Advances in the Stille Reaction and New Methods for Continuous Flow Pd–Catalyzed C–N Bond Forming Reactions

By

John R. Naber

B.Sc. Chemistry (Honours)
University of Victoria – Victoria, BC, 2004

Submitted to the Department of Chemistry in Partial Fulfillment of the Requirement for the Degree of

DOCTOR OF PHILOSOPHY IN ORGANIC CHEMISTRY

at the
Massachusetts Institute of Technology

June 2010

Signature of Author: _____
Department of Chemistry
May 17, 2010

Certified by:_____
Stephen L. Buchwald
Camille Dreyfus Professor of Chemistry
Thesis Supervisor

Accepted by: _____
Robert W. Field
Haslam and Dewey Professor of Chemistry
Chairman, Departmental Committee on Graduate Students

This doctoral thesis has been examined by a committee of the Department of Chemistry as follows:

Professor Timothy M. Swager: _____
Thesis Committee Chair

Professor Stephen L. Buchwald: _____
Thesis Supervisor

Professor Timothy F. Jamison: _____

Recent Advances in Palladium–Catalyzed Carbon–Carbon Bond–Forming Reactions and Continuous Flow Methods for Palladium–Catalyzed Carbon–Nitrogen Bond–Forming Reactions

By

John R. Naber

Submitted to the Department of Chemistry on May 21, 2010
in Partial Fulfillment of the Requirement for the Degree of Doctor of Philosophy
at the Massachusetts Institute of Technology

ABSTRACT

Chapter 1

A highly active catalyst system based upon a biaryl monophosphine ligand, XPhos, for the palladium-catalyzed Stille reaction has been developed. This method allows for the coupling of aryl chlorides with a range of tributylarylstannanes to produce the corresponding biaryl compounds in good to excellent yields (61-98%) in short reaction times (4 h). Palladium(II) acetate [$Pd(OAc)_2$] and XPhos in a 1:1.1 ratio were milled into a fine powder that was used as pre-catalyst for these reactions.

Chapter 2

A catalyst system for the Stille cross-coupling reactions of aryl mesylates and tosylates is reported. Using the combination of $Pd(OAc)_2$, XPhos, and CsF in t-BuOH an array of aryl and heteroaryl sulfonates were successfully employed in these reactions. Morever, heteroarylstannanes, such as furyl, thienyl, and N-methylpyrrolyl, which are often prone to decomposition, were efficiently coupled under these conditions. Ortho-substitution on the stannane coupling partner was well tolerated; however, the presence of ortho substituents on the aryl sulfonates greatly reduced the efficiency of these reactions.

Chapter 3

A continuous-flow, multistep Heck synthesis was made possible by integrating microreactors, liquid-liquid extraction, and microfluidic distillation. The microfluidic distillation enabled solvent exchange from CH_2Cl_2 in the first reaction step to *N*,*N*-dimethylformamide (DMF) in the final reaction step.

Chapter 4

A method to mitigate clogging of microsystems during Pd-catalyzed C–N bond-forming reactions under continuous flow conditions was developed. Bridging of particles across the channel and deposition of materials on the walls of the microreactor were both found to be causes that led to clogging and techniques to minimize their effects using sonication were developed. This system allows Pd-catalyzed amination reactions for the formation of a diaryl amines to proceed for extended periods of time without significant pressure increase in the reactor.

Chapter 5

A highly efficient method for the Pd-catalyzed coupling of aryl chloride and anilines has been developed. Catalysts based on allyl palladium chloride dimer and BrettPhos, using biphasic reaction conditions of toluene and water with KOH as a base, provided excellent yields for these reactions. The use of a packed bed reactor allowed for these reactions to be run in a continuous flow manner.

Thesis Supervisor: Stephen L. Buchwald
Title: Camille Dreyfus Professor of Chemistry

Acknowledgements

I wouldn't have been able to complete this work without the support of Marie-Eve. She has been a constant during my time here, and while it hasn't always been easy, I think we have made the absolute most of these past five years. Thank you for being there for me, even when I made it more difficult than it needed to be.

There are countless people that I would to thank, so I sure that some deserving people will be missed. However, I would like to start by thanking my family for helping me get to this point. It is a credit to my parents that I always believed that I could accomplish any task that I started, and this quality was invaluable during my time here at MIT.

A big thank you also goes to Steve for his support, and for accepting me into his group. I know there is a tendency for him to 'blame Canada' and that his trips to Quebec are often filled with travel hassles, but I hope that I was able to convince him that we don't just hunt moose, play hockey and drink Molson, eh?

During the last three years, I have had the pleasure of working on the Novartis project and through the project I have worked with many talented people. I would like to thank Klavs Jensen and Tim Jamison for taking the leap along with Steve and giving us the opportunity to work on continuous flow chemistry, which has been very both interesting, and in my case, the path to my first job. I also want to thank Ryan Hartman and Jon McMullen for being patient with me and teaching me about chemical engineering. My collaborations with Ryan have been great experiences, and Jon was always willing to explain things and exchange ideas.

In addition to the engineering collaborators, I am extremely grateful to the Buchwald flow team. Pat was there from the beginning and along with Matthew we were the original three. We learned a lot about how to clog, melt, break and burst polymer tubing, to say nothing about the damage we did to the fancy silicon microreactors that were so generous provided by the engineers. In the end, we put that knowledge to

good use in turning out some very interesting work, and also laid the groundwork for the future of the flow subgroup. Dima, Elliot, Pengfei and Tim are going to keep the project alive and I hope that some of what we have learned will be useful to them.

That just leaves the Buchwald group. I have had the pleasure of working with several waves of people that have made their ways through the labs here on the 3rd floor, and they have all contributed to my experience. The list of graduate students is a little shorter, so I am going to start there. My classmates, Carrie and Rich, helped me through my first year. Studying for exams, making it to class on time and trying to settle into a routine in the lab were all easier as a group. Joe and Tim were like the odd couple. Joe seemed very idealistic and Tim was one of the most cynical people I have ever met. Combining the advice from the two of them, or splitting the difference was generally my plan for staying centered. I didn't spend too much time with Ryan and Alan, but I always knew that if I had a question about chemistry, or how to handle something in the lab, they were there, and willing to answer questions. Nicole, Felix, Georgiy and Todd have all come after me in the lab, and I hope that I was able to provide some guidance for them about how to survive in the lab and in grad school.

I also want to thank the postdocs that have been part of the lab during my stay. They have been some of the most talented and driven scientists that I have ever met, and I'm sure I will be reading of their successes for many years to come. The people that were here when I joined the group really set the tone for how I felt a lab should operate. They seemed very serious and business-like, but I got to see how to work hard and how to accomplish much. For this I would like to thank Alex (Shafir), Marta, Nan, Peter, Ruben, Takashi and Tom (Clarke). As the group began to turn over, I was treated to a new batch of postdocs. I was more established in the lab, and began to see them as peers and as such, there are several people from this time that I consider close friends. Thanks to Alex (Taylor), Ana, Brijesh, Don, Jackie, Rachel and Yoshi. Lastly, we have the current crop of Buchwald postdocs. I was firmly established in the lab at this point, so I feel that I was able to help acclimate these colleagues to the Buchwald lab. They have helped my finish up my work here, and have taken over the majority of the group governance and

relieved a lot of that pressure. Therefore, thanks to Chong, Deb, Eun Jin, Gavin, Jaclyn, Jorge, Luca, Matthias, Tom (Kinzel), Tom (Maimone), Xiaoqiang, Xiaoxing and Yong. I would be remiss if I didn't acknowledge David, who has been a constant throughout my time here in the group. I couldn't decide which group to put him in, as he satisfies all of the criteria.

One postdoc who was not only a very talented chemist, and incredibly hard worker, but is truly one of the nicest people that I have ever met, is Gordon Brasche. Gordon worked in the same bay as me, and is someone that I will never forget, and hope to remain friends with for a long time. We spent many Saturdays listening to the Bundesliga (in German) and cheering on Werder Bremen. He was gracious enough to act as a tour guide when we visited Berlin, and still manages to find time in his new life to call, email and chat on a regular basis. I could always count on Gordon if I was feeling down, and can't thank him enough.

I mentioned Pat earlier as a member of the flow project, but would like to thank Pat Bazinet again. In addition to being the only other Canadian in the group and helping to absorb some of the blame, Pat got us moving on flow, revolutionized the group inventory, found himself (and subsequently me) a job, introduced me to running and also became a good friend. I'm looking forward to the opportunity to work with Pat again, and it can't hurt to have a francophone around if I ever want to have a decent conversation with my in-laws.

That just leaves two people. Kelvin 'PJ' Billingsley and Brett Fors. One older grad student and one younger grad student were the people that held it all together for me. I will never forget PJ's recruiting pitch of liking the Buchwald lab "because it's all dudes". While this may not sound memorable, you should know that I was visiting the lab with Carrie Jones. Maybe surprisingly, this didn't deter her from joining the lab. PJ wasn't the easiest person to get to know as he pretty much kept to himself, but a mutual love of basketball, an interest in all sports and a taste for fine beer was enough to gain access into his confidence. After that he was a source of advice, a co-conspirator in noon-ball, a squash convert and an always-willing drinking buddy. I will always have more than a passing interest in the successes of the

Gamecocks and a desire to visit South Carolina to see if it is all he made it out to be. For all of this, a big 'thanks, buddy' to PJ.

Contrary to getting to know PJ, getting to know Brett took almost no work. I guess this stems from the fact that we have so much in common, having grown up in the same province. Montana may border both Alberta and Saskatchewan, but from what I have heard and seen, it is really just Saskatchewan South. Brett's friendship has been invaluable over the past 3 years. Whether it is a trip to the student center for some fries, someone to get lunch with, someone to go get a keg for Steve's party with or any number of other things Brett is reliable. In addition to being a great friend, he has also been an inspiration in terms of lab work, a fount of chemistry expertise and a valuable proofreader. In addition to all of the help in the lab, Marie-Eve and I are grateful to both Brett and Carly for their friendship outside of the lab. While we may not have lobster with them again, we look forward to many more dinners and parties with them.

Preface

This thesis has been adapted from the following published articles co-written by the author:

"Palladium-Catalyzed Stille Cross-Coupling Reaction of Aryl Chlorides using a Pre-Milled Palladium Acetate and XPhos Catalyst System" Naber, J.R.; Buchwald, S.L. *Adv. Synth. Catal*. **2008**, *350*, 957-961.

"Stille Cross-Coupling Reactions of Aryl Mesylates and Tosylates Using a Biarylphosphine Based Catalyst System" Naber, J.R.; Fors, B.P.; Wu, X.; Gunn, J.T.; Buchwald, S.L. *Heterocycles*, **2010**, *80*, 1215-1226.

"Multistep Microchemical Synthesis Enabled by MicroFluidic Distillation" Hartman, R.L.; Naber, J.R.; Buchwald, S.L.; Jensen, K.F. *Angew. Chem. Int. Ed.* **2010**, *49*, 899-903.

"Overcoming the challenges of bridging and constriction during Pd-Catalyzed C-N bond formation in micro-flow" Hartman, R.L.; Naber, J.R.; Zaborenko, N.; Buchwald, S.L.; Jensen, K.F. Prepared Manuscript.

"Biphasic, Continuous-Flow Palladium-Catalyzed C-N Bond Formation Enabled by Packed Bed Reactors" Naber, J.R.; Buchwald, S.L. Prepared Manuscript.

Respective Contributions

This thesis is the result of the collaborative research efforts of the author and other workers at the Massachusetts Institute of Technology. An overview of the specific contributions of the collaborators is included below.

The work described in Chapter 2 was the result of collaboration between the author, Brett P. Fors, Dr. Xiaoxing Wu and Jonathan T. Gunn. The responsibility for the results in Table 1 was shared between the author and Dr. Wu while the responsibility for the results in Table 2 was shared between all of the collaborators with the author synthesizing Entries 3, 9 and 12.

The work described in Chapters 3 and 4 was the result of collaborative efforts between the author and Dr. Ryan Hartman of Prof. Klavs F. Jensen's group in the MIT chemical engineering department. The author was responsible for all method development for the chemical reactions described within these two chapters along with the preparation of all reagent solutions, all sample analysis, product isolation, product purification and all product characterization. In addition the setup for the microfluidic equipment used for the experiments described in Table 3-3, Figure 3-4, Figure 4-9, Figure 4-12, Figure 4-13 and Table 4-1 was performed by the author. Dr. Hartman was responsible for the remainder of the equipment setup, the development of the micro-distillation method used in Chapter 3, and for all of the operation of the micro-distillation system described herein. Additionally, all modeling was performed by Dr. Hartman. In Chapter 4, Dr. Hartman was again responsible for all modeling, all of the equipment setup not detailed above, the operation of all experiments involving pressure monitoring, X-ray diffraction analysis and particle size analysis. Reactor design and reactor surface modification was performed by Dr. Hartman and Nikolay Zaborenko and was included for continuity. Additionally, the analysis of the waveform produced by the ultrasonic bath was performed by Nikolay Zaborenko and was also included for continuity.

Table of Contents

Introduction

Since their discovery, palladium-catalyzed cross-coupling processes have become some of the most important reactions in organic chemistry.[1] While a variety of bonds can be formed by Pd catalysis, carbon-carbon and carbon-nitrogen bond-forming reactions are the most common. Within the subset of C–C bond-forming reactions, many derivatives exist that are differentiated by the aryl (or alkyl) nucleophiles that are employed. Aryl or alkyl lithiums (Murahashi),[2] Grignard reagents (Kumada-Corriu),[3] organostannanes (Stille),[4] organozinc reagents (Negeshi),[5] aryl silanes (Hiyama)[6] and boronic acids and esters (Suzuki-Miyaura)[7] are all utilized in these reactions, with many methods having been described to encompass the coupling of a wide range of aryl electrophiles.

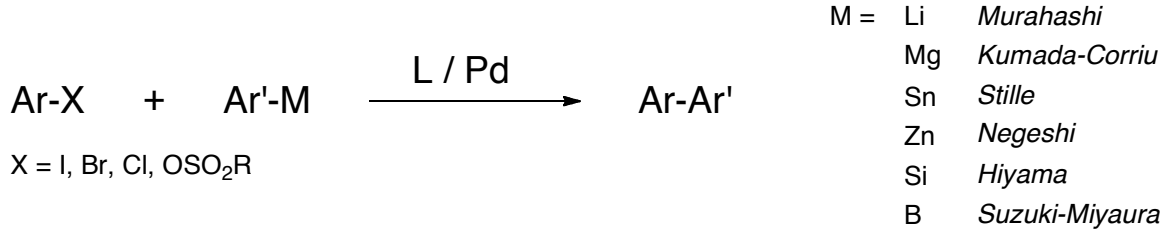

Scheme 1. Types of Pd-catalyzed C–C cross-coupling reactions.

Similarly, a range of reaction conditions and catalyst systems have been reported for Pd-catalyzed C–N bond-forming reactions (Buchwald-Hartwig)[8] that enable the coupling of aryl electrophiles with a host of nitrogen nucleophiles.

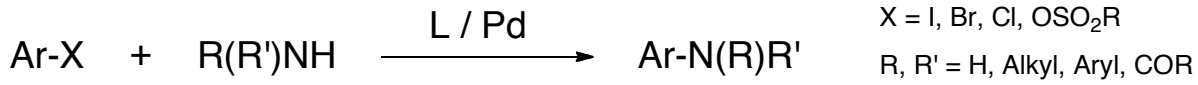

Scheme 2. Pd-catalyzed C–N cross-coupling reactions.

The heart of the research devoted to developing new methods for these reactions focuses on the design of new supporting ligands for palladium. The selection of the appropriate ligand can mean the difference between a highly active catalyst and a catalyst with no activity whatsoever. A family of electron-rich

bulky biaryl monophosphine ligands have been developed that form highly active Pd catalysts for a wide range of coupling reactions.[9]

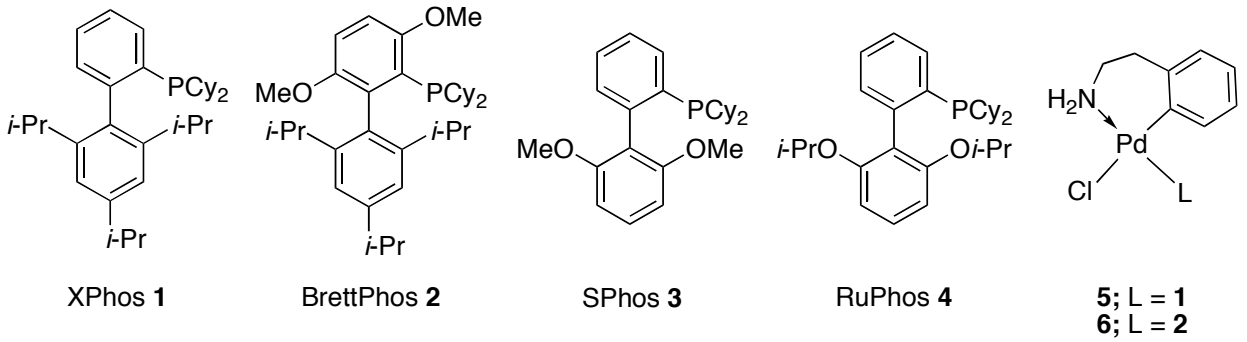

XPhos **1** BrettPhos **2** SPhos **3** RuPhos **4** **5;** L = **1** **6;** L = **2**

Figure 1. Biaryl Monophosphine Ligands.

In recent years, a great deal of research has been directed towards the development of methods for the Suzuki-Miyaura reaction and it has become a favorite of chemists for C–C bond formation. In contrast, the Stille reaction has received less attention, likely due to the toxicity associated with the organotin byproducts formed during the course of the reaction. While this toxicity is undesirable, there are a number of reasons why the Stille reaction remains a valuable tool for organic chemistry including the air and moisture stability of the organostannanes used in these reactions, and the excellent function group tolerance of these transformations.

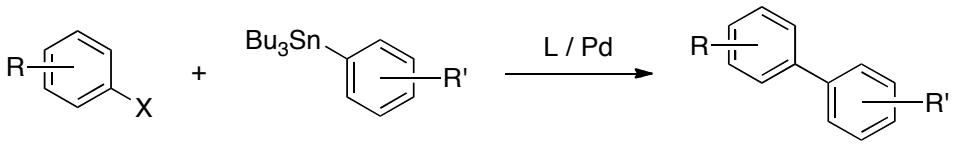

X = I, Br, Cl, OSO_2R

R, R' = CO_2R, COR, CHO, NO_2, CN

ArSnBu3 = air and moisture stable

Scheme 3: The Stille reaction.

In this work, Chapters 1 and 2 deal with new methods for Stille cross-coupling reactions that have been developed. These methods are based on XPhos as a supporting ligand and use cesium fluoride as an

activating agent for the organostannanes. The remainder of this work is focused on new methods for continuous-flow based chemistry; specifically, Pd-catalyzed coupling reactions.

Complex organic molecules, such as active pharmaceutical ingredients, are synthesized via multiple reactions, which require work-up and isolation of the intermediates. Recent interest in microfluidic systems for continuous-flow synthesis has motivated the integration of multiple chemical reactions and separations in an attempt to streamline the process. Microreactor networks provide advantages for chemical synthesis such as enhanced heat and mass transfer characteristics, safety of operation, isolation of sensitive reactions from air or moisture and a reduction of hazardous waste, while potentially providing a fundamental understanding of how production-scale processes operate.[10]

The work presented in Chapter 3 describes the use of a novel microfluidic tool, an on-chip distillation,[11] to develop a system for a two step synthesis comprised of the formation of a triflates followed by the Heck coupling of the triflates with an alkene. The two steps of the synthesis were performed in different solvents and the distillation enabled the switch from dichloromethane to dimethylformamide.

Finally, Chapters 4 and 5 deal with the development of flow-based methods for the Pd-catalyzed C–N bond-forming reaction. Chapter 4 focuses on the chemical engineering required to design a system that can deal with heterogeneous reaction mixture in micro scale flow, and Chapter 5 describes a new flow method for the coupling of aryl chlorides with anilines using an aqueous solution of potassium hydroxide as the base.

References

1. For reviews of Pd-catalyzed cross-coupling, see: a) *Metal-catalyzed Cross-coupling Reactions*, 2nd Edition, Eds.: A. de Meijere and F. Diederich, Wiley-VCH, Weinheim, **2004.** b) J. Tsuji, *Palladium Reagents and Catalysis*, 2nd Edition, Wiley, Chichester, **2004**.
2. M. Yamamura, I. Moritani, S.-I. Murahashi, *J. Organomet. Chem*. **1975**, *91*, C39-C42.
3. a) R.J.P. Corriu, J.P. Masse, *J. Chem. Soc., Chem. Commun*. **1972**, 144-144. b) K. Tamao, K.

Sumitani, M. Kumada, *J. Am. Chem. Soc*. **1972**, *94*, 4374-4376.

4. a) M. Kosugi, K, Sasazawa, Y. Shimizu and T. Migita, *Chem. Lett*., **1977**, 301. b) D. Milstein and J. K. Stille, *J. Am. Chem. Soc*., **1978**, *100*, 3636-3638. c) D. Milstein and J. K. Stille, *J. Org. Chem*., **1979**, *44*, 1613-1618.

5. S. Babu, E.-I. Negishi, *J. Am. Chem. Soc*. **1976**, *98*, 6729-6731.

6. a) Y. Hatanaka, T. Hiyama, *J. Org. Chem*. **1988**, *53*, 918-920. b) Y. Hatanaka, S. Fukushima, T. Hiyama, *Chem. Lett*. **1989**, 1711-1714.

7. a) N. Miyaura, A. Suzuki, *J. Chem. Soc., Chem. Commun*. **1979**, 866-867. b) N. Miyaura, T. Yanagi, A. Suzuki, *Synth. Commun*. **1981**, *11*, 513-519.

8. For recent reviews of Pd-catalyzed aminations, see: a) D.S. Surry, S.L. Buchwald, *Angew. Chem. Int. Ed.* **2008**, *47*, 6338-6361. b) S.L. Buchwald, L. Jiang, In *Metal-Catalyzed Cross-Coupling Reactions*; A. deMeijere, F. Diederich, Eds.; Wiley-VCH: Weinheim, 2004, p 699. c) J.F. Hartwig, *Acc. Chem. Res*. **2008**, *41*, 1534-1544. d) N. Marion, S.P. Nolan, *Acc. Chem. Res*. **2008**, *41*, 1440-1449.

9. a) X. Huang, K.W. Anderson, D. Zim, L. Jiang, A. Klapars, S.L. Buchwald, *J. Am. Chem. Soc*. **2003**, *125*, 6653-6655. b) S. D. Walker, T. E. Barder, J. R. Martinelli, S. L. Buchwald, *Angew. Chem. Int. Ed.* **2004**, *43*, 1871-1876. c) J. E. Milne and S. L. Buchwald, *J. Am. Chem. Soc.,* **2004**, **126**, 13028-13032. d) B.P. Fors, D.A. Watson, M.R. Biscoe, S.L. Buchwald, *J. Am. Chem. Soc*. **2008**, *130*, 13552-13554.

10. For a review of synthetic chemistry application performed in flow, see: Hartman, R. L.; Jensen, K. F. *Lab Chip* **2009**, *9*, 2495–2507.

11. R.L. Hartman, H.R. Sahoo, B.C. Yen, K.F. Jensen, *Lab Chip*, **2009**, *9*, 1843-1849.

Chapter 1 - Stille Cross-Coupling Reactions of Aryl Chlorides

1.1 Introduction

The Stille cross-coupling reaction has proven to be a powerful method for combining aryl halides and arylstannanes to give ready access to biaryl motifs,[1] which are found in numerous biologically active compounds including both natural products and pharmaceutically interesting molecules.[2] Recent advances in the general area of cross-coupling have led to the development of highly active catalyst systems that were capable of transforming aryl chlorides, which are less expensive and more readily available than aryl iodides and bromides.[1f] While considerable research has been devoted to the Suzuki-Miyaura reaction,[1f, 3] there have been fewer reports of catalytic methods for the reaction of aryl chlorides with organostannanes.[4] Although the tin byproducts generated in the Stille reaction tend to have relatively high molecular weights and are toxic, the air- and moisture-stability of organostannanes combined with the broad functional group tolerance of the Stille reaction ensures it's continued relevance, particularly as a tool for discovery chemists[5] and in natural product synthesis.[6] Herein, we describe a highly active catalyst system for the coupling of aryl chlorides with arylstannanes.

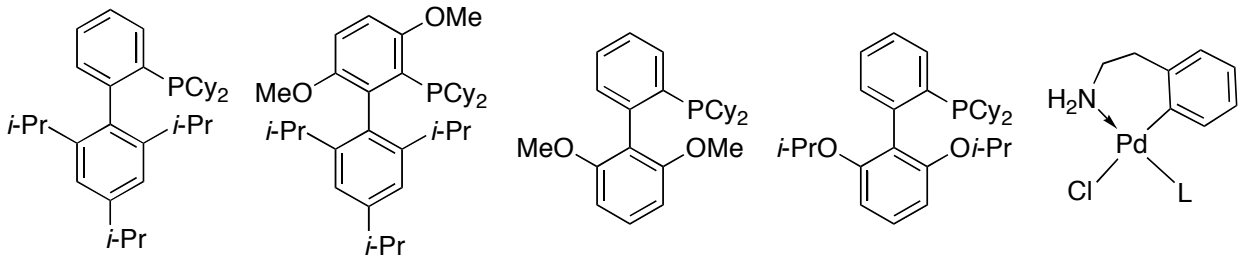

XPhos **1** BrettPhos **2** SPhos **3** RuPhos **4** **5;** L = **1** **6;** L = **2**

Figure 1. Biaryl Monophosphine Ligands.

A family of air-stable biaryl monophosphine ligands has been developed in our laboratories and have proven useful as components of highly active catalyst systems for C-C and C-N bond-forming reactions.[3b-c, 7] Based on previous work in our group and initial screening results, XPhos was chosen as a supporting ligand and was combined with $Pd(OAc)_2$ to generate a highly active catalyst system that was used for further optimization.

1.2 Results and Discussion

Recent work has shown that the addition of a fluoride source increases the reactivity of arylstannanes and results in a significant rate enhancement.[4a-c,f-h] While the use of TBAF and KF provided moderate results, CsF provided the greatest enhancement in the reaction rate (Table 1, entries 1-4). A further optimization showed that reactions in ethereal solvents or *t*-butanol provided the desired biaryl in a greater yield. Dimethoxyethane (DME) was chosen over *t*-butanol as the solvent for further studies due to the high melting point of *t*-butanol.

Table 1. Examination of reaction conditions for the coupling of 4-chloroanisole.

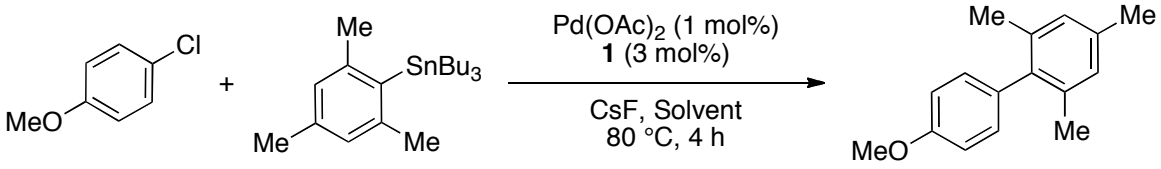

Entry	Solvent	CsF (equiv)	Conv (%)	Yield (%)[b]
1	toluene	0.0	13	0
2	toluene	1.0	47	33
3	toluene	2.0	76	67
4	toluene	2.2	80	70
5	DCE	2.2	53	38
6	NMP	2.2	89	73
7	n-butanol	2.2	100	33
8	t-butanol	2.2	100	100
9	DEM	2.2	100	91
10	1,4-dioxane	2.2	100	92
11	DME	2.2	100	100

[a] Reaction Conditions; 1.0 equiv of Ar-Cl, 1.1 equiv of Ar-Sn, 1.0 mol% of $Pd(OAc)_2$, 3.0 mol% of **1**, 1.0 mL of solvent/mmol of Ar-Cl, DCE = 1,2-dichloroethane, NMP = N-methylpyrrolidine, DME = dimethoxyethane, DEM = diethoxymethane. [b] GC Yield.

Table 2. Stille cross-coupling reactions of unactivated aryl chlorides and deactivated chlorides.

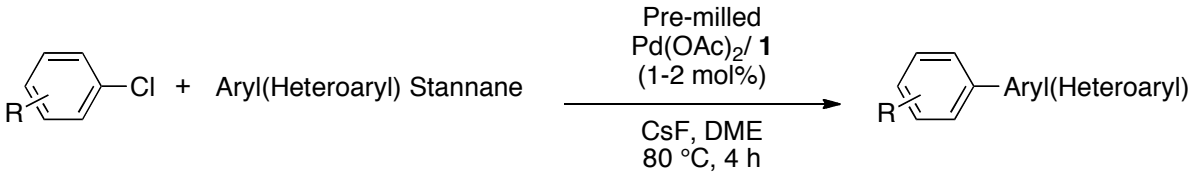

Entry	Aryl Chloride	Product	Yield (%)[b]
1	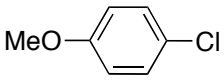	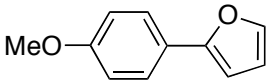	97[c]
2	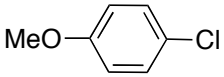	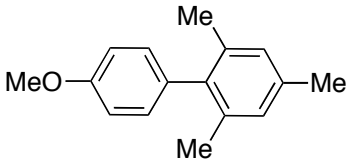	96
3	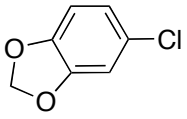	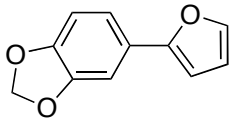	97
4	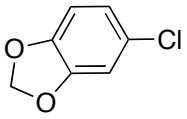	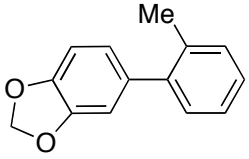	94
5			95[d]
6	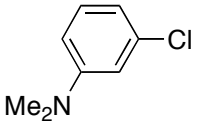	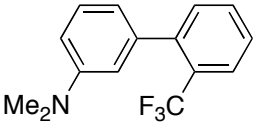	89[c]
7	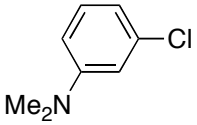	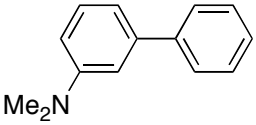	90[c]

[a] Reactions Conditions: 1.0 equiv of Ar-Cl, 1.1 equiv of Ar-$SnBu_3$, 2.2 equiv of CsF, 1.0 mol% of pre-milled $Pd(OAc)_2$: **1** (1:1.1), 1.0 mL of DME/mmol of Ar-Cl. [b] Isolated yields (average of two runs). [c] 2.0 mol% of pre-milled $Pd(OAc)_2$:XPhos (1:1.1) [d] 1.0 mol% $Pd(OAc)_2$ and 1.1 mol% **1** added as separate solids.

We found that very similar results were obtained with ligand:Pd ratios of 1:1, 2:1 and 3:1, thus reactions were conducted with only a slight excess of ligand (1.1:1, L:Pd). A mixture of palladium acetate and XPhos, in the aforementioned ratio, was milled with a mortar and pestle to give a fine, beige powder that was used in subsequent reactions. The milling process allowed for excellent control of the palladium to ligand ratio and facilitated precision when weighing samples for reactions. The results of reaction run with the powder were identical to those performed with separate $Pd(OAc)_2$ and XPhos (Table 2, entries 4 and 5) and the powder could be stored in a bench top dessicator with no loss of activity over a six-month period.

Encouraged by these results, we sought to examine the scope of this process. The results are shown in Table 2. These conditions constitute the lowest temperature reactions and shortest reaction times reported for the coupling of unactivated aryl chlorides with arylstannanes reported to date. Chloroanilines, as a class of compounds, have not previously been used to generate biaryl compounds via the Stille reaction.[8] One example of this class of compounds, *N,N*-dimethyl-3-chloroaniline, using our conditions, was successfully coupled with a both aryl- and heteroarylstannanes (Table 2, entries 5 and 6). Similarly, while 4-chloroanisole has been combined with arylstannanes, the best reported conditions required that the reactions be conducted at 100 °C for 48 hours.[4a,c] Employing our catalyst system this substrate, in combination with both a hindered arylstannane and a heteroarylstannane, provided excellent yields of product in 4 hours at 80 °C (Table 2, entries 1 and 2). Additionally, 5-chlorobenzo[*d*][1,3]dioxole (Table 2, entries 3 and 4), could be coupled in excellent yields with both aryl- and heteroarylstannanes. Previously, this substrate has been used in the Stille reaction to form a biaryl in only one other instance in which longer reaction times and higher temperatures (45 h and 110 °C) were required.[4h]

Table 3. Stille cross-coupling reactions of aryl chlorides and heteroaryl chlorides.

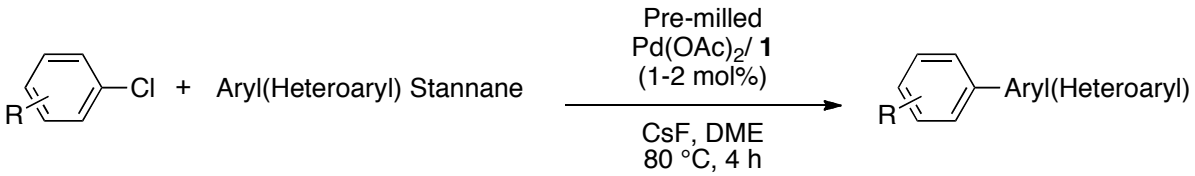

Entry	Aryl Chloride	Product	Yield (%)[b]
1	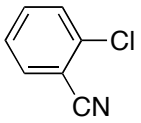	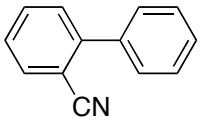	86
2	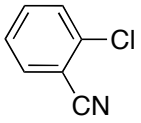	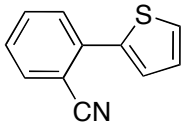	92
3	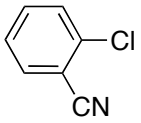	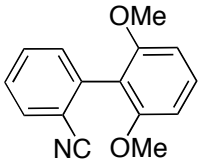	74
4	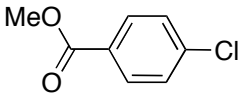	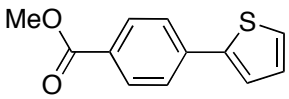	91
5	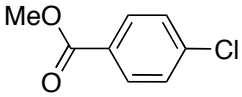	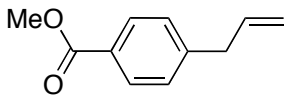	84
6	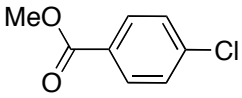	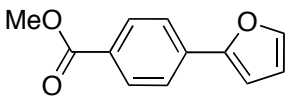	97
7	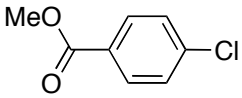	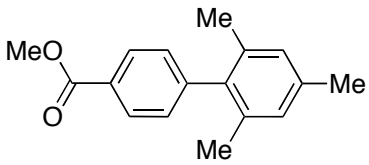	96
8	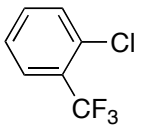	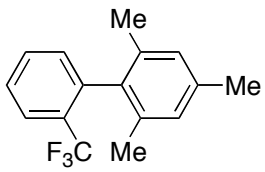	61[c]

[a] Reactions Conditions: 1.0 equiv of Ar-Cl, 1.1 equiv of Ar-$SnBu_3$, 2.2 equiv of CsF, 1.0 mol% of pre-milled $Pd(OAc)_2$: **1** (1:1.1), 1.0 mL of DME/mmol of Ar-Cl. [b] Isolated yields (average of two runs). [c] 2.0 mol% of pre-milled $Pd(OAc)_2$: **1** (1:1.1) [d] Reactions run in dioxane at 100 °C, with 2.0 mol% pre-milled $Pd(OAc)_2$: **1** (1:3).

Table 3 (cont).

Entry	Aryl Chloride	Product	Yield (%)[b]
9	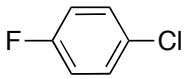	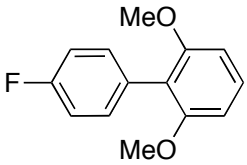	93[c]
10	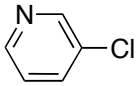	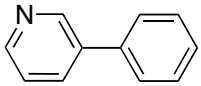	92[d]
11	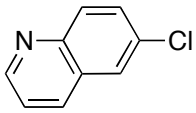	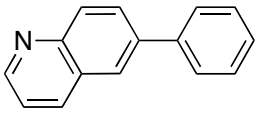	98[d]

[a] Reactions Conditions: 1.0 equiv of Ar-Cl, 1.1 equiv of Ar-$SnBu_3$, 2.2 equiv of CsF, 1.0 mol% of pre-milled $Pd(OAc)_2$: **1** (1:1.1), 1.0 mL of DME/mmol of Ar-Cl. [b] Isolated yields (average of two runs). [c] 2.0 mol% of pre-milled $Pd(OAc)_2$: **1** (1:1.1) [d] Reactions run in dioxane at 100 °C, with 2.0 mol% pre-milled $Pd(OAc)_2$: **1** (1:3).

While the results in Table 3 do not represent the lowest temperature reaction conditions reported for Stille reactions with activated aryl chlorides,[9] they do represent a significant decrease over most of the reaction times reported and one of lowest operating temperatures of available Stille methods with these substrates. For instance, the coupling 2-chlorobenzonitrile has been previously reported at temperatures greater than 100 °C with reaction times longer than 24 hours.[4h, 10] By using our standard protocol, 2-chlorobenzonitrile was efficiently coupled with aryl, heteroaryl and electron-rich arylstannanes (Table 3, entries 1-3). Entries 4-7 of Table 3 show coupling reactions with methyl-4-chlorobenzoate and a variety of stannanes including allyl, heteroaryl and sterically-demanding arylstannanes. While the importance of fluorinated aromatic rings in pharmaceutically active compounds as a means to alter a molecules pharmacokinetics is well known,[11] examples of Stille reactions of fluoride-containing aryl chlorides are relatively scarce. In the lone example of coupling an aryl chloride with an ortho trifluoromethyl group, the process was carried out at for 48 hours at 150 °C;[12] only one example was found for a Stille coupling of fluorinated aryl chlorides.[13] By using our conditions, both o-chlorobenzotrifluoride and p-

fluorochlorobenzene could be efficiently coupled with arylstannanes (Table 3, entries 8 and 9). Additionally, we found that by increasing the reaction temperature to 100 °C and choosing 1,4-dioxane as a solvent to accommodate the increased temperature, it was possible to couple heteroaryl chlorides (Table 3, entries 10 and 11) with tributyl(phenyl)stannane.[14]

With regard to the arylstannane component: heteroaryl (Table 2, entries 1 and 3, Table 3, entries 2, 4 and 6), electron-rich aryl (Table 3, entries 3 and 9), electron-deficient aryl (Table 2, entry 6) and allylstannanes (Table 3, entry 5) were all coupled in high yields. It is noteworthy to mention that 2,6-dimethoxyphenyltributylstannane, which has not previously been used in Stille cross-coupling reactions,[15] was found to perform well under our conditions (Table 3, entries 3 and 9).

1.3 Conclusion

In conclusion, we have developed a highly active catalyst system for the reaction of a diverse range of aryl chlorides with a variety of arylstannanes. The use of CsF as an activator allows for a reduction of the temperatures commonly used in Stille reactions, and the use of ethereal solvents such as DME along with XPhos as a ligand allow for the reduction of the reaction times regularly used in these reactions.

1.4 Experimental

General. All reactions were carried out under an argon atmosphere. Dimethoxyethane (DME 99.5%, Anhydrous) and 1,4-dioxane (99.8%, Anhydrous) were purchased from Aldrich Chemical Co. Commercially available materials were used without further purification unless otherwise noted. XPhos was synthesized in our laboratories but is commercially available from Aldrich Chemical Co. or Strem Chemicals, Inc. Aryl halides were purchased from Aldrich Chemical Co. or Alfa Aesar. Phenyl- furyl- thiophenyl- and allyltributylstannanes were purchased from Aldrich Chemical Co. or Gelest, Inc. In analogy to the procedures described by Littke and Fu,[16] other stannanes were prepared by lithiation of the corresponding aryl bromides with *n*-BuLi (2.5 M in hexanes, Aldrich) followed by quenching with tributyltin chloride; 1-lithio-2,6-dimethoxybenzene was prepared by directed lithiation[17] and quenched

with tributyltin chloride. Cesium fluoride (99.9%) was purchased from Aldrich Chemical Co. and stored in a bench-top dessicator. Palladium acetate was supplied by BASF. All products from coupling reactions were characterized by ^{1}H NMR, ^{13}C NMR, IR spectroscopy, elemental analysis and melting points for solids. Known compounds were compared to their literature values. ^{1}H and ^{13}C NMR spectra were recorded on a Bruker Advance 400. Infrared spectra were recorded on a Perkin-Elmer Model 2000 FT-IR using NaCl plates (thin film). Elemental analyses were performed by Atlantic Microlabs Inc., Norcross, GA. All ^{1}H NMR experiments are reported in parts per million (ppm) downfield of TMS and were measured relative to the signals for chloroform (7.24 ppm). All ^{13}C NMR spectra were reported in ppm relative to residual chloroform (77.23 ppm) and were obtained with ^{1}H decoupling. Melting points were obtained on a Mel-Temp capillary melting point apparatus. Gas chromatographic analyses were preformed on Hewlett-Packard 6890 gas chromatography instrument with a FID detector using 25m x 0.20 mm capillary column with cross-linked methyl siloxane as a stationary phase. The yields in Tables 2 and 3 refer to isolated yields (average of two runs) of compounds estimated to be $\geq$ 95% pure as determined by ^{1}H NMR and GC analysis and/or combustion analysis. The procedures described in this section are representative and may differ slightly from those given in Tables 2 and 3.

$Pd(OAc)_2$ (225 mg, 1.00 mmol) and XPhos (524 mg, 1.10 mmol) were ground together using a mortar and pestle until a fine beige powder was formed. This powder (effective molecular weight: 749 g/mol) was stored in a bench-top dessicator for up to six months with no loss of activity and was used as the catalyst for all reactions described in this paper except where noted.

General Procedure A:

Pre-milled $Pd(OAc)_2$/XPhos and CsF (334 mg, 2.20 mmol) were added to an oven-dried test tube. The tube was fitted with a rubber septum, sealed with electrical tape, and evacuated and backfilled with argon (this process was repeated a total of 3 times). Dimethoxyethane (DME, 1.0 mL), aryl chloride (1.00 mmol) and stannane (1.10 mmol) were added via syringe to the tube. The reaction was heated to 80 °C with stirring for 4 h. At this time the reaction was removed from the oil bath, allowed to cool to room

temperature, diluted with ethyl acetate (5 mL) and filtered through a pad of silica gel, eluting with ethyl acetate (150 mL). The solvent was removed with the aid of a rotary evaporator, and the residue was taken up in dichloromethane (20 mL) and added to silica gel (~1 g). The solvent was concentrated under reduced pressure and the residue (adsorbed on silica) was loaded onto the top of a Biotage 25M column and purified by flash chromatography using a Biotage SP4.

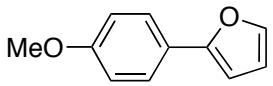

2-(4-Methoxyphenyl)furan (Table 2, entry 1).[18] Following general procedure A, 4-chloroanisole (123 μL, 1.00 mmol), tributyl(2-furanyl)stannane (346 μL, 1.10 mmol), pre-milled $Pd(OAc)_2$/XPhos (15.0 mg, 0.020 mmol) and CsF (334 mg, 2.20 mmol) were heated to 80 °C in DME with stirring for 4 h. The crude product was adsorbed on silica, loaded onto the top of a Biotage 25M column and purified by flash chromatography using a Biotage SP4 to provide the titled compound in 99% yield (173 mg) as a white solid, mp 55-56 °C. ^{1}H NMR (400 MHz, $CDCl_3$) δ 7.59 (d, *J* = 9.0 Hz, 2H), 7.41 (dd, *J* = 1.5, 0.5 Hz, 1H), 6.91 (d, *J* = 9.0 Hz, 2H), 6.50 (dd, *J* = 3.5, 0.5 Hz, 1H), 6.43 (dd, *J* = 3.5, 1.5 Hz, 1H), 3.82 (s, 3H); ^{13}C NMR (100 MHz, $CDCl_3$) δ 159.2, 154.2, 141.6, 125.4, 124.2, 114.3, 111.7, 103.5, 55.5; IR (neat, cm^{-1}) 3450, 2958, 2837, 1515, 485, 1254, 1026, 834, 801, 734. Anal. Calc'd. for $C_{11}H_{10}O_2$: C, 75.84; H, 5.79. Found C, 75.71; H, 5.77.

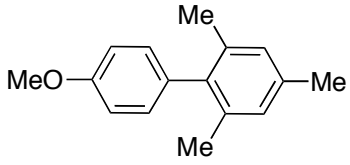

4'-Methoxy-2,4,6-trimethylbiphenyl (Table 2, entry 2).[19] Following general procedure A, 4-chloroanisole (123 μL, 1.00 mmol), tributyl(2,4,6-mesityl)stannane (401 μL, 1.10 mmol), pre-milled $Pd(OAc)_2$/XPhos (7.5 mg, 0.010 mmol) and CsF (334 mg, 2.20 mmol) were heated to 80 °C in DME with stirring for 4 h. The crude product was adsorbed on silica, loaded onto the top of a Biotage 25M column and purified by flash chromatography using a Biotage SP4 to provide the titled compound in 95% yield

(215 mg) as a white solid, mp 75-77 °C. ^{1}H NMR (400 MHz, $CDCl_3$) δ 7.04 (d, *J* = 9.0 Hz, 2H), 6.94 (d, *J* = 9.0 Hz, 2H), 6.93 (s, 2H), 3.84 (s, 3H), 2.37 (s, 3H), 2.00 (s, 6H); ^{13}C NMR (100 MHz, $CDCl_3$) δ 158.3, 138.8, 136.6, 133.4, 130.5, 128.2, 113.9, 55.4, 21.2, 21.0; IR (neat, cm^{-1}) 2933, 2833, 1609, 1514, 1285, 1245, 1042, 854, 832, 733. Anal. Calc'd. for $C_{16}H_{18}O$: C, 84.91; H, 8.02. Found C, 84.81; H, 8.04.

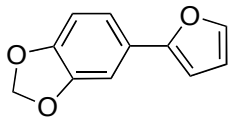

5-(2-Furanyl)benzo[*d*][1,3]dioxole (Table 2, entry 3).[20] Following general procedure A, 5-chlorobenzo[*d*][1,3]dioxole (117 μL, 1.00 mmol), tributyl(2-furanyl)stannane (346 μL, 1.10 mmol), pre-milled $Pd(OAc)_2$/XPhos (7.5 mg, 0.010 mmol) and CsF (334 mg, 2.20 mmol) were heated to 80 °C in DME with stirring for 4 h. The crude product was adsorbed on silica, loaded onto the top of a Biotage 25M column and purified by flash chromatography using a Biotage SP4 to provide the titled compound in 95% yield (178 mg) as a yellow oil. ^{1}H NMR (400 MHz, $CDCl_3$) δ 7.40 (d, *J* = 2.0 Hz, 1H), 7.16 (dd, *J* = 8.0, 2.0 Hz, 1H), 7.13 (d, *J* = 2.0 Hz, 1H), 6.81 (d, *J* = 8.0 Hz, 1H), 6.48 (d, *J* = 3.0 Hz, 1H), 6.42 (dd, *J* = 3.0, 2.0 Hz, 1H), 5.96 (s, 2H); ^{13}C NMR (100 MHz, $CDCl_3$) δ 153.9, 148.1, 147.1, 141.6, 125.5, 117.7, 111.7, 108.7, 104.7, 104.0, 101.2; IR (neat, cm^{-1}) 3457, 2894, 1507, 1479, 1451, 1257, 1227, 1040, 811, 733. Anal. Calc'd. for $C_{11}H_8O_3$: C, 70.21; H, 4.29. Found C, 70.16; H, 4.21.

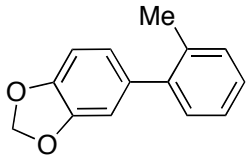

5-*o*-Tolylbenzo[*d*][1,3]dioxole (Table 2, entry 4).[21] Following general procedure A, 5-chlorobenzo[*d*][1,3]dioxole (117 μL, 1.00 mmol), tributyl(*o*-tolyl)stannane (373 μL, 1.10 mmol), pre-milled $Pd(OAc)_2$/XPhos (7.5 mg, 0.010 mmol) and CsF (334 mg, 2.20 mmol) were heated to 80 °C in DME with stirring for 4 h. The crude product was adsorbed on silica, loaded onto the top of a Biotage 25M column and purified by flash chromatography using a Biotage SP4 to provide the titled compound in

91% yield (192 mg) as a colorless oil. ^{1}H NMR (400 MHz, $CDCl_3$) δ 7.23 (m, 4H), 6.86 (d, J = 8.0 Hz, 1H), 6.82 (d, J = 1.5 Hz, 1H), 6.77 (dd, J = 8.0, 1.5 Hz, 1H), 5.99 (s, 2H), 2.28 (s, 3H); ^{13}C NMR (100 MHz, $CDCl_3$) δ 147.5, 146.6, 141.7, 136.0, 135.7, 130.5, 130.0, 127.3, 125.9, 122.7, 110.0, 108.2, 101.2, 20.7; IR (neat, cm^{-1}) 2460, 2889, 1504, 1478, 1246, 1221, 1040, 760, 731. Anal. Calc'd. for $C_{14}H_{12}O_2$: C, 79.22; H, 5.70. Found C, 79.14; H, 5.84.

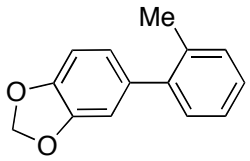

5-*o*-Tolylbenzo[*d*][1,3]dioxole (Table 2, entry 5).[21] Modification to general procedure A, 5-chlorobenzo[*d*][1,3]dioxole (117 μL, 1.00 mmol), tributyl(*o*-tolyl)stannane (373 μL, 1.10 mmol), $Pd(OAc)_2$ (2.3 mg 0.010 mmol), XPhos (5.2 mg, 0.011 mmol) and CsF (334 mg, 2.20 mmol) were heated to 80 °C in DME with stirring for 4 h. The crude product was adsorbed on silica, loaded onto the top of a Biotage 25M column and purified by flash chromatography using a Biotage SP4 to provide the titled compound in 96% yield (203 mg) as a colorless oil. ^{1}H NMR (400 MHz, $CDCl_3$) δ 7.25 (m, 4H), 6.88 (d, J = 8.0 Hz, 1H), 6.84 (d, J = 1.5 Hz, 1H), 6.79 (dd, J = 8.0, 1.5 Hz, 1H), 6.01 (s, 2H), 2.30 (s, 3H); ^{13}C NMR (100 MHz, $CDCl_3$) δ 147.4, 146.6, 141.7, 136.0, 135.6, 130.5, 130.0, 127.3, 125.9, 122.6, 110.0, 108.2, 101.1, 20.7.

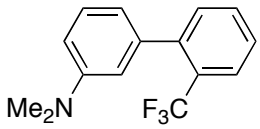

***N,N*-Dimethyl-2'-(trifluoromethyl)biphenyl-3-amine (Table 2, entry 6).** Following general procedure A, 3-chloro-*N,N*-dimethylaniline (137 μL, 1.00 mmol), tributyl(2-(trifluoromethyl)phenyl)stannane (389 μL, 1.10 mmol), pre-milled $Pd(OAc)_2$/XPhos (15.0 mg, 0.020 mmol) and CsF (334 mg, 2.20 mmol) were heated to 80 °C in DME with stirring for 4 h. The crude product was adsorbed on silica, loaded onto the top of a Biotage 25M column and purified by flash chromatography using a Biotage SP4 to provide the

titled compound in 87% yield (229 mg) as a pale yellow oil. ^{1}H NMR (400 MHz, $CDCl_3$) δ 7.72 (d, *J* = 7.5 Hz, 1H), 7.53 (t, *J* = 7.5 Hz, 1H), 7.43 (t, *J* = 7.5 Hz, 1H), 7.36 (d, *J* = 7.5 Hz, 1H), 7.25 (t, *J* = 8.0 Hz, 1H), 6.75 (d, *J* = 8.0 Hz, 1H), 6.66 (m, 2H), 2.95 (s, 6H); ^{13}C NMR (100 MHz, $CDCl_3$) δ 150.0, 142.5, 140.8, 132.2, 131.4, 128.6, 128.6 (q, *J* = 30 Hz), 127.3, 126.2 (q, *J* = 5 Hz), 124.5 (q, *J* = 272 Hz), 117.6, 113.6, 111.8, 40.7; IR (neat, cm^{-1}) 2888, 1601, 1491, 1314, 1170, 1128. 1109, 768, 701. Anal. Calc'd. for $C_{15}H_{14}F_3N$: C, 67.91; H, 5.32. Found C, 67.98; H, 5.42.

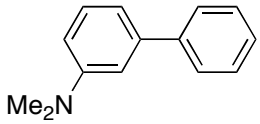

***N,N*-Dimethylbiphenyl-3-amine (Table 2, entry 7).**[22] Following general procedure A, 3-chloro-*N,N*-dimethylaniline (137 μL, 1.00 mmol), tributyl(phenyl)stannane (359 μL, 1.10 mmol), pre-milled $Pd(OAc)_2$/XPhos (15.0 mg, 0.020 mmol) and CsF (334 mg, 2.20 mmol) were heated to 80 °C in DME with stirring for 4 h. The crude product was adsorbed on silica, loaded onto the top of a Biotage 25M column and purified by flash chromatography using a Biotage SP4 to provide the titled compound in 90% yield (178 mg) as a pale yellow oil. ^{1}H NMR (400 MHz, $CDCl_3$) δ 7.68 (d, *J* = 8.0 Hz, 2H), 7.50 (t, *J* = 7.5 Hz, 2H), 7.39 (m, 2H), 7.02 (m, 2H), 6.81 (dd, *J* = 8.0, 2.5 Hz, 1H), 3.06 (s, 6H); ^{13}C NMR (100 MHz, $CDCl_3$) δ 151.1, 142.4, 142.4, 129.6, 128.8, 127.5, 127.3, 116.0, 111.8, 111.7, 40.9; IR (neat, cm^{-1}) 3030, 2881, 2801, 1598, 1491, 1354, 755, 698; Anal. Calc'd. for $C_{14}H_{15}N$: C, 85.24; H, 7.66. Found C, 85.21; H, 7.66.

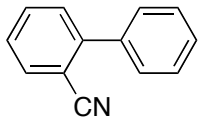

Biphenyl-2-carbonitrile (Table 3, entry 1).[23] Following general procedure A, 2-chlorobenzonitrile (138 mg, 1.00 mmol), tributyl(phenyl)stannane (359 μL, 1.10 mmol), pre-milled $Pd(OAc)_2$/XPhos (7.5 mg, 0.010 mmol) and CsF (334 mg, 2.20 mmol) were heated to 80 °C in DME with stirring for 4 h. The crude product was adsorbed on silica, loaded onto the top of a Biotage 25M column and purified by flash

chromatography using a Biotage SP4 to provide the titled compound in 88% yield (158 mg) as a colorless oil. ^{1}H NMR (400 MHz, $CDCl_3$) δ 7.75 (dd, *J* = 8.0, 1.0 Hz, 1H), 7.63 (td, *J* = 8.0, 1.0 Hz, 1H), 7.48 (m, 7H); ^{13}C NMR (100 MHz, $CDCl_3$) δ 145.6, 128.3, 133.9, 133.0, 130.3, 128.9, 128.9, 128.9, 127.7, 118.9, 111.4; IR (neat, cm^{-1}) 3064, 2963, 2223, 1261, 1076, 1027, 799, 758; Anal. Calc'd. for $C_{13}H_9N$: C, 87.12; H, 5.06. Found C, 86.87; H, 5.09.

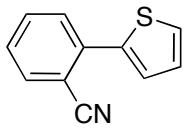

2-(2-Thiophenyl)benzonitrile (Table 3, entry 2).[23] Following general procedure A, 2-chlorobenzonitrile (138 mg, 1.00 mmol), tributyl(2-thiophenyl)stannane (349 μL, 1.10 mmol), pre-milled $Pd(OAc)_2$/XPhos (7.5 mg, 0.010 mmol) and CsF (334 mg, 2.20 mmol) were heated to 80 °C in DME with stirring for 4 h. The crude product was adsorbed on silica, loaded onto the top of a Biotage 25M column and purified by flash chromatography using a Biotage SP4 to provide the titled compound in 92% yield (171 mg) as a colorless oil. ^{1}H NMR (400 MHz, $CDCl_3$) δ 7.72 (dd, *J* = 8.0, 1.0 Hz, 1H), 7.62 (dd, *J* = 3.5, 1.0 Hz, 1H), 7.58 (m, 2H), 7.42 (dd, *J* = 5.0, 1.0 Hz, 1H), 7.37 (td, *J* = 8.0, 1.5 Hz, 1H), 7.14 (dd, *J* = 5.0, 3.5 Hz, 1H); ^{13}C NMR (100 MHz, $CDCl_3$) δ 139.6, 137.7, 134.5, 133.2, 129.9, 128.4, 127.8, 127.7, 127.5, 119.1, 110.1; IR (neat, cm^{-1}) 3107, 2224, 1595, 1482, 1444, 760, 702. Anal. Calc'd. for $C_{11}H_7NS$: C, 71.32; H, 3.81. Found C, 71.40; H, 3.59.

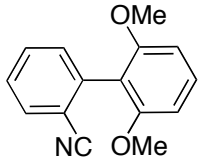

2',6'-Dimethoxybiphenyl-2-carbonitrile (Table 3, entry 3).[24] Following general procedure A, 2-chlorobenzonitrile (138 mg, 1.00 mmol), tributyl(2,6-dimethoxyphenyl)stannane (403 μL, 1.10 mmol), pre-milled $Pd(OAc)_2$/XPhos (7.5 mg, 0.010 mmol) and CsF (334 mg, 2.20 mmol) were heated to 80 °C in DME with stirring for 4 h. The crude product was adsorbed on silica, loaded onto the top of a Biotage

25M column and purified by flash chromatography using a Biotage SP4 to provide the titled compound in 76% yield (181 mg) as a white solid, mp 100-101 °C. ^{1}H NMR (400 MHz, $CDCl_3$) δ 7.71 (d, *J* = 7.5 Hz, 1H), 7.59 (td, *J* = 7.5, 1.5 Hz, 1H), 7.38 (m, 2H), 7.34 (t, *J* = 8.5 Hz, 1H), 6.66 (d, *J* = 8.5 Hz, 2H), 3.75 (s, 6H); ^{13}C NMR (100 MHz, $CDCl_3$) δ 157.7, 138.9, 132.7, 132.3, 132.1, 130.6, 127.3, 118.9, 115.7, 115.7, 114.6, 104.3, 56.0; IR (neat, cm^{-1}) 2940, 2838, 2225, 1590, 1473, 1250, 1108. Anal. Calc'd. for $C_{15}H_{13}NO_2$: C, 75.30; H, 5.48. Found C, 75.19; H, 5.32.

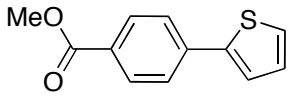

Methyl 4-(2-thiophenyl)benzoate (Table 3, entry 4).[25] Following general procedure A, methyl 4-chlorobenzoate (171 mg, 1.00 mmol), tributyl(2-thiophenyl)stannane (349 μL, 1.10 mmol), pre-milled $Pd(OAc)_2$/XPhos (7.5 mg, 0.010 mmol) and CsF (334 mg, 2.20 mmol) were heated to 80 °C in DME with stirring for 4 h. The crude product was adsorbed on silica, loaded onto the top of a Biotage 25M column and purified by flash chromatography using a Biotage SP4 to provide the titled compound in 89% yield (195 mg) as a white solid, mp 140-141 °C. ^{1}H NMR (400 MHz, $CDCl_3$) δ 8.02 (d, *J* = 8.5 Hz, 2H), 7.66 (d, *J* = 8.5 Hz, 2H), 7.41 (dd, *J* = 3.5, 1.0 Hz, 1H), 7.34 (dd, *J* = 5.0, 1.0 Hz, 1H), 7.10 (dd, *J* = 5.0, 3.5 Hz, 1H), 3.91 (s, 3H); ^{13}C NMR (100 MHz, $CDCl_3$) δ 166.9, 143.1, 138.7, 130.4, 128.8, 128.5, 126.4, 125.6, 124.6, 52.3; IR (neat, cm^{-1}) 1712, 1282, 1261, 1113, 769, 724, 698. Anal. Calc'd. for $C_{12}H_{10}O_2S$: C, 66.03; H, 4.62. Found C, 66.00; H, 4.67.

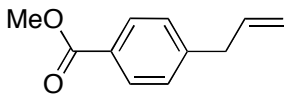

Methyl 4-allylbenzoate (Table 3, entry 5).[26] Following general procedure A, methyl 4-chlorobenzoate (171 mg, 1.00 mmol), allyltributylstannane (341 μL, 1.10 mmol), pre-milled $Pd(OAc)_2$/XPhos (7.5 mg, 0.010 mmol) and CsF (334 mg, 2.20 mmol) were heated to 80 °C in DME with stirring for 4 h. The crude product was adsorbed on silica, loaded onto the top of a Biotage 25M column and purified by flash chromatography using a Biotage SP4 to provide the titled compound in 86% yield (152 mg) as a colorless

oil. ^{1}H NMR (400 MHz, $CDCl_3$) δ 7.95 (d, *J* = 8.0 Hz, 1H), 7.24 (d, *J* = 8.0 Hz, 1H), 5.94 (ddt, *J* = 17.5, 9.0, 6.5 Hz, 1H), 5.09 (dd, *J* = 9.0, 1.0 Hz, 1H), 5.08 (dd, *J* = 17.6, 1.0 Hz, 1H), 3.88 (s, 3H), 3.42 (d, *J* = 6.5 Hz, 1H); ^{13}C NMR (100 MHz, $CDCl_3$) δ 167.3, 145.7, 136.6, 130.0, 128.8, 128.3, 116.8, 52.2, 40.4; IR (neat, cm^{-1}) 2952, 1723, 1611, 1435, 1280, 1178, 1109, 758, 707. Anal. Calc'd. for $C_{11}H_{12}O_2$: C, 74.98; H, 6.86. Found C, 75.11; H, 6.90.

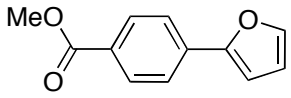

Methyl 4-(2-furanyl)benzoate (Table 3, entry 6).[27] Following general procedure A, methyl 4-chlorobenzoate (171 mg, 1.00 mmol), tributyl(2-furanyl)stannane (346 μL, 1.10 mmol), pre-milled $Pd(OAc)_2$/XPhos (7.5 mg, 0.010 mmol) and CsF (334 mg, 2.20 mmol) were heated to 80 °C in DME with stirring for 4 h. The crude product was adsorbed on silica, loaded onto the top of a Biotage 25M column and purified by flash chromatography using a Biotage SP4 to provide the titled compound in 97% yield (196 mg) as a white solid, mp 120-121 °C. ^{1}H NMR (400 MHz, $CDCl_3$) δ 8.03 (d, *J* = 8.5 Hz, 2H), 7.71 (d, *J* = 8.5 Hz, 2H), 7.50 (d, *J* = 1.5 Hz, 1H), 6.77 (d, *J* = 3.5 Hz, 1H), 6.49 (dd, *J* = 3.5, 1.5 Hz, 1H), 3.91 (s, 3H); ^{13}C NMR (100 MHz, $CDCl_3$) δ 166.9, 153.0, 143.2, 134.8, 130.2, 128.6, 123.5, 112.1, 107.4, 52.2; IR (neat, cm^{-1}) 1718, 1282, 1114, 772, 743, 701. Anal. Calc'd. for $C_{12}H_{10}O_3$: C, 71.28; H, 4.98. Found C, 71.09; H, 4.84.

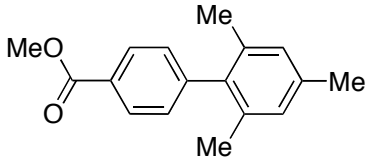

Methyl 2',4',6'-trimethylbiphenyl-4-carboxylate (Table 3, entry 7).[28] Following general procedure A, methyl 4-chlorobenzoate (171 mg, 1.00 mmol), tributyl(2,4,6-mesityl)stannane (401 μL, 1.10 mmol), pre-milled $Pd(OAc)_2$/XPhos (7.5 mg, 0.010 mmol) and CsF (334 mg, 2.20 mmol) were heated to 80 °C in DME with stirring for 4 h. The crude product was adsorbed on silica, loaded onto the top of a Biotage 25M column and purified by flash chromatography using a Biotage SP4 to provide the titled compound in

94% yield (238 mg) as a white solid, mp 125-126 °C. ^{1}H NMR (400 MHz, $CDCl_3$) δ 8.08 (d, *J* = 8.0 Hz, 2H), 7.21 (d, *J* = 8.0 Hz, 2H), 6.93 (s, 2H), 3.92 (s, 3H), 2.38 (s, 3H), 1.96 (s, 6H); ^{13}C NMR (100 MHz, $CDCl_3$) δ 167.3, 146.5, 138.2, 137.3, 135.7, 129.9, 129.7, 128.7, 128.4, 52.3, 21.2, 20.8; IR (neat, cm^{-1}) 2948, 1720, 1437, 1285, 1116, 1099, 858. Anal. Calc'd. for $C_{17}H_{18}O_2$: C, 80.28; H, 7.13. Found C, 80.02; H, 7.09.

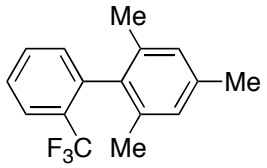

2,4,6-Trimethyl-2'-(trifluoromethyl)biphenyl (Table 3, entry 8). Following general procedure A, 2-chlorobenzotrifluoride (131 μL, 1.00 mmol), tributyl(2,4,6-mesityl)stannane (401 μL, 1.10 mmol), pre-milled $Pd(OAc)_2$/XPhos (15.0 mg, 0.020 mmol) and CsF (334 mg, 2.20 mmol) were heated to 80 °C in DME with stirring for 4 h. The crude product was adsorbed on silica, loaded onto the top of a Biotage 25M column and purified by flash chromatography using a Biotage SP4 to provide the titled compound in 59% yield (157 mg) as a colorless oil. ^{1}H NMR (400 MHz, $CDCl_3$) δ 7.77 (d, *J* = 7.5 Hz, 1H), 7.58 (t, *J* = 7.5 Hz, 1H), 7.46 (t, *J* = 7.5 Hz, 1H), 7.16 (d, *J* = 7.5 Hz, 1H), 6.92 (s, 2H), 2,33 (s, 3H), 1.90 (s, 6H); ^{13}C NMR (100 MHz, $CDCl_3$) δ 140.3, 137.3, 136.3, 136.0, 132.2, 131.7, 128.9, 127.9, 137.4, 126.5 (q, *J* = 5.0 Hz), 122.8, 21.3, 20.6; IR (neat, cm^{-1}) 3442, 2923, 1315, 1172, 1128, 1035, 763. Anal. Calc'd. for $C_{16}H_{15}F_3$: C, 72.71; H, 5.72. Found C, 72.56; H, 5.73.

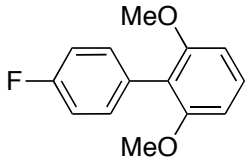

4'-Fluoro-2,6-dimethoxybiphenyl (Table 3, entry 9). Following general procedure A, 1-chloro-4-fluorobenzene (107 μL, 1.00 mmol), tributyl(2,6-dimethoxyphenyl)stannane (403 μL, 1.10 mmol), pre-milled $Pd(OAc)_2$/XPhos (15.0 mg, 0.020 mmol) and CsF (334 mg, 2.20 mmol) were heated to 80 °C in DME with stirring for 4 h. The crude product was adsorbed on silica, loaded onto the top of a Biotage

25M column and purified by flash chromatography using a Biotage SP4 to provide the titled compound in 93% yield (215 mg) as a white solid, mp 127-128 °C. ^{1}H NMR (400 MHz, $CDCl_3$) δ 7.28 (m, 3H), 7.07 (t, *J* = 8.5 Hz, 2H), 6.64 (d, *J* = 8.5 Hz, 2H), 3.72 (s, 6H); ^{13}C NMR (100 MHz, $CDCl_3$) δ 161.9 (d, *J* = 244 Hz), 157.8, 132.7 (d, *J* = 8 Hz), 130.0 (d, *J* = 3 Hz), 129.0, 118.5, 114.9 (d, *J* = 21 Hz), 104.3, 56.1; IR (neat, cm^{-1}) 2835, 1585, 1517, 1472, 1245, 1114, 830, 725, 711. Anal. Calc'd. for $C_{14}H_{13}FO_2$: C, 72.40; H, 5.64. Found C, 72.38; H, 5.65.

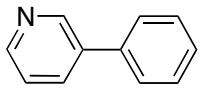

3-Phenylpyridine (Table 3, entry 10).[29] Modification to general procedure A, 3-chloropyridine (95 μL, 1.00 mmol), tributyl(phenyl)stannane (393 μL, 1.20 mmol), pre-milled $Pd(OAc)_2$:XPhos (1:3 ratio, 33.0 mg, 0.020 mmol) and CsF (334 mg, 2.20 mmol) were heated to 100 °C in 1,4-dioxane with stirring for 4 h. The crude product was purified by flash chromatography using a Biotage SP4 and 25M cartridge to provide the titled compound in 91% yield (141 mg) as a colorless oil. ^{1}H NMR (400 MHz, $CDCl_3$) δ 8.82 (d, J = 1.5 Hz, 1H), 8.55 (dd, J = 4.5, 1.5 Hz, 1H), 7.81 (dt, J = 7.5, 1.5 Hz, 1H), 7.53 (d, J = 7.5 Hz, 2H), 7.43 (t, J = 7.5 Hz, 2H), 7.36 (t, J = 7.5 Hz, 1H), 7.30 (dd, J = 7.5, 4.5 Hz, 1H); ^{13}C NMR (100 MHz, $CDCl_3$) δ 148.5, 148.4, 137.8, 136.6, 134.3, 129.1, 128.1, 127.2, 123.6; IR (neat, cm^{-1}) 3031, 1581, 1473, 1450, 1407, 1005, 754, 712.

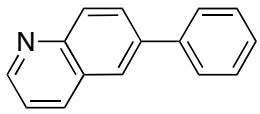

6-Phenylquinoline (Table 3, entry 11).[30] Modification to general procedure A, 6-chloroquinoline (164 mg, 1.00 mmol), tributyl(phenyl)stannane (393 μL, 1.20 mmol), pre-milled $Pd(OAc)_2$:XPhos (1:3 ratio, 33.0 mg, 0.020 mmol) and CsF (334 mg, 2.20 mmol) were heated to 100 °C in 1,4-dioxane with stirring for 4 h. The crude product was purified by flash chromatography using a Biotage SP4 and 25M cartridge to provide the titled compound in 96% yield (197 mg) as a white solid, mp 110-112 °C. ^{1}H NMR (400

MHz, $CDCl_3$) δ 8.87 (dd, J = 4.0, 1.5 Hz, 1H), 8.15 (d, J = 8.5 Hz, 1H), 8.08 (d, J = 8.5 Hz, 1H), 7.92 (m, 2H), 7.65 (d, J = 7.5 Hz, 2H), 7.44 (t, J = 7.5 Hz, 2H), 7.34 (m, 2H); ^{13}C NMR (100 MHz, $CDCl_3$) δ 150.4, 147.7, 140.2, 139.2, 136.2, 129.9, 129.2, 129.0, 128.4, 127.8, 127.5, 125.5, 121.5; IR (neat, cm^{-1}) 3060, 1576, 1460, 1352, 1326, 1122, 891, 844, 784, 765, 700.

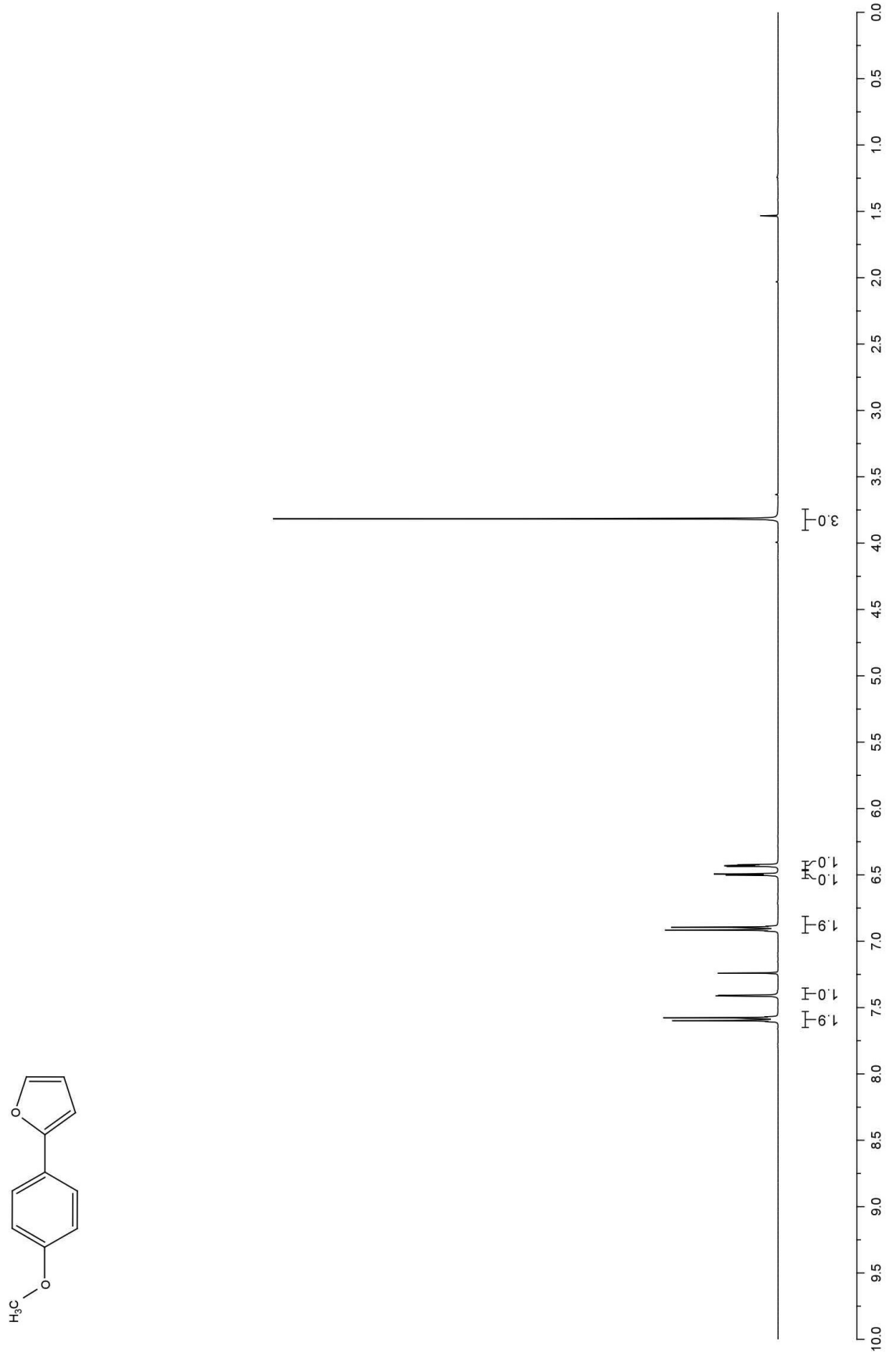
3.0
1.0
1.0
1.9
1.0
1.9
0.0
0.5
1.0
1.5
2.0
2.5
3.0
3.5
4.0
4.5
5.0
5.5
6.0
6.5
7.0
7.5
8.0
8.5
9.0
9.5
10.0
O
O
H3C

159.1
154.2
141.6
125.4
124.2
114.3
111.7
103.5
77.5
77.2
76.9
55.5
O
O
H3C

6.2
3.0
3.0
2.0
4.0
0.0
0.5
1.0
1.5
2.0
2.5
3.0
3.5
4.0
4.5
5.0
5.5
6.0
6.5
7.0
7.5
8.0
8.5
9.0
9.5
10.0
CH3
H3C
H3C
O
H3C

158.3
138.8
136.6
133.4
130.5
128.2
113.9
77.5
77.2
76.9
55.3
21.2
21.0
CH3
H3C
H3C
O
H3C

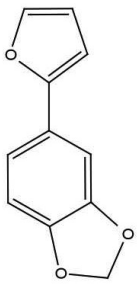

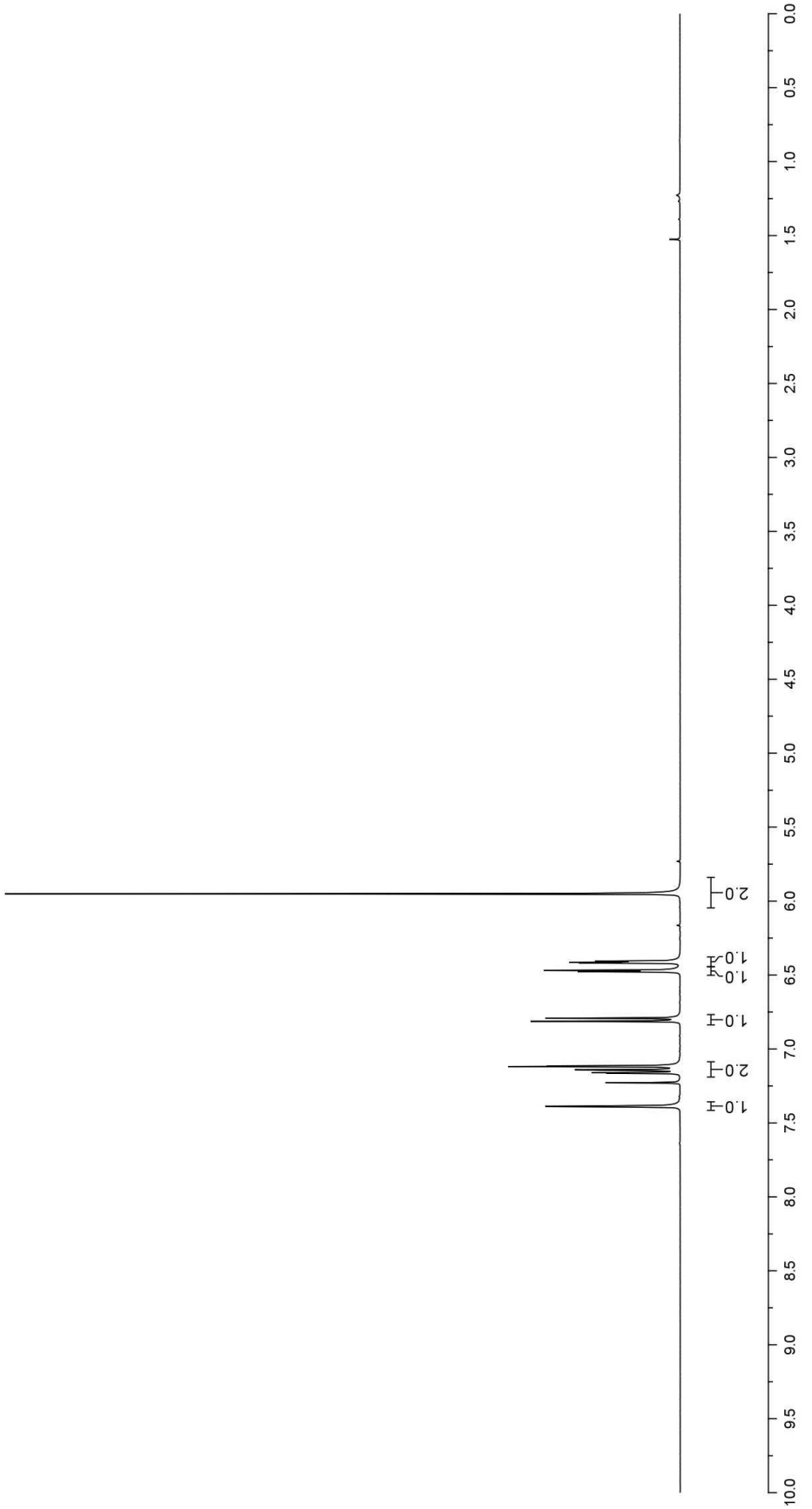
2.0
1.0
1.0
1.0
2.0
1.0
0.0
0.5
1.0
1.5
2.0
2.5
3.0
3.5
4.0
4.5
5.0
5.5
6.0
6.5
7.0
7.5
8.0
8.5
9.0
9.5
10.0

153.9
148.1
147.1
141.6
125.5
117.7
111.7
108.7
104.7
104.0
101.2
77.6
77.2
76.9
-10
0
10
20
30
40
50
60
70
80
90
100
110
120
130
140
150
160
170
180
190
200
210

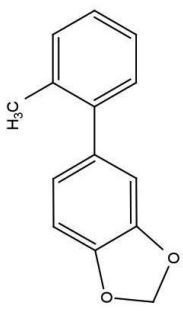
H3C
O
O

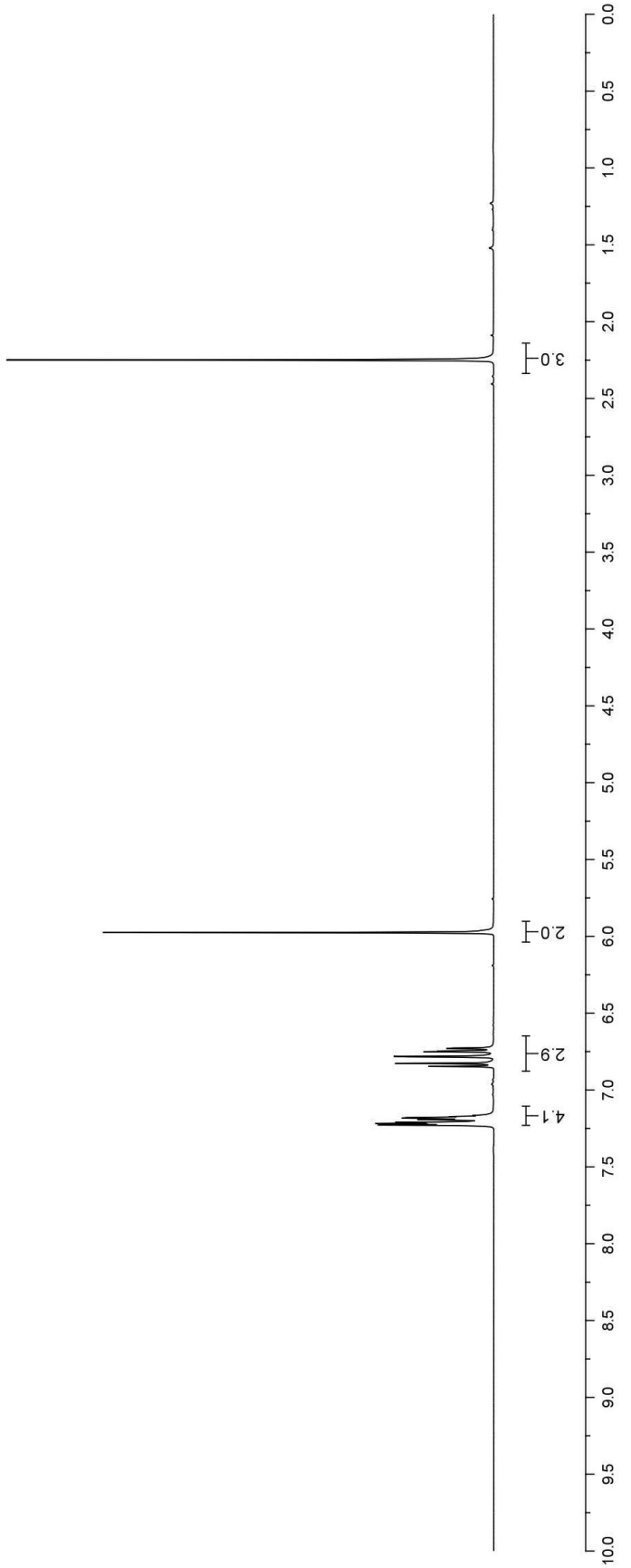
3.0
2.0
2.9
4.1
0.0
0.5
1.0
1.5
2.0
2.5
3.0
3.5
4.0
4.5
5.0
5.5
6.0
6.5
7.0
7.5
8.0
8.5
9.0
9.5
10.0

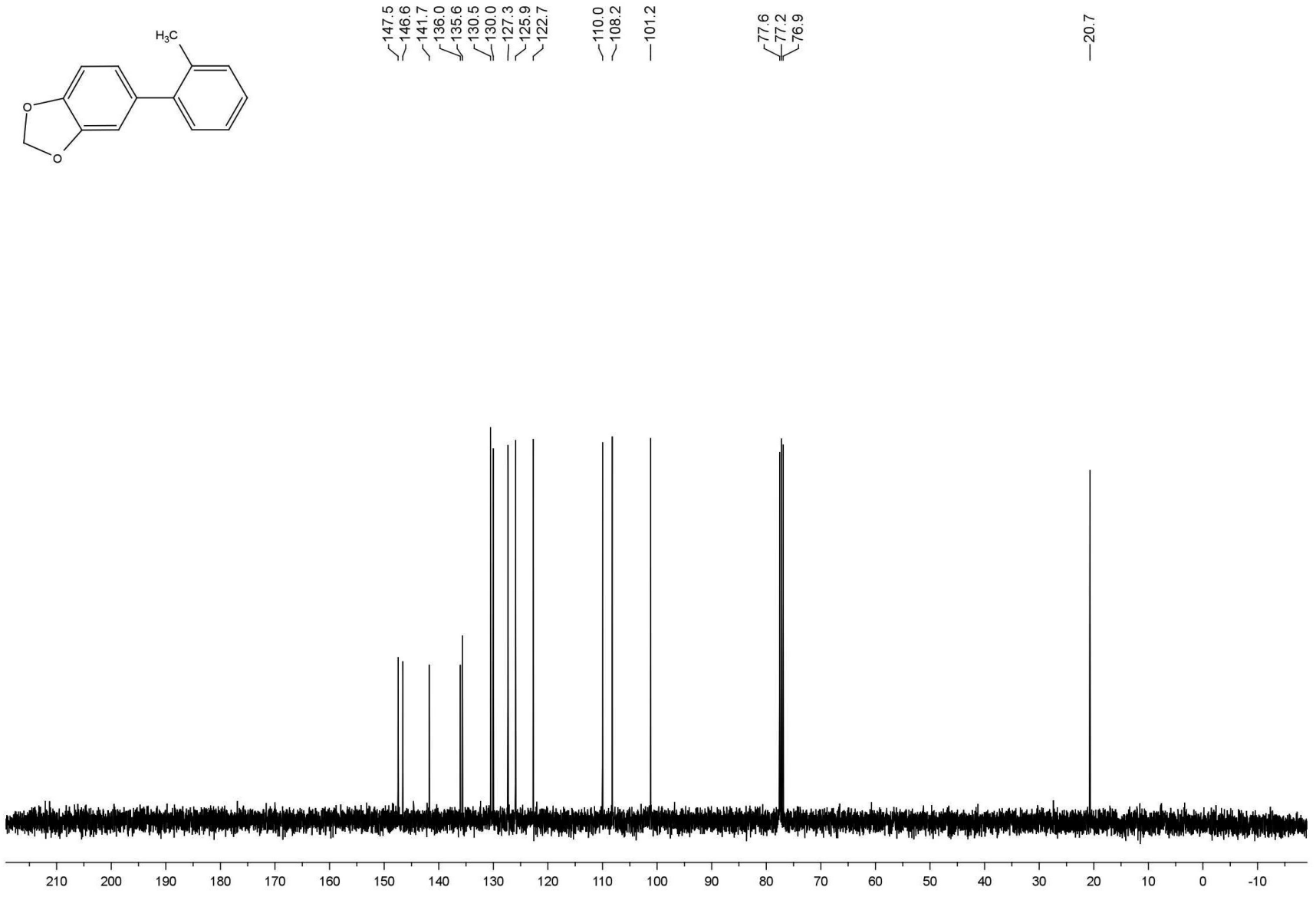
H3C
O
O
147.5
146.6
141.7
136.0
135.6
130.5
130.0
127.3
125.9
122.7
110.0
108.2
101.2
77.6
77.2
76.9
20.7
210
200
190
180
170
160
150
140
130
120
110
100
90
80
70
60
50
40
30
20
10
0
-10

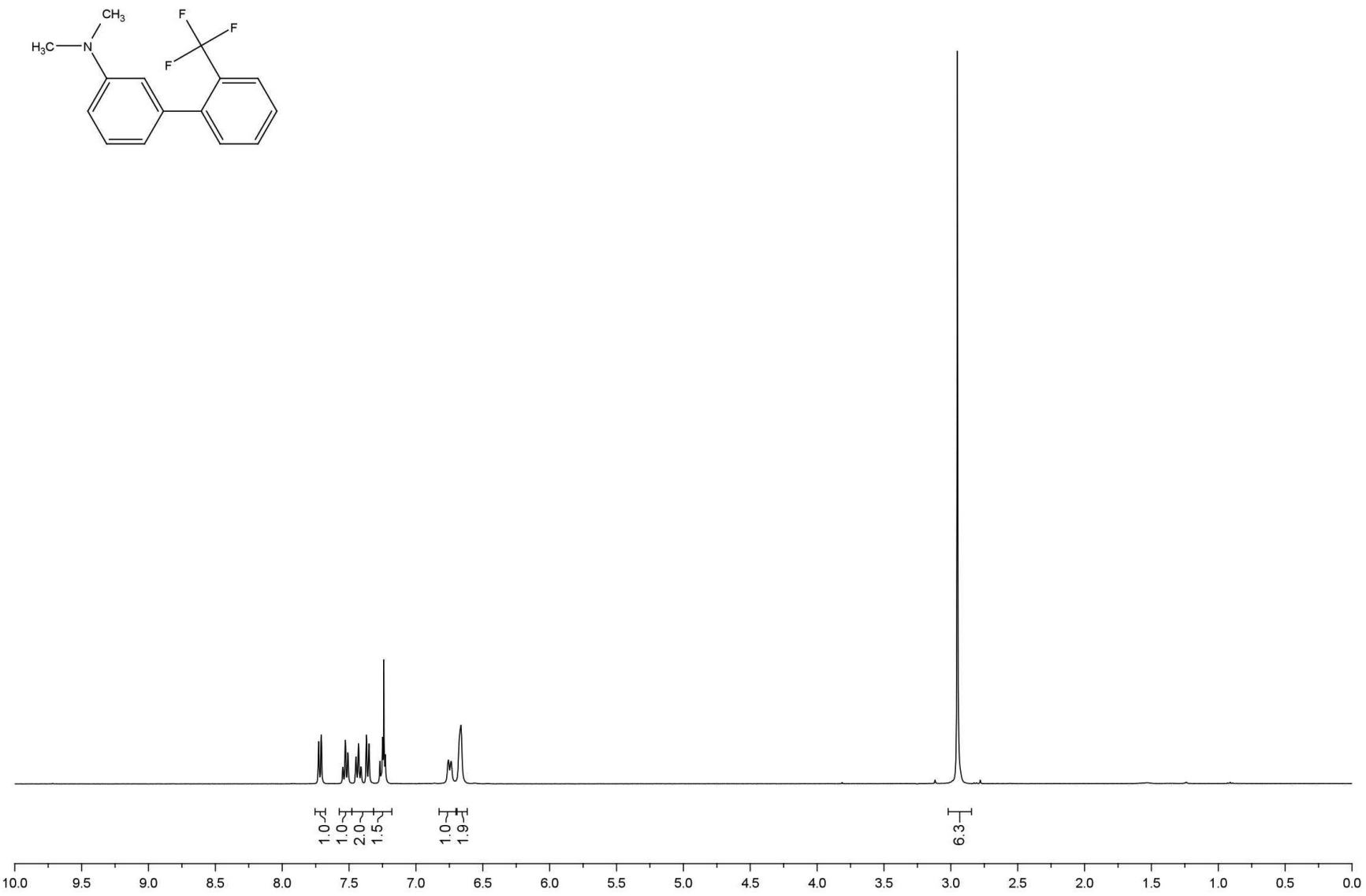
CH3
H3C
N
F
F
F
1.0
1.0
2.0
1.5
1.0
1.9
6.3
10.0
9.5
9.0
8.5
8.0
7.5
7.0
6.5
6.0
5.5
5.0
4.5
4.0
3.5
3.0
2.5
2.0
1.5
1.0
0.5
0.0

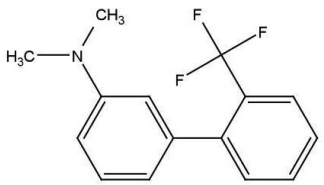

150.0
142.5
140.8
132.2
131.4
129.0
128.7
128.6
128.4
128.1
127.3
126.2
126.2
126.1
126.1
125.8
123.1
120.4
117.6
113.6
111.9
77.6
77.2
76.9
40.7

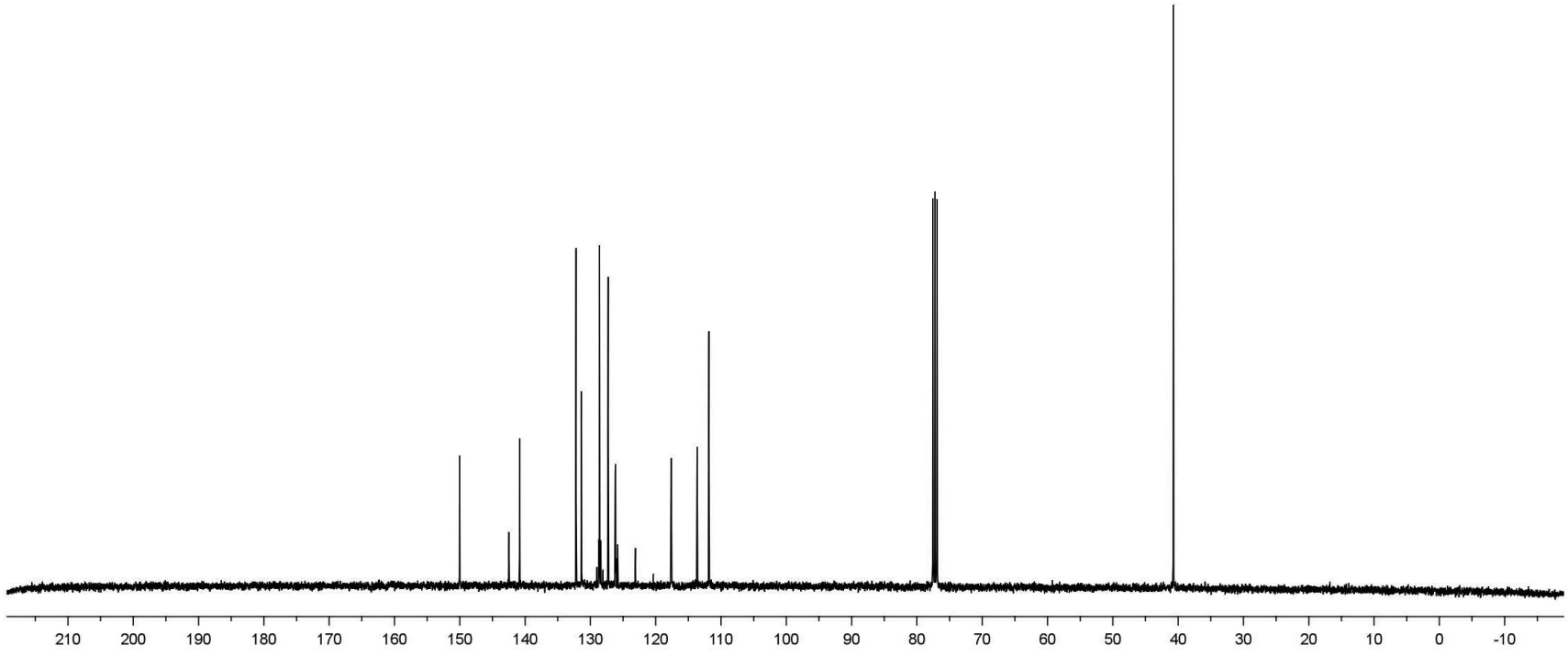

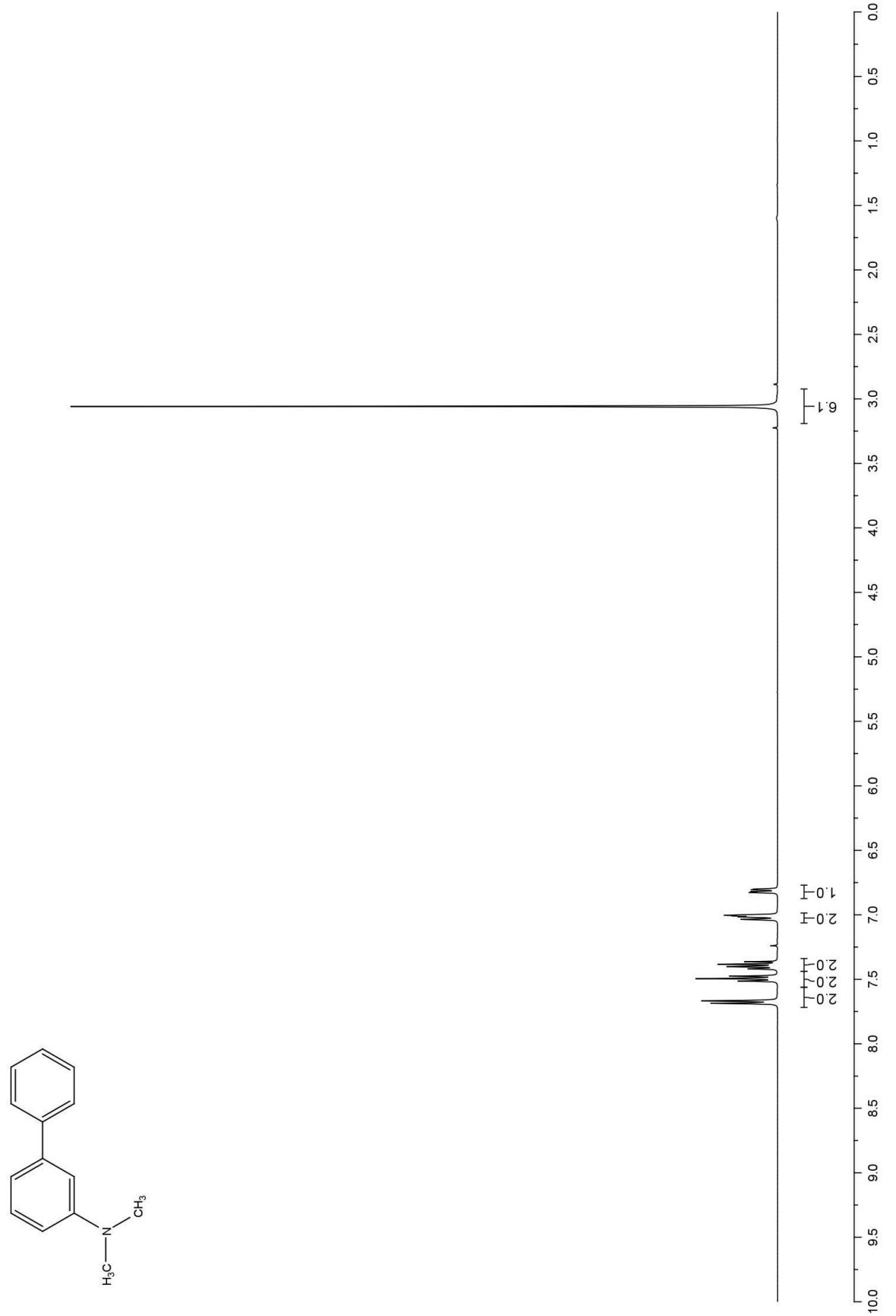
N
CH3
H3C
6.1
1.0
2.0
2.0
2.0
2.0
0.0
0.5
1.0
1.5
2.0
2.5
3.0
3.5
4.0
4.5
5.0
5.5
6.0
6.5
7.0
7.5
8.0
8.5
9.0
9.5
10.0

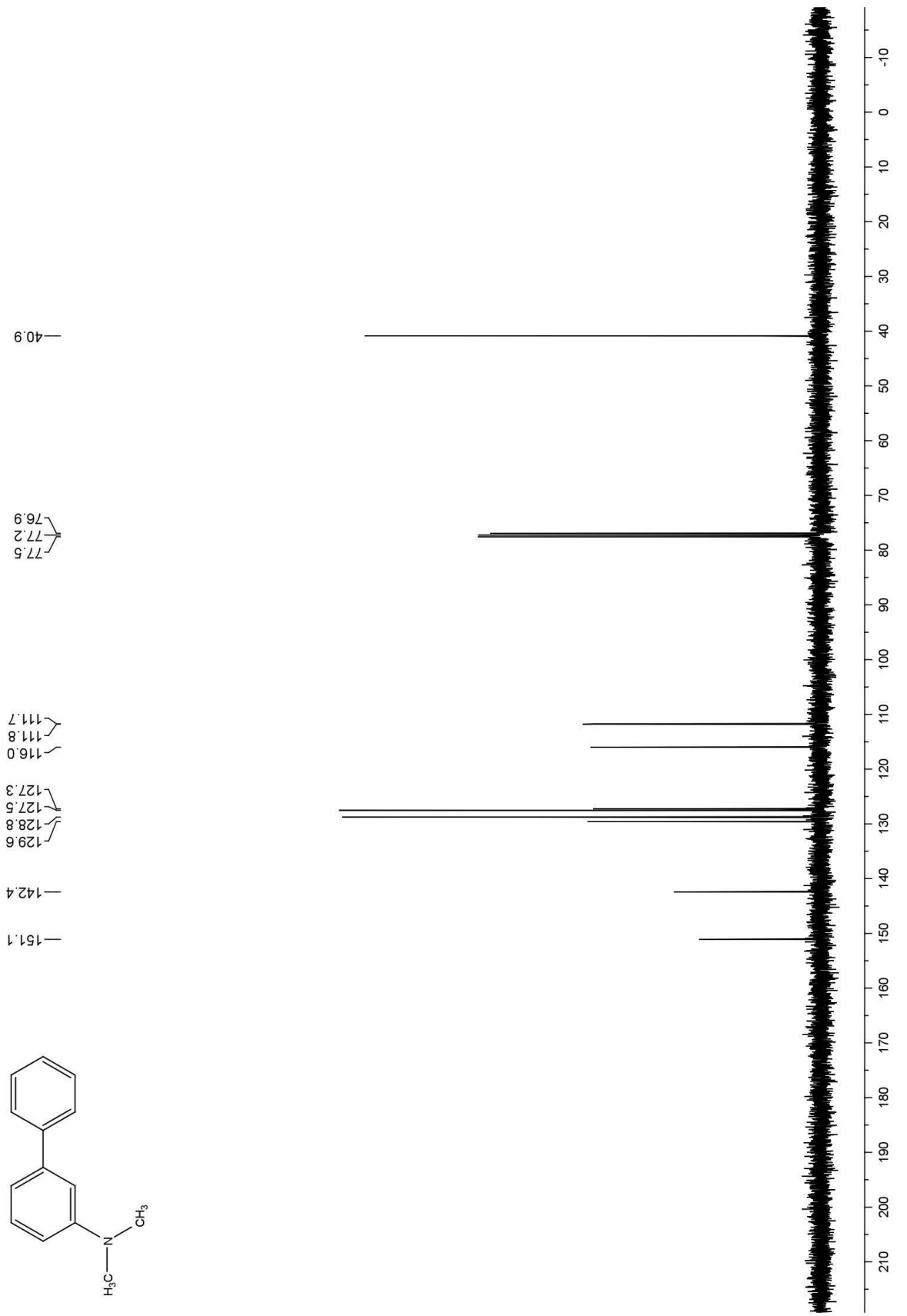
151.1
142.4
129.6
128.8
127.5
127.3
116.0
111.8
111.7
77.5
77.2
76.9
40.9
N
CH3
H3C

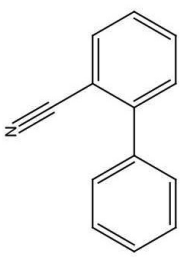

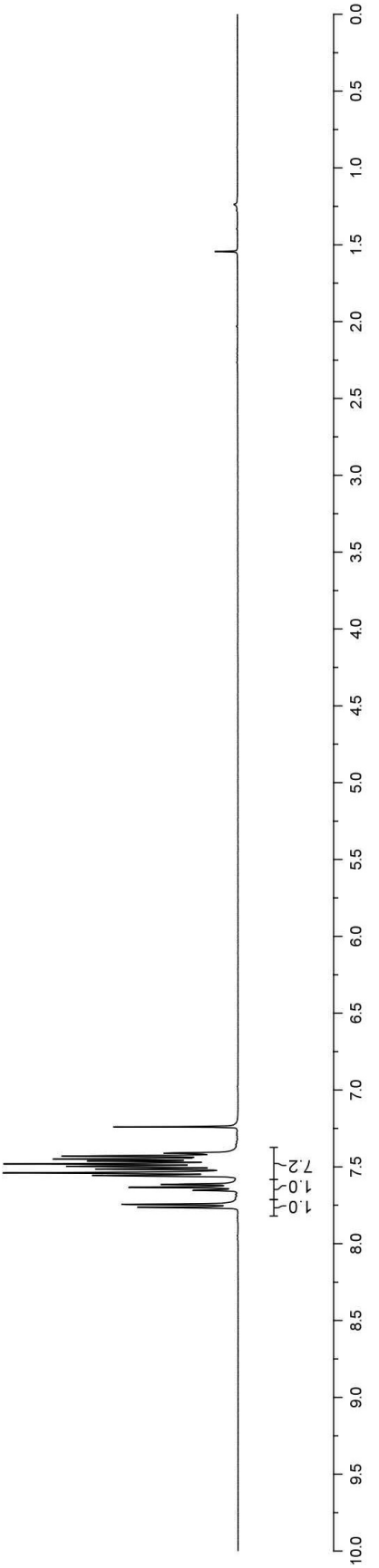
7.2
1.0
1.0
0.0
0.5
1.0
1.5
2.0
2.5
3.0
3.5
4.0
4.5
5.0
5.5
6.0
6.5
7.0
7.5
8.0
8.5
9.0
9.5
10.0

145.6
138.2
133.9
133.0
130.2
128.9
128.9
128.8
127.7
118.9
111.3
77.5
77.2
76.9
N
0
10
20
30
40
50
60
70
80
90
100
110
120
130
140
150
160
170
180
190
200
210

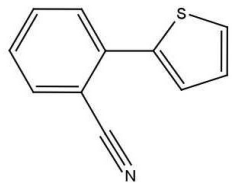
S
N

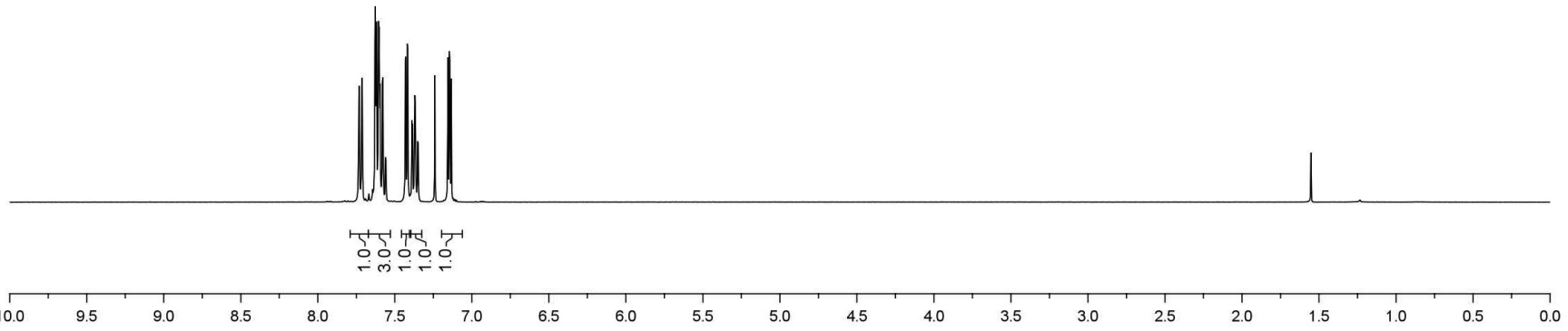
1.0
3.0
1.0
1.0
1.0
10.0
9.5
9.0
8.5
8.0
7.5
7.0
6.5
6.0
5.5
5.0
4.5
4.0
3.5
3.0
2.5
2.0
1.5
1.0
0.5
0.0

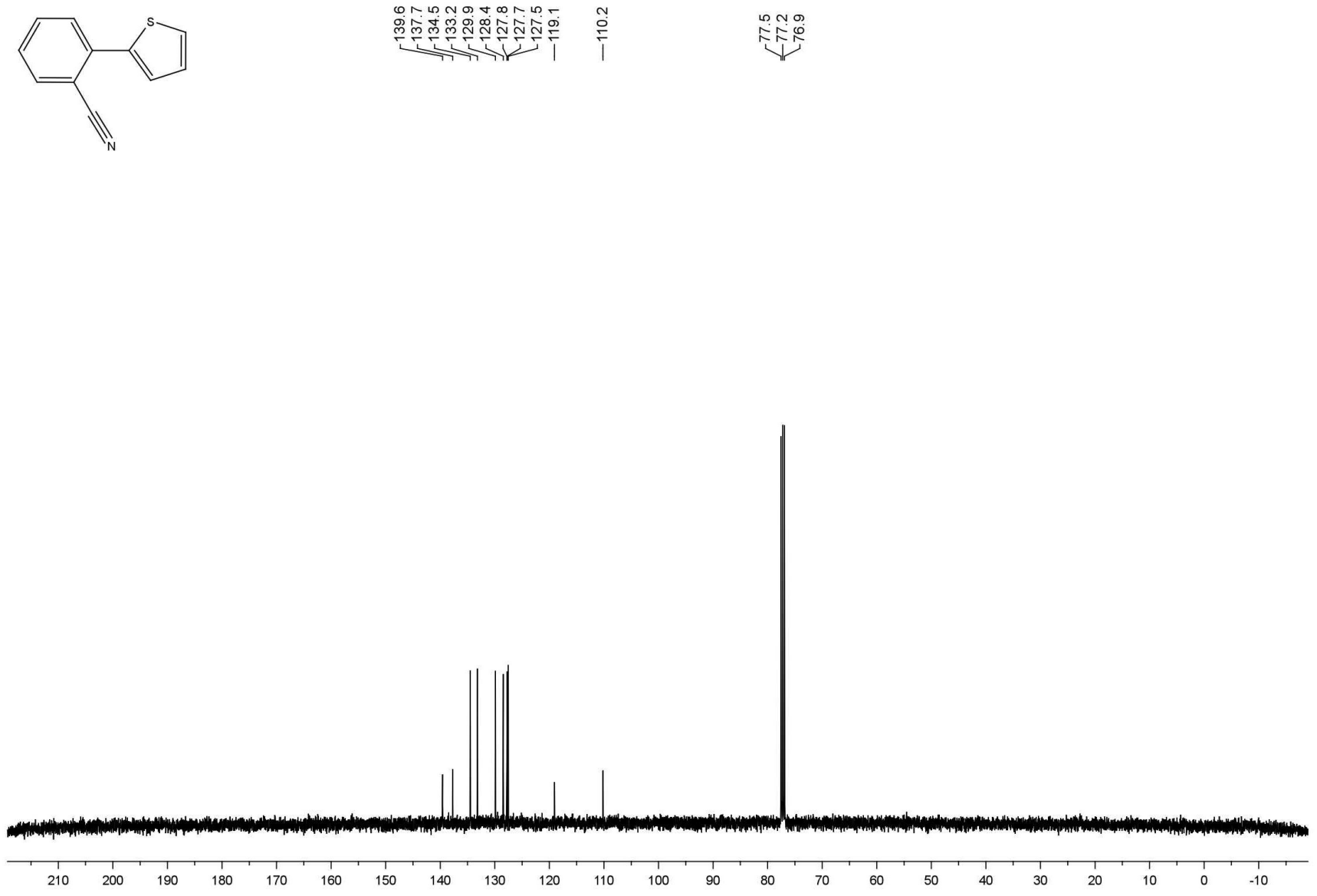
S
N
139.6
137.7
134.5
133.2
129.9
128.4
127.8
127.7
127.5
119.1
110.2
77.5
77.2
76.9
210
200
190
180
170
160
150
140
130
120
110
100
90
80
70
60
50
40
30
20
10
0
-10

6.3
2.0
3.1
1.0
1.0
0.0
0.5
1.0
1.5
2.0
2.5
3.0
3.5
4.0
4.5
5.0
5.5
6.0
6.5
7.0
7.5
8.0
8.5
9.0
9.5
10.0
N
O
H3C
O
CH3

56.0
76.9
77.2
77.5
104.3
114.6
115.7
118.9
127.3
130.6
132.1
132.3
132.7
138.9
157.7
N
O
O
CH3
H3C

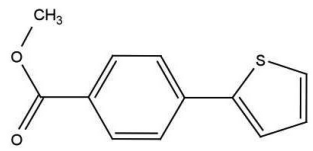
CH3
O
O
S

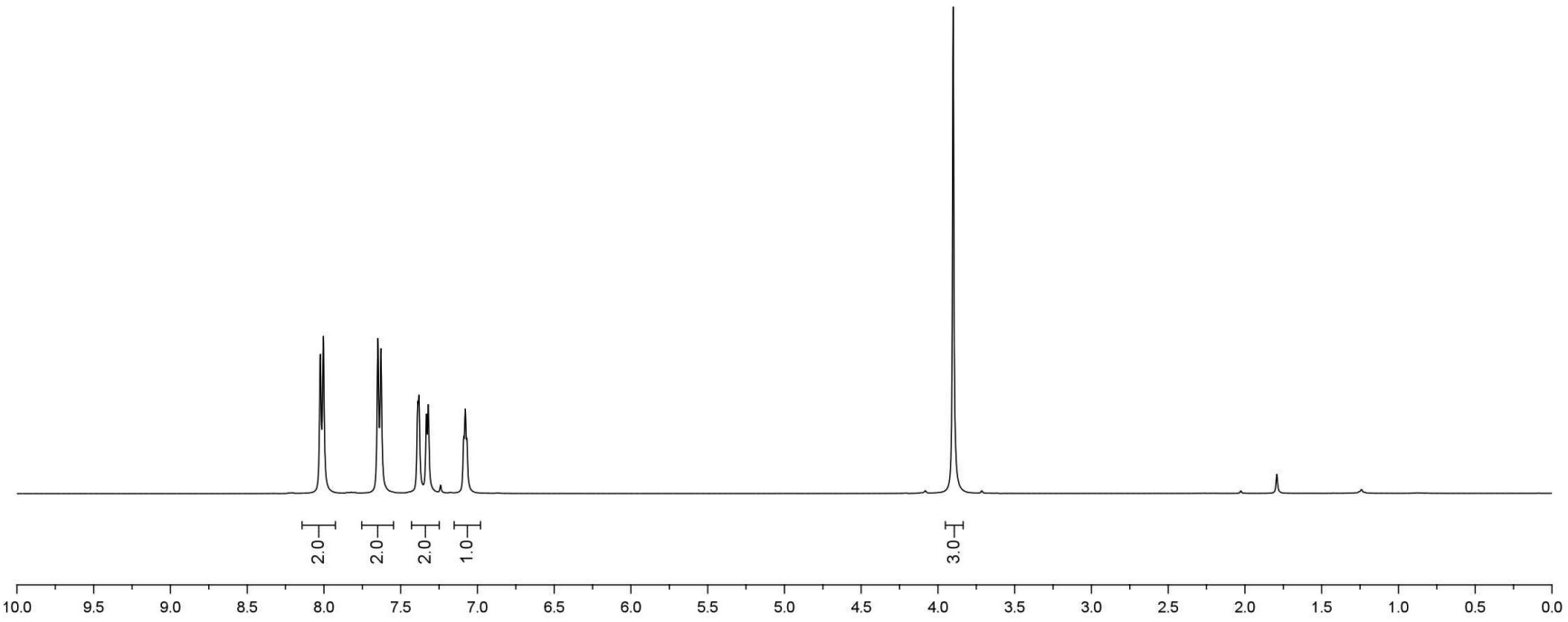
2.0
2.0
2.0
1.0
3.0
10.0
9.5
9.0
8.5
8.0
7.5
7.0
6.5
6.0
5.5
5.0
4.5
4.0
3.5
3.0
2.5
2.0
1.5
1.0
0.5
0.0

166.9
143.1
138.7
130.4
128.8
128.5
126.4
125.6
124.6
77.5
77.2
76.9
52.3
S
O
O
CH3

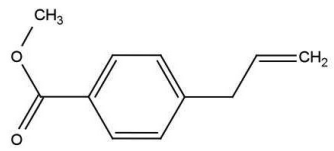
CH3
O
O
CH2

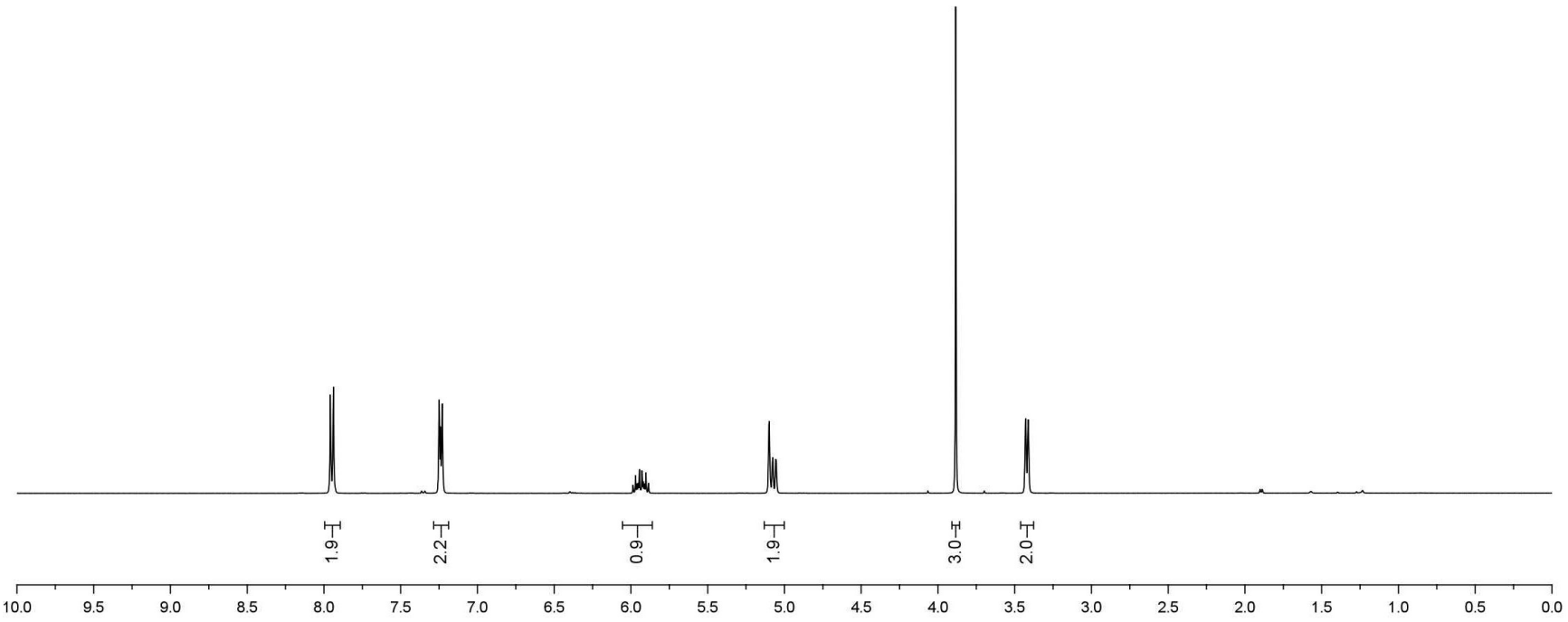
1.9
2.2
0.9
1.9
3.0
2.0
10.0
9.5
9.0
8.5
8.0
7.5
7.0
6.5
6.0
5.5
5.0
4.5
4.0
3.5
3.0
2.5
2.0
1.5
1.0
0.5
0.0

167.1
145.5
136.4
129.8
128.6
128.1
116.6
77.4
77.1
76.7
52.0
40.2
CH3
O
O
O
CH2
210
200
190
180
170
160
150
140
130
120
110
100
90
80
70
60
50
40
30
20
10
0
-10

3.0
0.9
1.0
0.9
2.0
2.0
0.0
0.5
1.0
1.5
2.0
2.5
3.0
3.5
4.0
4.5
5.0
5.5
6.0
6.5
7.0
7.5
8.0
8.5
9.0
9.5
10.0
O
O
O
CH3

166.9
153.0
143.2
134.8
130.2
128.6
123.5
112.1
107.4
77.5
77.2
76.9
52.2
CH3
O
O
O

CH3
H3C
H3C
CH3
O
O

6.1
3.0
3.1
2.0
2.0
2.0
0.0
0.5
1.0
1.5
2.0
2.5
3.0
3.5
4.0
4.5
5.0
5.5
6.0
6.5
7.0
7.5
8.0
8.5
9.0
9.5
10.0

167.3
146.5
138.2
137.3
135.7
129.9
129.7
128.7
128.4
77.5
77.2
76.9
52.3
21.2
20.8
CH3
H3C
H3C
O
O
CH3
210
200
190
180
170
160
150
140
130
120
110
100
90
80
70
60
50
40
30
20
10
0
-10

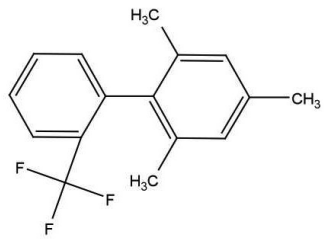
H3C
CH3
H3C
F
F
F

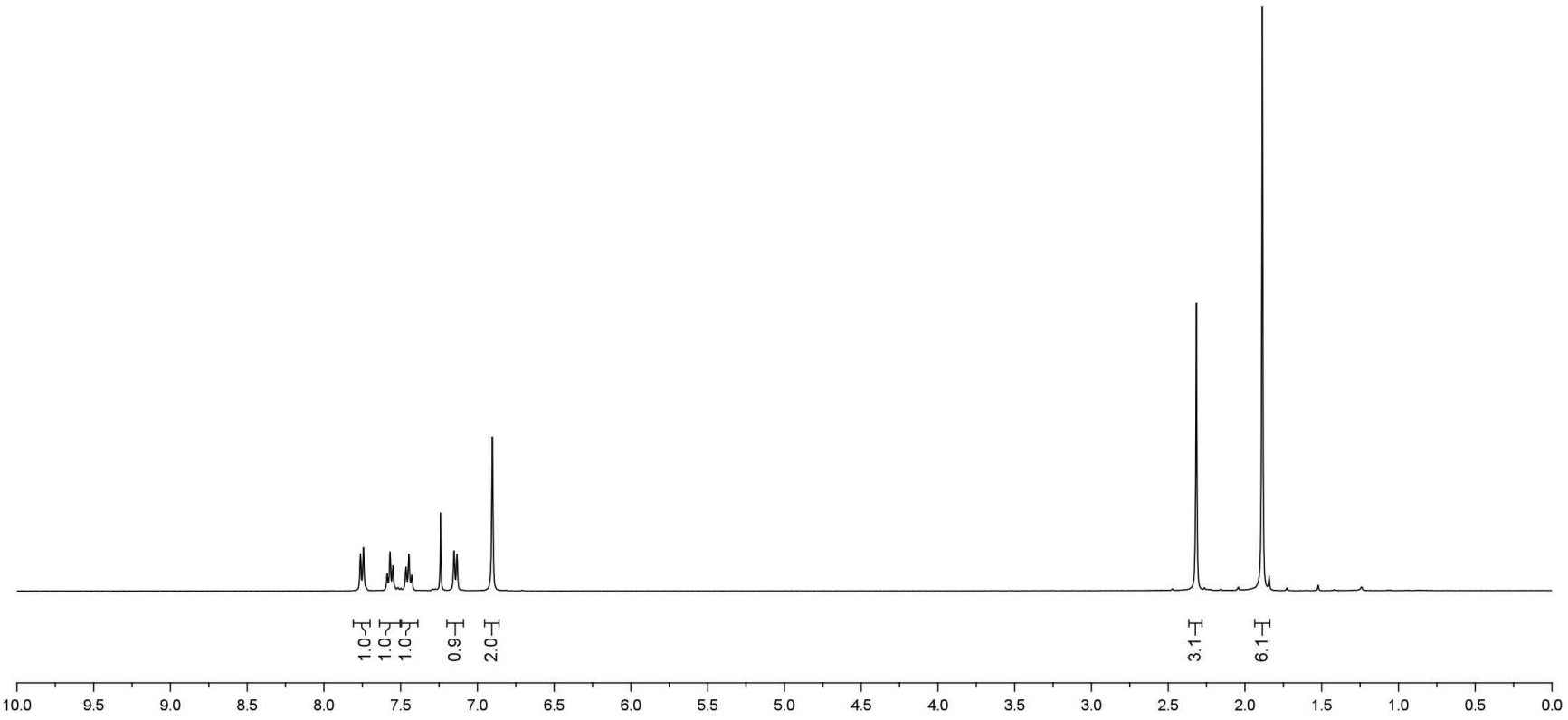
1.0
1.0
1.0
0.9
2.0
3.1
6.1
10.0
9.5
9.0
8.5
8.0
7.5
7.0
6.5
6.0
5.5
5.0
4.5
4.0
3.5
3.0
2.5
2.0
1.5
1.0
0.5
0.0

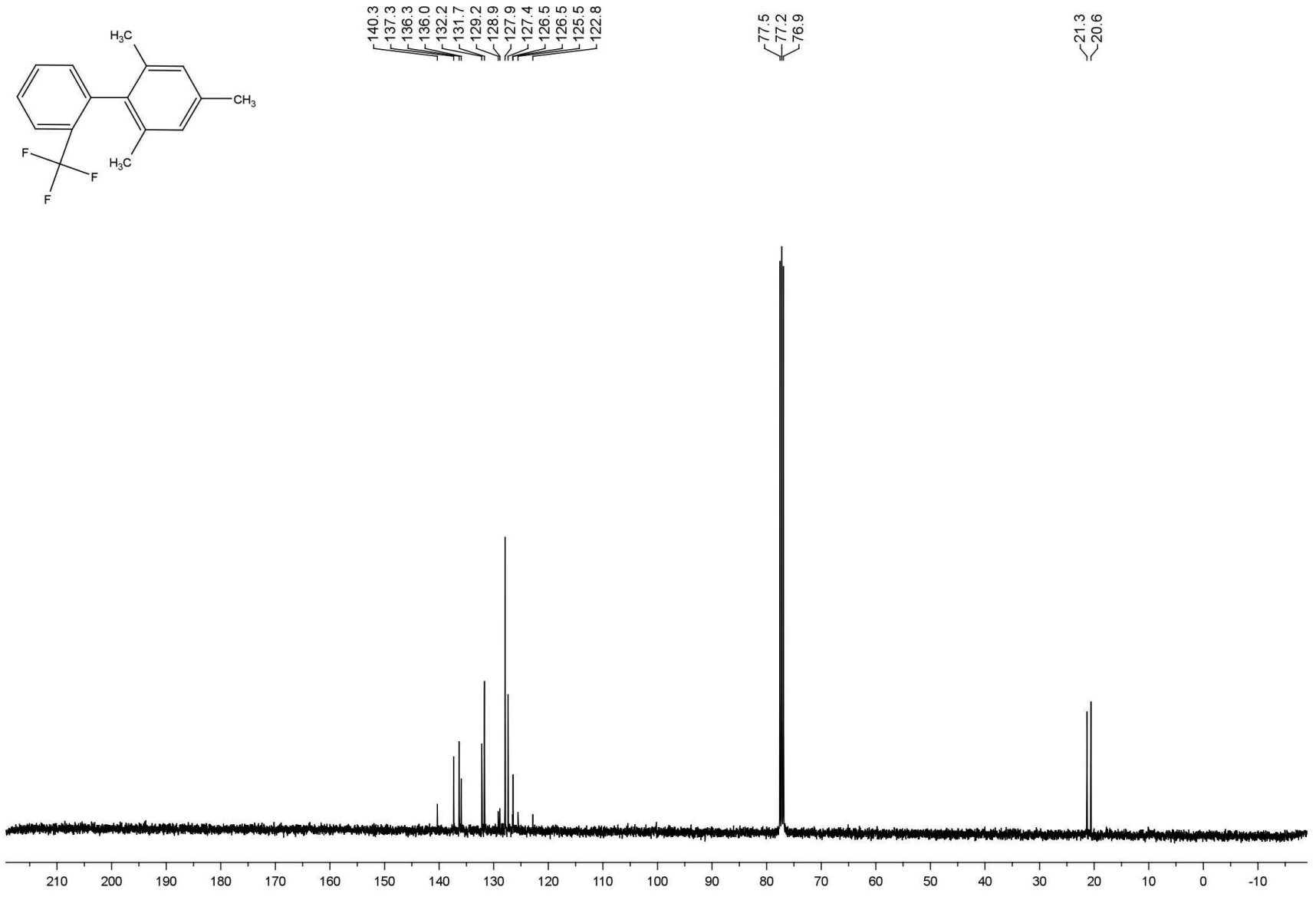
H3C
CH3
H3C
F
F
F
140.3
137.3
136.3
136.0
132.2
131.7
129.2
128.9
127.9
127.4
126.5
126.5
125.5
122.8
77.5
77.2
76.9
21.3
20.6
210
200
190
180
170
160
150
140
130
120
110
100
90
80
70
60
50
40
30
20
10
0
-10

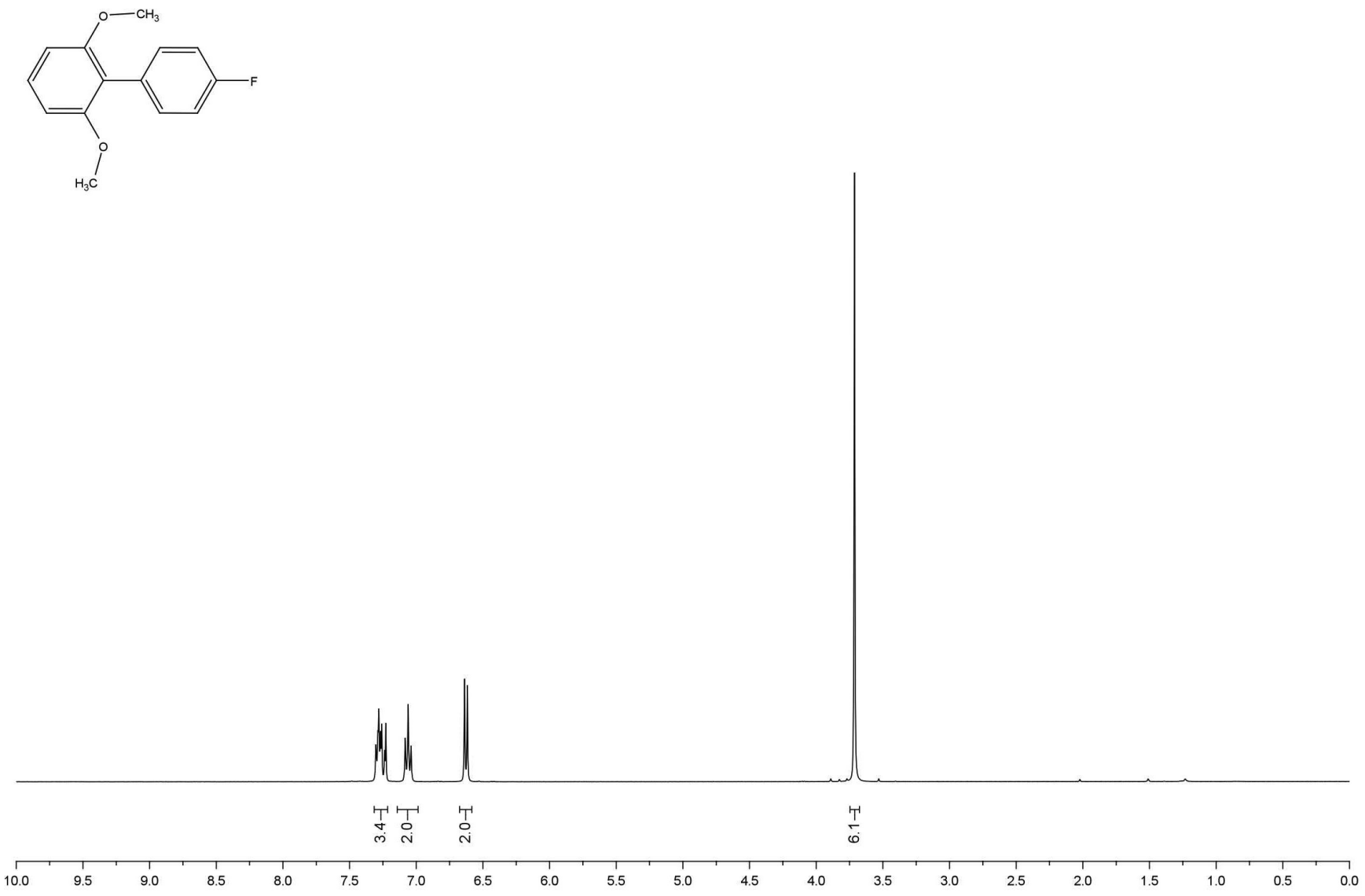
O
CH3
F
O
H3C
3.4
2.0
2.0
6.1
10.0
9.5
9.0
8.5
8.0
7.5
7.0
6.5
6.0
5.5
5.0
4.5
4.0
3.5
3.0
2.5
2.0
1.5
1.0
0.5
0.0

56.0
76.9
77.2
77.5
104.3
114.7
114.9
118.5
129.0
130.0
132.7
132.7
157.8
160.7
163.1
F
O
CH3
O
H3C

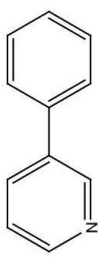

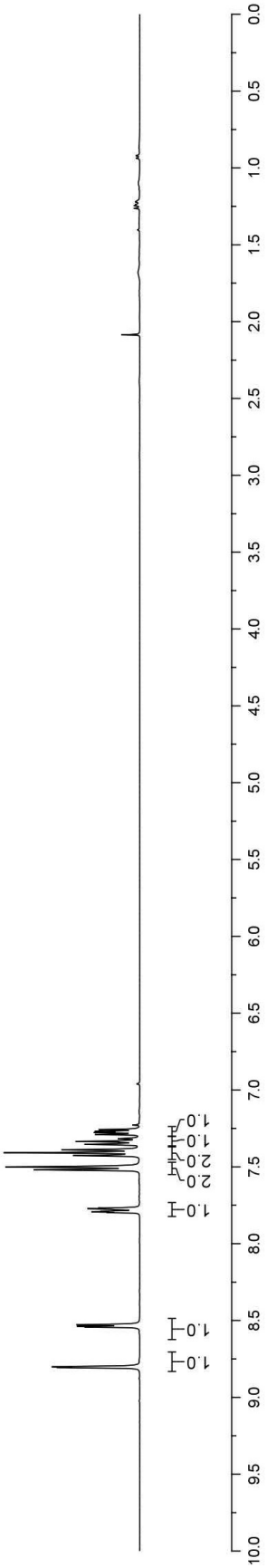
1.0
1.0
1.0
1.0
2.0
1.0
0.0
0.5
1.0
1.5
2.0
2.5
3.0
3.5
4.0
4.5
5.0
5.5
6.0
6.5
7.0
7.5
8.0
8.5
9.0
9.5
10.0

148.5
148.3
137.8
136.6
134.3
129.1
128.1
127.1
123.5
77.5
77.2
76.9
N
210
200
190
180
170
160
150
140
130
120
110
100
90
80
70
60
50
40
30
20
10
0
-10

1.0
1.0
2.0
2.0
2.0
2.7
10.0
9.5
9.0
8.5
8.0
7.5
7.0
6.5
6.0
5.5
5.0
4.5
4.0
3.5
3.0
2.5
2.0
1.5
1.0
0.5
0.0

150.4
147.6
140.2
139.2
136.2
129.9
129.2
129.0
128.4
127.8
127.4
125.5
121.5
77.5
77.2
76.9
N

1.5 References

1. For reviews of the Stille reaction see: a) J. K. Stille, *Pure Appl. Chem.* **1985**, *57*, 1771-1780; b) M. Pereyre, J. P. Quintard, A. Rahm, *Tin in Organic Synthesis*; Butterworth: London, **1987**, pp. 185-210; c) V. Farina, V. Krishnamurthy, W. J. Scott, *Org. React.* **1997**, *50*, 1-652; d) V. Farina, V. Krishnamurthy, W. J. Scott, *The Stille Reaction*, John Wiley & Sons, New York, NY, **1998**, pp. 1-652; e) J. Hassa, M. Svignon, C. Gozzi, E. Schulz, M. Lemaire, *Chem. Rev.* **2002**, *102*, 1359-1470; f) A. F. Littke, G. C. Fu, *Angew. Chem. Int. Ed.* **2002**, *41*, 4176-4211; g) T. N. Mitchell, in *Metal-catalyzed Cross-coupling Reactions*, 2nd Edition (Eds.: A. de Meijere and F. Diederich), Wiley-VCH, Weinheim, **2004**, pp. 125; h) P. Espinet, A. M. Echavarren, *Angew. Chem. Int. Ed.* **2004**, *36*, 4704-4734.

2. a) P. Manitto, *Biosynthesis of Natural Products*, Ellis Horwood, Chichester, **1981**, pp. 365-429; b) M. Gill, in *The Chemistry of Natural Products,* 2nd Edition (Ed.: R. H. Thomson), Blackie Academic & Professional, Glasgow, **1993**, pp. 60-105; h) G. B. Smith, G. C. Dezeny, D. L. Hughes, A. O. King, T. R. Verhoeven, *J. Org. Chem.* **1994**, *59*, 8151-8156; c) R. S. Coleman, M. L. Madaras, in *The Chemical Synthesis of Natural Products*, (Ed.: K. J. Hale), Sheffield Academic Press, Sheffield, **2000**, pp. 144-179; d) G. Bringmann, D. Menche, *Acc. Chem. Res.* **2001**, *8*, 615-624; e) S. Kotha, K. Lahiri, D. Kashinath, *Tetrahedron* **2002**, *58*, 9633-9695; f) G. Bringmann, Y. Reichert, V. V. Kane, *Tetrahedron* **2004**, *60*, 3539-3574; g) T. W. Wallace, *Org. Biomol. Chem.* **2006**, *4*, 3197-3210; h) T. C. Roberts, P. A. Smith, R. T. Cirz, R. E. Romesberg, *J. Am. Chem. Soc.* **2007**, *129*, 15830-15838.

3. a) O. Navarro, R. A. Kelly, S. P. Nolan, *J. Am. Chem. Soc.* **2003**, *125*, 16194-16195; b) S. D. Walker, T. E. Barder, J. R. Martinelli, S. L. Buchwald, *Angew. Chem. Int. Ed.* **2004**, *43*, 1871-1876; c) T. E. Barder, S. D. Walker, J. R. Martinelli, S. L. Buchwald, *J. Am. Chem. Soc.* **2005**, *127*, 4685-4696; d) N. Marion, O. Navarro, J. Mei, E. D. Stevens, N. M. Scott, S. P. Nolan, *J. Am. Chem. Soc.* **2006**, *128*, 4101-4111.

4. a) A. F. Littke, G. C. Fu, *Angew. Chem. Int. Ed.* **1999**, *38*, 2411-2413; b) G. A. Grasa, S. P. Nolan, *Org. Lett.* **2001**, *3*, 119-122; c) A. F. Littke, G. C. Fu, *J. Am. Chem. Soc.* **2002**, *124*, 6343-6348; d) R. B. Bedford, S. L. Hazelwood, *Chem. Commun.* **2002**, 2608-2609; e) R. B. Bedford, S. L. Hazelwood, M. E. Limmert, D. A. Albisson, S. M. Draper, P. N. Scully, S. J. Coles, M. B. Hursthouse, *Chem.—Eur. J.* **2003**, *9*, 3216-3227; f) S. P. H. Mee, V. Lee, J. E. Baldwin, *Angew. Chem. Int. Ed.* **2004**, *43*, 1132-1136; g) W. Su, S. Urgaonkar, J. G. Verkade, *Org. Lett.* **2004**, *6*, 1421-1424; h) W. Su, S. Urgaonkar, P. A. McLaughlin, J. G. Verkade, *J. Am. Chem. Soc.* **2004**, *126*, 16433-16439; i) V. Calo, A. Nacci, A. Monopoli, F. Montigelli, *J. Org. Chem.* **2005**, *70*, 6040-6044; j) M. L. Kantam, S. Roy, M. Roy, B. Sreedhar, B. M. Choudary, *Adv. Synth. Cat.* **2005**, *347*, 2002-2008; k) S. P. H. Mee, V. Lee, J. E. Baldwin, *Chem. – Eur. J.* **2005**, *11*, 3294-3308.

5. For a selection of recent applications of the Stille reaction in drug discovery, see: a) D. Amans, V. Bellosta, J. Cossy, *Org. Lett.* **2007**, *9*, 4761-4764; b) M. D. Cullen, B. L. Deng, T. L. Hartman, K. M. Watson, R. W. Buckheit, C. Pannecouque, E. DeClercq, M. Cushman, *J. Med. Chem.* **2007**, *50*, 4854-4867; c) V. Uchil, B. Seo, V. Nair, *J. Org. Chem.* **2007**, *72*, 8577-8579.

6. For a selection of recent applications of the Stille reaction in natural product synthesis, see: a) S. Lopez, J. Montenegro, C. Saa, *J. Org. Chem.* **2007**, *72*, 9572-9581; b) D. Schweitzer, J. J. Kane, D. Strand, P. McHenry, M. Tenniswood, P. Helquist, *Org. Lett.* **2007**, *9*, 4619-4622; c) V. Sofiyev, G. Navarro, D. Trauner, *Org. Lett.* **2008**, *10*, 149-152.

7. For a selection of recent applications of biaryl monophosphine ligands see: a) J. E. Milne, S. L. Buchwald, *J. Am. Chem. Soc.* **2004**, *126*, 13028-13032; b) T. E. Barder, S. L. Buchwald, *J. Am. Chem. Soc.* **2007**, *129*, 12003-12010; c) K. Billingsley, S. L. Buchwald, *J. Am. Chem. Soc.* **2007**, *129*, 3358-3366; d) T. Ikawa, T. E. Barder, M. R. Biscoe, S. L. Buchwald, *J. Am. Chem. Soc.* **2007**, *129*, 13001-13007; e) R. Martin, S. L. Buchwald, *J. Am. Chem. Soc.* **2007**, *129*, 3844-3845.

8. The coupling of 4-chloroaniline with vinyltributylstannane in 61% yield has been reported, see

ref. 4c.

9. A general method for the coupling of activated aryl chlorides at 60 °C has been reported, see ref. 4h.

10. C. Wolf, R. Lerebours, *J. Org. Chem.* **2003**, *68*, 7551-7554.

11. a) S. M. Abel, D. J. Back, J. L. Maggs, B. K. Park, *J. Steroid Biochem. Mol. Biol.* **1993**, *46*, 833-839; b) B. K. Park, N. R. Kitteringham, *Drug Metab. Rev.* **1994**, *26*, 605-643; c) S. B. Rosenblum, T. Huynh, A. Afonso, H. R. Davis, Jr., N. Yumibe, J. W. Clader, D. A. Burnett, *J. Med. Chem.* **1998**, *41*, 973-980.

12. M. V. Ncube, M. H. Norman, V. I. Ognyanov, L. H. Pettus, US Patent 2005165015, **2005**.

13. M. P. Wentland, (Sterling Drug Inc., USA), US Patent 4959363, **1990**.

14. The coupling of 2-chloropyridine with tributyl(phenyl)stannane did not proceed to completion under these conditions. With a prolonged reaction time, 12 h at 100 °C a yield of 41 % was achieved.

15. A trimethylstannyl version has been reported as a coupling partner in two instances, see: a) J. M. Saa, G. Martorell, *J. Org. Chem.* **1993**, *58*, 1963-1966; b) A. M. Echavarren, N. Tamayo, D. J. Cardenas, *J. Org. Chem.* **1994**, *59*, 6075-6083.

16. A. F. Littke, G. C. Fu, *J. Am. Chem. Soc.* **2002**, *124*, 6343-6348.

17. T. E. Barder, S. D. Walker, J. R. Martinelli, S. L. Buchwald, *J. Am. Chem. Soc.* **2005**, *127*, 4685-4696.

18. S. P. Tanis, M. V. Deaton, L. A. Dixon, M. C. McMills, J. W. Raggon, M. A. Collins, *J. Org. Chem*. **1998**, *63*, 6914-6928.

19. L. Ackermann, R. Born, J. H. Spatz, D. Meyer, *Angew. Chem. Int. Ed*. **2005**, *44*, 7216-7219.

20. A. S. K. Hashmi, J-H. Choi, J. W. Bats, *J. Prakt. Chem.* **1999**, *341*, 342-357.

21. N. Kataokia, Q. Shelby, J. P. Stambuli, J. F. Hartwig, *J. Org. Chem*. **2002**, *67*, 5553-5566.

22. J-M. Becht, A. Gissot, A. Wagner, C. Mioskowski, *Chem. – Eur. J.* **2003**, *9*, 3209-3215.

23. B. Sain, J. S. Sandhu, *J. Org. Chem.* **1990**, *55*, 2545-2546.

24. C. Song, Y. Ma, Q. Chai, C. Ma, W. Jiang, M. B. Andrus, *Tetrahedron* **2005**, *61*, 7438-7446.

25. S-K. Kang, S-K. Yoon, K-H. Lim, H-J. Son, T-G. Baik, *Synth. Commun*, **1998**, *28*, 3645-3655.

26. P. Goems, C. Gosmini, J. Perichon, *Org. Lett.* **2003**, *5*, 1043-1045.

27. Y. Kobayashi, A. D. William, R. Mizojiri, *J. Organomet. Chem*. **2002**, *653*, 91-97.

28. G. Hafelinger, F. Hack, G. Westermayer, *Chem. Ber.* **1978**, *111*, 1323-1329.

29. W. Su, S. Urgaonkar, J. G. Verkade, *Org. Lett.* **2004,** *6*, 1421-1424.

30. A. K. Sahoo, T. Oda, Y. Nakao, T. Hiyama, *Adv. Synth. Catal.* **2004***, 346*, 1715-1727.

Chapter 2 - Stille Cross-Coupling of Aryl Mesylates

2.1 Introduction

The Stille cross-coupling reaction is a versatile method for the formation of carbon–carbon bonds and the construction of molecules containing sp^2-sp^2 bonds.[1] Since its introduction by Migita[2] and its subsequent exploration by Stille,[3] it has evolved into one of the most robust of the palladium-catalyzed cross-coupling reactions and has found applications in drug discovery,[4] natural products synthesis,[5] and materials chemistry.[6] The toxicity of organostannanes,[7] and the difficulty in the removal of the tin byproducts have lead to an increase in the popularity of other C–C cross-coupling methods, specifically the Suzuki-Miyaura reaction,[8] but for difficult cases and late stage synthetic transformations the Stille reaction is still widely employed due to its reliable nature.

A great deal of effort in the field of Pd-catalyzed cross-coupling has been devoted to the development of catalysts that allow for less reactive and more stable aryl halides or pseudohalides to be employed in these reactions. Early methods utilized activated electrophilic coupling partners, such as aryl iodides, electron-deficient aryl bromides, and in the case of the Stille reaction, acid chlorides.[3] The advent of more active catalysts, based on electron-rich phosphine ligands, has allowed for reactions of unactivated aryl bromides, aryl chlorides, and aryl sulfonates to be carried out efficiently.[9] Aryl triflates were initially the most successfully employed aryl sulfonates for cross-coupling reactions.[10] However, due to the fact that aryl tosylates and mesylates are less expensive and more stable than the corresponding aryl triflates, recent research has focused on utilizing these substrates in many cross-coupling reactions.[11] Specifically, aryl tosylates have been shown to be effective coupling partners in Suzuki-Miyaura, Kumada-Corriu, and C-N cross-coupling reactions;[12] aryl mesylates have been efficiently employed in Hiyama, Suzuki-Miyaura, and C–N cross-coupling reactions, as well as Pd-catalyzed carbonylation reactions.[13] Further, vinyl tosylates have also been utilized in Stille cross-coupling reactions;[14] however, to date no examples of the Stille cross-coupling reactions of aryl tosylates and mesylates have been reported. Herein, we report a catalyst, based on **1** (XPhos), for the Pd-catalyzed Stille cross-coupling reactions of aryl mesylates and tosylates.

2.2 Results and Discussion

We began our studies by investigating the reaction of 3-methoxyphenyl methanesulfonate and tri-*n*-butyl(phenyl)stannane. Attempts to use reaction conditions previously reported by our group for the Stille reaction of aryl chlorides,[15] employing $Pd(OAc)_2$ and **1** in either 1,4-dioxane or DME as solvent provided very low yields (Table 1, entries 1 and 2). An examination of the use of non-ethereal solvents showed that a polar aprotic solvent, DMF, gave no desired product; while alcoholic solvents proved to be the best, with *t*-BuOH giving the highest yield (Table 1, entries 3-5).

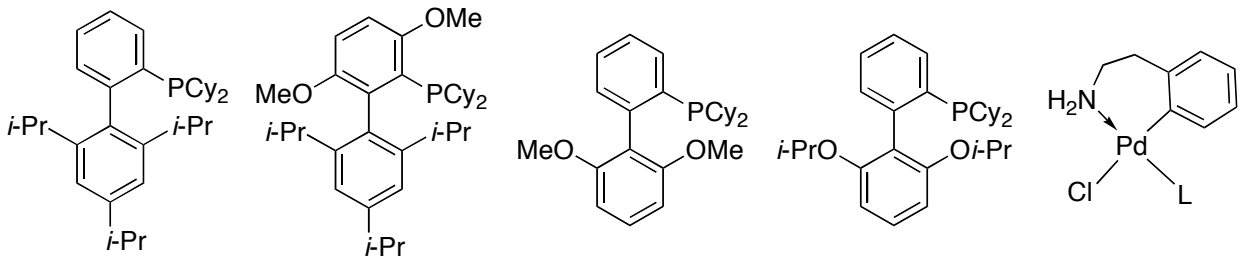

XPhos **1** BrettPhos **2** SPhos **3** RuPhos **4** **5;** L = **1** **6;** L = **2**

Figure 1: Biaryl-monophosphine Ligands

We next explored other biarylphosphine ligands and Pd sources in this reaction. Catalysts based on **2** (BrettPhos), which has been shown to form an efficient catalyst for the C–N cross-coupling of aryl mesylates, and **3** (SPhos) provided yields of 60% and 52% respectively (Table 1, entries 6 and 7). Using a catalyst comprised of $Pd(OAc)_2$ and **4** (RuPhos**)** increased the yield of the reaction to 76% (Table 1, entry 8); however, **1** formed the most efficient catalyst system and furnished the desired product in 93% yield (Table 1, entry 3). While other Pd sources, such as allylpalladium chloride dimer and **5**, a single component precatalyst developed in our group,[16] gave results similar to palladium acetate for this reaction, we chose to continue our studies with the latter because of its low cost and stability (Table 1, entries 8 and 9). Pd_2dba_3 was also examined, and its use only produced a 22% yield of the desired product (Table 1, entry 10). Finally, we wanted to explore the effect of increasing the L:Pd ratio on the efficiency of the reaction. Entries 12-14 show these results. While the yields of the three ratios of L:Pd examined

were similar, we found that a 2:1 ratio was optimal (Table 1, entries 11-13).

Table 1. Examination of reaction conditions for the coupling of 3-methoxyphenyl methanesulfonate.

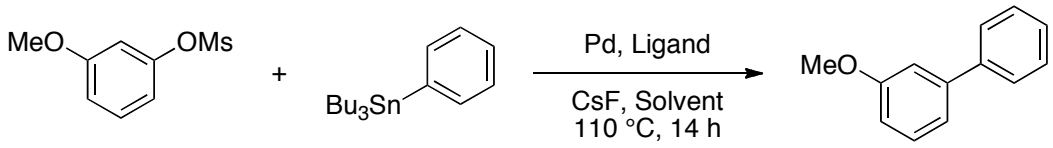

Entry	Solvent	Ligand	Pd Source	L:Pd	Yield (%)[b]
1	1,4-dioxane	**1**	$Pd(OAc)_2$	1.5:1	4
2	DME	**1**	$Pd(OAc)_2$	1.5:1	0
3	t-BuOH	**1**	$Pd(OAc)_2$	1.5:1	93
4	n-BuOH	**1**	$Pd(OAc)_2$	1.5:1	48
5	DMF	**1**	$Pd(OAc)_2$	1.5:1	0
6	t-BuOH	**2**	$Pd(OAc)_2$	1.5:1	60
7	t-BuOH	**3**	$Pd(OAc)_2$	1.5:1	52
8	t-BuOH	**4**	$Pd(OAc)_2$	1.5:1	76
9	t-BuOH	**1**	$(AllylPdCl)_2$	1.5:1	88
10	t-BuOH	**1**	Pd_2dba_3	1.5:1	22
11	t-BuOH	**1**	**5**	1.5:1	86
12	t-BuOH	**1**	$Pd(OAc)_2$	1.1:1	83
13	t-BuOH	**1**	$Pd(OAc)_2$	2:1	96
14	t-BuOH	**1**	$Pd(OAc)_2$	3:1	95

[a] Reaction Conditions: 0.5 mmol of Ar-OMs, 0.6 mmol of Ar-$SnBu_3$, 1.1 mmol of CsF, 1.0 mL of t-BuOH, 2.0 mol% of [Pd], DME = dimethoxyethane, DMF = dimethylformamide. [b] GC Yield.

Table 2. Stille cross-couplings of aryl sulfonates with XPhos.

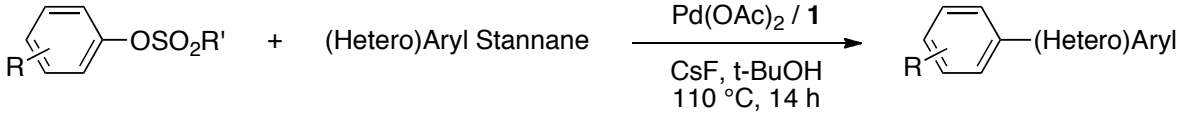

Entry	Sulfonate	Stannane	Product	Yield (%)[b]
1	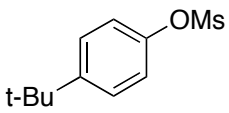	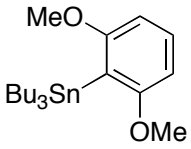	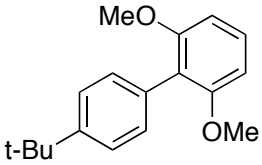	78
2	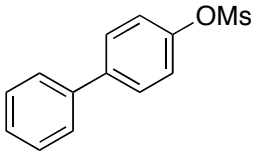	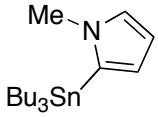	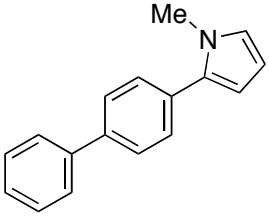	63[d]
3	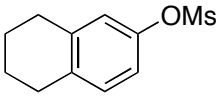	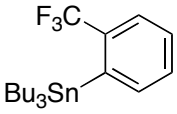	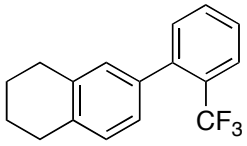	64
4	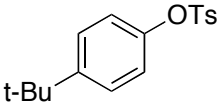	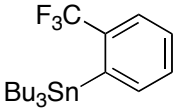	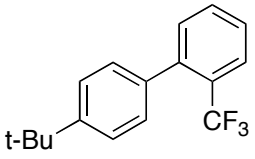	58[c]
5	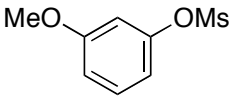	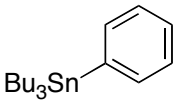	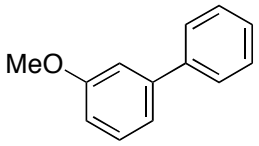	78
6	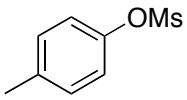	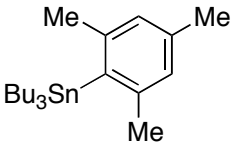	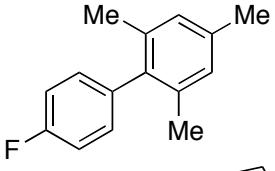	51
7	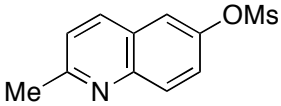	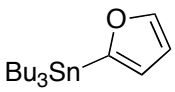	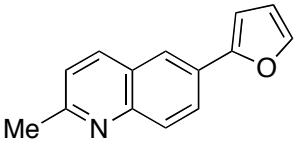	78
8	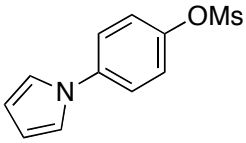	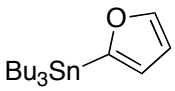	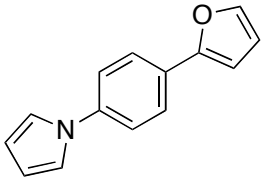	58

[a] Reaction Conditions: 1.0 mmol of Ar-OMs, 1.2 mmol of Ar-$SnBu_3$, 2.2 mmol of CsF, 2.0 mol% of $Pd(OAc)_2$, 4.0 mol% of **1**, 2.0 mL of t-BuOH. [b] Isolated yields (average of two runs). [c] 2.0 mol% of pre-milled $Pd(OAc)_2$: **1** (1:2). [d] 4.0 mol% of $Pd(OAc)_2$, 8.0 mol% of 1.

Table 2 (cont.):

Entry	Sulfonate	Stannane	Product	Yield (%)[b]
9	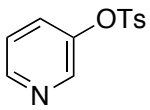	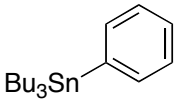	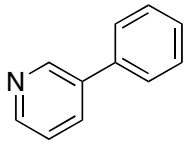	60[c]
10	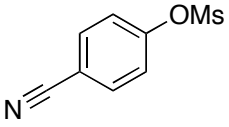	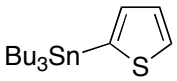	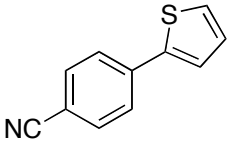	64
11	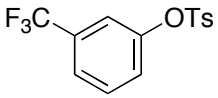	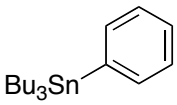	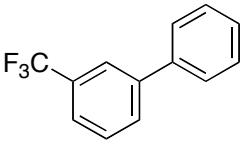	84
12	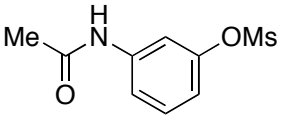	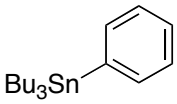	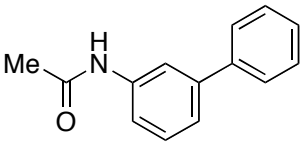	61[c]

[a] Reaction Conditions: 1.0 mmol of Ar-OMs, 1.2 mmol of Ar-$SnBu_3$, 2.2 mmol of CsF, 2.0 mol% of $Pd(OAc)_2$, 4.0 mol% of **1**, 2.0 mL of t-BuOH. [b] Isolated yields (average of two runs). [c] 2.0 mol% of pre-milled $Pd(OAc)_2$: **1** (1:2). [d] 4.0 mol% of $Pd(OAc)_2$, 8.0 mol% of **1**.

With these conditions in hand, we wanted to explore the scope of the Stille cross-coupling reaction of aryl sulfonates using $Pd(OAc)_2$ and XPhos. The results are summarized in Table 2. We found that a variety of aryl and heteroaryl mesylates and tosylates could be coupled in moderate to good yields with aryl stannanes. These results represent the first reported Stille couplings of these sulfonates. Unactivated aryl mesylates and tosylates were coupled in good yields (Table 2, entries 1-4). Slightly activated aryl mesylates, such as 3-methoxyphenyl mesylate and 4-fluorophenyl mesylate were also suitable coupling partners (Table 2, entries 5-6). Heteroaryl containing mesylates (Table 2, entries 7-8), which have been difficult substrates in other cross-coupling reactions, and a heteroaryl tosylate (Table 2, entry 9) were successfully combined with arylstannanes in good to moderate yields.

For example, the reaction of 2-methylquinolin-6-yl methanesulfonate and tri-*n*-butyl(furan-2-yl)stannane provided the desired product in 78% yield. Finally, reactions were carried out with aryl sulfonates containing functional groups. Electron-withdrawing groups such as nitriles and trifluoromethyl groups

were tolerated in this reaction (Table 2, entries 10-11), as well as an acetamide that contained a free N–H (Table 2, entry 12).

A range of tri-*n*-butylarylstannanes were also explored and found to work well in these coupling reactions. The simplest arylstannane, tri-*n*-butyl(phenyl)stannane, was combined with weakly activated mesylates (Table 2, entry 5), functional group containing mesylates (Table 2, entries 11-12) and heteroaryl tosylates (Table 2, entry 9) with high efficiency. Arylstannanes containing *ortho* substitution, such as tri-*n*-butyl(2,6-dimethoxyphenyl)stannane (Table 2, entry 1), tri-*n*-butyl(2-(trifluoromethyl)-phenyl)stannane (Table 2, entries 3-4), and tri-*n*-butyl(mesityl)-stannane (Table 2, entry 6) were effectively reacted with unactivated mesylates and tosylates. Additionally, heteroarylstannanes such as 2-furyl-, 2-thienyl-, and 2-(N-methylpyrrolyl)tri-*n*-butylstannane were shown to be proficient substrates in these reactions. (Table 2, entries 2, 7, 8 and 10).

While we have revealed that this method tolerates a range of substrates, we also discovered some limitations in its scope. As described above, steric hindrance was well tolerated on the arylstannane, as shown by the reactions of tin reagents containing an *o*-CF_3 group, two *o*-OMe groups, and even two *o*-Me groups. However, attempts to utilize *ortho*-substituted aryl sulfonate resulted in greatly reduced reaction rates.[17] In addition, there were certain classes of heterocycles that were not tolerated under these reaction conditions. While 3-pyridyltosylate was successfully coupled, the analogous mesylate, along with 2-pyridylmesylate provided no product; in both cases only the products of hydrolysis (3-hydroxypyridine and 2-pyridone, respectively) were observed. Similarly, use of several heteroarylstannanes provided no coupling product and only decomposition of the mesylate coupling partners to their parent phenols were observed. These stannanes included the 2-thiazole, 2-oxazole, 2-pyrazinyl and 2-pyridyl derivatives.

2.3 Conclusion

In conclusion, a catalyst system comprised of XPhos and $Pd(OAc)_2$ used with CsF in t-BuOH was developed for the Stille cross-coupling of aryl mesylates and aryl tosylates with aryl- and heteroaryl-stannanes. A total of 11 examples were reported including unactivated aryl mesylates and aryl tosylates,

functional group containing aryl mesylates and both heteroaryl mesylates and heteroaryl tosylates. The biaryl products were obtained in yields that ranged from 51-84%, and represent the first biaryl compounds made by Stille cross-coupling of aryl mesylates and tosylates.

2.4 Experimental

General Reagent Information

All reactions were carried out under an argon atmosphere. The *tert*-butanol, 1,4-dioxane, DME, and DMF were purchased from Aldrich Chemical Company in Sure-Seal bottles and were used as received. Toluene was purchased from J.T. Baker in CYCLE-TAINER® solvent-delivery kegs and vigorously purged with argon for 2 h. The solvent was further purified by passing it under argon pressure through two packed columns of neutral alumina and copper (II) oxide. Aryl mesylates, tosylates, and benzenesulfonates were synthesized using literature procedures. Aryl tin reagents were purchased from Aldrich Chemical Company, Alfa Aesar, and Gelest and were used as received. **2**,[14] **4**,[18] and **5**[17] were synthesized using literature procedures. Ligands **1**[19] and **3**[20] were purchased from Strem Chemicals and the CsF, $Pd_2(dba)_3$, $PdCl_2(CH_3CN)_2$, and $[(allyl)PdCl]_2$ were purchased from Aldrich Chemical Company. $Pd(OAc)_2$ was received as a gift from BASF. Flash chromatography was performed using a Biotage SP4 instrument with pre-packed silica cartridges.

General Analytical Information

All compounds were characterized by ^1H NMR, ^{13}C NMR, and IR spectroscopy. Copies of the ^1H and ^{13}C spectra can be found at the end of the experimental section. Nuclear Magnetic Resonance spectra were recorded on a Varian 300 MHz instrument or a Bruker 400 MHz instrument. All ^1H NMR experiments are reported in δ units, parts per million (ppm), and were measured relative to the signals for residual chloroform (7.26 ppm) in the deuterated solvent, unless otherwise stated. All ^{13}C NMR spectra are reported in ppm relative to deuterochloroform (77.23 ppm), unless otherwise stated, and all were obtained with ^1H decoupling. All IR spectra were taken on a Perkin – Elmer 2000 FTIR. All GC analyses were

performed on a Agilent 6890 gas chromatograph with an FID detector using a J & W DB-1 column (10 m, 0.1 mm I.D.).

General Procedure for Table 1

An oven-dried test tube, which was equipped with a magnetic stir bar and fitted with a Teflon screw-cap septum, was charged with the Pd source (2 mol% Pd), ligand (4 mol%), and CsF (1.1 mmol). The vessel was evacuated and backfilled with argon (this process was repeated a total of 3 times) and then the 3-methoxyphenyl methanesulfonate (101 mg, 0.5 mmol), tri-*n*-butyl(phenyl)stannane (221 mg, 0.6 mmol), and *t*-BuOH (1 mL) were added via syringe. The solution was heated to 110 °C for 14 h and then the reaction mixture was cooled to room temperature and filtered through a plug of silica (eluting with EtOAc). Biphenyl was then added as an internal standard and the reaction was analyzed by GC.

General Procedure for Table 2

An oven-dried test tube, which was equipped with a magnetic stir bar and fitted with a Teflon screw-cap septum, was charged with the $Pd(OAc)_2$ (2 mol%), **1** (4 mol%), and CsF (2.2 mmol). The vessel was evacuated and backfilled with argon (this process was repeated a total of 3 times) and then the aryl sulfonate (1.0 mmol), stannane (1.2 mmol), and *t*-BuOH (2 mL) were added via syringe (aryl mesylates, tosylates, or benzenesulfonates that were solids at room temperature were added with the catalyst and base). The solution was heated to 110 °C for 44 h and then the reaction mixture was cooled to room temperature, filtered through a plug of silica (eluting with EtOAc), concentrated in vacuo, and purified via the Biotage SP4 (silica-packed 50 or 100 g snap cartridge).

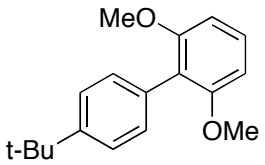

4'-*tert*-Butyl-2,6-dimethoxybiphenyl[21] (Table 2, entry 1) Following the general procedure, a mixture of 4-*tert*-butylphenyl methanesulfonate (228 mg, 1.0 mmol), tri-*n*-butyl(2,6-dimethoxyphenyl)stannane (514

mg, 1.2 mmol), $Pd(OAc)_2$ (4.4 mg, 2.0 mol%), **1** (19 mg, 4 mol%), CsF (334 mg, 2.2 mmol), and *t*-BuOH (2 mL) was heated to 110 °C for 14 h. The crude product was purified via the Biotage SP4 (silica-packed 50 g snap column; 0-5% EtOAc/hexanes) to provide the title compound as a white solid (211 mg, 87%), mp = 129 – 130 °C. ^{1}H NMR (300 MHz, $CDCl_3$) δ: 7.43 (d, *J* = 8.7 Hz, 2H), 7.32 – 7.22 (m, 3H), 6.46 (d, *J* = 8.4 Hz, 2H), 3.75 (s, 6H), 1.37 (s, 9H) ppm. ^{13}C NMR (75 MHz, $CDCl_3$) δ: 157.9, 149.3, 131.0, 130.6, 128.6, 124.8, 119.5 ppm. IR (neat, cm^{-1}): 2961, 1587, 1471, 1430, 1384, 1245, 1109, 825, 723, 563.

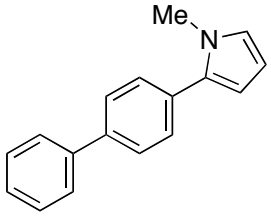

2-(Biphenyl-4-yl)-1-methyl-1*H*-pyrrole (Table 2, entry 2) Following the general procedure, a mixture of biphenyl-4-yl methanesulfonate (248 mg, 1.0 mmol), 1-methyl-2-(tri-*n*-butylstannyl)-1*H*-pyrrole (445 mg, 1.2 mmol), $Pd(OAc)_2$ (8.8 mg, 4.0 mol%), **1** (38 mg, 8 mol%), CsF (334 mg, 2.2 mmol), and *t*-BuOH (2 mL) was heated to 110 °C for 14 h. The crude product was purified via the Biotage SP4 (silica-packed 50 g snap column; 0-40% EtOAc/hexanes) to provide the title compound as a white solid (151 mg, 65%), mp = 125 – 127 °C. ^{1}H NMR (300 MHz, $CDCl_3$) δ: 7.64 (m, 4H), 7.49 (m, 4H), 7.39 (m, 1H), 6.76 (t, *J* =2.4 Hz, 1H), 6.30 (m, 1H), 6.25 (t, *J* = 2.4 Hz, 1H), 3.73 (s, 3H) ppm. ^{13}C NMR (75 MHz, $CDCl_3$) δ: 140.9, 139.6, 134.4, 132.5, 129.1, 129.0, 127.5, 127.3, 127.2, 124.1, 109.0, 108.1, 35.4 ppm. IR (neat, cm^{-1}): 2953, 1478, 1446, 1408, 1309, 1061, 846, 765, 713, 695.

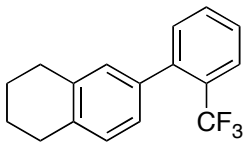

6-(2-(Trifluoromethyl)phenyl)-1,2,3,4-tetrahydronaphthalene (Table 2, entry 3) Following the general procedure, a mixture of 5,6,7,8-tetrahydronaphthalen-2-yl methanesulfonate (237 mg, 1.0 mmol), tri-*n*-

butyl(2-(trifluoromethyl)phenyl)stannane (522 mg, 1.2 mmol), $Pd(OAc)_2$ (4.4 mg, 2.0 mol%), **1** (19 mg, 4 mol%), CsF (334 mg, 2.2 mmol), and *t*-BuOH (2 mL) was heated to 110 °C for 14 h. The crude product was purified via the Biotage SP4 (silica-packed 50 g snap column; 0-10% EtOAc/hexanes) to provide the title compound as a yellow oil (152 mg, 55%). ^{1}H NMR (300 MHz, $CDCl_3$) δ: 7.78 (d, J = 7.8 Hz, 1H), 7.58 (t, J = 7.5 Hz, 1H), 7.47 (t, J = 7.5 Hz, 1H), 7.38 (d, J = 6.9 Hz, 1H), 7.14 (m, 2H), 7.09 (s, 1H), 2.86 (m, 4H), 1.89 (m, 4H) ppm. ^{13}C NMR (75 MHz, $CDCl_3$) δ: 141.9, 141.8, 137.2, 136.7, 136.7, 132.4, 131.4, 131.4, 129.8, 129.8, 129.8, 129.8, 129.3, 128,8, 128.6, 128.4, 127.2, 126.3, 126.2, 126.1, 126.1, 125.6, 122.6, 29.6, 29.4, 23.6, 23.4 ppm. IR (neat, cm^{-1}): 2931, 1604, 1486, 1449, 1315, 1168, 1127, 1036, 768, 650.

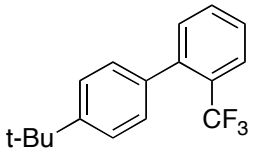

4'-*tert*-Butyl-2-(trifluoromethyl)biphenyl[22] (Table 2, entry 4) Following the general procedure, a mixture of 4-*tert*-butylphenyl 4-tolylsulfonate (304 mg, 1.0 mmol), tri-*n*-butyl(2-(trifluoromethyl)-phenyl)stannane (522 mg, 1.2 mmol), $Pd(OAc)_2$ (2.0 mol%) and **1** (4 mol%) as a pre-milled mixture (23.6 mg), CsF (334 mg, 2.2 mmol), and *t*-BuOH (2 mL) was heated to 110 °C for 14 h. The crude product was purified via the Biotage SP4 (silica-packed 50 g snap column; hexanes) to provide the title compound as a colorless oil (170 mg, 61%). ^{1}H NMR (400 MHz, $CDCl_3$) δ: 7.75 (d, J =7.5 Hz, 1H), 7.54 (t, J =7.5 Hz, 1H), 7.44 (m, 3H), 7.34 (d, J =7.5 Hz, 1H), 7.28 (d, J =7.5 Hz, 2H), 1.38 (s, 9H) ppm. ^{13}C NMR (100 MHz, $CDCl_3$) δ: 150.7, 141.7, 141.7, 137.1, 132.4, 131.5, 129.1, 128.8, 128.8, 128.5, 128.2, 127.3, 126.3, 126.3, 126.2, 126.2, 125.8, 124.9, 123.1, 34.8, 31.6 ppm. IR (neat, cm^{-1}): 2965, 2869, 1606, 1488, 1315, 1171, 1131, 1069, 1036, 768.

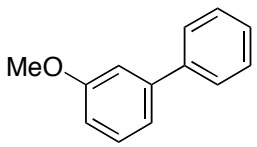

3-Methoxybiphenyl[23] (Table 2, entry 5) Following the general procedure, a mixture of 3-methoxyphenyl methanesulfonate (202 mg, 1.0 mmol), tri-*n*-butyl(phenyl)stannane (440 mg, 1.2 mmol), $Pd(OAc)_2$ (4.4 mg, 2.0 mol%), **1** (19 mg, 4 mol%), CsF (334 mg, 2.2 mmol), and *t*-BuOH (2 mL) was heated to 110 °C for 14 h. The crude product was purified via the Biotage SP4 (silica-packed 50 g snap column; 0-10% EtOAc/hexanes) to provide the title compound as a yellow oil (145 mg, 79%). ^{1}H NMR (300 MHz, $CDCl_3$) δ: 7.60 (d, *J* = 6.9 Hz, 2H), 7.45 (t, *J* = 7.2 Hz, 2H), 7.37 (m, 2H), 7.19 (d, *J* = 7.8 Hz, 1H), 7.14 (m, 1H), 6.91 (m, 1H), 3.89 (s, 3H) ppm. ^{13}C NMR (75 MHz, $CDCl_3$) δ: 160.1, 143.0, 141.3, 130.0, 128.9, 127.6, 127.4, 119.9, 113.1, 112.8, 55.5 ppm. IR (neat, cm^{-1}): 2937, 1599, 1573, 1479, 1421, 1296, 1213, 1020, 757, 697.

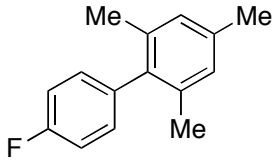

4'-Fluoro-2,4,6-trimethylbiphenyl[24] (Table 2, entry 6) Following the general procedure, a mixture of 4-fluorophenyl methanesulfonate (190 mg, 1.0 mmol), tri-*n*-butyl(mesityl)-stannane (491 mg, 1.2 mmol), $Pd(OAc)_2$ (4.4 mg, 2.0 mol%), **1** (19 mg, 4 mol%), CsF (334 mg, 2.2 mmol), and *t*-BuOH (2 mL) was heated to 110 °C for 14 h. The crude product was purified via the Biotage SP4 (silica-packed 50 g snap column; 0-5% EtOAc/hexanes) to provide the title compound as a white solid (116 mg, 54%), mp = 65 – 67 °C (literature 64 – 65 °C). ^{1}H NMR (300 MHz, $CDCl_3$) δ: 7.14 (s, 2H), 7.11 (s, 2H), 6.97 (s, 2H) ppm. ^{13}C NMR (75 MHz, $CDCl_3$) δ: 163.5, 160.3, 138.2, 137.0, 137.0, 136.4, 131.1, 130.9, 128.3, 115.7, 115.4, 109.9, 21.2, 21.0 ppm. IR (neat, cm^{-1}): 2921, 1601, 1511, 1478, 1217, 1151, 1087, 1008, 854, 815.

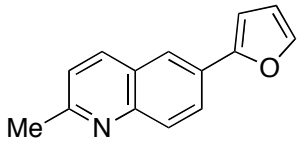

6-(Furan-2-yl)-2-methylquinoline (Table 2, entry 7) Following the general procedure, a mixture of 2-methylquinolin-6-yl methanesulfonate (237 mg, 1.0 mmol), tri-*n*-butyl(furan-2-yl)stannane (430 mg, 1.2

mmol), $Pd(OAc)_2$ (4.4 mg, 2.0 mol%), **1** (19 mg, 4 mol%), CsF (334 mg, 2.2 mmol), and *t*-BuOH (2 mL) was heated to 110 °C for 14 h. The crude product was purified via the Biotage SP4 (silica-packed 50 g snap column; 0-40% EtOAc/hexanes) to provide the title compound as a white solid (175 mg, 84%), mp = 57 – 59 °C. ^{1}H NMR (300 MHz, $CDCl_3$) δ: 7.97 (m, 4H), 7.48 (s, 1H), 7.19 (d, *J* =8.4 Hz, 1H), 6.71 (d, *J* = 3.3 Hz, 1H), 6.47 (m, 1H), 2.69 (s, 3H) ppm. ^{13}C NMR (75 MHz, $CDCl_3$) δ: 158.9, 153.5, 147.3, 142.6, 136.3, 129.1, 128.1, 126.7, 125.9, 122.6, 121.5, 112.0, 106.1 ppm. IR (neat, cm^{-1}): 1640, 1385, 1125, 1385, 1125, 885, 816, 744, 596, 456.

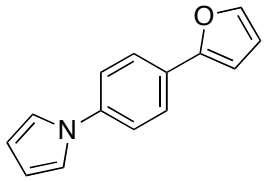

1-(4-(Furan-2-yl)phenyl)-1*H*-pyrrole (Table 2, entry 8) Following the general procedure, a mixture of 4-(1*H*-pyrrol-1-yl)phenyl methanesulfonate (237 mg, 1.0 mmol), tri-*n*-butyl(furan-2-yl)stannane (430 mg, 1.2 mmol), $Pd(OAc)_2$ (4.4 mg, 2.0 mol%), **1** (19 mg, 4 mol%), CsF (334 mg, 2.2 mmol), and *t*-BuOH (2 mL) was heated to 110 °C for 14 h. The crude product was purified via the Biotage SP4 (silica-packed 50 g snap column; 0-40% EtOAc/hexanes) to provide the title compound as a white solid (123 mg, 59%), mp = 189 – 191 °C. ^{1}H NMR (300 MHz, $CDCl_3$) δ: 7.72 (d, *J* = 9.0 Hz, 2H), 7.49 (d, *J* = 1.8 Hz, 1H), 7.41 (d, *J* = 9.0 Hz, 2H), 7.12 (t, *J* = 2.4 Hz, 2H), 6.65 (d, *J* = 3.3 Hz, 1H), 6.49 (m, 1H), 6.37 (t, *J* = 2.4 Hz, 2H) ppm. ^{13}C NMR (75 MHz, $CDCl_3$) δ: 153.4, 142.3, 139.8, 128.5, 125.1, 120.7, 119.3, 112.0, 110.8, 105.1 ppm. IR (neat, cm^{-1}): 2360, 1523, 1329, 1250, 1007, 831, 718, 594.

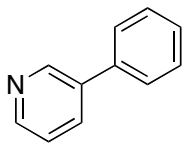

3-Phenylpyridine[25] (Table 2, entry 9) Following the general procedure, a mixture of pyridin-3-yl 4-methylbenzenesulfonate (249 mg, 1.0 mmol), tri-*n*-butyl(phenyl)stannane (440 mg, 1.2 mmol), $Pd(OAc)_2$ (2.0 mol%) and **1** (4 mol%) as a pre-milled mixture (23.6 mg), CsF (334 mg, 2.2 mmol), and *t*-BuOH (2

mL) was heated to 110 °C for 14 h. The crude product was purified via the Biotage SP4 (silica-packed 25 g snap column; 20% EtOAc/hexanes) to provide the title compound as a pale yellow oil (85 mg, 55%). ^{1}H NMR (400 MHz, $CDCl_3$) δ: 8.82 (s, 1H), 8.55 (d, *J* =5.0 Hz, 1H), 7.82 (d, *J* =7.5 Hz, 1H), 7.54 (d, *J* =7.5 Hz, 2H), 7.44 (t, *J* =7.5 Hz, 2H), 7.37 (m, 1H), 7.31 (dd, *J* = 7.5, 5.0 Hz, 1H) ppm. ^{13}C NMR (100 MHz, $CDCl_3$) δ: 148.7, 148.5, 138.0, 136.8, 134.6, 129.3, 128.3, 127.3, 123.8 ppm. IR (neat, cm^{-1}): 3400, 3031, 1581, 1473, 1450, 1407, 1006, 754, 711, 698.

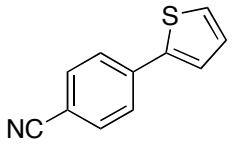

4-(Thien-2-yl)benzonitrile[26] (Table 2, entry 10) Following the general procedure, a mixture of 4-cyanophenyl methanesulfonate (197 mg, 1.0 mmol), tri-*n*-butyl(thiophen-2-yl)stannane (448 mg, 1.2 mmol), $Pd(OAc)_2$ (4.4 mg, 2.0 mol%), **1** (19 mg, 4 mol%), CsF (334 mg, 2.2 mmol), and *t*-BuOH (2 mL) was heated to 110 °C for 14 h. The crude product was purified via the Biotage SP4 (silica-packed 50 g snap column; 0-40% EtOAc/hexanes) to provide the title compound as a white solid (120 mg, 65%), mp = 90 – 92 °C (literature 91 – 92 °C). ^{1}H NMR (300 MHz, $CDCl_3$) δ: 7.68 (m, 4H), 7.41 (m, 2H), 7.13 (m, 1H) ppm. ^{13}C NMR (75 MHz, $CDCl_3$) δ: 142.1, 138.7, 132.8, 128.7, 119.0, 110.6 ppm. IR (neat, cm^{-1}): 2218, 1600, 1424, 852, 821, 718, 551.

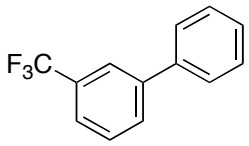

3-(Trifluoromethyl)biphenyl[24] (Table 2, entry 11) Following the general procedure, a mixture of 3-trifluoromethylphenyl tosylate (300 mg, 1.0 mmol), tri-*n*-butyl(phenyl)stannane (442 mg, 1.2 mmol), $Pd(OAc)_2$ (4.4 mg, 2.0 mol%), **1** (19 mg, 4 mol%), CsF (334 mg, 2.2 mmol), and *t*-BuOH (2 mL) was heated to 110 °C for 14 h. The crude product was purified via the Biotage SP4 (silica-packed 50 g snap column; 0-3% EtOAc/hexanes) to provide the title compound as a clear oil (194 mg, 86%). ^{1}H NMR (300

MHz, $CDCl_3$) δ: 7.93 (s, 1H), 7.82 (d, *J* = 7.5 Hz, 1H), 7.70 – 7.47 (m, 7H) ppm. ^{13}C NMR (75 MHz, $CDCl_3$) δ: 142.3, 140.0, 131.6, 131.2, 130.7, 130.7, 129.5, 129.3, 128.3, 127.5, 126.3, 124.3, 124.2, 124.2, 124.1, 124.1, 122.7 ppm. IR (neat, cm^{-1}): 3037, 1425, 1335, 1262, 1167, 1097, 1047, 899, 759, 702.

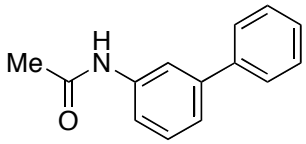

***N*-(Biphenyl-3-yl)acetamide**[27] (Table 2, entry 12) Following the general procedure, a mixture of 3-acetamidophenyl methanesulfonate (229 mg, 1.0 mmol), tri-*n*-butyl(phenyl)stannane (440 mg, 1.2 mmol), $Pd(OAc)_2$ (2.0 mol%) and **1** (4 mol%) as a pre-milled mixture (23.6 mg), CsF (334 mg, 2.2 mmol), and *t*-BuOH (2 mL) was heated to 110 °C for 14 h. The crude product was purified via the Biotage SP4 (silica-packed 50 g snap column; 20-60% EtOAc/hexanes) to provide the title compound as a white solid (120 mg, 57%), mp = 143 - 145 °C (literature 146 °C). ^1H NMR (400 MHz, $CDCl_3$) δ: 7.98 (s, 1H), 7.73 (s, 1H), 7.50 (m, 3H), 7.37 (t, *J* =7.2 Hz, 2H), 7.30 (m, 3H), 2.14 (s, 3H) ppm. ^{13}C NMR (100 MHz, $CDCl_3$) δ: 169.1, 142.2, 140.9, 138.6, 129.5, 129.0, 127.7, 127.3, 123.3, 119.1, 119.0, 24.7 ppm. IR (neat, cm^{-1}): 3294, 1665, 1555, 1480, 1402, 1317, 1013, 891, 759, 700.

MeO
OMe
t-Bu
ppm
1
2
3
4
5
6
7
9.00
5.74
1.85
3.64
1.98

31.608
34.707
56.092
76.807
77.230
77.653
104.297
119.465
124.845
128.566
130.602
130.954
149.274
157.897
MeO
OMe
t-Bu
ppm
20
40
60
80
100
120
140
160

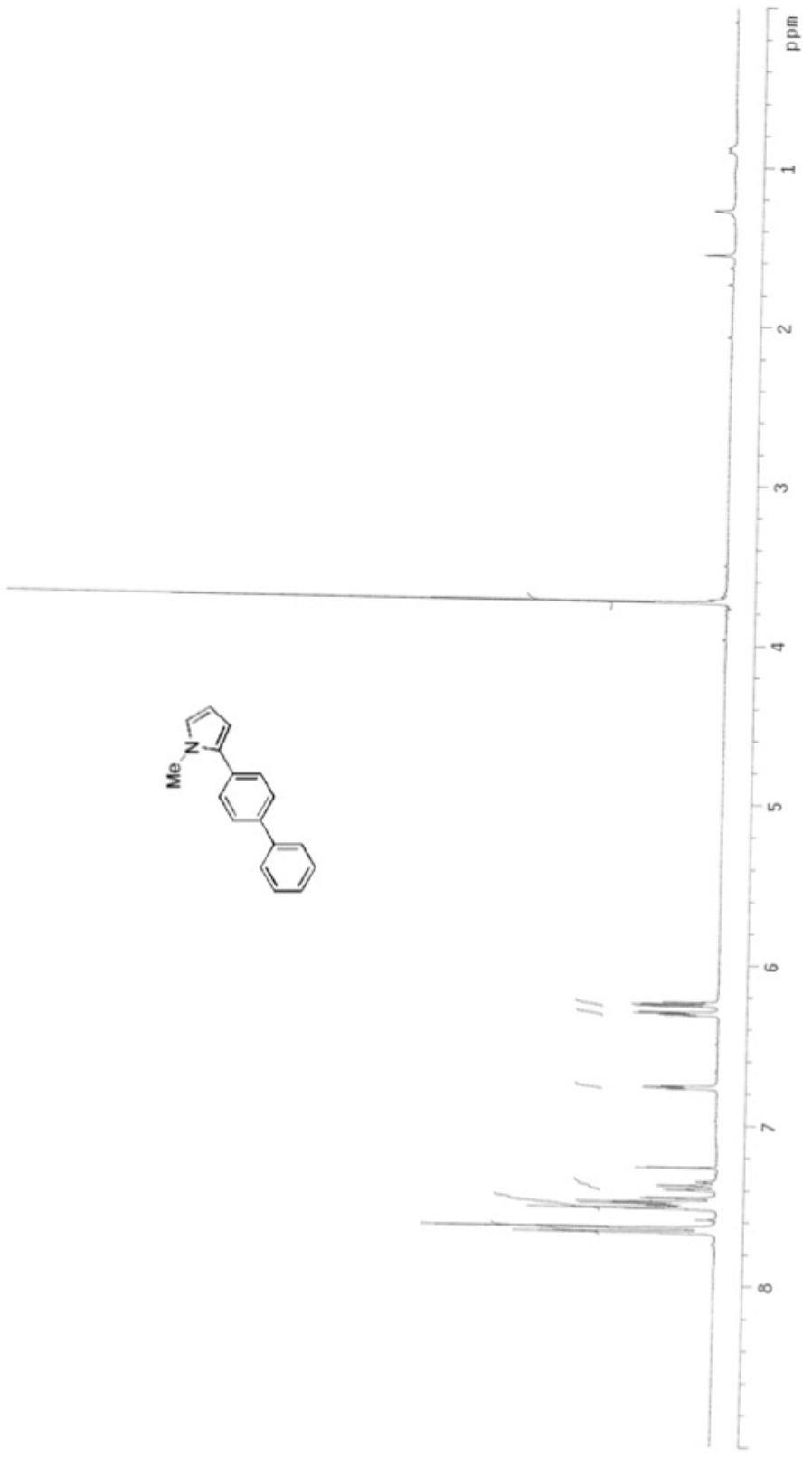
Me
N
ppm
1
2
3
4
5
6
7
8

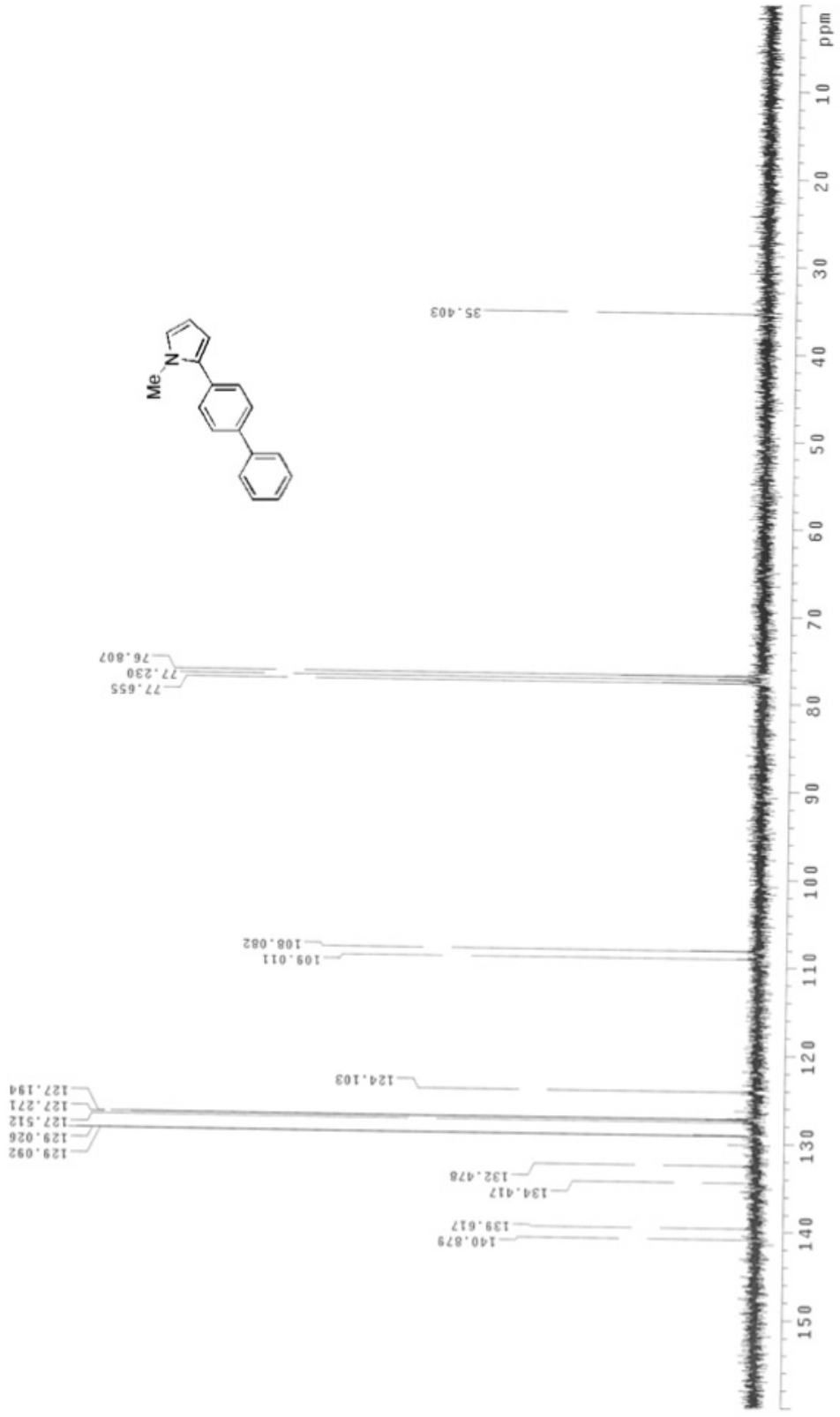
Me
N
35.403
76.807
77.230
77.655
108.082
109.011
124.103
127.194
127.271
127.512
129.026
129.092
132.478
134.417
139.617
140.879
ppm

CF3
ppm
1
2
3
4
5
6
7
8

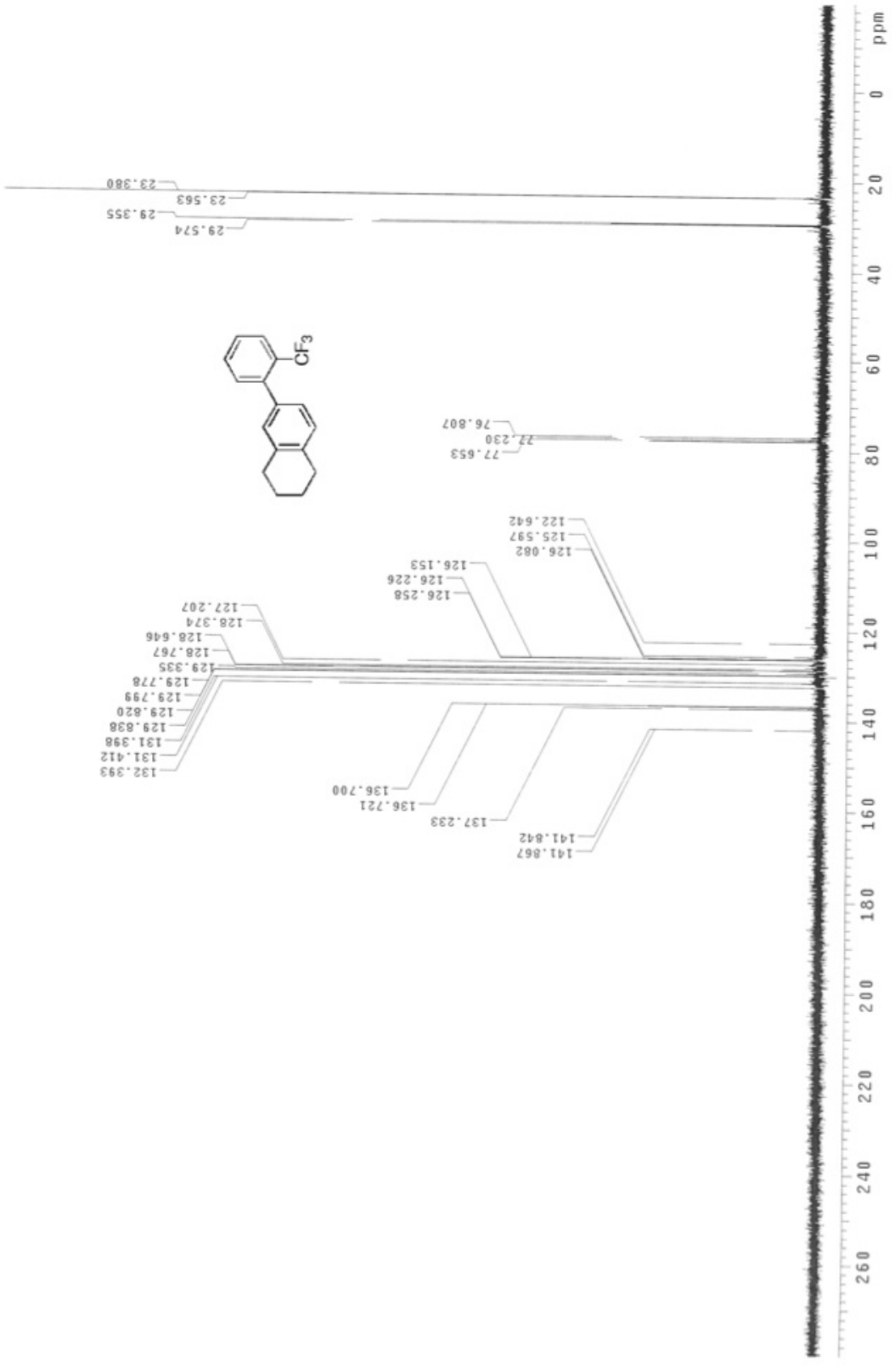
CF3
23.380
23.563
29.355
29.574
76.807
77.230
77.653
122.642
125.597
126.082
126.153
126.226
126.258
127.207
128.374
128.646
128.767
129.335
129.778
129.799
129.820
129.838
131.398
131.412
132.393
136.700
136.721
137.233
141.842
141.867
ppm

Current Data Parameters
NAME JN5-108-010
EXPNO 1
PROCNO 1
F2 - Acquisition Parameters
Date_ 20090731
Time 1.57
INSTRUM spect
PROBHD 5 mm BBO BB-1H
PULPROG zg30
TD 65536
SOLVENT
NS 16
DS 2
SWH 8278.146 Hz
FIDRES 0.126314 Hz
AQ 3.9584243 sec
RG 40.3
DW 60.400 usec
DE 6.00 usec
TE 293.2 K
D1 1.00000000 sec
TD0 1
======== CHANNEL f1 ========
NUC1 1H
P1 15.07 usec
PL1 0.00 dB
SFO1 400.1324710 MHz
F2 - Processing parameters
SI 65536
SF 400.1300212 MHz
WDW EM
SSB 0
LB 0.30 Hz
GB 0
PC 1.00
1.380
9.000
0.968
1.030
2.915
0.994
1.926
7.756
7.736
7.537
7.519
7.457
7.438
7.418
7.355
7.336
7.288
7.268
CF3
t-Bu
ppm

Current Data Parameters
NAME JN5-108-010
EXPNO 13
PROCNO 1
F2 - Acquisition Parameters
Date_ 20090731
Time 2.01
INSTRUM spect
PROBHD 5 mm BBO BB-1H
PULPROG zgpg30
TD 65536
SOLVENT CDCl3
NS 71
DS 2
SWH 23980.814 Hz
FIDRES 0.365918 Hz
AQ 1.3664756 sec
RG 16384
DW 20.850 usec
DE 6.00 usec
TE 293.2 K
D1 2.00000000 sec
d11 0.03000000 sec
DELTA 1.89999998 sec
TD0 1
======== CHANNEL f1 ========
NUC1 13C
P1 8.75 usec
PL1 -3.00 dB
SFO1 100.6228298 MHz
======== CHANNEL f2 ========
CPDPRG2 waltz16
NUC2 1H
PCPD2 90.00 usec
PL2 -1.00 dB
PL12 14.52 dB
PL13 18.00 dB
SFO2 400.1316005 MHz
F2 - Processing parameters
SI 65536
SF 100.6127514 MHz
WDW EM
SSB 0
LB 1.00 Hz
GB 0
PC 1.40
31.591
34.784
76.914
77.231
77.549
123.095
124.879
125.818
126.174
126.226
126.280
126.332
127.305
128.232
128.527
128.807
128.821
129.118
131.453
132.443
137.102
141.718
141.737
150.650
CF3
t-Bu
ppm
20
40
60
80
100
120
140
160
180

MeO
ppm
1
2
3
4
5
6
7
8

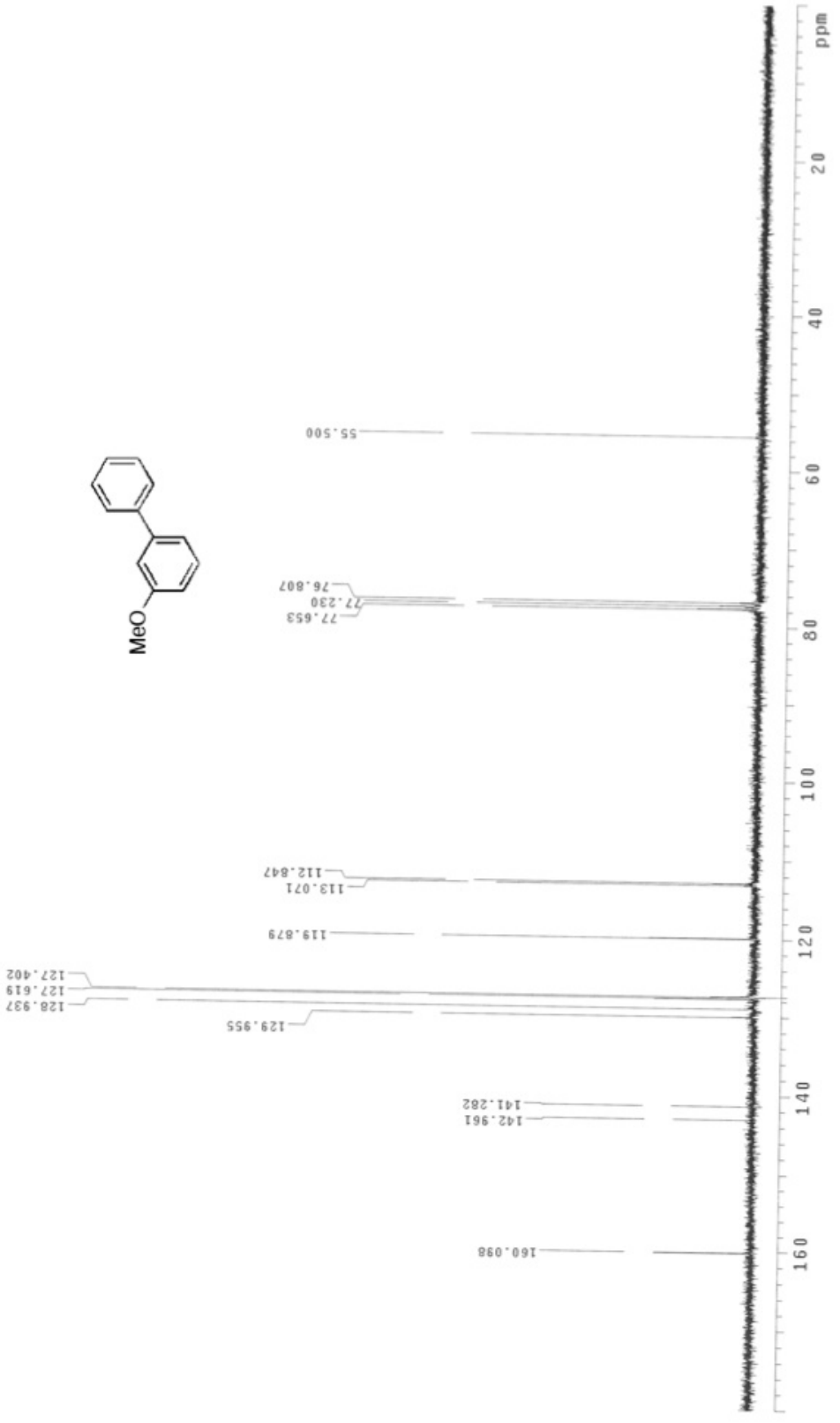
MeO
55.500
77.653
77.230
76.807
112.847
113.071
119.879
127.402
127.619
128.937
129.955
141.282
142.961
160.098
ppm
20
40
60
80
100
120
140
160

2.017
2.355
7.111
6.969
6.967
7.136
7.134
ppm
1
2
3
4
5
6
7
5.92
2.98
1.88
1.93
1.95
Me
Me
Me
F

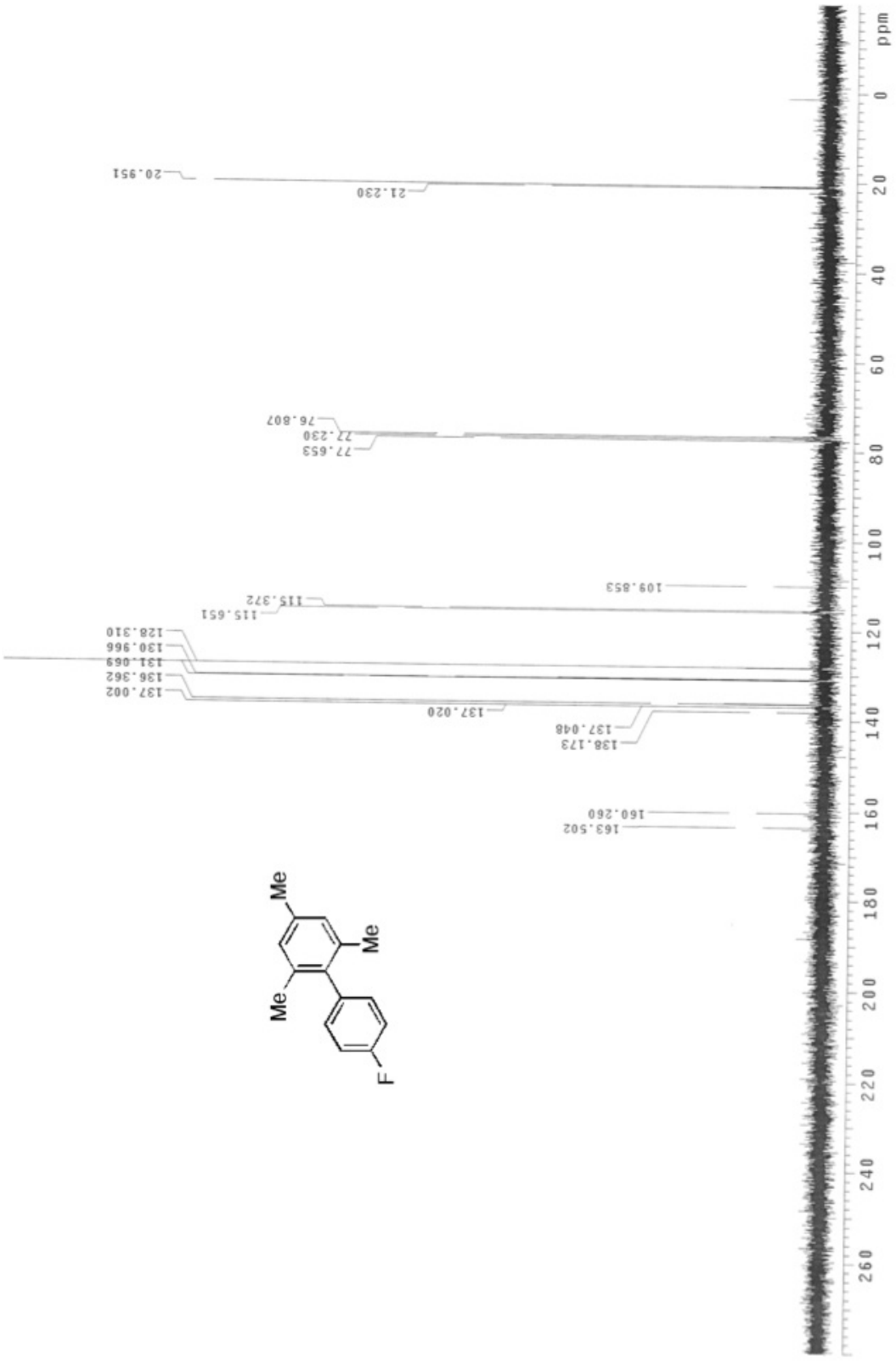
20.951
21.230
76.807
77.230
77.653
109.853
115.372
115.651
128.310
130.966
131.069
136.362
137.002
137.020
137.048
138.173
160.260
163.502
Me
Me
Me
F
ppm

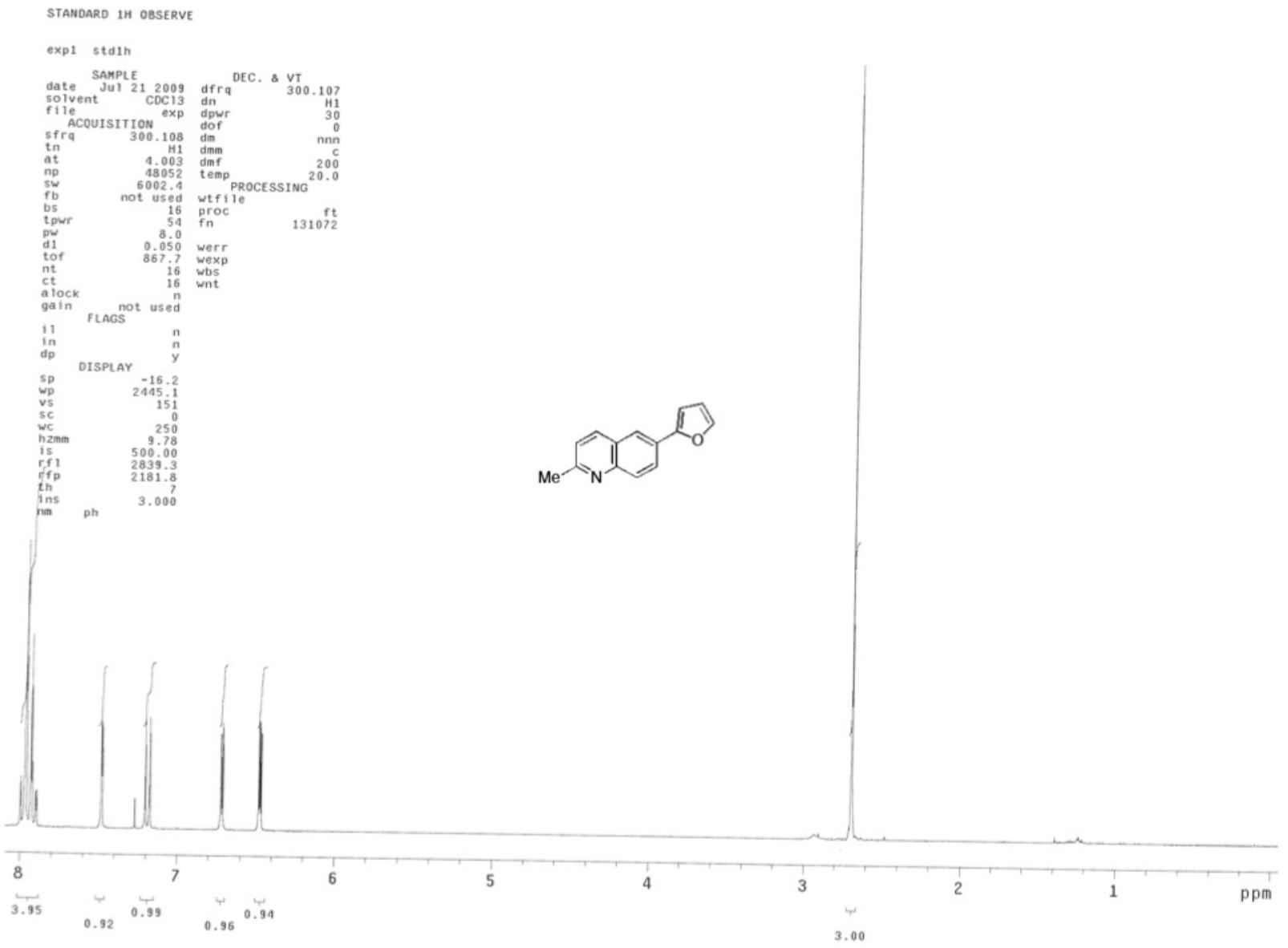
STANDARD 1H OBSERVE
exp1 std1h
SAMPLE
date Jul 21 2009
solvent CDCl3
file exp
ACQUISITION
sfrq 300.108
tn H1
at 4.003
np 48052
sw 6002.4
fb not used
bs 16
tpwr 54
pw 8.0
d1 0.050
tof 867.7
nt 16
ct 16
alock n
gain not used
FLAGS
il n
in n
dp y
DISPLAY
sp -16.2
wp 2445.1
vs 151
sc 0
wc 250
hzmm 9.78
is 500.00
rfl 2839.3
rfp 2181.8
th 7
ins 3.000
nm ph
DEC. & VT
dfrq 300.107
dn H1
dpwr 30
dof 0
dm nnn
dmm c
dmf 200
temp 20.0
PROCESSING
wtfile
proc ft
fn 131072
werr
wexp
wbs
wnt
Me
N
O
8
7
6
5
4
3
2
1
ppm
3.95
0.92
0.99
0.96
0.94
3.00

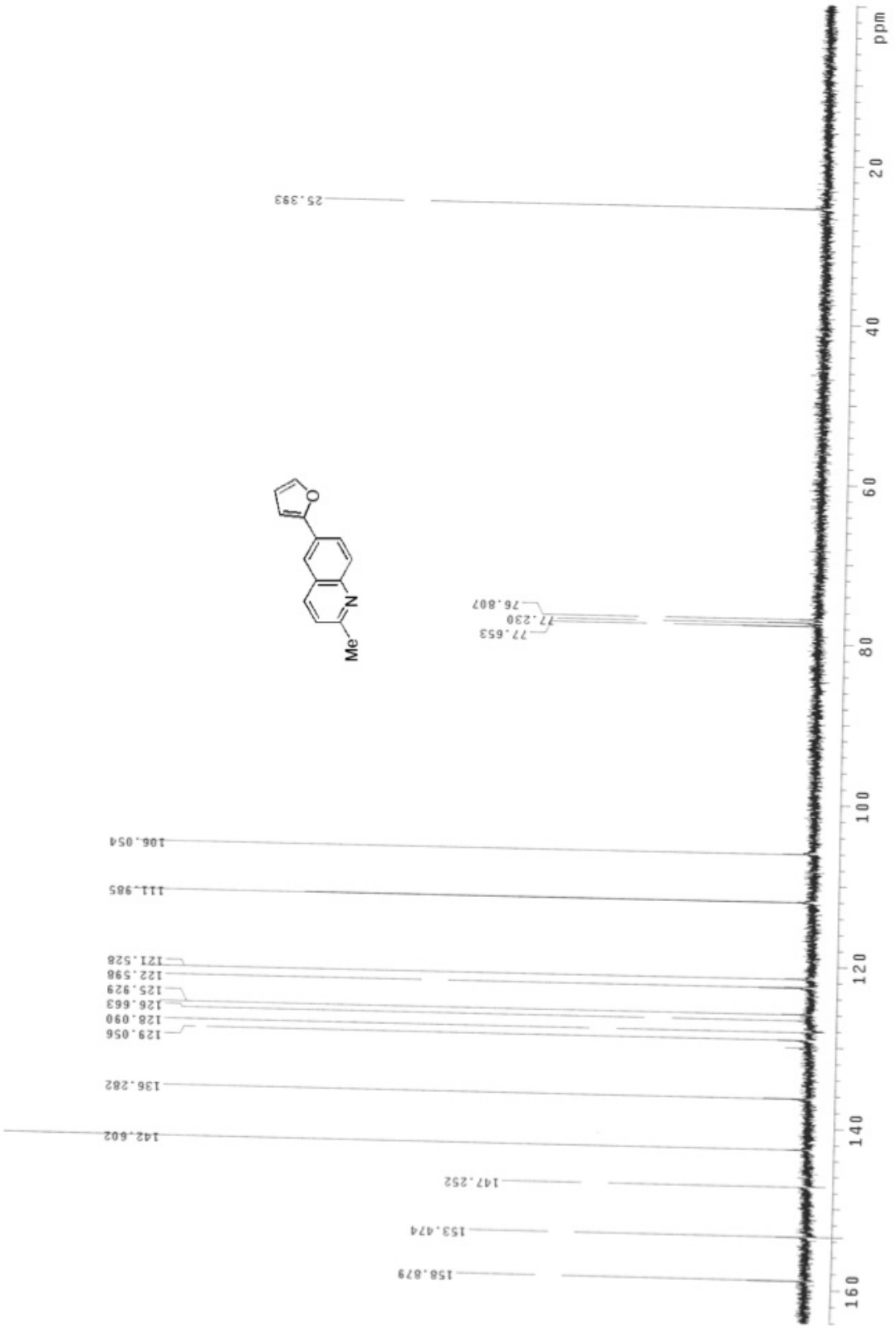
25.393
76.807
77.230
77.653
106.054
111.985
121.528
122.598
125.929
126.663
128.090
129.056
136.282
142.602
147.252
153.474
158.879
Me
N
O
ppm
20
40
60
80
100
120
140
160

O
N

ppm
1
2
3
4
5
6
7
8

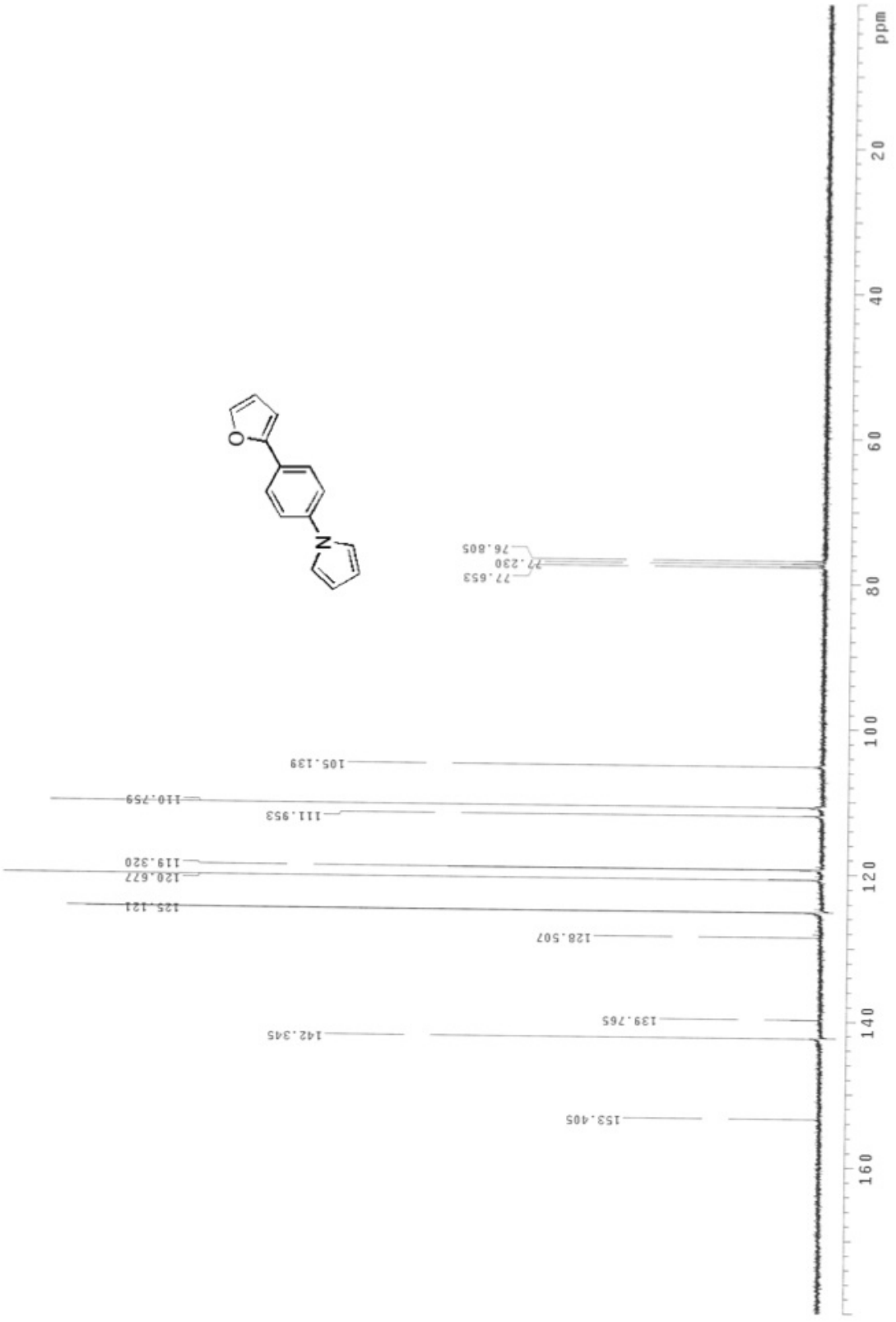
153.405
142.345
139.765
128.507
125.121
120.677
119.320
111.953
110.759
105.139
77.653
77.230
76.805
O
N
ppm
160
140
120
100
80
60
40
20

BRUKER
Current Data Parameters
NAME JN5-101-1
EXPNO 1
PROCNO 1
F2 - Acquisition Parameters
Date_ 20090728
Time 17.13
INSTRUM spect
PROBHD 5 mm BBO BB-1H
PULPROG zg30
TD 65536
SOLVENT CDCl3
NS 16
DS 2
SWH 8278.146 Hz
FIDRES 0.126314 Hz
AQ 3.9584243 sec
RG 57
DW 60.400 usec
DE 6.00 usec
TE 293.2 K
D1 1.00000000 sec
TD0 1
======== CHANNEL f1 ========
NUC1 1H
P1 15.07 usec
PL1 0.00 dB
SFO1 400.1324710 MHz
F2 - Processing parameters
SI 65536
SF 400.1300212 MHz
WDW EM
SSB 0
LB 0.30 Hz
GB 0
PC 1.00
8.818
8.561
8.549
7.837
7.818
7.552
7.533
7.460
7.442
7.423
7.385
7.367
7.349
7.333
7.321
7.314
7.301
N
0.990
1.003
1.000
2.006
2.004
2.046
9
8
7
6
5
4
3
2
1
ppm

Current Data Parameters
NAME JN5-101-1
EXPNO 13
PROCNO 1
F2 - Acquisition Parameters
Date_ 20090728
Time 17.16
INSTRUM spect
PROBHD 5 mm BBO BB-1H
PULPROG zgpg30
TD 65536
SOLVENT CDCl3
NS 33
DS 2
SWH 23980.814 Hz
FIDRES 0.365918 Hz
AQ 1.3664756 sec
RG 8192
DW 20.850 usec
DE 6.00 usec
TE 293.2 K
D1 2.00000000 sec
d11 0.03000000 sec
DELTA 1.89999998 sec
TD0 1
======== CHANNEL f1 ========
NUC1 13C
P1 8.75 usec
PL1 -3.00 dB
SFO1 100.6228298 MHz
======== CHANNEL f2 ========
CPDPRG2 waltz16
NUC2 1H
PCPD2 90.00 usec
PL2 -1.00 dB
PL12 14.52 dB
PL13 18.00 dB
SFO2 400.1316005 MHz
F2 - Processing parameters
SI 65536
SF 100.6127514 MHz
WDW EM
SSB 0
LB 1.00 Hz
GB 0
PC 1.40
77.621
77.303
76.985
148.672
148.529
138.012
136.814
134.554
129.282
128.301
127.348
123.753
N
180
160
140
120
100
80
60
40
20
ppm

S
NC
ppm
1
2
3
4
5
6
7
8

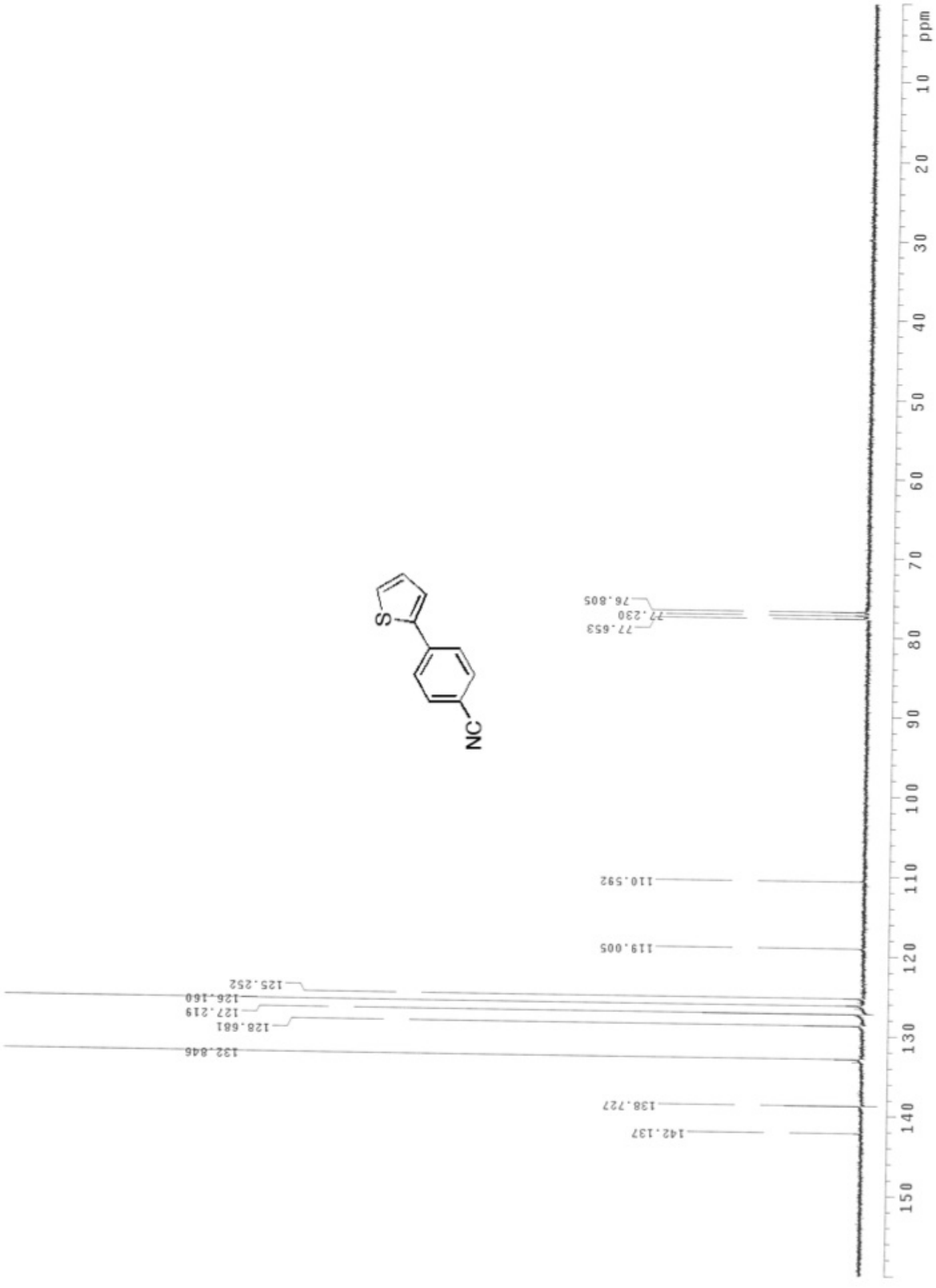
S
NC
142.137
138.727
132.846
128.681
127.219
126.160
125.252
119.005
110.592
77.653
77.230
76.805
ppm

F3C
ppm
1
2
3
4
5
6
7
8

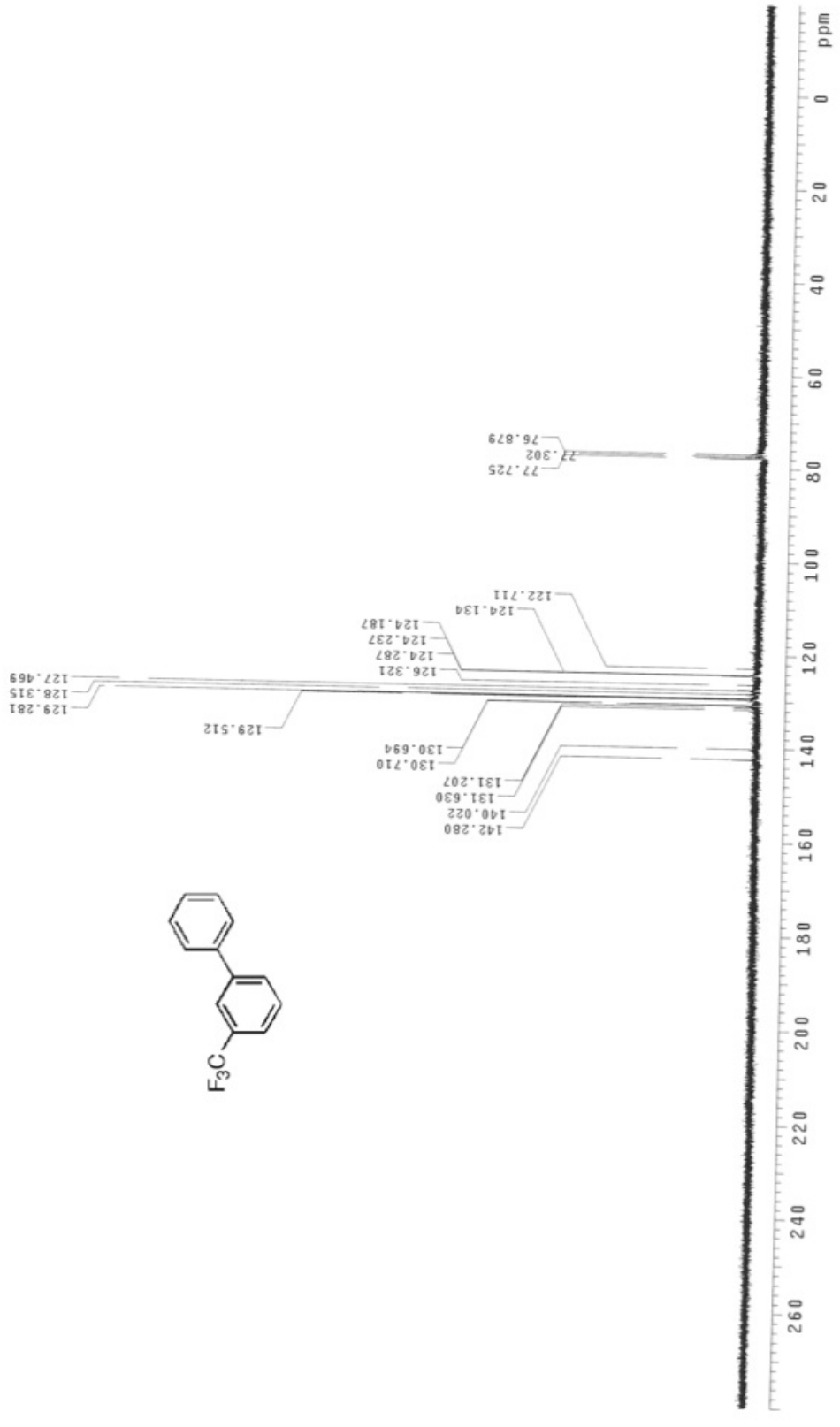
F3C
142.280
140.022
131.630
131.207
130.710
130.694
129.512
129.261
128.315
127.469
126.321
124.287
124.237
124.187
124.134
122.711
77.725
77.302
76.879
ppm

Current Data Parameters
NAME JN5-96-030
EXPNO 1
PROCNO 1
F2 - Acquisition Parameters
Date_ 20090731
Time 2.13
INSTRUM spect
PROBHD 5 mm BBO BB-1H
PULPROG zg30
TD 65536
SOLVENT CDCl3
NS 16
DS 2
SWH 8278.146 Hz
FIDRES 0.126314 Hz
AQ 3.9584243 sec
RG 57
DW 60.400 usec
DE 6.00 usec
TE 293.2 K
D1 1.00000000 sec
TD0 1
======== CHANNEL f1 ========
NUC1 1H
P1 15.07 usec
PL1 0.00 dB
SFO1 400.1324710 MHz
F2 - Processing parameters
SI 65536
SF 400.1300212 MHz
WDW EM
SSB 0
LB 0.30 Hz
GB 0
PC 1.00
2.139
7.983
7.728
7.533
7.514
7.499
7.482
7.392
7.374
7.356
7.319
7.301
7.286
Me
H
N
O
3.339
0.949
1.000
3.221
2.157
2.929
ppm

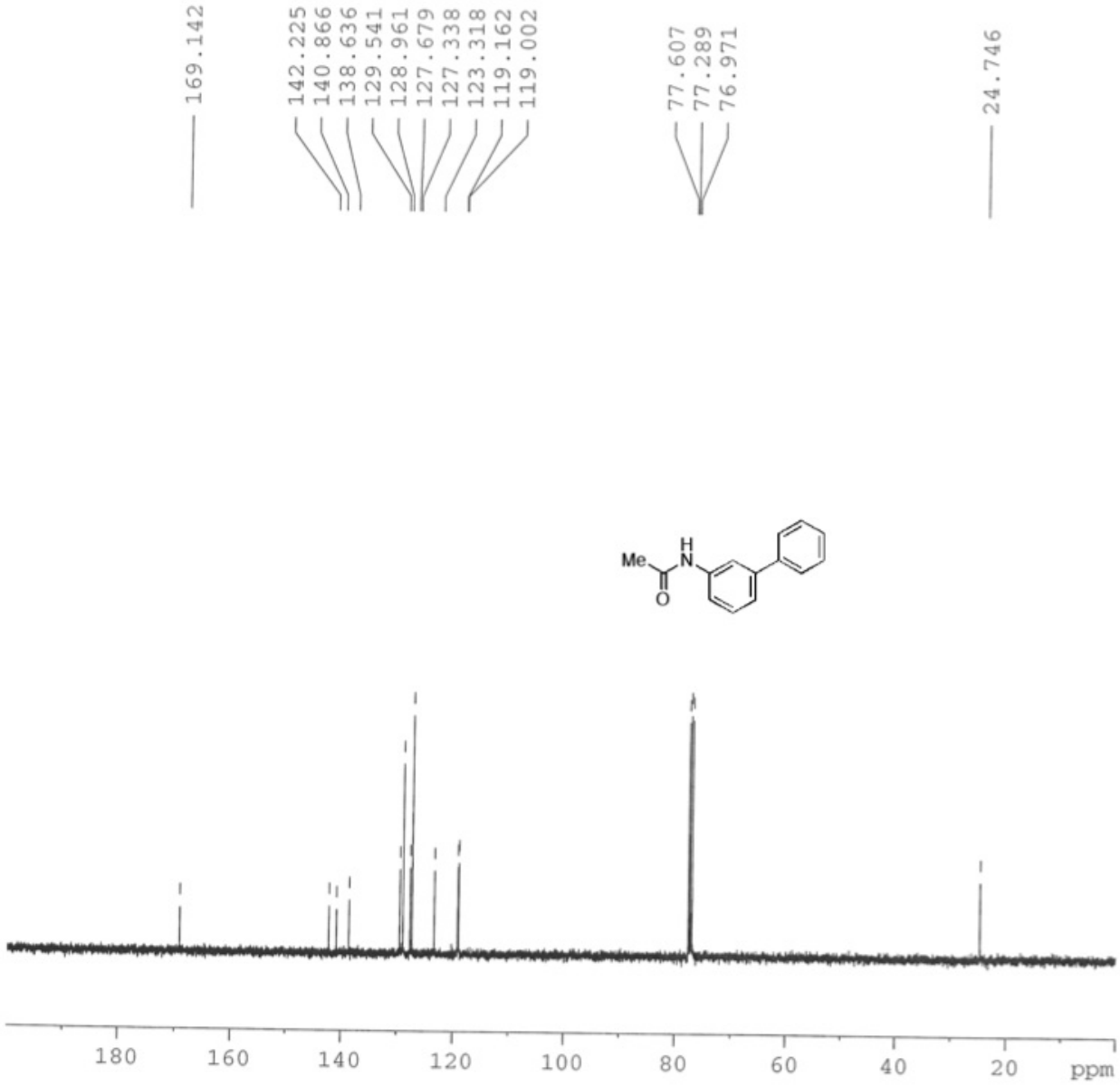

BRUKER

Current Data Parameters
NAME JN5-96-030
EXPNO 13
PROCNO 1

F2 - Acquisition Parameters
Date_ 20090731
Time 2.19
INSTRUM spect
PROBHD 5 mm BBO BB-1H
PULPROG zgpg30
TD 65536
SOLVENT CDCl3
NS 40
DS 2
SWH 23980.814 Hz
FIDRES 0.365918 Hz
AQ 1.3664756 sec
RG 9195.2
DW 20.850 usec
DE 6.00 usec
TE 293.2 K
D1 2.00000000 sec
d11 0.03000000 sec
DELTA 1.89999998 sec
TD0 1

======== CHANNEL f1 ========
NUC1 13C
P1 8.75 usec
PL1 -3.00 dB
SFO1 100.6228298 MHz

======== CHANNEL f2 ========
CPDPRG2 waltz16
NUC2 1H
PCPD2 90.00 usec
PL2 -1.00 dB
PL12 14.52 dB
PL13 18.00 dB
SFO2 400.1316005 MHz

F2 - Processing parameters
SI 65536
SF 100.6127514 MHz
WDW EM
SSB 0
LB 1.00 Hz
GB 0
PC 1.40

2.5 References

1. For reviews of the Stille reaction see: T. N. Mitchell, in: 'Metal-catalyzed Cross-coupling Reactions, 2nd edition, ed. by: A. de Meijere and F. Diederich, Wiley-VCH, Weinheim, 2004, pp 125; P. Espinet and A. M. Echavarren, *Angew. Chem. Int. Ed*., 2004, **43**, 4704.

2. M. Kosugi, K, Sasazawa, Y. Shimizu and T. Migita, *Chem. Lett*., 1977, 301

3. Milstein and J. K. Stille, *J. Am. Chem. Soc*., 1978, **100**, 3636; D. Milstein and J. K. Stille, *J. Org. Chem*., 1979, **44**, 1613; J. K. Stille, *Pure Appl. Chem.,* 1985, **57**, 1771.

4. A.-M. Lord, M. F. Mahon, M. D. Lloyd and M. D. Threadgill, *J. Med. Chem*., 2009, **52**, 868; D. Amans, V. Bellosta and J. Cossy, *Org. Lett*., 2007, **9**, 4761; M. D. Cullen, B. L. Deng, T. L. Hartman, K. M. Watson, R. W. Buckheit, C. Pannecouque, E. DeClercq and M. Cushman, *J. Med. Chem*., 2007, **50**, 4854; V. Uchil, B. Seo and V. Nair, *J. Org. Chem*., 2007, **72**, 8577.

5. V. Sofiyev, G. Navarro and D. Trauner, *Org. Lett*., 2008, **10**, 149; S. Lopez, J. Montenegro and C. Saa, *J. Org. Chem*., 2007, **72**, 9572; D. Schweitzer, J. J. Kane, D. Strand, P. McHenry, M. Tenniswood and P. Helquist, *Org. Lett*., 2007, **9**, 4619.

6. C. Song and T. M. Swager, *Macromolecules,* 2009, **42**, 1472; T. Qi, Y. Liu, W. Qiu, H. Zhang, X. Gao, Y. Liu, K. Lu, C. Du, G. Yu and D. Zhu, *J. Mater. Chem*., 2008, **18**, 1131; J. Gau, L. Li, Q. Meng, R. Li, H. Jiang, H. Li and W. Hu, *J. Mater. Chem*., 2007, **17**, 1421; K. R. J. Thomas, J. T. Lin, Y.-T. Tao and C. H. Chuen, *J. Mater. Chem*., 2002, **12**, 3516.

7. S. M. Jenkins, K. Ehman and S. Barone Jr., *Dev. Brain Res*., 2004, **151**, 1; A. S. Stasinakis, N. S. Thomaidis and T. D. Lekkas, *Ecotox. Environ. Safe*., 2001, **49**, 275; N. J. Snoeij, A. H. Penninks and W. Seinen, *Environ. Res*., 1987, *44*, 335;

8. For recent reviews of the Suzuki-Miyaura reaction see: R. Martin and S. L. Buchwald, *Acc. Chem. Res*., 2008, **41**, 1461; H. Doucet, *Eur. J. Org. Chem*., 2008, 2013.

9. F. Littke and G. C. Fu, *Angew. Chem. Int. Ed*., 2002, **41**, 4176.

10. Corbet and G. Mignani, *Chem. Rev*., 2006, **106**, 2651; A. L. Casado, P. Espinet and A. M. Gallego, *J. Am. Chem. Soc*., 2000, **122**, 11771; V. Farina, V. Krishnamurthy and W. J. Scott, 'The Stille Reaction', John Wiley & Sons, New York, NY, 1998.

11. R. H. Munday, J. R. Martinelli and S. L. Buchwald, *J. Am. Chem. Soc*. 2008, **130**, 2754.

12. Coupling of aryl tosylates, for the Suzuki-Miyaura reaction, see: H. N. Nguyen, X. Huang and S. L. Buchwald, *J. Am. Chem. Soc*. 2003, **125**, 11818; L. Ziang, T. Meng and J. Wu, *J. Org. Chem*. 2007, **72**, 9346; C. M. So, C. P. Lau, A. S. C. Chan and F. Y. Kwong, *J. Org. Chem*. 2008, **73**, 7731; for the Kumada-Corriu reaction, see: A. M. Roy and J. F. Hartwig, *J. Am. Chem. Soc*. 2003, **125**, 8704; L. Ackermann and A. Althammer, *Org. Lett*. 2006, **8**, 2457; for C–N cross-coupling, see: B. C. Hamann and J. F. Hartwig, *J. Am. Chem. Soc*., 1998, **120**, 7369; X. Huang, K. W. Anderson, D. Zim, L. Jiang, A. Klapars and S. L. Buchwald, *J. Am. Chem. Soc*., 2003, **125**, 6653.

13. Coupling of aryl mesylates, for the Hiyama reaction, see: L. Zhang, J. Qing, P. Yang and J. Wu, *Org. Lett*., 2008, **10**, 4971; for the Suzuki-Miyaura reaction, see: C. M. So, C. P. Lau and F. Y. Kwong, *Angew. Chem. Int. Ed*., 2008, **47**, 8059; for the C–N cross-coupling, see: C. M. So, C. P. Lau and F. Y. Kwong, *Angew. Chem. Int. Ed*., 2008, **47**, 8059; B. P. Fors, D. A. Watson, M. R. Biscoe and S. L. Buchwald, *J. Am. Chem. Soc*., 2008, **130**, 13552.

14. L. Schio, F. Chatreaux and M. Klich, *Tetrahedron Lett*., 2000, **41**, 1543; D. Steinhuebel, J. M. Baxter, M. Palucki and I. W. Davies, *J. Org. Chem*., 2005, **70**, 10124.

15. J. R. Naber and S. L. Buchwald, *Adv. Synth. Catal.,* 2008, **250**, 957.

16. M. R. Biscoe, B. P. Fors and S. L. Buchwald, *J. Am. Chem. Soc.,* 2008, **130**, 6686.

17. For the coupling of 2-methylphenyltosylate and 2,4,6-trimethylphenyltributylstannane the GC conversion was measured to be 40% after the standard reaction conditions of 14 h at 110 °C with 2 mol% Pd.

18. J. E. Milne and S. L. Buchwald, *J. Am. Chem. Soc.,* 2004, **126**, 13028.

19. X. Huang, K. W. Anderson, D. Zim, L. Jiang and S. L. Buchwald, *J. Am. Chem. Soc.,* 2003, **125**, 6653.

20. E. Barder, S. D. Walker, J. R. Martinelli and S. L. Buchwald *J. Am. Chem. Soc.,* 2005, **127**, 4685.

21. J. Becht and C. Le Drian, *Org. Lett.,* 2008, **10**, 3161.

22. K. Fuchibe and T. Akiyama, *J. Am. Chem. Soc.,* 2006, **128**, 1434.

23. D. Saha, K. Chattopadhyay and B. C. Ranu, *Tetrahedron Lett.,* 2009, **50**, 1003.

24. H. Lipshutz, T. B. Petersen and A. R. Abela, *Org. Lett.,* 2008, **10**, 1333.

25. E. Alacid and C. Najera, *Org. Lett.,* 2008, **10**, 5011.

26. S. E. Denmark and J. D. Baird, *Org. Lett.,* 2006, **8**, 793.

27. Z. Bosshand, *Helv. Chim. Acta,* 1961, **44**, 1985.

Chapter 3 - Multistep Microchemical Synthesis Enabled by Microfluidic Distillation

3.1 Introduction

Complex organic molecules, such as active pharmaceutical ingredients, are synthesized via multiple reactions, which require work-up and isolation of the intermediates. Recent interest in microfluidic systems for continuous-flow synthesis has motivated the integration of multiple chemical reactions and separations in an attempt to streamline the process.[1-4] Microreactor networks provide advantages for chemical synthesis such as enhanced heat and mass transfer characteristics, safety of operation, isolation of sensitive reactions from air or moisture and a reduction of hazardous waste, while potentially providing a fundamental understanding of how production-scale processes operate.[5-16] Nevertheless, studies combining multiple steps in a flow system are relatively limited.[1-3, 17-25] Recently, multiple reaction steps were combined with intermediate liquid-liquid extractions to provide a continuous-flow synthesis of carbamates, which proceeded via a Curtius rearrangement of organic azides followed by a reaction of the isocyanate with an alcohol.[1] This example illustrates the advantage of forming and immediately using small quantities of potentially hazardous intermediates (organic azides) in continuous-flow. By taking advantage of the high interfacial area in micro-scale multiphase flow systems, intermediate extraction steps allowed for the completion of three sequential reaction steps.[1] Other reports have combined reactions with a liquid-liquid extraction for the determination of Co(II) concentration in a Co/Cu mixture,[3] multiple reaction steps without intermediate separations,[19, 22] multiple steps with off-line workups using solid-supported reagents and catalysts,[17, 21] and solvent exchange by evaporation through porous poly(dimethylsiloxane).[18] The integration of reactions with analysis on chip has also advanced the field of micro total analysis systems (μTAS).[20, 26, 27] These studies underscore the importance of integrating different unit operations to perform synthetic transformations.

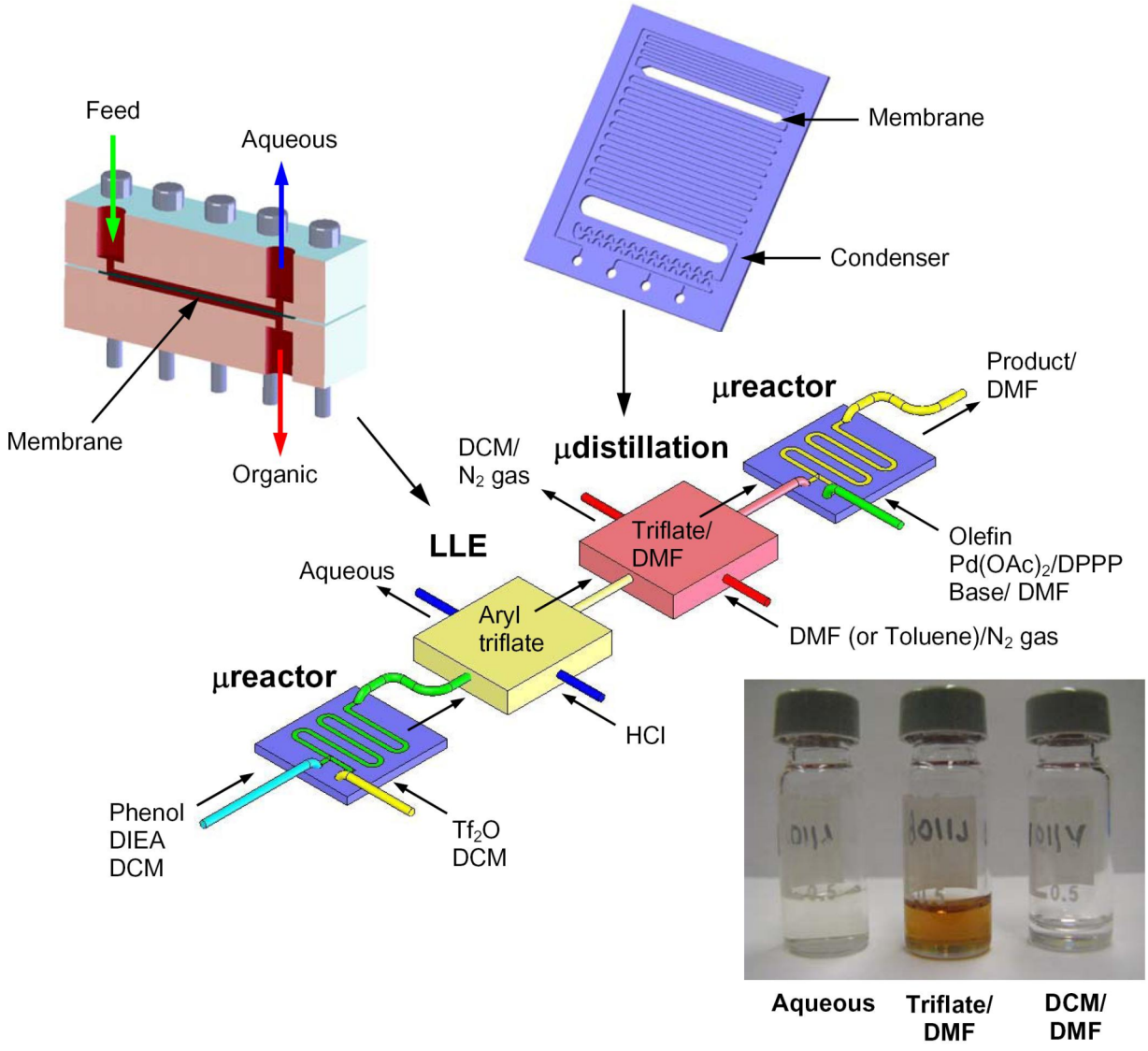

Figure 1. Reaction and separation scheme for continuous-flow synthesis involving solvent switch using microfluidic distillation.

A typical batch synthesis requires a variety of reactions, separation techniques and purifications. Separations are equally essential for continuous-flow chemistry, with single-step liquid-liquid extraction[28-30] and microevaporation[18, 31-35] having already been demonstrated. Distillation is an important method for separating liquid mixtures and can allow for both purification and solvent exchange. Distillation processes operate by exploiting the difference in volatility between the components in a liquid mixture. Microfluidic distillation, based exclusively on boiling point differences, is challenging because

surface forces dominate over body forces at these length scales. By using gas-liquid segmented flow in conjunction with gas-liquid separators, limitations were overcome to enable the separation of binary solvent mixtures.[36] Combining microfluidic distillation with multiple reaction steps would offer an instrumental tool for synthetic organic chemistry and would provide a deeper understanding of how multi-step microfluidic processes operate. In the current work, we present the first example of a multi-step chemical synthesis employing a microfluidic distillation to exchange reaction solvents (Figure 1).

The Heck reaction is a versatile transformation in organic chemistry[37, 38] that finds applications in the production of active pharmaceutical ingredients[39], natural product synthesis[40, 41] and fine chemical production[42]. In addition to aryl halides, aryl triflates and nonaflates can be used as coupling partners to extend the scope of the reaction to a wider range of starting materials and to access regioisomeric products.[43] Because of this, examples of Heck reactions with aryl triflates are common; however, the almost complete lack of commercial availability of aryl triflates necessitates their preparation prior to their use in Heck reactions[44-48].

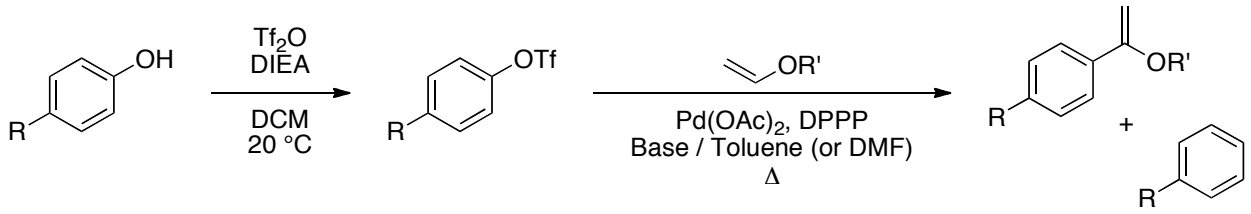

Scheme 1. Model chemistry for continuous-flow solvent exchange (R = t-Bu, R' = n-Bu).

Triflates are commonly prepared in chlorinated solvents from phenols and trifluoromethanesulfonic anhydride using stoichiometric amine bases. After the reaction, a general workup procedure can include removal of the chlorinated solvent and addition of another solvent such as ethyl acetate (EA) to facilitate the workup. Liquid-liquid extraction of the reaction mixture with aqueous acid, base and brine to remove salt byproducts and excess reagents, followed by removal of the solvent and often purification of the triflate. In the second reaction step, the purified triflate, alkene coupling partner, amine base, palladium precatalyst and ligand are combined in a polar aprotic solvent, such as DMF, and heated to 100 °C or

higher for the duration of the reaction (see Scheme 1).

3.2 Results and Discussion

In the continuous flow process, we wanted to take advantage of both the glassware-like compatibility and excellent heat transfer properties of silicon based microreactors to perform the chemistry, and the high interfacial area that results from the small length scales of the microsystems to increase the efficiency of the liquid-liquid extraction.[28] The first reaction step, the synthesis of an aryl triflate from a phenol and triflic anhydride (see Scheme 1), was carried out in a microreactor as illustrated in Figure 1. The syntheses of two different aryl triflates were investigated at 20 ºC: 4-tert-butylphenyl trifluoromethanesulfonate and (*S*)-1,1'-binaphthyl-2,2'-diyl bis(trifluoromethanesulfonate). Upon exiting the microreactor, the product was combined with 2.0 M hydrochloric acid (HCl) and segmented flow was established.[49-51] Side-by-side contact of HCl slugs with the organic phase enhanced mass transport of DIEA to the aqueous droplets, making possible a single-stage liquid-liquid extraction.[1, 28, 49-51]

As shown in the reaction sequence of Figure 1, purified aryl triflate exiting the liquid-liquid extraction was combined with pure toluene (or DMF). The resulting stream (with a DCM-to-toluene volumetric ratio of 1:4) was then delivered to the microfluidic distillation device (Figure 1). Gas-liquid segmented flow was established by combining nitrogen gas with the liquid stream, which enabled controlled flashing. The temperature of the distillation device (70 ºC) was maintained above the boiling point of DCM (i.e., 40 ºC) yet below the boiling point of toluene (i.e., 110 ºC) or DMF (i.e., 153 ºC). Consequently, the vapor phase was enriched with DCM while the liquid phase was comprised mostly of toluene (or DMF) and aryl triflate. The liquid and vapor phases were further separated by exploiting the differences in their surface tensions. The device was designed such that the liquid (i.e., reaction products and solvent) flowed through an integrated PTFE membrane (0.5 μm pore size) while the vapor did not. Detailed pressure drop calculations, device fabrication, and theory of operation have been previously reported.[36]

In addition to the multi-step experiment, samples of the aqueous phase, vapor condensate and product streams were collected after the distillation stage for analysis. A photograph of a set of these samples is shown in Figure 1. It can be seen in this figure that the distillate appeared to be colorless while the product stream was orange-brown. NMR analysis confirmed that the triflate remained in the liquid product stream in the case of DCM-to-toluene solvent exchange, and that the starting material was converted to the triflate in 91-95% yield. The analysis also identified that 93% of the DIEA was extracted into the aqueous phase while the remaining 7% was in the liquid product stream. The vapor condensate exiting the distillation stage was exclusively comprised of DCM and toluene as confirmed by NMR analysis.

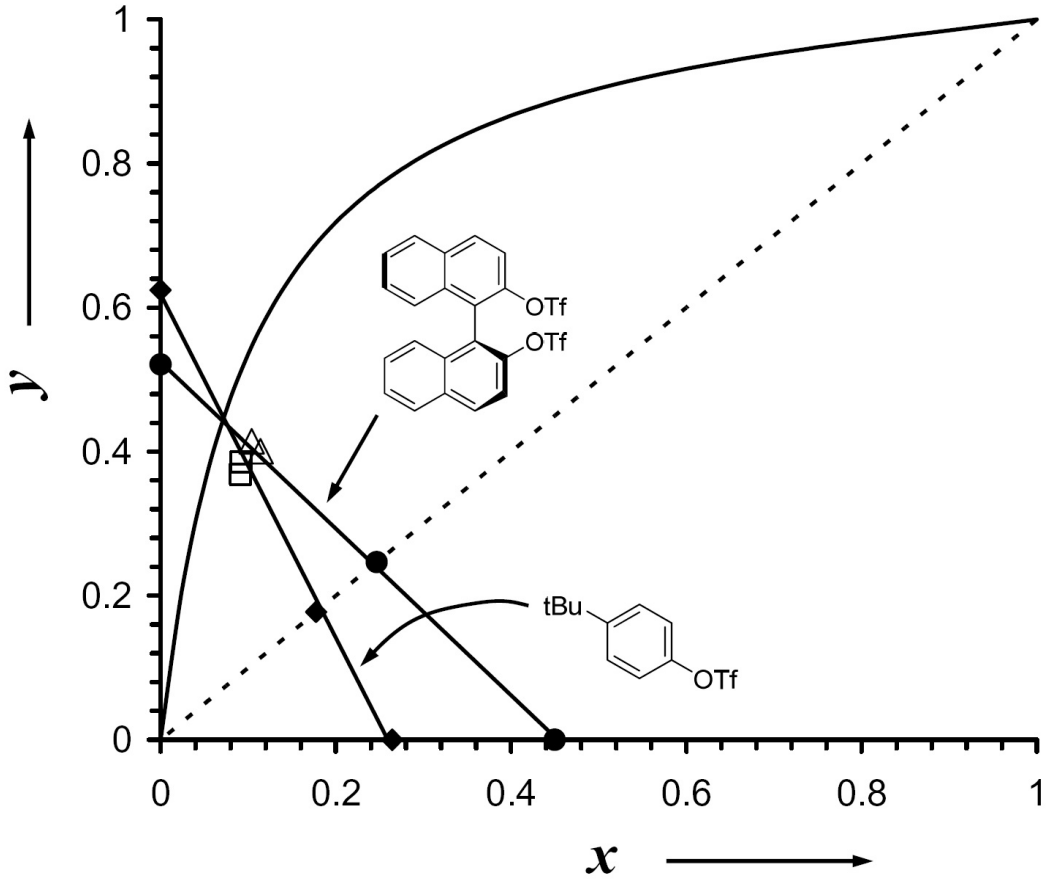

Figure 2. Mole fraction of DCM in the liquid stream (x) versus the mole fraction of DCM in the vapor condensate stream (y) for the separation of DCM and toluene at 70 ºC in the presence of two different triflates.

When a liquid mixture is comprised of two or more components with different volatilities, a phase equilibrium of the varying compositions exists and can be represented by a McCabe-Thiele diagram (see the experimental section for more details).[52, 53] Figure 2 shows the McCabe-Thiele diagram for the DCM-toluene solvent exchange that was studied.

In Figure 2, the theoretical equilibrium of a DCM-toluene binary mixture (at 70.0 ºC) is shown by the curved line. The straight lines are described by Equation (**3**) and represent the mass balance during the separation of DCM and toluene for both triflate syntheses. Details on how these operating lines were obtained can be found in the Experimental section. For the synthesis of (*S*)-1,1'-binapthyl-2,2'-diyl bis(trifluoromethanesulfonate) (BINOL-triflate), we observed that DCM compositions of 0.11 ± 0.01 (liquid product stream) and 0.41 ± 0.01 (vapor condensate stream) were close to those predicted by the equilibrium diagram (△ in Figure 2). Similarly, values of 0.09 ± 0.01 (liquid product stream) and 0.38 ± 0.01 (vapor condensate stream) were measured during the synthesis and separation of 4-tert-butylphenyl triflate (□ in Figure 2). Careful analysis of Figure 2 also shows that the DCM content of the feed stream was reduced from 0.2 (or 0.25 for BINOL-triflate) to 0.1 mol fraction. Thus, diluting the product stream from the first reaction step and carrying out one distillation step resulted in a switch of the solvent composition from 100% DCM to 90:10 toluene:DCM.

The synthesis of 4-tert-butylphenyl trifluoromethanesulfonate (**1**) and subsequent solvent exchange from DCM to DMF was also investigated (Figure 3). We observed that increasing the distillation temperature from 120 ºC to 125 ºC resulted in a fundamental change in operation. At 120 ºC, the slope of the operating line (i.e., the ratio of molar flowrate of liquid stream to vapor condensate) was > 1, however, at 125 ºC the slope was < 1. Such control over flowrates is advantageous for continuous-flow chemical processes. Adjusting temperature alone can potentially change the entire outcome of the downstream microchemical process. Trace amounts of aryl triflate (< 0.3 mol%) were found in the vapor condensate collected during solvent exchange from DCM to DMF, implying that operation at higher temperatures resulted in product vaporization. Calculation of the total molar flowrates through the system revealed that

the mol fraction of aryl triflate vaporized, *f*, ranged from 0.07 to 0.22. Loss of product in a chemical process is undesirable, but can potentially be minimized using a more selective separation process. For example, multi-stage distillation would enable lower operating temperatures, maximizing solvent separation, and minimizing product losses.

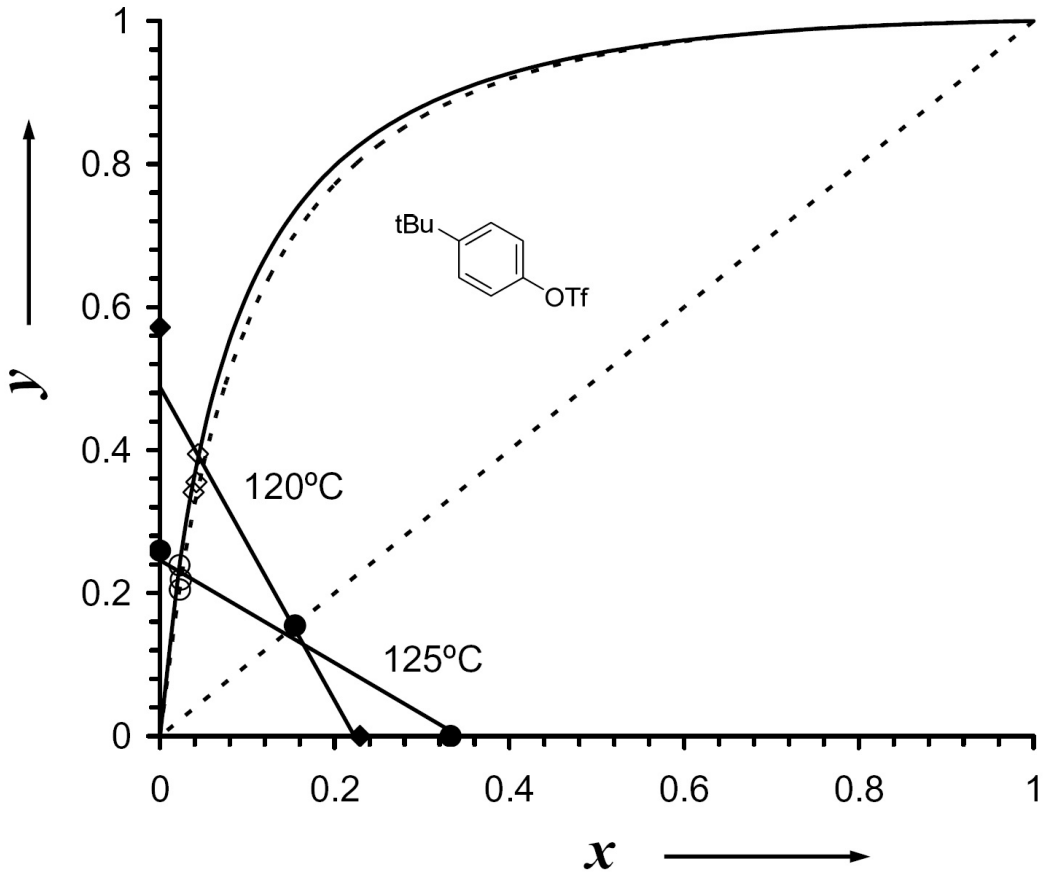

Figure 3. Mole fraction of DCM in the liquid stream (*x*) versus the mole fraction of DCM in the vapor condensate stream (*y*) for the separation of DCM and DMF at 120 °C and 125 ºC in the presence of **1**. The curved dashed line represents the change in equilibrium.

In the final reaction step (see Scheme 1), a palladium-catalyzed coupling of **1** with n-butyl vinyl ether was carried out by combining the product stream exiting the microfluidic distillation stage with the other reagents and a catalyst in a downstream microreactor at 125 ºC (see Figure 1). Analysis of the samples exiting the microreactor elucidated the extent of the reaction. Table 1 shows the residence time, DCM

composition, conversion of aryl triflate, and yield of the Heck product, 1-(1-Butoxyvinyl)-4-*tert*-butylbenzene (**2**), with increasing distillation stage temperature.

Table 1. Residence time, DCM composition, conversion, and yield as a function of distillation temperature.

Temp (°C)	Res. Time (min)	DCM (vol%)	Conv. (%)[a]	Yield (%)[a]
110	5.1	9.6	47.1 ± 8.7	42.8 ± 5.9
120	5.5	7.1	67.6 ± 4.5	57.5 ± 4.1
125	8.1	6.0	96.3 ± 0.4	76.8 ± 0.7

[a] Average of three samples with standard deviation

Increasing the temperature increases the amount of volatile solvent separated from the product stream, which decreased the volume fraction of DCM, increased the concentration of the triflate and decreased the flowrate of the product stream. Concentrating the aryl triflate entering the final reactor increased the reaction rate while decreasing the total flowrate resulted in a longer residence time for the reaction (Table 1). Batch experiments were performed to elucidate the influence of residual DCM on the Heck reaction. Table 3 shows that the reaction was most efficient in pure DMF and increasing the fraction of DCM decreased the product yield, which was in agreement with the results in flow. As shown in Scheme 1, reduction of the triflate was also observed during the Heck reaction. The selectivity for the **2** relative to the reduced product remained constant and was estimated to be ~15:1.

The preparation of an aryl triflate followed by a Heck reaction of this triflate represented a case study for multistep synthesis with integrated microfluidic distillation. Continuous operation of the scheme presented in this paper could produce uninterrupted quantities of 1-(1-butoxyvinyl)-4-tert-butyl benzene. Based on data reported in Table 1 and the residence times investigated, approximately 32 mg/hr (or 0.135 mmol/hr) of product could be synthesized. In order to test this, an experiment was repeated using the conditions from line 3 of Table 1 and the product stream was collected for 5.5 hours. As described in the

experimental section, the product was hydrolyzed to the methyl ketone (**3**)[54], which was isolated in a 69% yield. Just as importantly, the working principles can be applied to other chemical reactions to achieve continuous-flow syntheses. For example, toluene could be removed to concentrate the isocyanate intermediated in the flow synthesis of carbamates without the need for a collection/boiling tank.[1] In addition to performing manipulations with solvents during a synthesis, microfluidic distillation can potentially be used as a product purification process or as a separation step to facilitate reagent recycling.

3.3 Conclusion

In conclusion, we have designed a microfluidic distillation operation, which exploits differences in volatility between components in liquid mixtures. Microfluidic distillation was used to allow the completion of a microchemical synthesis involving multiple reaction and separation steps. A triflate was synthesized in DCM, after which the solvent was switched to either toluene or DMF, and a palladium-catalyzed Heck reaction was performed. Microfluidic distillation offers new opportunities for continuous-flow chemical synthesis that requires a separation between the reaction steps. Moving forward, however, is not without challenges. Strategies for handling solids in microchemical systems will enable multistep synthesis using solid reagents and/or catalysts, or when solid by-products or products are formed. Furthermore, the integration of multiple distillation stages promises more selective separations.

3.4 Experimental

A DCM solution of the substrate (1.0 M), base (1.5 M DIEA) and internal standard (0.2 M) was loaded into a syringe and a DCM solution of Tf_2O (1.2 M) was loaded into a separate syringe (Hamilton Gastight 2.5 mL) and delivered to the first microreactor (see Figure 1) using a Harvard Apparatus syringe pump (3 to 4 μL/min). Two additional pumps and five separate syringes were used to deliver 2.0 M HCl (24 μL/min), pure toluene or DMF (24 μL/min), and DMF solutions of 4.0 M *n*-butyl vinyl ether, 4.0 M base, and 0.033 M $Pd(OAc)_2$/0.050 M DPPP (all at 2 μL/min) in subsequent steps according to Figure 1. Nitrogen gas was delivered to the microdistillation stage directly from a gas tank fitted with a regulator. The three inlets and outlet of each microreactor were cooled (20 ºC) using chucks that have been

described previously,[36] while the main reaction channels were heated using cartridge heaters in conjunction with PID controllers and aluminum chucks.

Sample analysis: NMR spectroscopy was used to identify the product and quantify concentrations of DCM, toluene, and DMF in all streams. GC analysis was used to quantify concentrations of the reagents and products in all streams.

General Reagent Information

All reactions were carried out under an argon atmosphere. The DMF was purchased from Aldrich Chemical Company in Sure-Seal bottles and was used as received. Toluene and dichloromethane (DCM) were purchased from J.T. Baker in CYCLE-TAINER® solvent-delivery kegs and vigorously purged with argon for 2 h. The solvent was further purified by passing it under argon pressure through two packed columns of neutral alumina and copper (II) oxide. Phenols, amine bases, biphenyl and trifluoromethanesulfonic anhydride were purchased from Aldrich Chemical Company, Alfa Aesar, and TCI America and were used as received. Diphenylphosphinopropane (dppp) was purchased from Aldrich Chemical Company. $Pd(OAc)_2$ was received as a gift from BASF. Flash chromatography was performed by standard technique on SilicaFlash® F60 silica gel available from Silicycle.

General Analytical Information

All compounds were characterized by ^1H NMR, ^{13}C NMR, IR spectroscopy, as well as, in most instances, elemental analysis. Copies of the ^1H and ^{13}C spectra can be found at the end of the experimental section. Nuclear Magnetic Resonance spectra were recorded on a Bruker 400 MHz instrument. All ^1H NMR experiments are reported in δ units, parts per million (ppm), and were measured relative to the signals for residual chloroform (7.26 ppm) in the deuterated solvent, unless otherwise stated. All ^{13}C NMR spectra are reported in ppm relative to deuterochloroform (77.23 ppm), unless otherwise stated, and all were obtained with ^1H decoupling. All IR spectra were taken on a Perkin – Elmer 2000 FTIR. All GC analyses were performed on a Agilent 6890 gas chromatograph with an FID detector using a J & W DB-1 column

(10 m, 0.1 mm I.D.). Elemental analyses were performed by Atlantic Microlabs Inc., Norcross, GA.

Table 2: Mass flowrates that were measured during the collection of product, which correspond to the data reported in Table 1.

Test	Temp (°C)	Aqueous (mg/min)	Distillate (mg/min)	Final Reactor (mg/min)
1	110	26.2	8.5	22.0
2	110	25.2	8.9	24.0
3	110	26.5	8.5	23.2
4	120	26.5	11.0	21.2
5	120	23.2	11.1	21.1
6	120	27.0	10.2	20.8
7	125	28.1	20.2	12.7
8	125	28.1	18.9	16.3
9	125	26.2	18.1	14.2

McCabe-Thiele Diagram Analysis (Figures 2 and 3)

The most elementary form of distillation is binary flash distillation. Flash distillation represents a building block, around which many other forms of distillation can be constructed, including equilibrium stages and column distillation. In flash distillation, part of a feed stream is vaporized, and the vapor and liquid in equilibrium are separated. Writing an overall mole balance on a flash distillation process gives **1** where F, L, and V are the feed, liquid, and vapor molar flowrates (mol/min), respectively.

$$F = L + V \quad \textbf{1}$$

$$zF = xL + yV \quad \textbf{2}$$

$$y = -\frac{L}{V}x + \frac{F}{V}z \quad \textbf{3}$$

When a liquid mixture is comprised of two or more components with different volatilities, the mole balance can be written as equation **2** where, z, x, and y are mole fractions of the more volatile component in the feed, liquid, and vapor streams. Combining Equations **1** and **2** and rearranging yields the operating

line for a flash distillation process, Equation **3**.

Binary vapor-liquid equilibrium data can be represented graphically by plotting the vapor mole fraction *y* as a function of the liquid mole fraction *x*. When the vapor-liquid equilibrium of a binary mixture is known, Equation **3** can be applied and its intersection with the equilibrium curve predicts the equilibrium composition (i.e., McCabe-Thiele diagram). What is more, the slope (*L/V*) and y-intercept (*zF/V*) of Equation **3** define the operation of a flash distillation process, and control vapor and liquid compositions.

Closing the mass balance around the distillation stage enabled estimation of *x*, *y*, and *z* for each component in the different streams. Thus, Equation **3** was applied to generate the data in Figures 2 and 3. The different lines within Figures 2 and 3 represent experiments each carried out under separate conditions. Consequently, the slope (i.e., *L/V*) was observed to change by manipulating temperature or injection rate. It should be noted that the vapor-liquid equilibrium curves in Figures 2 and 3 were obtained from thermodynamic simulations using Aspen Plus 2006.5.

Table 3: Yield of 1-(1-butoxyvinyl)-4-tert-butyl benzene as a function of the percent of DCM in DMF at 125 ºC and 5 min residence time.

Temp (°C)	Time (min)	DMF (μL)	DCM (μL)	DCM (vol%)	Conv. (%)[a]	Yield (%)[a]
125	5.0	2.0	0	0	98	97
125	5.0	2.0	100	5	75	71
125	5.0	2.0	200	10	66	62
125	5.0	2.0	400	20	53	49

[a] GC yields

General Procedure for Table 3

An oven-dried volumetric flask (5.00 mL), which was equipped with a magnetic stir bar and fitted with a Teflon screw-cap septum, was charged with the $Pd(OAc)_2$ (16.8 mg, 1.5 mol%) and dppp (46.4 mg, 2.3 mol%). The vessel was evacuated and backfilled with argon (this process was repeated a total of 3 times) and then DMF (~5 mL, make solution up to 5.00 mL) was added and the solution was stirred for 15 minutes to ensure complete dissolution (Solution 1). An oven-dried screw-top volumetric flask (5.00 mL) was evacuated and backfilled with argon (this process was repeated a total of 3 times) and then was charged with compound 1 (1.41 g, 5.0 mmol), 1-(vinyloxy)butane (1.00 g, 10.0 mmol), triethylamine (758 mg, 7.5 mmol) and DMF (~3 mL, make solution up to 5.00 mL) to give Solution 2. An oven-dried Schlenk tube equipped with a magnetic stir bar and a Teflon stopper was cooled to room temperature under vacuum and backfilled with argon. Under a positive flow of argon, the Teflon stopper was exchanged for a rubber septum, Solution 1 (1.0 mL), Solution 2 (1.0 mL) and DCM (100-400 μL, 5-20 %) were added sequentially by syringe. Under a positive flow of argon, the rubber septum was replaced with a Teflon stopper, the tube was sealed and heated to 125 °C for 5 minutes. The reactions were immediately placed in an ice bath, and after cooling, ethyl acetate, water and an internal standard (biphenyl) were added. An aliquot of the organic layer was passed through a plug of silica, eluting with ethyl acetate and the reactions were analyzed by GC.

General Procedure for Figure 4

An oven-dried volumetric flask (5.00 mL), which was equipped with a magnetic stir bar and fitted with a Teflon screw-cap septum, was charged with the $Pd(OAc)_2$ (16.8 mg, 1.5 mol%) and dppp (46.4 mg, 2.3 mol%). The vessel was evacuated and backfilled with argon (this process was repeated a total of 3 times) and then DMF (~5 mL, make solution up to 5.00 mL) was added and the solution was stirred for 15 minutes to ensure complete dissolution (Solution 1). An oven-dried screw-top volumetric flask (5.00 mL) was evacuated and backfilled with argon (this process was repeated a total of 3 times) and then was charged with compound 1 (1.41 g, 5.0 mmol), 1-(vinyloxy)butane (1.00 g, 10.0 mmol), triethylamine

(758 mg, 7.5 mmol) and DMF (~3 mL, make solution up to 5.00 mL) to give Solution 2. An oven-dried Schlenk tube equipped with a magnetic stir bar and a Teflon stopper was cooled to room temperature under vacuum and backfilled with argon. Under a positive flow of argon, the Teflon stopper was exchanged for a rubber septum, Solution 1 (1.0 mL) and Solution 2 (1.0 mL) were added sequentially by syringe. Under a positive flow of argon, the rubber septum was replaced with a Teflon stopper, the tube was sealed and heated to 125 °C for 1-5 minutes. The reactions were immediately placed in an ice bath, and after cooling, ethyl acetate, water and an internal standard (biphenyl) were added. An aliquot of the organic layer was passed through a plug of silica, eluting with ethyl acetate and the reactions were analyzed by GC.

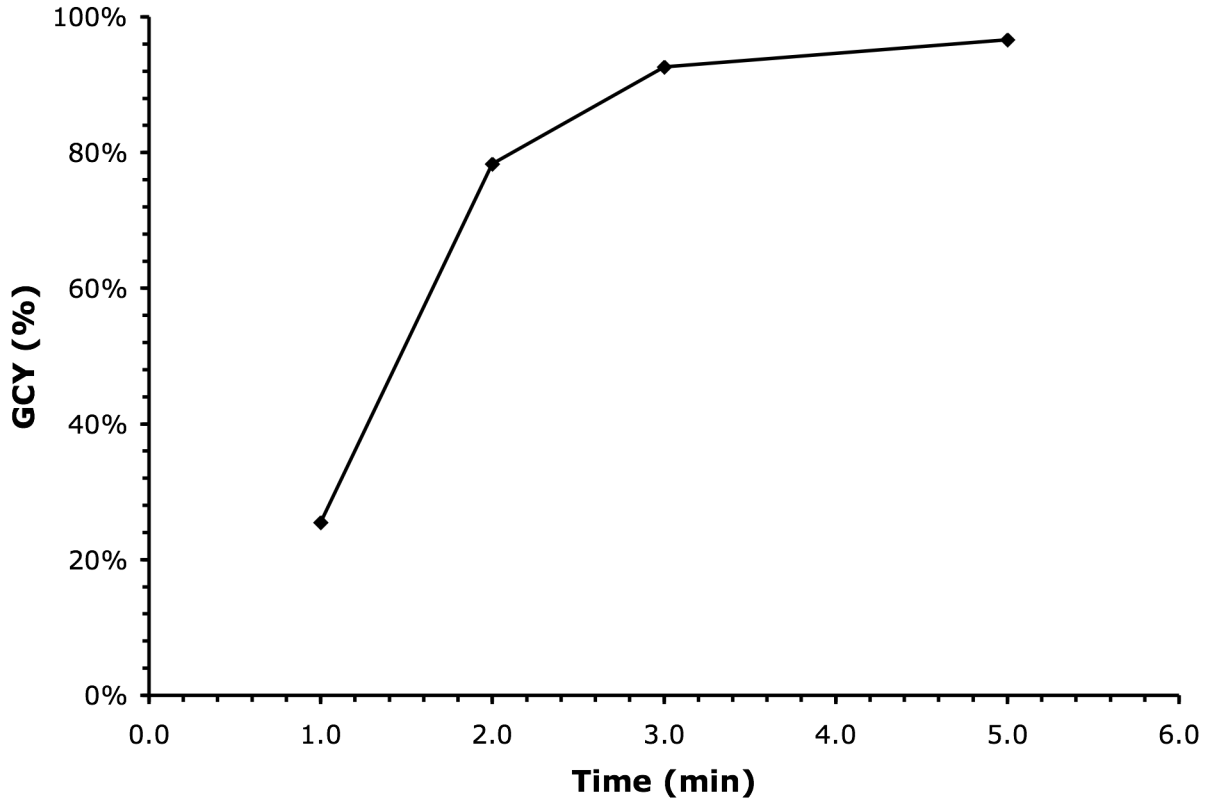

Figure 4: Yield of 1-(1-butoxyvinyl)-4-tert-butylbenzene as a function of reaction time at 125 °C

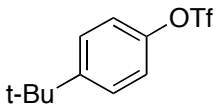

4-*tert*-Butylphenyl trifluoromethanesulfonate (1). An oven-dried round-bottomed flask that was fitted with a magnetic stirbar and a rubber septum was charged with 4-tert-butylphenol (1.50 g, 10.0 mmol). The vessel was evacuated and backfilled with argon (this process was repeated a total of 3 times) and then DIEA (1.94 g, 15.0 mmol) and DCM (20 mL) were added by syringe. The solution was cooled to 0 °C and a solution of trifluoromethanesulfonic anhydride (3.38 g, 12.0 mmol) in DCM (20 mL) was added over a period of 30 minutes. The reaction was warmed to room temperature and stirred for 1 h. At this point the solution was concentrated in vacuo, EA (50 mL) was added and the solution was washed with aqueous HCl (2 M, 50 mL). The phases were separated and the organic phase was washed with saturated aqueous $NaHCO_3$ (50 mL) followed by saturated NaCl (50 mL). The organic phase was dried over anhydrous $MgSO_4$, concentrated in vacuo and purified by silica gel chromatography (50 g silica gel, eluting with hexanes) to provide the product as a pale yellow oil (2.7 g, 96%). ^{1}H NMR (400 MHz, $CDCl_3$) δ: 7.43 (d, J = 9.0 Hz, 2H), 7.17 (d, J = 9.0 Hz, 2H), 1.31 (s, 9H) ppm. ^{13}C NMR (100 MHz, $CDCl_3$) δ: 151.8, 147.6, 127.4, 120.9, 119.0 (q, J = 317 Hz), 34.9, 31.4 ppm. IR (neat, cm^{-1}): 2968, 1505, 1426, 1251, 1212, 1142, 1015, 891, 837, 611.

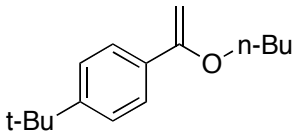

1-(1-Butoxyvinyl)-4-*tert*-butylbenzene (2). An oven-dried test tube, which was equipped with a magnetic stir bar and fitted with a Teflon screw-cap septum, was charged with the $Pd(OAc)_2$ (16.8 mg, 1.5 mol%) and dppp (46.4 mg, 2.3 mol%). The vessel was evacuated and backfilled with argon (this process was repeated a total of 3 times) and then DMF (5.0 mL) was added and the solution was stirred for 15 minutes to ensure complete dissolution. An oven-dried screw-top volumetric flask (5.00 mL) was evacuated and backfilled with argon (this process was repeated a total of 3 times) and then was charged with compound 1 (1.41 g, 5.0 mmol), 1-(vinyloxy)butane (1.00 g, 10.0 mmol), triethylamine (758 mg, 7.5

mmol) and DMF (~3 mL, make solution up to 5.00 mL). This solution of reagents was added via syringe to the stirred solution of $Pd(OAc)_2$ and dppp and the resulting solution was heated to 110 °C for 1 h. The reaction was cooled. EA (20 mL) was added, and the solution was washed with saturated $NaHCO_3$ (3 x 25 mL) and with saturated NaCl (25 mL). The organic layer was dried over anhydrous $MgSO_4$, concentrated in vacuo and purified by passing it through a short plug of silica gel, providing the product as a pale yellow oil (1.13 g, 97%). ^{1}H NMR (400 MHz, $CDCl_3$) δ: 7.62 (d, *J* = 8.5 Hz, 2H), 7.41 (d, *J* = 8.5 Hz, 2H), 4.65 (d, *J* = 2.0 Hz, 1H), 4.20 (d, *J* = 2.0 Hz, 1H), 3.90 (t, *J* = 2.0 Hz, 2H), 1.83 (pentet, *J* = 7.5 Hz, 2H), 1.57 (sextet, *J* = 7.5 Hz, 2H), 1.37 (s, 9H), 1.04 (t, *J* = 7.5 Hz, 3H) ppm. ^{13}C NMR (100 MHz, $CDCl_3$) δ: 160.2, 151.5, 134.2, 125.6, 125.2, 81.5, 67.5, 34.7, 31.5, 31.4, 19.7, 14.1 ppm. IR (neat, cm^{-1}): 2961, 2871, 1640, 1606, 1462, 1315, 1300, 1282, 1135, 841, 793.

Equipment Setup

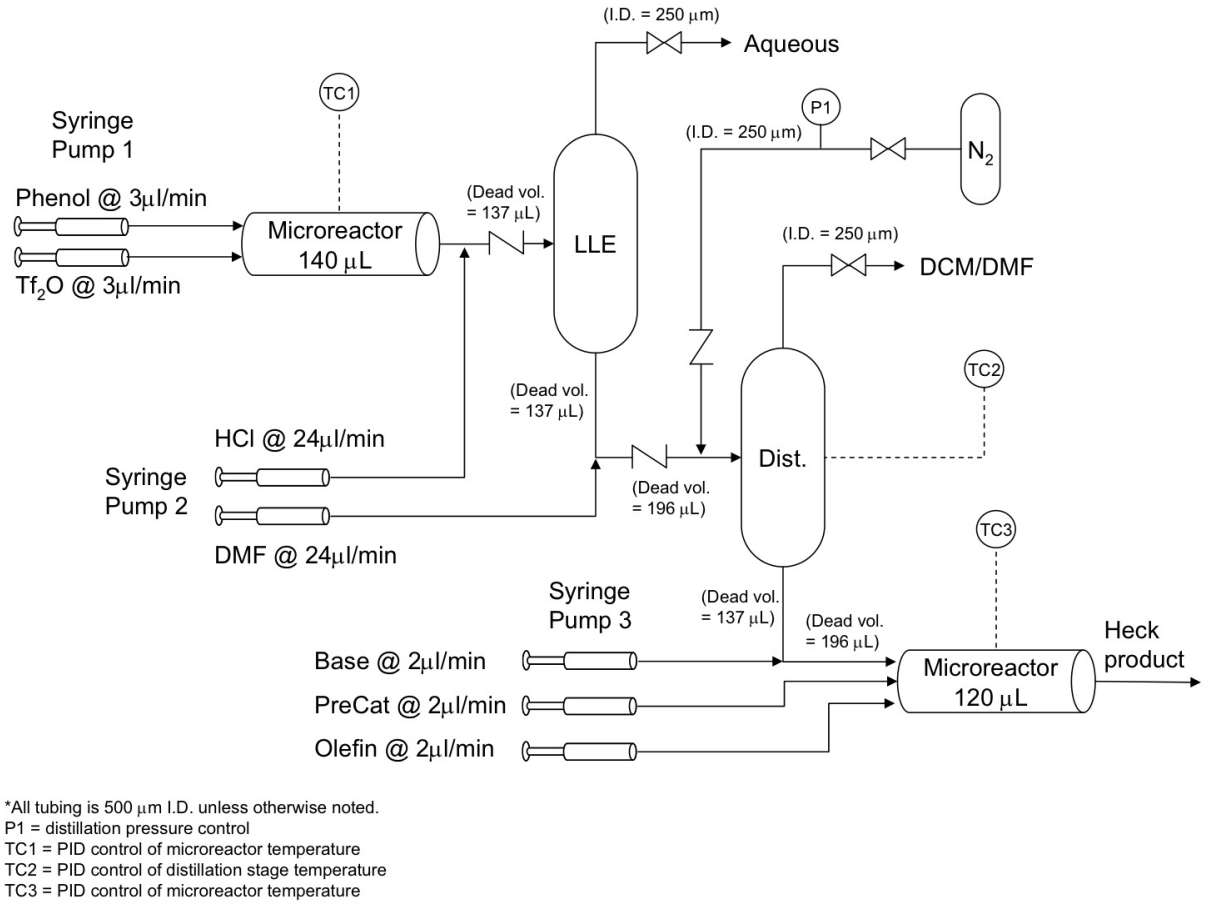

*All tubing is 500 μm I.D. unless otherwise noted.
P1 = distillation pressure control
TC1 = PID control of microreactor temperature
TC2 = PID control of distillation stage temperature
TC3 = PID control of microreactor temperature

Figure 5: Process flow diagram for the multistep synthesis platform.

Figure 5 details the equipment layout and specifications of Figure 1. The microreactors were fabricated from a double-polished silicon wafer and a Pyrex wafer (both 150 mm in diameter and 650 μm thick). The fabrication process involved several photolithography steps, deep reactive ion etching of silicon, and low-pressure chemical vapor deposition of silicon nitride. Pyrex anodic bonding capped silicon nitride features, and thus formed the final microfluidic devices. The fabricated microchannels were 0.4 x 0.4 x 875 mm. Standard machining techniques were employed to produce compression chucks (316 Stainless Steel). Each microreactor was fitted with a compression chuck that controlled the temperature of inlets and outlet (to 20ºC) using a Thermo Scientific NESLAB RTE-7 refrigerating bath. Consequently, reagent mixing was made feasible under cooled conditions. A second compression chuck was used in each device to maintain a high temperature in the primary microfluidic channel. The heated sections of each device were driven by an Omega 120V cartridge heater controlled by an Omega CN9000 series PID controller. Further details of the design and fabrication of the liquid-liquid extraction and microfuidic distillation devices can be found in References [24] and [32], respectively.

General Procedure for Multi-step Reactions

An oven-dried volumetric flask (5.00 mL), which was fitted with a Teflon screw-cap septum, was charged with biphenyl (308 mg, 2.0 mmol) and 4-*tert*-butylphenol (750 mg, 5.0 mmol). The vessel was evacuated and backfilled with argon (this process was repeated a total of 3 times) and then was charged with DIEA (1.3 mL, 7.5 mmol) and DCM (~4 mL, make solution up to 5.00 mL) to give Solution 1. An oven-dried screw-top volumetric flask (5.00 mL) was evacuated and backfilled with argon (this process was repeated a total of 3 times) and then was charged with triflic anhydride (1.0 mL, 6.0 mmol) and DCM (~4 mL, make solution up to 5.00 mL) to give Solution 2. Three oven-dried volumetric flasks (5.00 mL), which were fitted with a Teflon screw-cap septa were used to make Solutions 3-5. Two of these flasks were evacuated and backfilled with argon (this process was repeated a total of 3 times). The first was charged with triethylamine (2.8 mL, 20.0 mmol) and the second with n-butyl vinyl ether (2.6 mL, 20.0 mmol) and n-tetradecane (400 μL, 1.5 mmol). The flasks were then made up to volume with DMF to give Solutions 3

and 4, respectively. The fifth flask was charged with $Pd(OAc)_2$ (37.8 mg, 0.17 mmol) and dppp (104 mg, 0.25 mmol) prior to evacuation and backfilling with argon (repeated a total of 3 times). The flask was then filled with DMF (~5 mL) and mixed for 10 minutes to ensure complete dissolution (Solution 5). These solutions were loaded into Hamilton Gastight syringes and connected to the microfluidic system as diagrammed in Figure S3. The product stream was collected on ice and after cooling, ethyl acetate and water were added. An aliquot of the organic layer was passed through a plug of silica, eluting with ethyl acetate and the reactions were analyzed by GC.

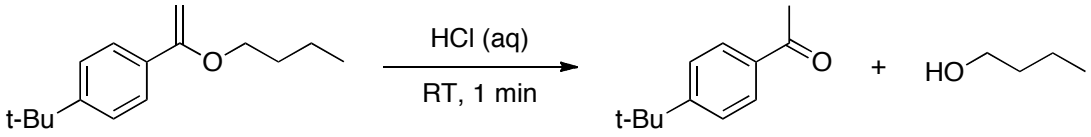

Scheme 2: Hydrolysis of **2** to give 1-(4-(tert-butyl)phenyl)ethanone (**3**)

Procedure for obtaining an isolated yield from the multi-step process:

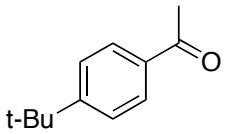

1-(4-(*tert*-Butyl)phenyl)ethanone (3). Products such as **2** are well known to be acid sensitive, and as such hydrolysis to the aryl methyl ketones facilitates isolation [see reference 54]. Solutions 1-5 were prepared following the general procedure described above, with the omission of the n-tetradecane from solution 4. The solutions were loaded into Hamilton Gastight syringes and connected to the microfluidic system as diagrammed in Figure 5. Once the flowrates and pressures had stabilized to a steady-state, a sample was collected over saturated $NaHCO_3$ (aq) for 5.5 hours. The sample was transferred to a separatory funnel, ethyl acetate (EA) and water were added and mixed thoroughly. GC analysis of the organic layer determined the yield of **2** to be 79.8% relative to the biphenyl internal standard. The aqueous layer was removed, and 20 mL of 2 M HCl (aq) was added. After washing, GC analysis of the organic layer determined the yield of **3** to be 78.8% relative to the internal standard. The organic layer

was concentrated and purified by silica gel chromatography to give a volatile yellow oil (95 mg, 69% isolated yield). ^{1}H NMR (400 MHz, $CDCl_3$) δ: 7.87 (d, J = 8.5 Hz, 2H), 7.45 (d, J = 8.5 Hz, 2H), 2.55 (s, 3H), 1.31 (s, 9H) ppm. ^{13}C NMR (100 MHz, $CDCl_3$) δ: 197.9, 156.8, 134.6, 128.3, 125.5, 35.1, 31.1, 26.6 ppm. IR (neat, cm^{-1}): 2965, 1684, 1606, 1406, 1357, 1271, 1113, 957, 838, 598.

BRUKER

```
Current Data Parameters
NAME                  JN5-82-010
EXPNO                          1
PROCNO                         1

F2 - Acquisition Parameters
Date_                   20090707
Time                       18.03
INSTRUM                    spect
PROBHD    5 mm BBO BB-1H
PULPROG                     zg30
TD                         65536
SOLVENT                    CDCl3
NS                            16
DS                             2
SWH                     8278.146 Hz
FIDRES                  0.126314 Hz
AQ                      3.9584243 sec
RG                          35.9
DW                        60.400 usec
DE                         6.00 usec
TE                        293.2 K
D1                   1.00000000 sec
TD0                            1

======== CHANNEL f1 ========
NUC1                          1H
P1                        15.07 usec
PL1                        0.00 dB
SFO1                400.1324710 MHz

F2 - Processing parameters
SI                         65536
SF                  400.1300212 MHz
WDW                           EM
SSB                            0
LB                         0.30 Hz
GB                             0
PC                          1.00
```

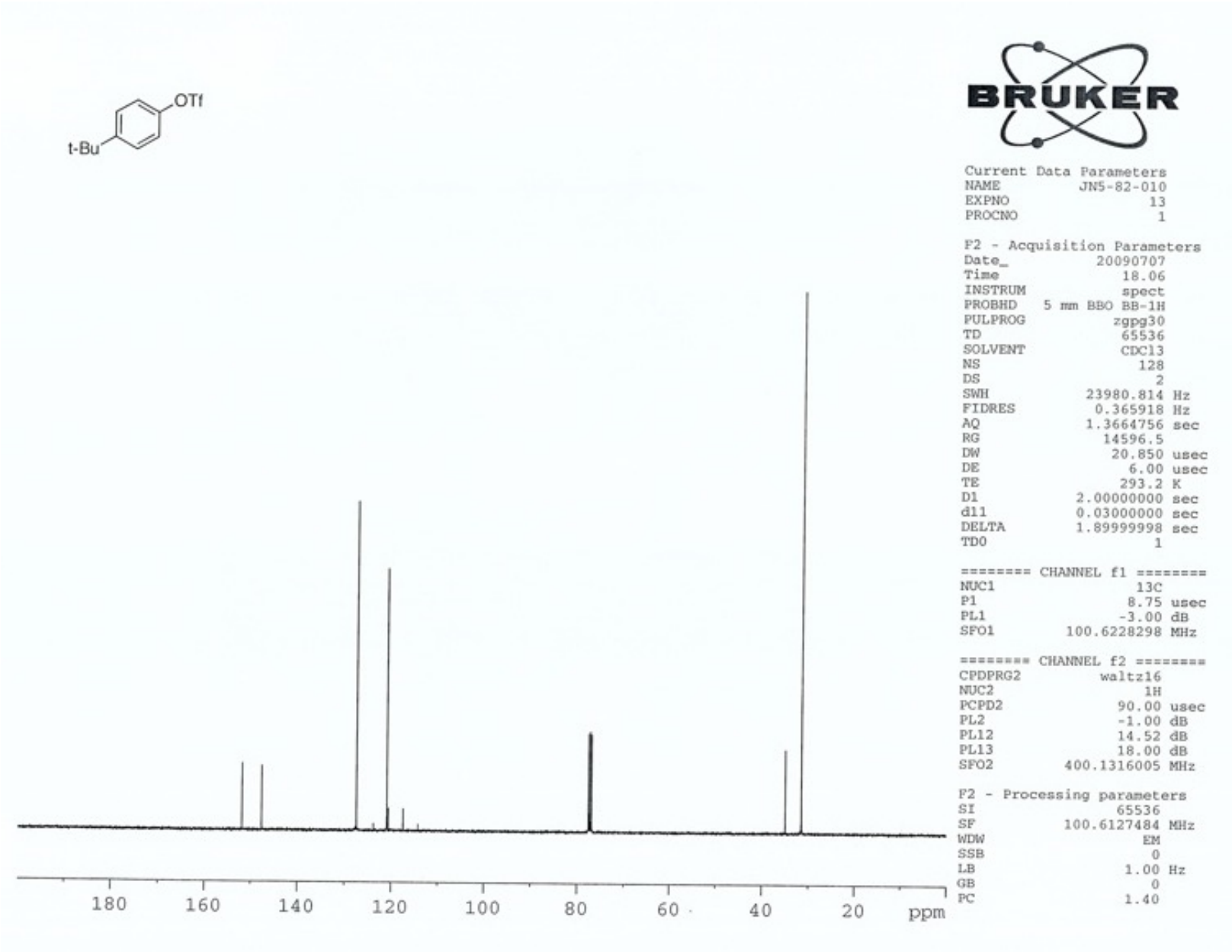

BRUKER

```
Current Data Parameters
NAME                  JN5-82-010
EXPNO                         13
PROCNO                         1

F2 - Acquisition Parameters
Date_                   20090707
Time                       18.06
INSTRUM                    spect
PROBHD    5 mm BBO BB-1H
PULPROG                   zgpg30
TD                         65536
SOLVENT                    CDCl3
NS                           128
DS                             2
SWH                    23980.814 Hz
FIDRES                  0.365918 Hz
AQ                      1.3664756 sec
RG                        14596.5
DW                         20.850 usec
DE                          6.00 usec
TE                         293.2 K
D1                     2.00000000 sec
d11                    0.03000000 sec
DELTA                  1.89999998 sec
TD0                            1

======== CHANNEL f1 ========
NUC1                         13C
P1                          8.75 usec
PL1                        -3.00 dB
SFO1                100.6228298 MHz

======== CHANNEL f2 ========
CPDPRG2                  waltz16
NUC2                         1H
PCPD2                      90.00 usec
PL2                        -1.00 dB
PL12                       14.52 dB
PL13                       18.00 dB
SFO2                400.1316005 MHz

F2 - Processing parameters
SI                         65536
SF                  100.6127484 MHz
WDW                           EM
SSB                            0
LB                          1.00 Hz
GB                             0
PC                          1.40
```


t-Bu
O
BRUKER
Current Data Parameters
NAME JNS-85-010
EXPNO 1
PROCNO 1
F2 - Acquisition Parameters
Date_ 20090710
Time 10.37
INSTRUM spect
PROBHD 5 mm BBO BB-1H
PULPROG zg30
TD 65536
SOLVENT
NS 8
DS 2
SWH 8278.146 Hz
FIDRES 0.126314 Hz
AQ 3.9584243 sec
RG 18
DW 60.400 usec
DE 6.00 usec
TE 293.2 K
D1 1.00000000 sec
TD0 1
======== CHANNEL f1 ========
NUC1 1H
P1 15.07 usec
PL1 0.00 dB
SFO1 400.1324710 MHz
F2 - Processing parameters
SI 65536
SF 400.1300212 MHz
WDW EM
SSB 0
LB 0.30 Hz
GB 0
PC 1.00
9
8
7
6
5
4
3
2
1
ppm
1.869
1.982
0.957
1.005
1.881
1.907
2.145
9.000
3.045

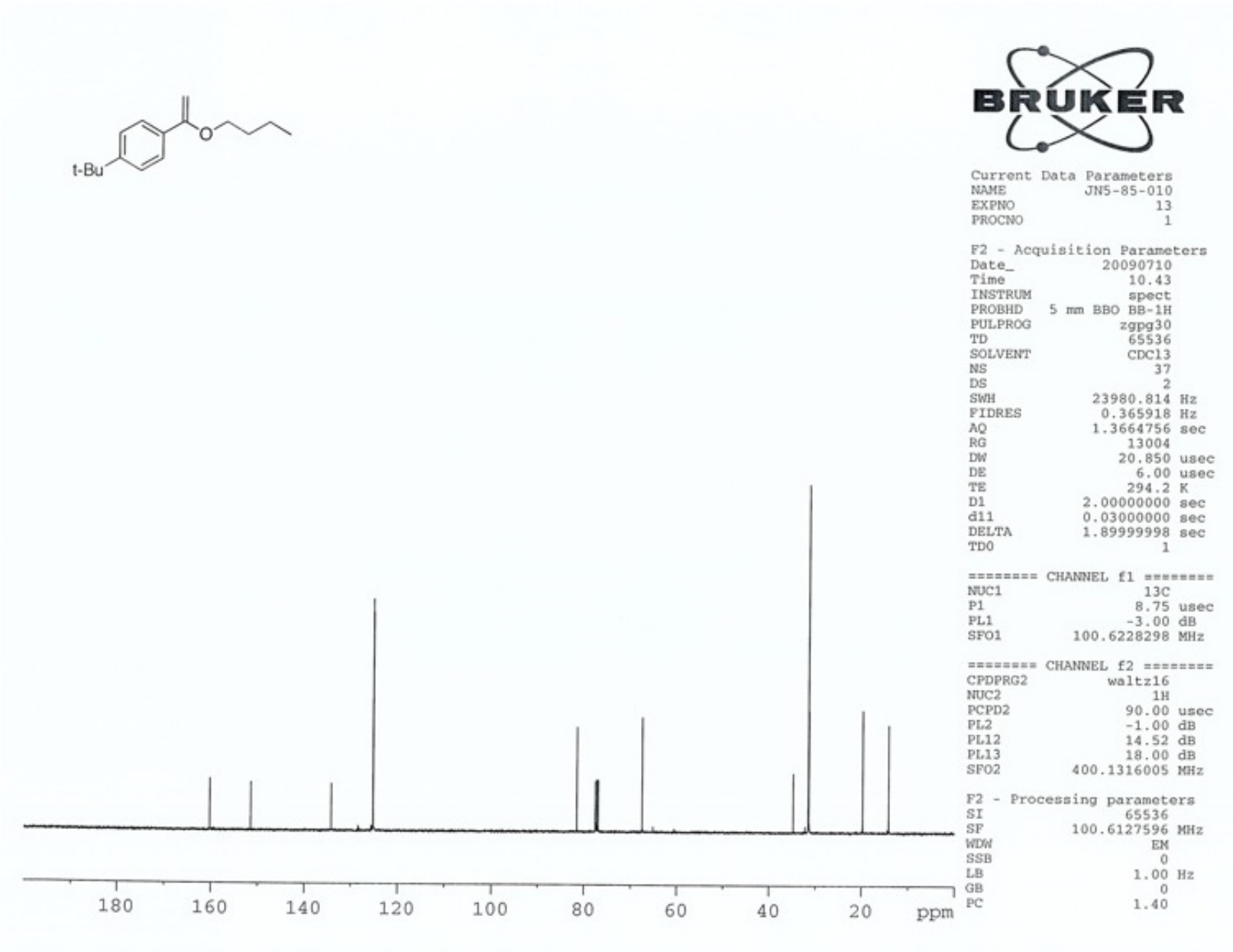

BRUKER

Current Data Parameters
NAME JN5-85-010
EXPNO 13
PROCNO 1

F2 - Acquisition Parameters
Date_ 20090710
Time 10.43
INSTRUM spect
PROBHD 5 mm BBO BB-1H
PULPROG zgpg30
TD 65536
SOLVENT CDCl3
NS 37
DS 2
SWH 23980.814 Hz
FIDRES 0.365918 Hz
AQ 1.3664756 sec
RG 13004
DW 20.850 usec
DE 6.00 usec
TE 294.2 K
D1 2.00000000 sec
d11 0.03000000 sec
DELTA 1.89999998 sec
TD0 1

======== CHANNEL f1 ========
NUC1 13C
P1 8.75 usec
PL1 -3.00 dB
SFO1 100.6228298 MHz

======== CHANNEL f2 ========
CPDPRG2 waltz16
NUC2 1H
PCPD2 90.00 usec
PL2 -1.00 dB
PL12 14.52 dB
PL13 18.00 dB
SFO2 400.1316005 MHz

F2 - Processing parameters
SI 65536
SF 100.6127596 MHz
WDW EM
SSB 0
LB 1.00 Hz
GB 0
PC 1.40

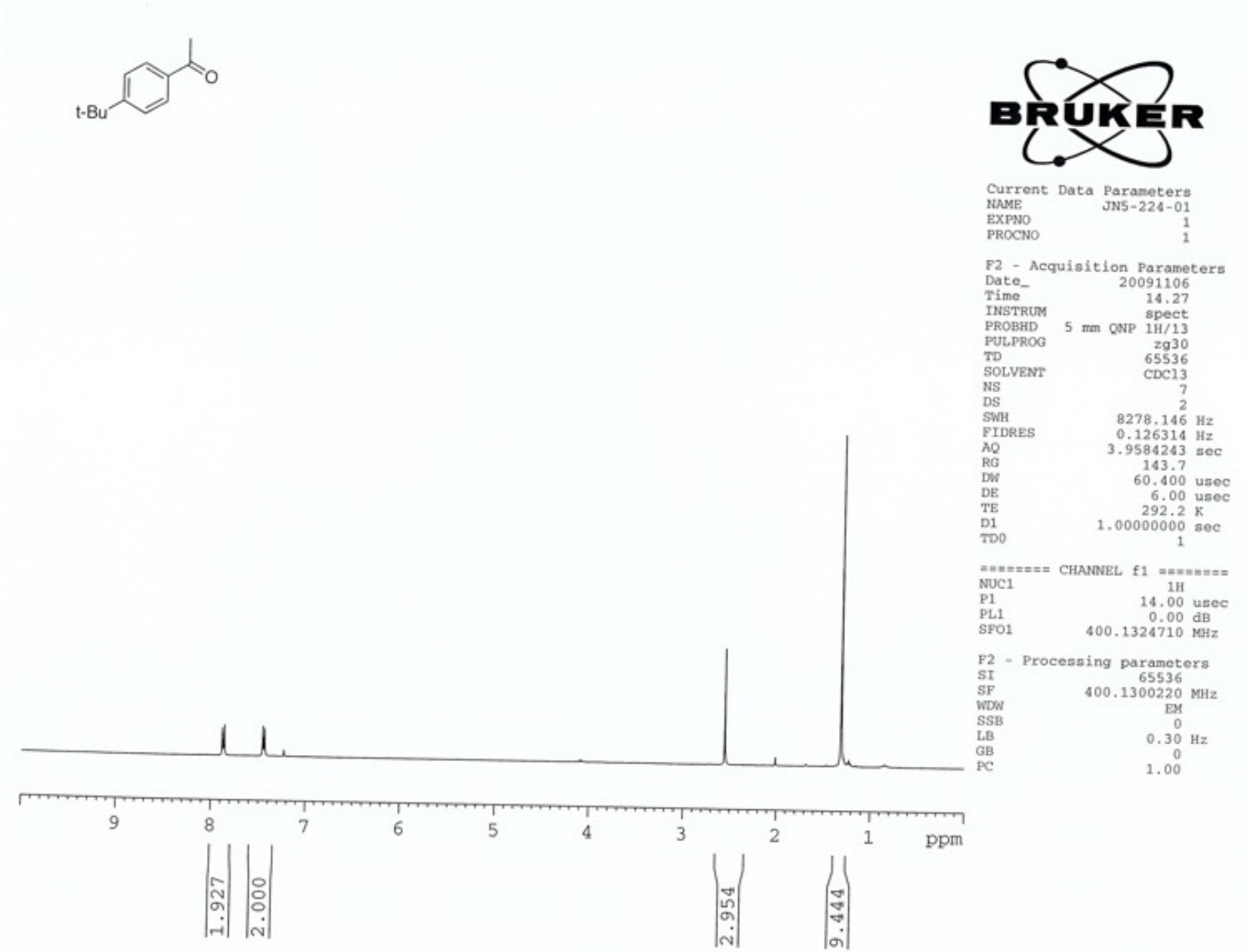
t-Bu
O
BRUKER
Current Data Parameters
NAME JN5-224-01
EXPNO 1
PROCNO 1
F2 - Acquisition Parameters
Date_ 20091106
Time 14.27
INSTRUM spect
PROBHD 5 mm QNP 1H/13
PULPROG zg30
TD 65536
SOLVENT CDCl3
NS 7
DS 2
SWH 8278.146 Hz
FIDRES 0.126314 Hz
AQ 3.9584243 sec
RG 143.7
DW 60.400 usec
DE 6.00 usec
TE 292.2 K
D1 1.00000000 sec
TD0 1
======== CHANNEL f1 ========
NUC1 1H
P1 14.00 usec
PL1 0.00 dB
SFO1 400.1324710 MHz
F2 - Processing parameters
SI 65536
SF 400.1300220 MHz
WDW EM
SSB 0
LB 0.30 Hz
GB 0
PC 1.00
9
8
7
6
5
4
3
2
1
ppm
1.927
2.000
2.954
9.444

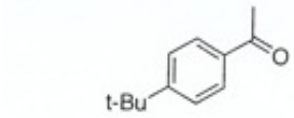

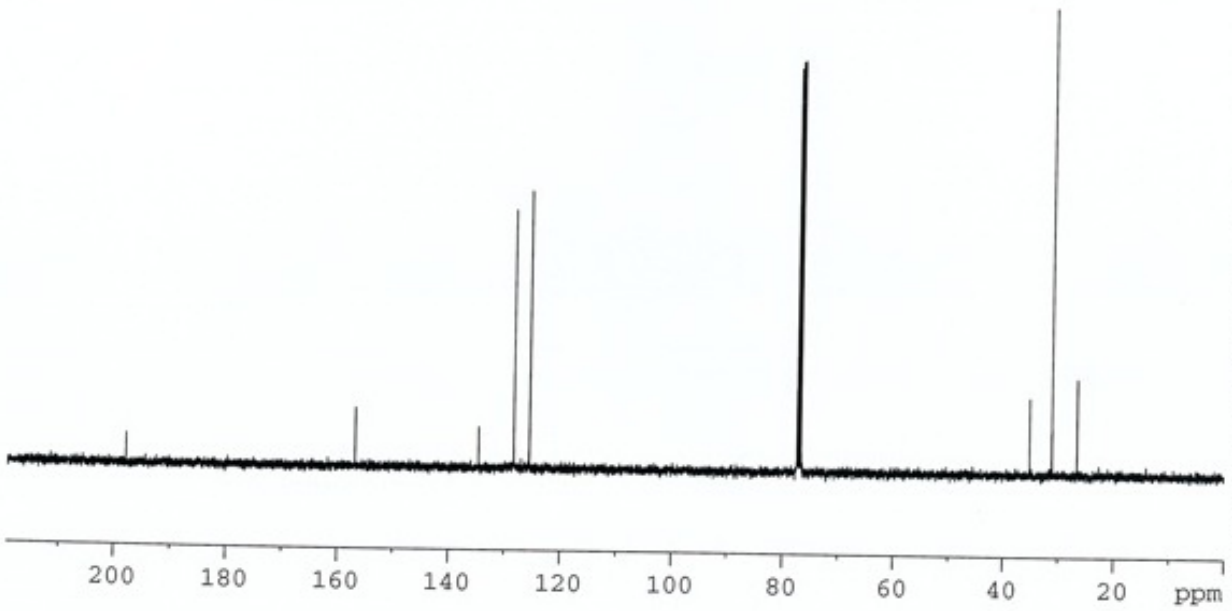

BRUKER

Current Data Parameters
NAME JN5-224-01
EXPNO 13
PROCNO 1

F2 - Acquisition Parameters
Date_ 20091106
Time 14.29
INSTRUM spect
PROBHD 5 mm QNP 1H/13
PULPROG zgpg30
TD 65536
SOLVENT CDCl3
NS 81
DS 4
SWH 23980.814 Hz
FIDRES 0.365918 Hz
AQ 1.3664756 sec
RG 1625.5
DW 20.850 usec
DE 6.00 usec
TE 292.2 K
D1 2.00000000 sec
d11 0.03000000 sec
DELTA 1.89999998 sec
TD0 1

======== CHANNEL f1 ========
NUC1 13C
P1 9.38 usec
PL1 0.00 dB
SFO1 100.6228298 MHz

======== CHANNEL f2 ========
CPDPRG2 waltz16
NUC2 1H
PCPD2 90.00 usec
PL2 0.00 dB
PL12 16.10 dB
PL13 19.00 dB
SFO2 400.1316005 MHz

F2 - Processing parameters
SI 32768
SF 100.6127690 MHz
WDW EM
SSB 0
LB 1.00 Hz
GB 0
PC 1.40

3.5 References

1. H. R. Sahoo, J. G. Kralj, K. F. Jensen, *Angew. Chem. Int. Ed.* **2007**, *46*, 5704.
2. H. Song, J. D. Tice, R. F. Ismagilov, *Angew. Chem. Int. Ed.* **2003**, *42*, 768.
3. M. Tokeshi, T. Minagawa, K. Uchiyama, A. Hibara, K. Sato, H. Hisamoto, T. Kitamori, *Anal. Chem.* **2002**, *74*, 1565.
4. R. L. Hartman, K. F. Jensen, *Lab Chip* **2009**, *9*, 2495–2507.
5. A. J. deMello, *Nature* **2006**, *442*, 394.
6. P. D. I. Fletcher, S. J. Haswell, E. Pombo-Villar, B. H. Warrington, P. Watts, S. Y. F. Wong, X. L. Zhang, *Tetrahedron* **2002**, *58*, 4735.
7. V. Hessel, H. Lowe, *Chem. Eng. Technol.* **2005**, *28*, 267.
8. K. Jahnisch, V. Hessel, H. Lowe, M. Baerns, *Angew. Chem. Int. Ed.* **2004**, *43*, 406.
9. K. F. Jensen, *Chem. Eng. Sci.* **2001**, *56*, 293.
10. K. F. Jensen, *MRS Bull.* **2006**, *31*, 101.
11. B. P. Mason, K. E. Price, J. L. Steinbacher, A. R. Bogdan, D. T. McQuade, *Chem. Rev.* **2007**, *107*, 2300.
12. H. Pennemann, P. Watts, S. J. Haswell, V. Hessel, H. Lowe, *Org. Process Res. Dev.* **2004**, *8*, 422.
13. P. Watts, C. Wiles, *Chem. Commun.* **2007**, 443.
14. P. Watts, C. Wiles, *Chem. Eng. Technol.* **2007**, *30*, 329.
15. N. Wang, T. Matsumoto, M. Ueno, H. Miyamura, S. Kobayashi, *Angew. Chem. Int. Ed.* **2009**, *48*, 4744.
16. J. Kobayashi, Y. Mori, K. Okamoto, R. Akiyama, M. Ueno, T. Kitamori, S. Kobayashi, *Science* **2004**, *304*, 1305.

17. I. R. Baxendale, J. Deeley, C. M. Griffiths-Jones, S. V. Ley, S. Saaby, G. K. Tranmer, *Chem. Commun.* **2006**, 2566.

18. C. C. Lee, G. D. Sui, A. Elizarov, C. Y. J. Shu, Y. S. Shin, A. N. Dooley, J. Huang, A. Daridon, P. Wyatt, D. Stout, H. C. Kolb, O. N. Witte, N. Satyamurthy, J. R. Heath, M. E. Phelps, S. R. Quake, H. R. Tseng, *Science* **2005**, *310*, 1793.

19. H. Usutani, Y. Tomida, A. Nagaki, H. Okamoto, T. Nokami, J. Yoshida, *J. Am. Chem. Soc.* **2007**, *129*, 3046.

20. D. Belder, M. Ludwig, L. W. Wang, M. T. Reetz, *Angew. Chem. Int. Ed.* **2006**, *45*, 2463.

21. I. R. Baxendale, C. M. Griffiths-Jones, S. V. Ley, G. K. Tranmer, *Synlett* **2006**, 427.

22. D. Grant, R. Dahl, N. D. P. Cosford, *J. Org. Chem.* **2008**, *73*, 7219.

23. W. Li, H. H. Pharn, Z. Nie, B. MacDonald, A. Guenther, E. Kumacheva, *J. Am. Chem. Soc.* **2008**, *130*, 9935.

24. C. Wiles, P. Watts, S. J. Haswell, *Lab Chip* **2007**, *7*, 322.

25. I. R. Baxendale, S. V. Ley, A. C. Mansfield, C. D. Smith, *Angew. Chem. Int. Ed.* **2009**, *48*, 4017.

26. O. Trapp, S. K. Weber, S. Bauch, T. Backer, W. Hofstadt, B. Spliethoff, *Chem. Eur. J.* **2008**, *14*, 4657.

27. O. Trapp, S. K. Weber, S. Bauch, W. Hofstadt, *Angew. Chem. Int. Ed.* **2007**, *46*, 7307.

28. J. G. Kralj, H. R. Sahoo, K. F. Jensen, *Lab Chip* **2007**, *7*, 256.

29. M. Tokeshi, T. Minagawa, T. Kitamori, *J. Chromatogr. A* **2000**, *894*, 19.

30. A. Aota, M. Nonaka, A. Hibara, T. Kitamori, *Angew. Chem. Int. Ed.* **2007**, *46*, 878.

31. D. A. Boyd, J. R. Adleman, D. G. Goodwin, D. Psagtis, *Anal. Chem.* **2008**, *80*, 2452.

32. A. Hibara, K. Toshin, T. Tsukahara, K. Mawatari, T. Kitamori, *Chem. Lett.* **2008**, *37*, 1064.

33. B. H. Timmer, K. M. van Delft, W. Olthuis, P. Bergveld, A. van den Berg, *Sensor. Actuat. B-Chem.* **2003**, *91*, 342.

34. R. C. R. Wootton, A. J. deMello, *Chem. Commun.* **2004**, 266.

35. Y. Zhang, S. Kato, T. Anazawa, *Chem. Commun.* **2009**, 2750.

36. R. L. Hartman, H. R. Sahoo, B. C. Yen, K. F. Jensen, *Lab Chip* **2009**, *9*, 1843.

37. I. P. Beletskaya, A. V. Cheprakov, *Chem. Rev.* **2000**, *100*, 3009.

38. F. Alonso, I. P. Beletskaya, M. Yus, *Tetrahedron* **2005**, *61*, 11771.

39. P. Mahavir, in *Topics in Organometallic Chemistry, Vol. 6*, Springer-Verlag Berlin Heidelberg, **2004**, pp. 181.

40. K. C. Nicolaou, P. G. Bulger, D. Sarlah, *Angew. Chem. Int. Ed.* **2005**, *44*, 4442.

41. A. B. Dounay, L. E. Overman, *Chem. Rev.* **2003**, *103*, 2945.

42. J. G. de Vries, *Can. J. Chem.-Rev. Can. Chim.* **2001**, *79*, 1086.

43. W. Cabri, I. Candiani, *Acc. Chem. Res.* **1995**, *28*, 2.

44. A. L. Hansen, T. Skrydstrup, *J. Org. Chem.* **2005**, *70*, 5997.

45. S. R. Gilbertson, Z. Fu, *Org. Lett.* **2001**, *3*, 161.

46. K. Olofsson, M. Larhed, A. Hallberg, *J. Org. Chem.* **2000**, *65*, 7235.

47. W. Cabri, I. Candiani, A. Bedeschi, R. Santi, *J. Org. Chem.* **1992**, *57*, 3558.

48. W. Cabri, I. Candiani, A. Bedeschi, S. Penco, R. Santi, *J. Org. Chem.* **1992**, *57*, 1481.

49. A. Gunther, K. F. Jensen, *Lab Chip* **2006**, *6*, 1487.

50. A. Gunther, M. Jhunjhunwala, M. Thalmann, M. A. Schmidt, K. F. Jensen, *Langmuir* **2005**, *21*, 1547.

51. A. Gunther, S. A. Khan, M. Thalmann, F. Trachsel, K. F. Jensen, *Lab Chip* **2004**, *4*, 278.

52. W. L. McCabe, E. W. Thiele, *Ind. Eng. Chem.* **1925**, *17*, 605.

53. P. C. Wankat, *Equilibrium-Staged Separations - Separations in Chemical Engineering*, Prentice Hall PTR, Englewood Cliffs, **1988**.

54. W. Cabri, I. Candiani, A. Bedeschi, *J. Org. Chem.* **1990**, *55*, 3654.

Chapter 4 – The Use of Sonication to Mitigate Clogging in Continuous Flow

4.1 Introduction

The problem of handling of solids in microfluidic systems has gained considerable attention in recent years as many interesting applications, from the manipulation of biological materials to a wide range of organic chemistry reactions, involve heterogeneous mixtures. For example, many important reactions in the synthesis of fine chemicals, including active pharmaceutical ingredients (APIs), require more than one phase, be it gas and liquid, liquid and liquid, or solid and liquid.[1-3] Microreactors have been widely applied in research to advance a deeper understanding of the physical and chemical rate processes that govern reactions,[4-16] yet their use for reactions involving solids has been relatively limited.[17-33] Understanding why solids lead to clogging in microsystems and the development of strategies to overcome this challenge are necessary in order to apply microsystems to a wider range of reaction discovery and process optimization.

A number of creative strategies have been employed to handle solids in both microreactors and simple microfluidic systems. While immobilization of the particles (e.g., catalyst or solid-supported reagent) can minimize the risk of microchannel clogging,[17-20,27] regenerating a packed bed necessitates the removal and/or recharging of such immobilized solids. The synthesis of nanoparticles[31-34] can mitigate clogging caused by flow-induced bridging but can lead to retention and build-up when the particles interact with the surfaces of the system. Another approach is to use multiphase liquid-liquid flow to prevent particles from interacting with the walls of the microchannels. Encapsulating particles in droplets[21,23,28] or establishing annular-type flow[30] not only limits the interactions between the particles and walls, but also constrains particle-to-particle interactions that may lead to clogging. However, these specialized systems often require the use of solvents that can be incompatible with certain reagents or can lead to changes in the efficiency of many organic reactions. Non-invasive approaches such as flow focusing and filtration have proven to be effective in separating particles based on hydrodynamic conditions.[35-38] These conditions, however, limit reaction screening applications and present challenges with systems that have high particle concentrations or particles that have an affinity for each other or the surfaces of the reactor.

Electrical potentials have also been used to sort particles in microfluidic systems.[39,40] Yet another non-invasive approach is the application of acoustic standing waves to order particles, such as the acoustic streaming of blood cells.[41-44] More recently, we have demonstrated the potential for using ultrasound to handle solids during the course of a chemical reaction,[45,46] while others have combined ultrasound and multiphase flow to facilitate the flow of solids during polymerization.[24] In general, the strategy for solids handling depends on the nature of the chemistry and warrants a deeper understanding of the mechanisms that lead to clogging.

The Pd-catalyzed C–N bond forming reaction is one of the most important reactions of the past 15 years, finding applications in the production of APIs, natural products, and specialty chemicals.[47-50] It is a versatile transformation that allows the coupling of aryl and vinyl halides, triflates, nonaflates and other sulfonates with a wide variety of nitrogen nucleophiles. These reactions, and many others used in fine chemical production, form inorganic salt byproducts and are often run in non-polar solvents, which leads to precipitation.

In the present work, we use the Pd-catalyzed amination reaction to investigate the mechanisms that govern the clogging of microreactors.[51] We will show that both bridging and constriction are important mechanisms that lead to clogging and serve to limit the application of microsystems to reactions that form insoluble byproducts. We present several approaches to overcome the challenge of plugging and thus enable continuous-flow microchemical synthesis of a biaryl amine. Consequently, the present work establishes the groundwork for further continuous-flow studies on both the mechanisms responsible for clogging and synthetic applications of Pd-catalyzed cross-coupling reactions.

4.2 Results and discussion

In this study of clogging on the micro-scale, we employed the coupling of 4-chloroanisole and aniline, catalyzed by a catalyst supported by one of the bulky, electron-rich, biaryl phosphine ligands developed in the Buchwald group, to form 4-methoxy-N-phenylaniline (Scheme 1).[52]

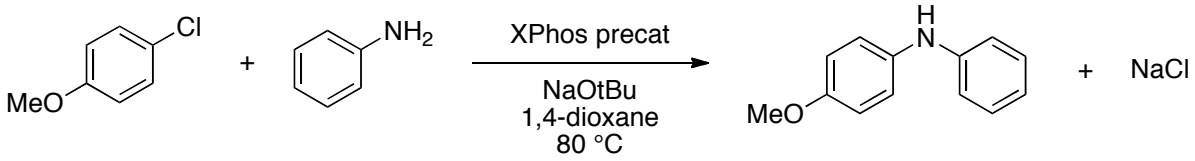

Scheme 1. Pd-catalyzed amination of an aryl chloride with aniline.

It can be seen in Scheme 1 that sodium chloride is formed as a stoichiometric byproduct in this reaction. Inorganic salts are generally insoluble in the solvents used to carry out this reaction (e.g., 1,4-dioxane, toluene, tetrahydrofuran). To complicate matters further, typical batch conditions for these reactions employ high concentrations (0.5-1.0 M) and the reactions are often complete in minutes resulting in fast salt formation. This is a process that is synthetically interesting, yet challenging to carry out under flow conditions; it served as a model to study solids handling in microsystems.

Clogging mechanisms. The aforementioned reaction was first carried out in a series of experiments using a silicon-based microreactor to allow the process to be followed visually. Figure 1 shows that the normalized pressure drop across the microreactor, $\Delta P/\Delta P_0$ (normalized to the initial, solvent-only, pressure drop), rapidly increased upon injecting the reagents at 20 μL/min (residence time (τ) = 7 min) and 80.0 °C, even when the concentration of aryl halide was only 0.1 M (concentrations refer to the reaction mixture after the two streams are combined). The sudden increase in pressure drop was followed by clogging of the microreactor to the point that no flow occurred. As is evident in Figure 1, the onset of clogging took place after less than 6 reactor volumes had been injected.

As shown in Figure 2a, clogging was caused by a white solid that accumulated at the 180° turns within the microreactor. Under increased magnification (Figure 2b) it can be seen that the solid material was crystalline in nature and the sizes of the particles found were on the same order as the channel dimensions (e.g., 400 μm). When the size of flowing and stable particles is on the order of the cross-sectional length of a channel, it has been shown that bridging takes place in micron-sized pore throats[53-55] and fabricated geometries.[56] The depiction in Figure 2c illustrates that particles can plug by forming a bridge across a microchannel. It is generally understood that particles can be retained when the aspect ratio (e.g., the

ratio of channel width to particle size, D/a) is in the range of 3-4.[53] It should be noted, however, that this type of bridging has been shown for stable particle suspensions that do not exhibit attractive interactions or that do not change size with time. Based on our experimental observations, it is evident that bridging also takes place during the amination reaction and is one of the mechanisms that leads to clogging.

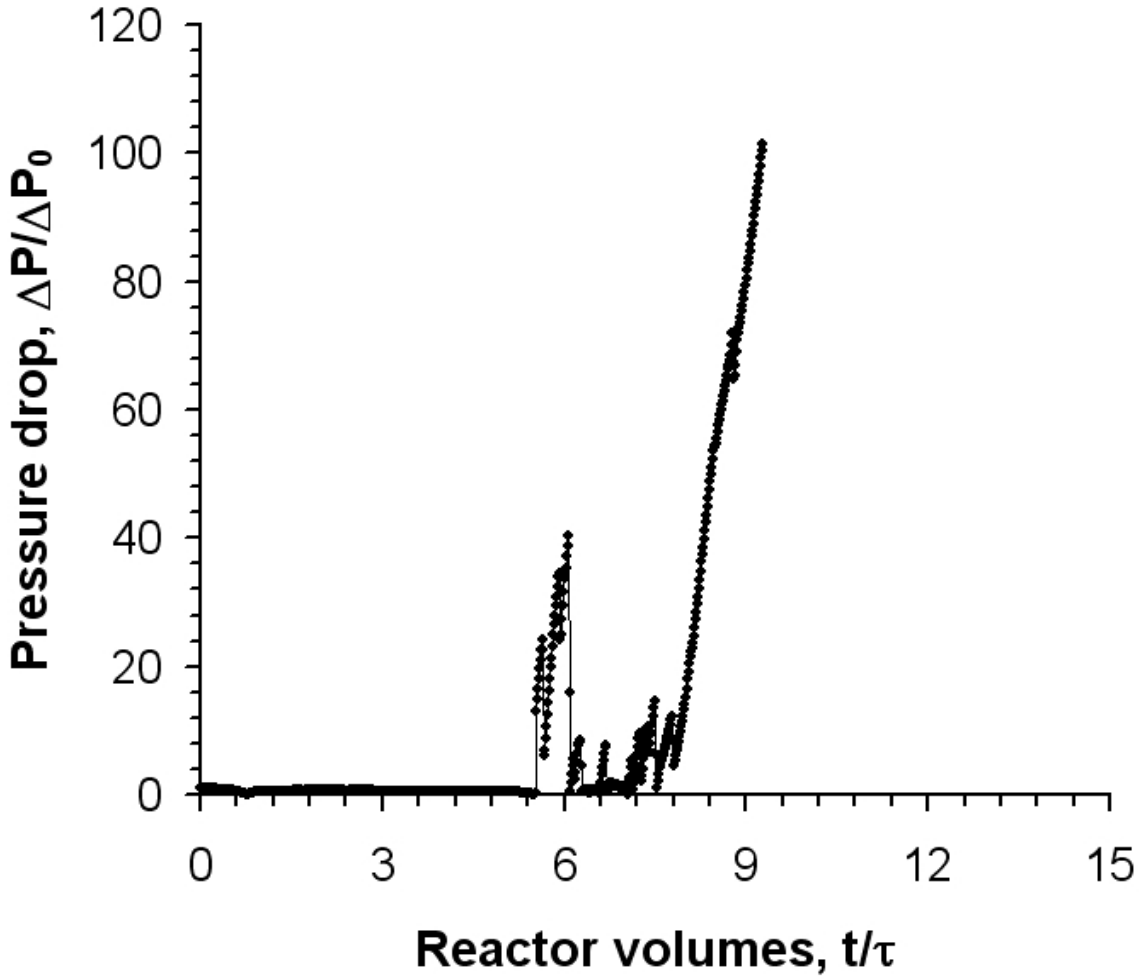

Figure 1: Pd–catalyzed amination leading to bridging in microreactors. Normalized pressure drop across a microreactor during the injection of the reagents and catalyst (at 20 μL/min and 80.0 °C) shown in Scheme 1.

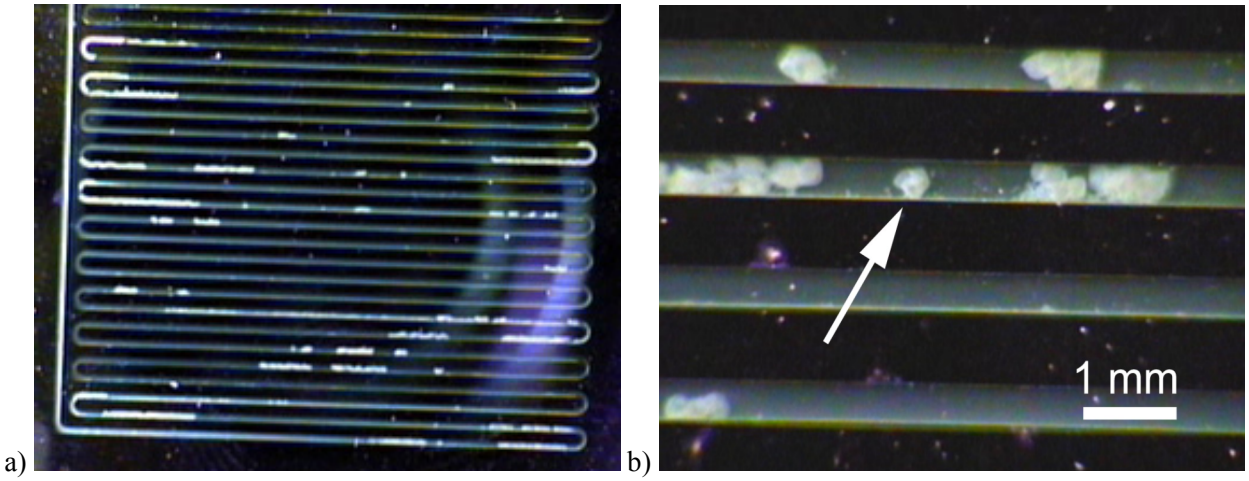

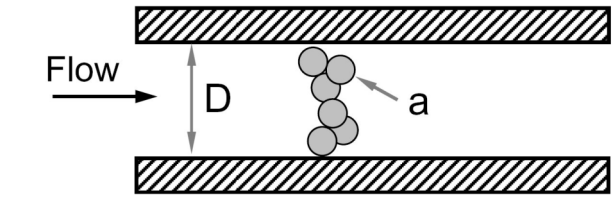

c) $\frac{D}{a} \approx 3 \text{ to } 4$

Figure 2: Pd–catalyzed amination leading to bridging in microreactors, pressure drop shown in Figure 1. a) A photograph of the microreactor illustrating the accumulation of white solid, primarily at 180° turns. b) An expanded view of the microchannel. c) A depiction of flow-induced bridging between two flat plates.

The clogged microreactor was replaced with a fresh device and the experiment was repeated with an increased injection rate of 70 μL/min (τ = 2 min). Figure 3 shows that the pressure drop once again increased to the point of clogging with the injection of only a few reactor volumes of the reaction. However, in this case the pressure drop gradually increased for 4 reactor volumes before suddenly rising and clogging.

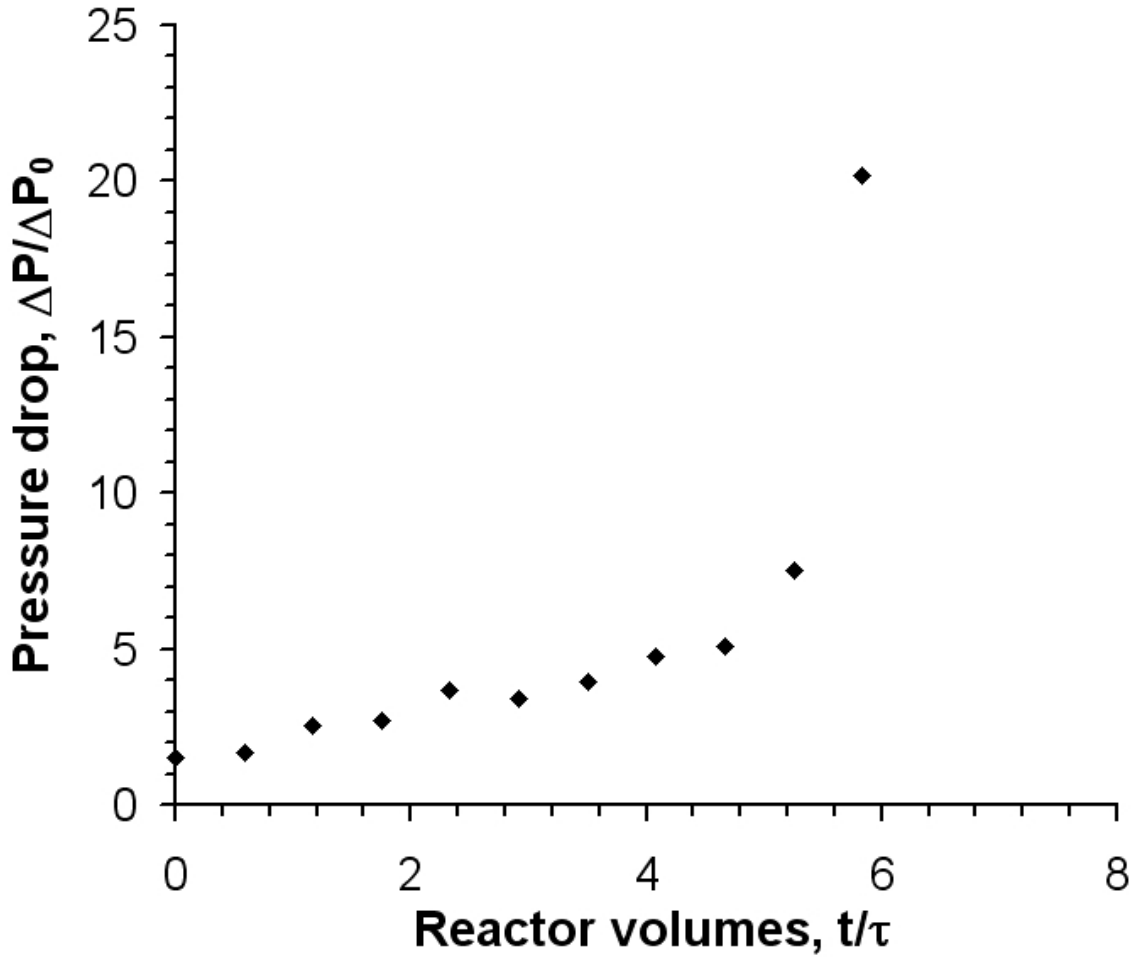

Figure 3. Pd-catalyzed amination resulting in constriction in a microreactor. a) Normalized pressure drop across a microreactor during the injection of the reagents and catalyst (at 70 μL/min and 80.0 °C) shown in Scheme 1.

Further inspection of the microreactor (Figure 4a) showed a white buildup on the reactor walls, attributed to NaCl and implying that material was deposited or grown on these surfaces. Both deposition[57-59] and nucleation followed by growth can lead to channel constriction, which is depicted in Figure 4b. A time-dependent decrease in cross-sectional diameter will likely bring about bridging in a system with particles suspended in the bulk solution. The presence of constriction in addition to bridging warrants more than one approach to address the clogging issues caused by the insoluble byproducts of the Pd-catalyzed amination.

a) 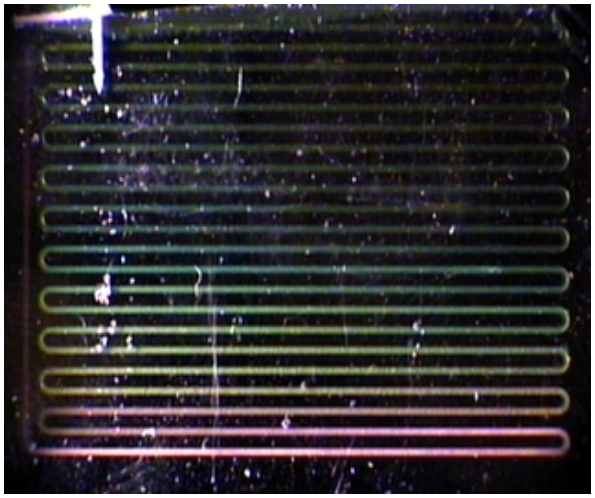 b)

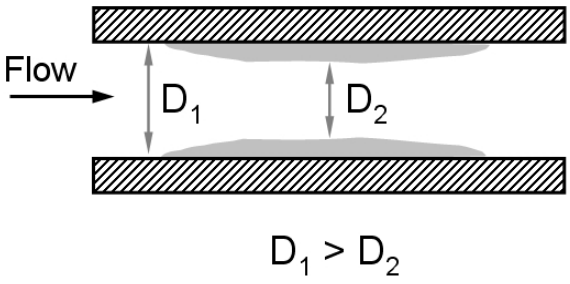

Figure 4. Pd-catalyzed amination resulting in constriction in a microreactor, pressure drop shown in figure 3. a) Photograph of the microreactor during reaction. b) A depiction of constriction when material grows or deposits on a channel wall.

Reactor design. Particle-to-wall interactions can take place in laminar flow when changes in the velocity occur (e.g., fluid flow around turns) or when the particle momentum is too large for particles to stay on a streamline path (e.g., inertial impaction).[57] To minimize these scenarios, we investigated the use of microreactors with gradual turns, as shown in Figure 5.

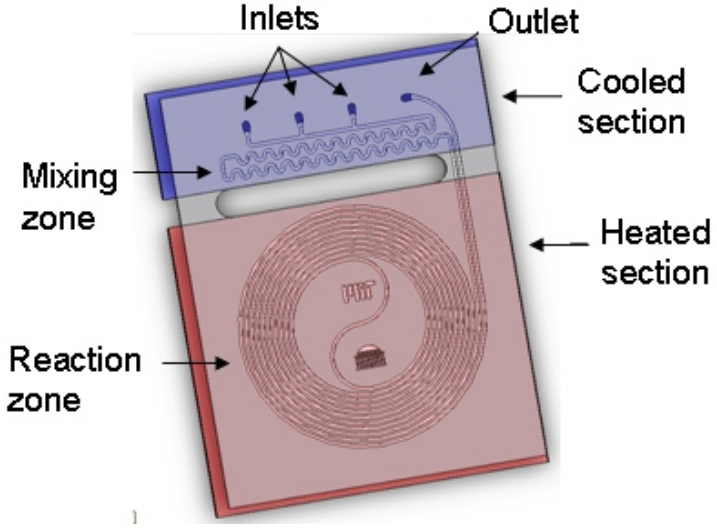

Figure 5. Silicon microreactor designed to eliminate 180° turns. The device has a gradual spiral in and out to imitate a long straight channel.

The reactor design was closely related to the previously described serpentine microreactor, retaining the same layout of ports and mixing zone, an equal volume, and an identical thermal isolation of the reaction zone from the ports. However, the nested spiral layout of the heated channel provided a gradual change in turning radius, with the sharpest turn having a much larger radius (4.4 mm) than the hairpin turns (0.4 mm) of the serpentine layout. When the experiment described in Figure 1 was repeated using the spiral reactor, we observed the solids flowed for several reactor volumes without the accumulation shown in Figure 2. Nevertheless, the microreactor wall (from the top down) gradually changed from transparent to white, and clogging eventually took place.

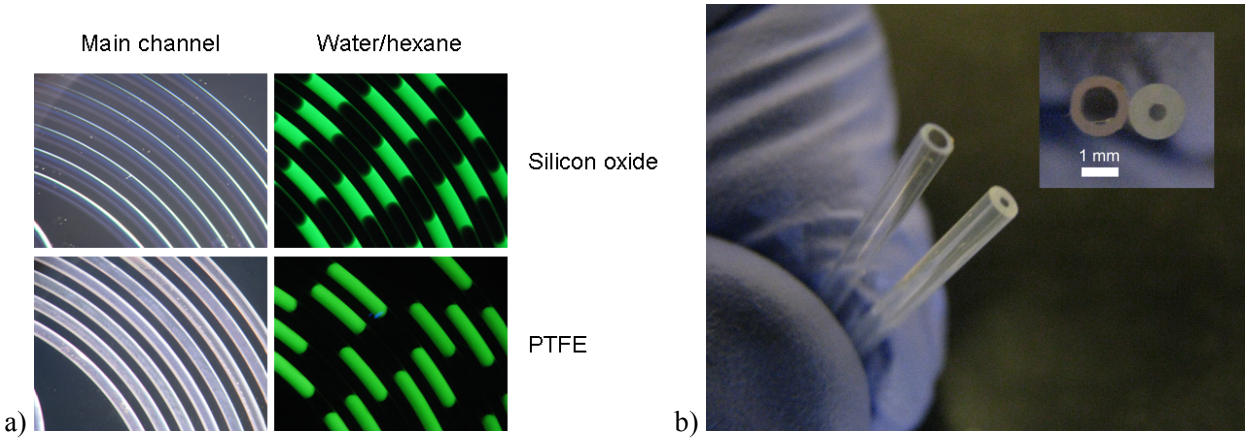

Figure 6. a) Coating the microreactor with PTFE enabled switching of the wetting characteristics from hydrophilic to hydrophobic as shown by the water-hexane segmented flow (the aqueous phase was laced with fluorescein dye and excited under a UV-lamp). b) PFA capillaries used as model reactors (ID = 500 and 1000 μm).

One approach to minimizing wall deposition or growth is the modification of microreactor surfaces with a fluorous coating. We have recently investigated such devices and have engineered silicon-Teflon®-hybrid microreactors by depositing fluoropolymer particles in annular-type flows.[60] As can be seen in Figure 6a, the coating of silicon microreactors with polytetrafluoroethylene (PTFE) switches the wetting characteristics of the channel from the hydrophilic properties of silicon oxide to the hydrophobic properties of PTFE, and has utility in a broad range of applications. Nevertheless, cracks and surface

imperfections in the coating present nucleation points for particle deposition and for attack by the strong organic and inorganic bases routinely used in C-N bond forming reactions. Because of this, we found simple PFA capillaries, (Figure 6b) to be useful as model reactors in studying the role of bridging and deposition.

Acoustic irradiation. It is commonly known that sound waves can impose a force on a system of particles.[61] Thus, we investigated the influence of acoustic waves on microreactor clogging during Pd-catalyzed C-N bond forming reactions. In the case of a standing wave, the amplitude of the primary radiation force acting on a particle (in the radial direction) flowing in a microchannel, F_r, has previously been described and given as Equation **1** where p_0 is the acoustic pressure amplitude, r is the particle radius, β_S is the compressibility of the solvent, and ϕ is a contrast factor, described in Equation **2** where ρ is density, and the subscripts P and S denote the particle and solvent, respectively.[41,42]

$$F_r = -\left(\frac{2\pi^2 p_0^2 r^3 \beta_S}{3\lambda}\right) \cdot \phi \cdot \sin\left(\frac{4\pi x}{\lambda}\right) \quad \textbf{1}$$

$$\phi = \left(\frac{5\rho_P - 2\rho_S}{2\rho_P + \rho_S}\right) - \frac{\beta_P}{\beta_S} \quad \textbf{2}$$

One observes in Equation **1** that the primary force is strongly dependent on particle radius; thus, the acoustic force weakens as the particle diameter is reduced. Furthermore, the primary force is driven by differences in density and compressibility, described by the contrast factor. The acoustic pressure amplitude also influences the primary radiation force and is dependent on the voltage and frequency under which piezoceramic operation takes place. Such forces have been exploited to order and separate particulates and biological matter when frequencies are in the range of MHz and wavelengths on the order of the channel dimensions.[41,42,62,63] We wanted to study whether these forces, with frequencies in the kHz range, could be used to overcome the particle-to-particle attractive interactions and hydrodynamic conditions that bring about bridging in laminar flow. See the experimental section for a description of the acoustic waveform applied in this study.

The reaction from Scheme 1 was carried out both with and without acoustic irradiation by injecting the reagents and base (0.1 M ArCl, τ = 7 min) into a PFA capillary (1000 μm I.D., 240 μL) coiled in an ultrasonic bath filled with water at 80.0 °C. Figure 7 shows that the microreactor clogged in the absence of ultrasound, shown by the rapid increase in Normalized pressure drop. Repeating the experiment with acoustic irradiation demonstrated that the presence of ultrasound prevented clogging, as the pressure drop remained negligible for approximately 20 reactor volumes. Removing the acoustic irradiation in the same experiment resulted in clogging of the microreactor, as shown in Figure 7, and subsequent investigations proved that reinitiating the ultrasonic bath did not unplug the reactor.

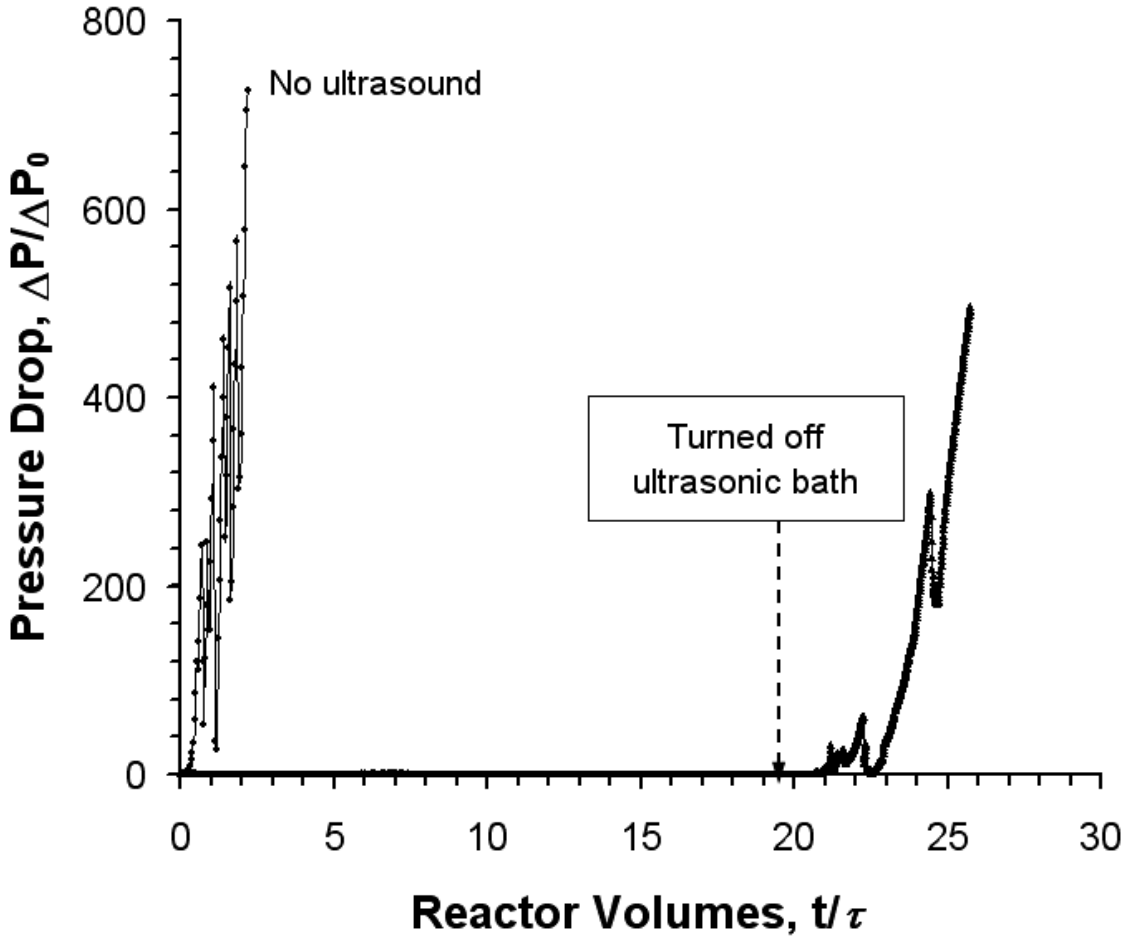

Figure 7. Normalized pressure drop during the reaction (τ = 7 min, 0.1 M ArCl) in a PFA capillary (1000 μm ID, 240 μL) at 80.0 °C. The figure illustrates that the presence of acoustic forces prevents the pressure drop from rapidly increasing.

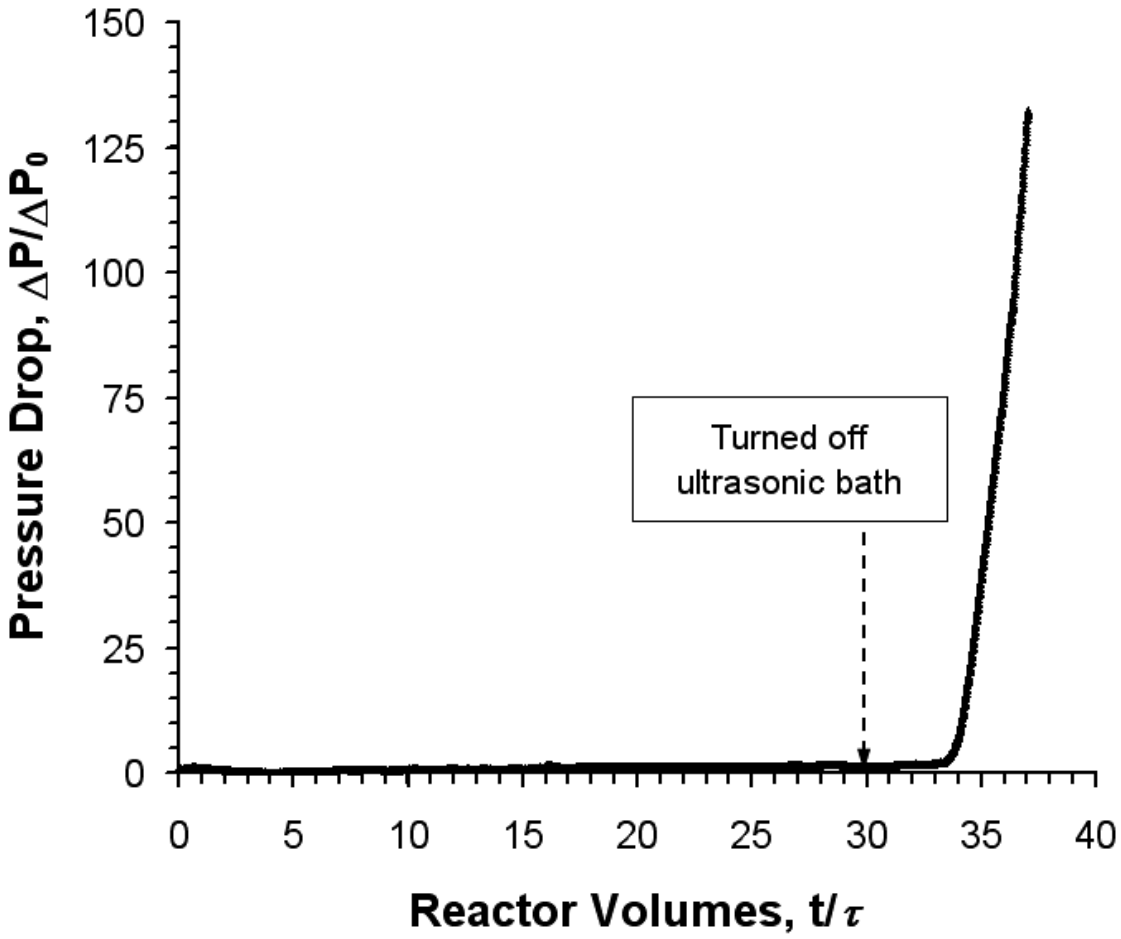

Figure 8. Normalized pressure drop during the reaction (τ = 7 min, 0.1 M ArCl) in a PFA capillary (500 μm I.D., 240 μL) at 80.0 °C. The figure illustrates the acoustic forces had a similar effect on the reaction in smaller diameter tubing.

The effect of channel dimensions on plugging was examined by repeating the experiment described in Figure 7 with a smaller capillary (500 μm I.D.). The reactor volume (240 μL) and injection rate (τ = 7 min) were held constant by increasing the reactor length. As shown in Figure 8, the Normalized pressure drop also remained small until the acoustic irradiation was removed. In both cases, samples were collected, and yield and conversion, relative to the internal standard, were determined by GC to be 100% and >95%, respectively. Given that the reaction rate increases with concentration we investigated whether acoustic-mediated transport would allow for uninterrupted flow when concentrations were closer to those

of traditional batch experiments (e.g., 1 M). However, we found that the solubility limit of NaO*t*-Bu in 1,4-dioxane at room temperature was approximately 1.0 M. Taking into account both the stoichiometry of the reaction and the dilution resulting from the combination of the base stream and the stream containing the remainder of the reagents, the maximum concentration was determined to be 0.36 M in ArCl. Under these conditions (τ = 1 min), flow was possible in the presence of ultrasound, samples were collected and the conversion and yield were measured to be 100% and >95% by GC, relative to internal standard. These observations were made for both 500- and 1000-μm PFA microreactors. Nevertheless, exactly why the ultrasound was preventing clogging remained ambiguous.

In order to elucidate the role of acoustic irradiation on flow, particles exiting the capillary (1000 μm I.D., τ = 1 min) were analyzed. The reaction mixture was collected (400 μL) into vials, under an argon atmosphere, containing 1,4-dioxane (400 μL), and the samples were analyzed using a Malvern Mastersizer 2000 laser diffraction analyzer. Reactions were run with catalyst loadings increasing from 0-1.0 mol% to give increasing conversions and yields without changing the flow conditions or the reagent concentrations of the experiments. As is evident in Figure 9 (left), varying the catalyst loading (in separate experiments) yielded particles ranging in diameter from approximately 0.15-36 μm. The different loadings resulted in different total particle concentrations (depending on the reaction conversion); however, the relative particle size distributions were equivalent in all cases.

In a separate set of experiments, we were able to flow the reaction for several reactor volumes in the absence of ultrasound without plugging. Samples were collected before plugging took place and particle size analysis revealed particles in the range of 0.15 to 112 μm, as shown in Figure 9 (right). The additional mode of particles observed can be attributed to the aggregation of the salt particles, and the combination of the results in Figures 9 demonstrate that ultrasonic forces can reduce the effective maximum particle size, which in turn prevents bridging. Thus, applying external forces such as ultrasonic irradiation can influence and even overcome the particle-to-particle interactions that can lead to clogging via bridging.

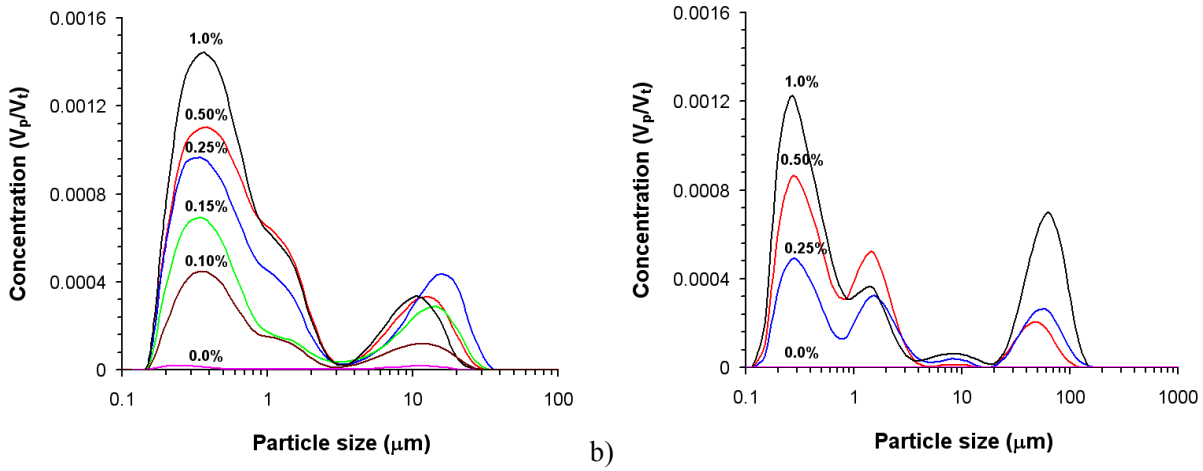

Figure 9. a) Particle size estimation for the reaction in the presence of ultrasound. b) Particle size estimation for the reaction in the absence of ultrasound. The figures show that acoustic irradiation reduces the maximum effective particle size – the larger particles are likely aggregates.

The experimental results shown in Figure 9 offer insight on potential microreactor designs that could prevent bridging for Pd-catalyzed aminations or other salt forming reactions. From the experiment in the presence of ultrasound, the aspect ratio (D/a) between the largest particle and the capillary (1000 μm ID) was 28. Without any ultrasound the system clogged even though the aspect ratio of 8.9 was greater than the previously stated cutoff of 4 that has been determined for stable colloids.[53] Attractive particle interactions likely contributed to clogging at this aspect ratio. Nevertheless, these observations imply that microreactors with channels of 400 μm could potentially tolerate NaCl particles in the range of 14 μm without bridging. It is possible, however, that particles larger than 14 μm but smaller than 45 μm (i.e., aspect ratio of 8.9) will not bridge. However, these conservative approximations neglect the time-dependent change in microchannel geometry caused by constriction *via* particle deposition or growth.

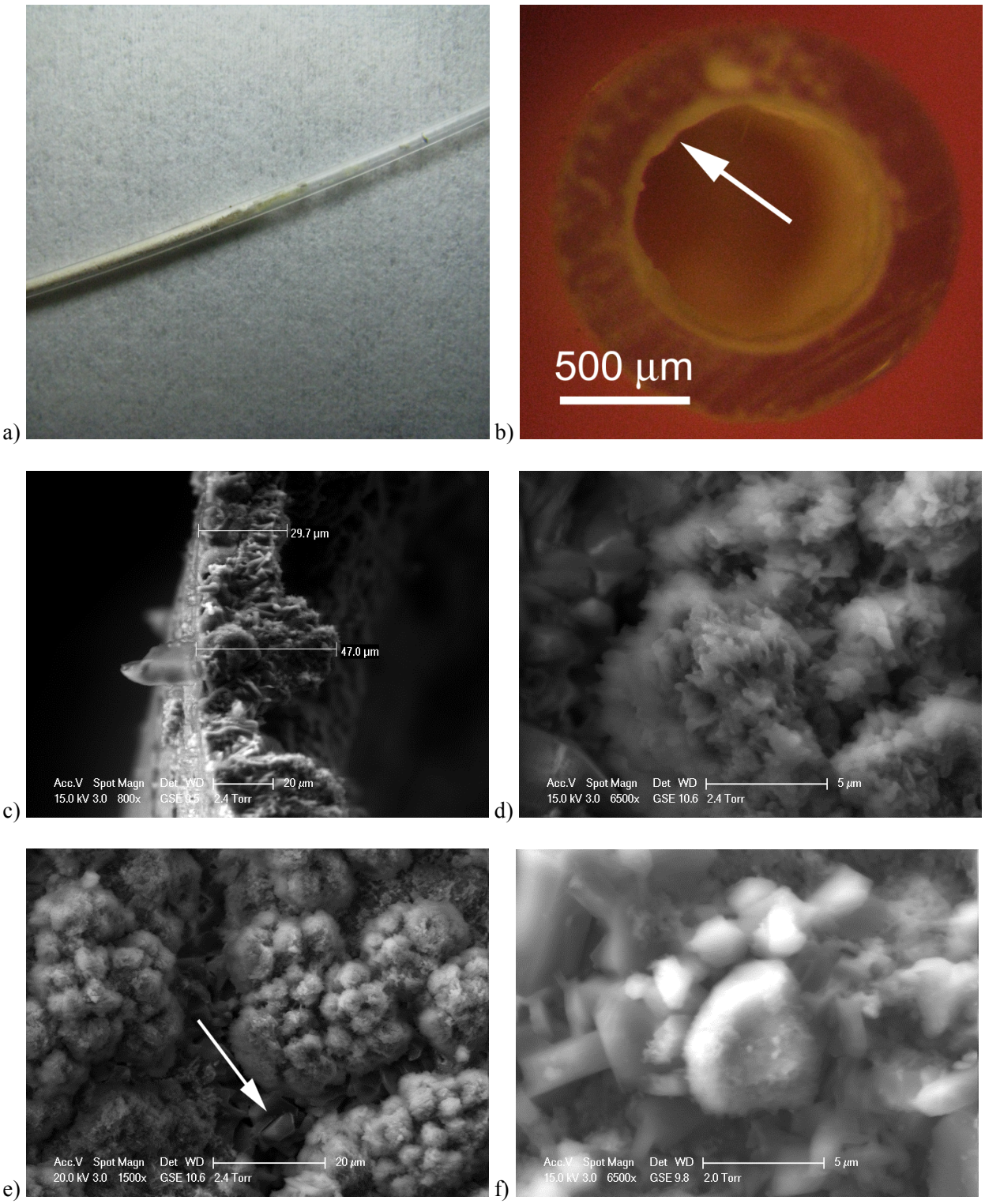

Figure 10. a) PFA capillary showing wall deposition after the reaction mixture exited the heated section exposed to acoustics. b) Cross-section of the capillary illustrating the wall deposit. c) SEM micrograph of the wall deposit in the axial direction. d) Expansion. e) SEM micrograph of the wall deposit in the radial direction. f) Expansion.

Constriction *via* deposition or growth. As was shown in the microreactor of Figure 4, constriction can take place in addition to bridging. To our surprise, switching the reactor surface from silicon nitride to fluoropolymer alone did not inhibit constriction, as white material gradually formed on the PFA capillary walls after injecting approximately 40 reactor volumes. It should be noted, however, that this material was observed to form upon the walls of the tubing after the heated zone where the exposure to ultrasound was limited. No wall deposits were observed to form in the section of the reactor exposed to ultrasound. Figure 8a and b illustrate the axial and radial cross-sections, respectively, of the capillary containing the wall deposits. The capillary was filled with reaction solvent (1,4-dioxane) and was cooled below the freezing point of the solvent (11.8 °C). Cuts were immediately made with a razor to preserve the deposited material on the capillary walls. Examination of these deposits with scanning electron microscopy illustrated the film thickness to range from 30-50 μm (Figure 10, middle left). As shown in Figure 10 (bottom left), the deposit was comprised of cauliflower-type clusters, which may or may not be particle aggregates. Further inspection of the film with SEM revealed the presence of different crystals, highlighted in Figure 10 (middle and bottom left) and enlarged in Figures 10 (middle and bottom right). X-ray diffraction later confirmed the material to be a composite of sodium chloride and an unknown organic crystal (see Experimental). Isolation and GCMS analysis of this unknown substance revealed that it is, at least in part, reaction product. Subsequent experiments proved that the deposited material could be easily removed by flushing with reaction solvent followed by water. In this case, constriction could be managed *via* periodic flushing schemes, especially when the deposition or growth rate is predictable.

When constriction takes place before heating of the reactants or after they have been cooled, the concentration of starting material or the particles formed remains relatively constant. It is under these conditions that the change in microchannel geometry is a constant, α, and expressed as Equation **3**.

$$\frac{dD}{dt} = -\alpha \qquad \textbf{3}$$

A reduction in cross-section diameter is readily monitored by measurement of the pressure drop. For laminar flow in a cylindrical pipe, pressure can be defined by Equation **4** when γ is defined by Equation **5**,

t^* is defined by Equation **6**, D_0 is the initial channel diameter, D is the diameter at time t, and τ is the residence time.

$$\frac{\Delta P}{\Delta P_0} = \frac{1}{(1-\gamma t^*)^4} \quad \textbf{4}$$

$$\gamma = \frac{\alpha\tau}{D_0} \quad \textbf{5}$$

$$t^* = \frac{t}{\tau} \quad \textbf{6}$$

Equation **4** can be applied to approximate a constriction rate, α, or to determine the clogging mechanism. When constriction takes place, one would expect the Normalized pressure drop to gradually increase before plugging, as was the case in Figure 4.

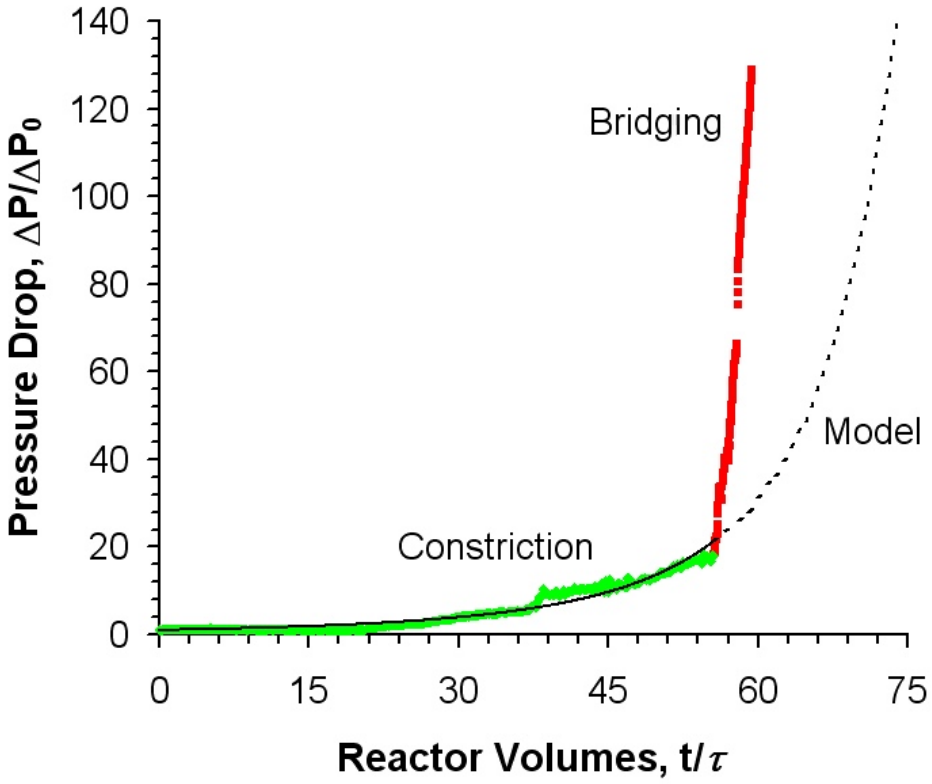

Figure 11. Normalized pressure drop during the reaction (τ = 3 min, 0.36 M ArCl) in a PFA capillary (1000 μm I.D., 240 μL) at 80.0 °C. The experimental data is plotted with the model of Equation **4**.

Repeating the experiment in a 1000-μm capillary (240 μL and τ = 3 min) and expanding the y-axis revealed an important observation. As can be seen in Figure 9, an abrupt increase took place after

injecting 57 reactor volumes, while the approximation of Equation **4** predicts the pressure increase at a later time. These results imply that constriction of the microreactor diameter eventually resulted in bridging. From Equation **5**, the constriction rate was estimated to be 3.2 μm/min.

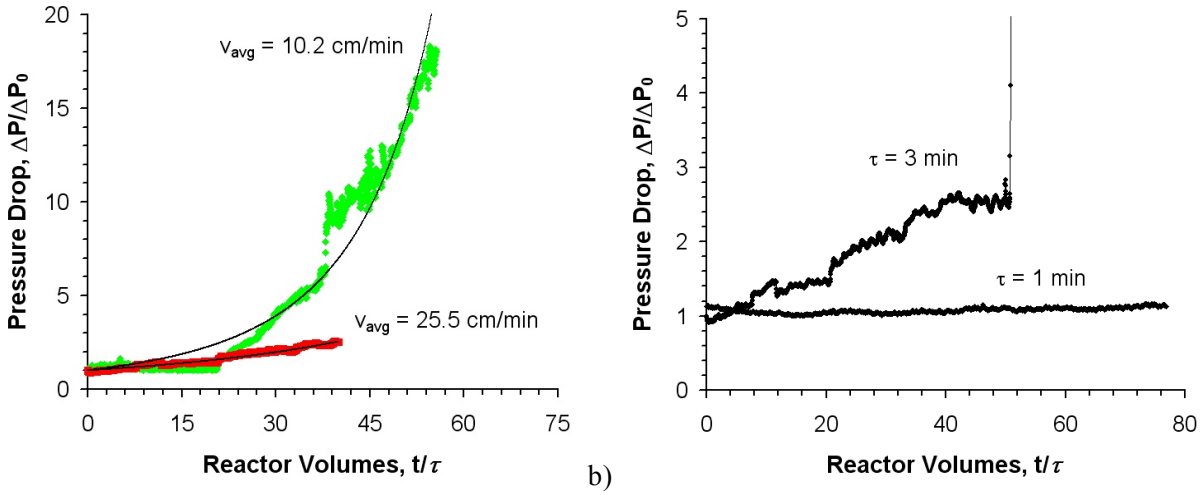

Figure 12. a) The influence of changing the average flow velocity from 10.2 to 25.5 cm/min on the normalized pressure drop. b) Reducing the residence time from 3 to 1 min further illustrates that increasing the velocity eliminates significant constriction and bridging.

Eliminating bridging and constriction. The rate at which salt byproduct accumulates on the surface is influenced by convection. To examine this influence, the experiment of Figure 11 was repeated, and the total reactor volume increased from 240 to 600 μL while maintaining a constant residence time of 3 min. The reactor volume exiting the ultrasonic bath was also held constant at 120 μL. One observes in Figure 10a that increasing the flowrate from 80 μL/min (average velocity v_{avg} = 10.2 cm/min) to 200 μL/min (v_{avg} = 25.5 cm/min) decreased the constriction rate. The solid curved lines of Figure 12 (left) represent Equation **4**. Applying Equations **4** and **5** yields a constriction rate of approximately 1.8 μm/min upon increasing the flowrate to 200 μL/min. These observations demonstrate that convective forces alone can potentially overcome the particle-to-particle or particle-to-wall interactions that lead to constriction. Moreover, the particles can interact mechanically with the deposit and limit growth *via* abrasion. Partial evidence of this phenomenon can be seen in Figure 12b. Reducing the residence time from 3 min to 1

min eliminated constriction and bridging altogether, despite the reaction being complete in all cases. Consequently, the normalized pressure drop remained constant even after injecting 76 reactor volumes.

Influence of acoustics on reaction. Ultrasound has proven to be a useful tool in enhancing the rate of organic transformations,[64,65] including reactions catalyzed by palladium.[66] It is generally understood that the energy emitted from cavitations can contribute to enhanced reaction rates in batch-scale systems that have temperature gradients. Recently, the research work of others has elucidated that ultrasound enhances mixing in microfluidic systems.[63,67,68] We questioned whether these temperature and mixing effects would impact the Pd-catalyzed C-N bond formation reaction in capillary flow.

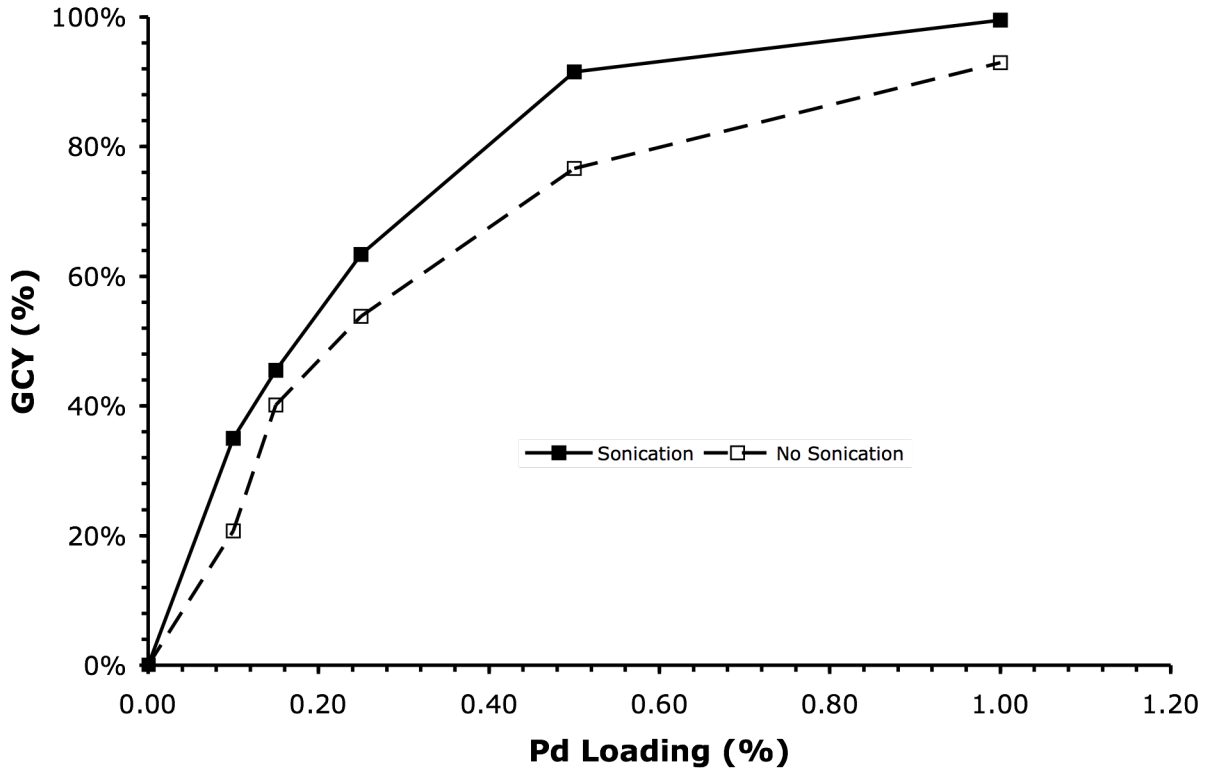

Figure 13. The influence of ultrasound on product yield for different catalyst loadings.

The coupling reaction was carried out in a PFA capillary at 80.0 °C and a residence time of 1 min. As shown in Figure 13, increasing the catalyst loading from 0-1.0 mol% resulted in increased conversion

from starting material to the biaryl amine product. Without any ultrasound, the yield was reduced for a given catalyst loading.

Table 1. Yields for a series of experiments (0.5 mol% catalyst, τ = 1 min) testing the influence of ultrasound on reaction yield.

exp.	Temp (°C)	Res. Time (min)	Yield w/ Ultrasound[a]	Yield w/o Ultrasound[a]
1	80	1.0	86	78
2[b]	80	1.0	80	77
3	80	1.0	86	81
4[b]	80	1.0	85	73
ave.	80	1.0	84 ± 3	77 ± 3
isolated	80	1.0	80[c]	74[c]

[a] Average of three samples with standard deviation
[b] Reaction performed in reverse order
[c] Combined isolated yield for exp. 1-4

The data in Table 1 show the results of a series of experiments performed to confirm the results in Figure 11. Solution 1 (1.0 M NaOtBu in 1,4-dioxane) and solution 2 (0.72 M ArCl, 0.86 M aniline, 0.14 M biphenyl and 3.6 mM XPhos precatalyst in 1,4-dioxane) were injected (120 μL/min each, τ = 1 min) into a PFA capillary (1/16" O.D., 1000 μm I.D., 240 μL heated, 360 μL total) submerged in an ultrasonic bath filled with water at 80 °C. While sonicating, the reaction was run for 5 minutes to achieve steady state at which point sample 1 was collected (5 reactor volumes). The sonication was stopped, and the reaction was run for 4 minutes to reach a new steady state at which point sample 2 was collected (5 reactor volumes). The injection was stopped and the reaction was flushed sequentially with dioxane, water, acetone and dioxane to remove all reagents, salt byproducts, water and acetone, respectively. The system was then ready for the next experiment. This process was repeated a total of four times, with the 2nd and 4th experiments being performed with sample 1 being the reaction with no sonication and sample 2 being the reaction during sonication. The 8 samples were analyzed by GC, and were subsequently combined

and isolated (see Table 1). These results support that the acoustic irradiation may have enhanced temperature, mixing, or both. Given that temperature gradients are less significant in microscale systems, one might expect an even more pronounced influence in larger-scale systems.

The preparation of a 4-methoxy-*N*-phenylaniline represented a case study for understanding how to handle salt byproducts in microsystems during Pd-catalyzed reactions. Based on the data reported in Figure 10b and the residence times investigated, approximately 2.6 g/hr of product could be synthesized, whereas continuous-flow synthesis under these conditions was previously not possible. Just as importantly, the working principles could be extended to other Pd-catalyzed C–N bond formation reactions. Consequently, the laboratory-scale production of fine chemicals prepared with these reactions is possible. Furthermore, microchemical systems may be applied to and the optimization of reaction conditions for individual reactions and complex synthetic pathways. Finally, the ability to handle salt byproducts in microsystems offers the opportunity to use these systems to discover the reaction kinetics and mechanisms of important transformations.

4.3 Conclusion

We have found that both bridging and constriction take place during Pd-catalyzed amination reactions in microreactors, leading to severe plugging. The use of acoustic irradiation reduced the maximum effective particle size of the salt byproduct and thus prevented bridging in PFA capillary-based reactors. It is likely that the magnitude of the acoustic forces exceeded the hydrodynamic and particle-to-particle attractive forces that led to bridging. Slurries of particles, the largest of which had aspect ratios of 28, flowed without severe plugging when acoustic irradiation was applied. In a system that did not include ultrasound, plugging was observed and the aspect ratio of the largest particles was estimated to be 8.9. Constriction was observed to be quite severe in silicon nitride coated devices, and interestingly, switching to a fluoropolymer capillary did not eliminate the problem. A composite of NaCl and product was formed on the surfaces that were not submerged in the ultrasonic bath and exposed to acoustic irradiation. When the flowrate was increased, it was observed that the pressure increased at a slower rate. Fitting this

data to a constriction model showed a correlation between the rate of wall deposition and flowrate and suggested that a further increase of the flowrate could potentially eliminate clogging due to constriction. Moreover, the presence of acoustic irradiation appeared to enhance the reaction rate, which may be the result of a temperature increase based on the energy emitted from cavitation and/or a result of enhanced mixing. Based on the results reported herein, general guidelines can be prescribed to handle salt byproducts during reactions in microsystems. It is important to limit the particle sizes to aspect ratios of ~9 either by removing them from the reactor before they grow to that size or by imposing an external force such as acoustic irradiation. The filtration of solvents and reagent mixtures can also be important in eliminating potential bridging. Additionally, increasing the flow velocity can help to mitigate constriction. Otherwise, an estimation of the constriction rate can be useful in determining how often solvents need be injected to remove deposits.

Although the handling of solids in microsystems offers new opportunities for chemical reactions that were previously difficult or not attainable, moving forward is not without challenges. Many of the routes to APIs involve solids, which can participate as reactants, products, and catalysts, in addition to salt byproducts. Strategies for handling other types of solids will prove useful for developing efficient flow-based syntheses. Furthermore, the need to operate in both the micro and macro scale reactors warrants a deeper understanding of solids handling. Additionally, deposition and growth on peripheral equipment, reactors, instruments, and transfer tubing surfaces is an important consideration that needs to be addressed when flowing salts suspended in organic solvents. Strategies and techniques to remove such deposits will find utility on all scales.

Scheme 2. Decision matrix for dealing with reactions that lead to plugging.

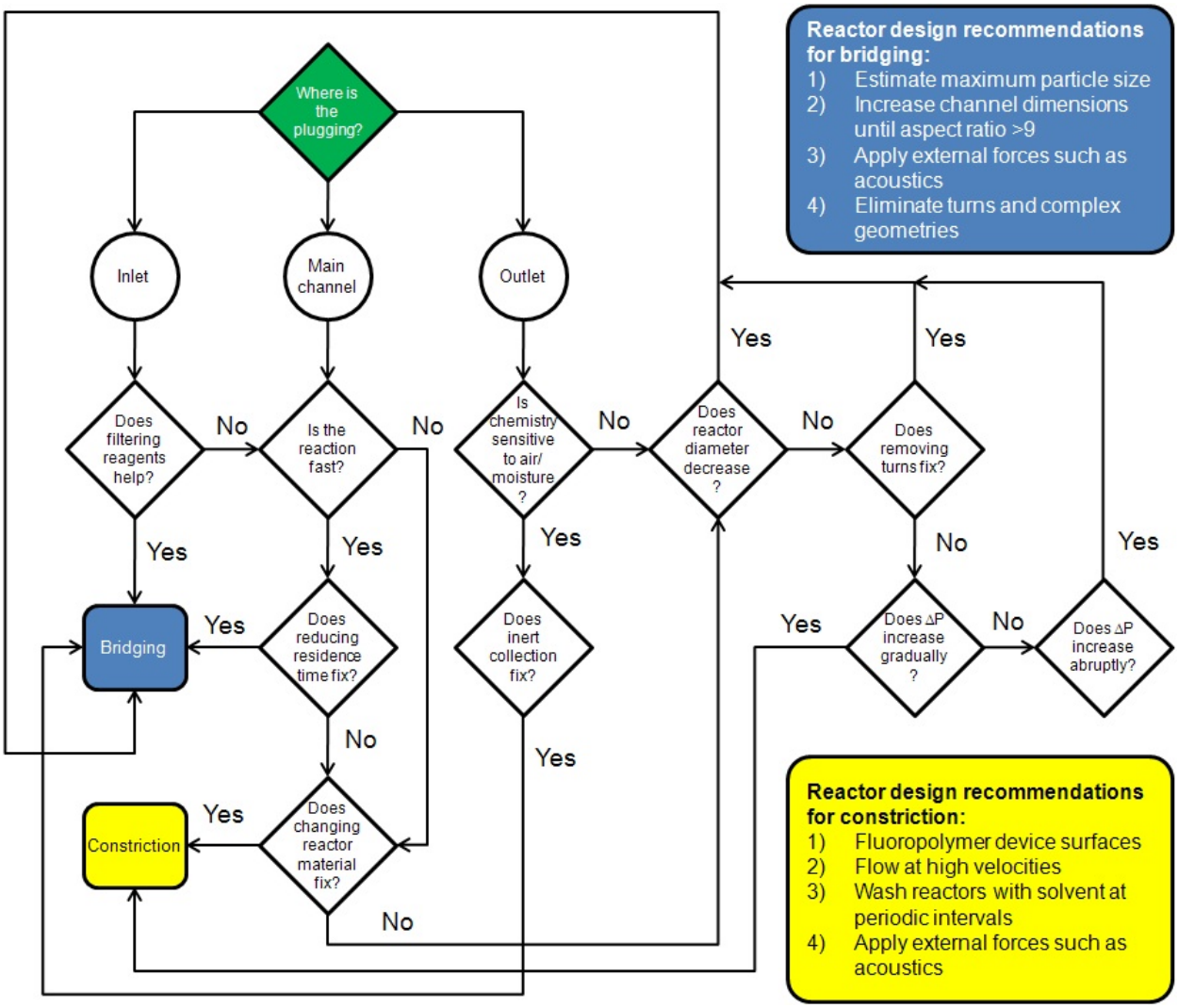

The conclusions that have been drawn from this work have been summarized into a chart that is shown in Scheme 2. By answering a series of questions about the nature of the flow system and the plugging that is occurring during the reaction, the mechanism of clogging can be determined and a series of recommendations are provided.

4.4 Experimental

Silicon fabricated microreactors. Microchannel devices were fabricated from a double-side-polished silicon wafer and capped with a Pyrex wafer (both 150 mm in diameter and 650 μm thick). As shown in Figure 14, the fabrication process involved several photolithography steps, deep reactive ion etching of the silicon, and growth of a low-stress silicon nitride coating (0.5 μm). Anodic bonding of the Pyrex wafer capped the etched silicon-nitride-coated features and completed the microfluidic device. The packaged device, with a serpentine microchannel (0.4 x 0.4 x 875 mm) is shown in Figure 15. As will be discussed later, a device with a spiral microchannel, of the same dimensions, was also fabricated in the same manner. The halo through-etch between the cooled inlets and outlet and main channel (Figure 15) provided thermal separation between the two parts of the reactor and allowed for operation with two separate temperature zones, each nearly isothermal, on a single chip.[34]

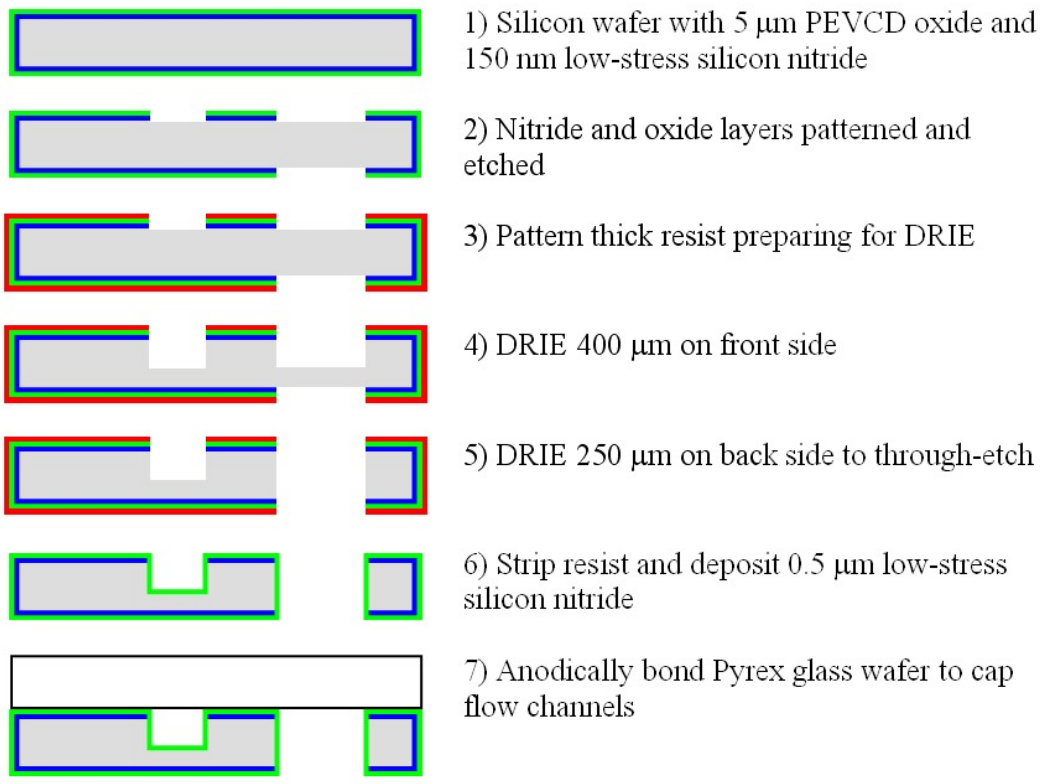

Figure 14. The microreactor fabrication process.

Standard machining techniques were employed to produce a compression chuck (316 Stainless Steel) with standard 10-32 coned-bottom fluidic ports for each microreactor. The microreactor inlets and outlet were compressed in this chuck (see Figure 15) using Kalrez® o-rings for chemical compatibility, and the chuck was cooled (to 20 °C) using a Thermo Scientific NESLAB RTE-7 refrigerating bath. A Kapton flexible heater (KHLV series, 28V) and an Omega CN9000 series PID controller were used to control the temperature in the heated section of the microchannel.

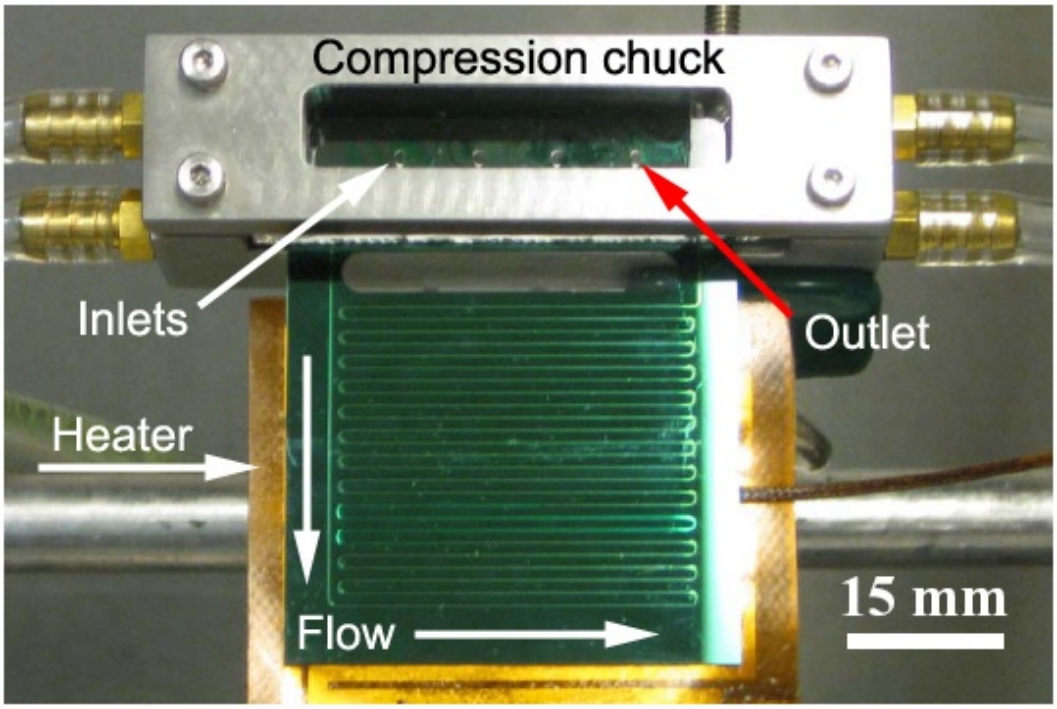

Figure 15. The silicon microreactor used to study solids handling. The image shows the compression chuck used to cool the inlets and outlet of the microchannel.

Experimental setup. Figure 16 illustrates the equipment configuration used for the present study. Reagents in glass syringes (10 mL, SGE), were delivered to the microreactor (see Figure 15) with Harvard Apparatus PHD2000 syringe pumps. A Honeywell stainless-steel pressure transducer (19C100PG4K) was plumbed directly into one of the reagent lines upstream to the mixing point. The pressure transducer was excited using a 10 V power supply, and the output was recorded using a National Instruments USB 9219 data acquisition card. Consequently, it was possible to constantly monitor the

pressure entering the reactor with National Instruments LabVIEW 8.5.1. Upon exiting the reactor, the mixture passed through approximately 120 μL of high purity polytetrafluoroethylene (PFA) tubing (1/16" OD, 1000 μm I.D.) at ambient temperature before it was collected in a vial that was under a constant pressure of argon, at 1.7 psig. All other fluidic connections were made using 1/4-28 PTFE fittings and PFA tubing (1/16" O.D., 500 μm I.D., IDEX Corporation). Images were captured with a high-speed color CCD camera (JAI CV-S3200 series). Experiments with acoustic irradiation were performed by replacing the microreactor of Figure 15 and Figure 16 with lengths of loosely coiled PFA tubing (1/16" OD, 500 or 1000 μm ID). The tubing was submerged in a VWR ultrasonic bath (Model 50HT) filled with de-ionized water. The bath temperature was monitored *via* a thermocouple and maintained with a Waage immersion heater controlled by a J-KEM Scientific Gemini PID controller. Upon exiting the bath, the reaction mixture was collected under argon as described above.

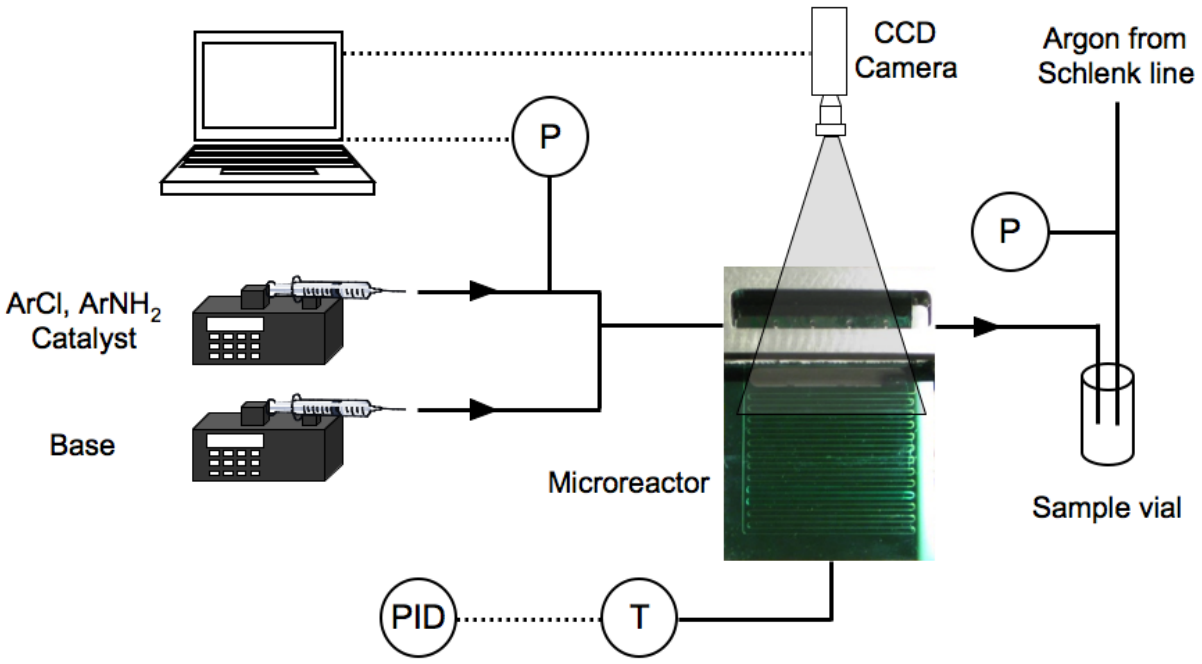

Figure 16. The experimental setup used to carry out solids handling experiments.

Reagents and analytical. All experiments were carried out using reagent grade solvents, and all solutions were prepared under argon atmospheres. 4-Chloroanisole, aniline, biphenyl, sodium *tert*-butoxide and 1,4-dioxane were purchased from Sigma-Aldrich chemical company and used as received. XPhos and the

XPhos precatalyst were prepared according to literature procedures.[52,69] Reaction solutions were prepared in screw-cap, oven-dried volumetric flasks. For the clogging experiments, two solutions were prepared. The first solution contained the base (NaO*t*-Bu) and was prepared in 1,4-dioxane. The second solution contained the aryl chloride (4-chloroanisole), amine (aniline), internal standard (biphenyl) and catalyst (XPhos precatalyst) and was also prepared in 1,4-dioxane. Reagents that were solids (biphenyl, XPhos precatalyst and NaO*t*-Bu) were added to the volumetric flasks that were then evacuated and refilled with argon. This process was repeated a total of 3 times. Liquid reagents were added by syringe, and the solutions were made up to the desired volume with 1,4-dioxane. The base solution was then taken up into a syringe and filtered through a PTFE membrane filter (0.4 μm porosity) into a second flask that had previously been oven-dried and purged with argon. The two solutions were then loaded into syringes and fitted in the syringe pumps for the experiments.

All compounds were characterized by ^{1}H NMR, ^{13}C NMR, and IR spectroscopy. Copies of the ^{1}H and ^{13}C spectra can be found at the end of the experimental section. Nuclear Magnetic Resonance spectra were recorded on a Bruker 400 MHz instrument. All ^{1}H NMR experiments are reported in δ units, parts per million (ppm), and were measured relative to the signals for residual chloroform (7.26 ppm) in the deuterated solvent, unless otherwise stated. All ^{13}C NMR spectra are reported in ppm relative to deuterochloroform (77.23 ppm), unless otherwise stated, and all were obtained with 1H decoupling. All IR spectra were taken on a Perkin – Elmer 2000 FTIR. All GC analyses were performed on a Agilent 6890 gas chromatograph with an FID detector using a J & W DB-1 column (10 m, 0.1 mm I.D.).

A Canon PowerShot S5IS camera fitted on a Diagnostic Instruments Leica MZ12 microscope was used to capture images of slugs made up of hexane and fluorescein (0.01 vol%) dissolved in water and to capture low resolution images of the wall deposits. High-resolution micrographs of the wall deposits were obtained with a FEI/Philips XL30 FEG ESEM. Analysis of particle sizes exiting the reactors was made possible with a Malvern Mastersizer 2000 laser diffractometer fitted with a Hydro 2000μP cell. In all cases, samples were collected under argon and diluted by a volumetric factor of 2 with 1,4-dioxane. The analysis was performed by injecting samples ranging from 0.2 to 0.8 mL into the 14.4 mL reservoir of the

diffractometer cell that was filled with 1,4-dioxane.

Workup and yields. Samples that were collected under argon were diluted with equal volumes of ethyl acetate and water and mixed vigorously. The organic phase was separated, filtered through a short plug of silica gel and analyzed by GC. Yield and conversion were determined based on the peak area, relative to the internal standard. In two examples, the water phase was extracted with ethyl acetate a total of three times and the organic phases were combined and concentrated. The crude material was then purified by column chromatography (Biotage Isolera, 25g SNAP column, hexanes and 0-20% ethyl acetate). Isolated yields were found to be in excellent agreement with the GC yields.

Acoustic Waveform

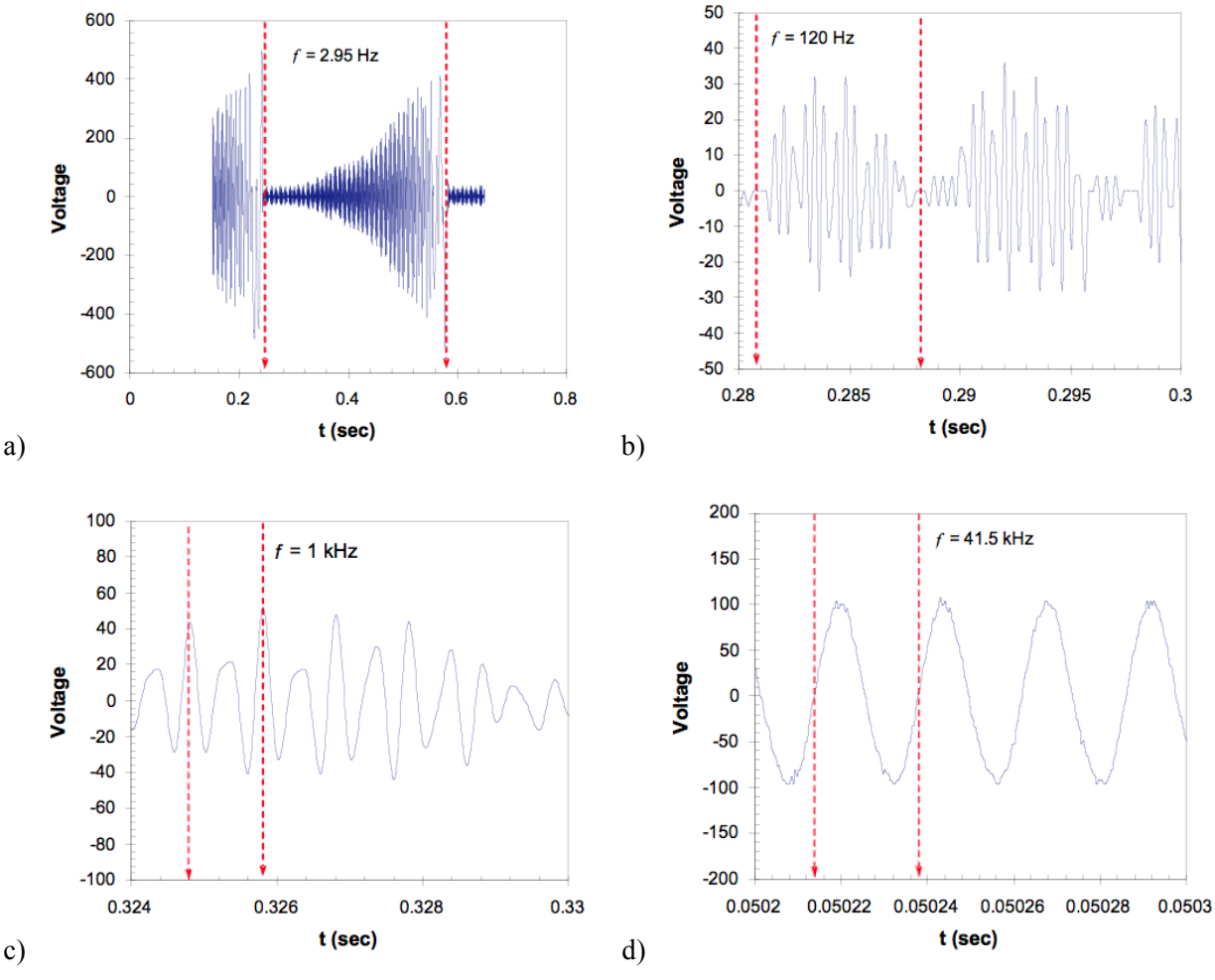

Figure 17. Ultrasonication bath waveform at different rates and resolutions of data capture.

The waveform produced by the transducer of the ultrasonic bath used in the experiments was recorded with an oscilloscope by measuring the voltage supplied to the transducer. The waveform was observed to have several different periodicities, as shown in Figure 17. The sinusoidal waves had a maximum voltage ranging from 25 – 500 V.

These figures were used to determine the frequencies of the acoustic signal and to create a function capable of reproducing it. The acoustic modes were seen to be a sinusoidal mode at 41.5 kHz (Figure S1d), a dual-sinusoid (every second peak is at half-height) at an overall frequency of 1 kHz, a "ringing" mode at 120 Hz, and a ramp-up followed by a drop at 2.95 Hz. The first mode can be easily written as Equation **7** and the second mode, a dual sinusoid, is a sum of a sine at twice the frequency and a half-value cosine and can be written as Equation **8**. The ringing mode is caused by a second sine wave added to the one in **8**, this one with a frequency such that the difference in frequencies of the two sine waves is the frequency of the ringing (Equation **9**).

$$f_1(t) = \sin(2\pi \cdot 41.5\,\text{kHz} \cdot t) = \sin(260752t) \quad \textbf{7}$$

$$f_2(t) = \sin(2\pi \cdot 2000\,\text{Hz} \cdot t) + \frac{1}{2}\cos(2\pi \cdot 1000\,\text{Hz} \cdot t) = \sin(12566t) + \frac{1}{2}\cos(6283t) \quad \textbf{8}$$

$$f_2(t) = \sin(2\pi \cdot (2000\,\text{Hz}+120\text{Hz}) \cdot t) = \sin(13320t) \quad \textbf{9}$$

The ramp was smoothed and fitted to determine the best approximation function, as shown in Figure 18. The exponential is a ramp with a period of 0.3386 seconds and as such it can be represented by a Laplacian, Equation **10** where the subscript *P* represents a single period, and *u*(*t*) is the Heaviside function. Thus, Equation **11** defines the Laplace of the periodic with a period of 0.3386 seconds.

$$f_P(t) = e^{9.5t}\left(u(t) - u(t-0.3386)\right) \quad \textbf{10}$$

$$L\left\{f(t)\right\} = \frac{1 - e^{3.2167-0.3386s}}{(s-9.5)\left(1-e^{-0.3386s}\right)} \quad \textbf{11}$$

Multiplying the inverse Laplace of this function by the sum of equations **7-9** yielded an overall function with the correct range of voltage and the appropriate periodicities, Equation **12**.

$$f(t) = L^{-1}\left\{\frac{1 - e^{3.2167-0.3386s}}{(s-9.5)\left(1-e^{-0.3386s}\right)}\right\}\left(\sin(260752t) + \sin(13320t) + \sin(12566t) + \frac{1}{2}\cos(6283t)\right) \quad \textbf{12}$$

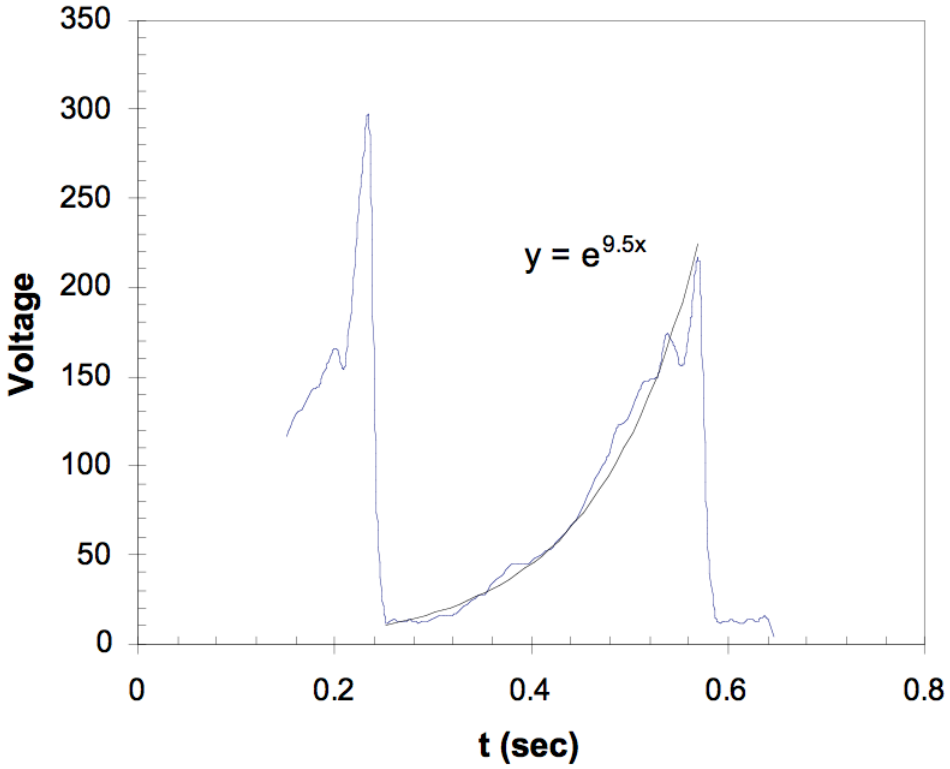

Figure 18. Smoothing of the absolute values of the data in Figure S1a, with a fitted exponential.

X-ray Diffraction and GCMS Analysis of the Wall Deposit

An X-ray diffraction analysis of the solid material of Figure 10 was made possible with a Rigaku high-power rotating anode X-Ray powder diffractometer. The solid deposit was washed from the microreactor walls with a 50:50 mixture of methanol:water (by volume) and recrystallized on an X-ray transparent sample stage. Figures 19 and 20 show the measured diffraction pattern compared with other possible components in the reaction mixture. As is evident, the pattern closely matches that of Halite (i.e., NaCl) that is the expected by-product formed during the reaction. Nevertheless, the intense peak between 5-10 2-theta and the less intense peaks from 30-40 2-theta do not correspond to NaCl. A comprehensive inorganic and organic crystallographic structure search did not reveal the identity of this unknown material. Therefore, a sample of the wall deposit was dissolved in de-ionized water and washed with ethyl acetate. Analysis of the organic phase by GCMS revealed that the crystals contained the reaction product, 4-methoxy-N-phenylaniline, in addition to NaCl.

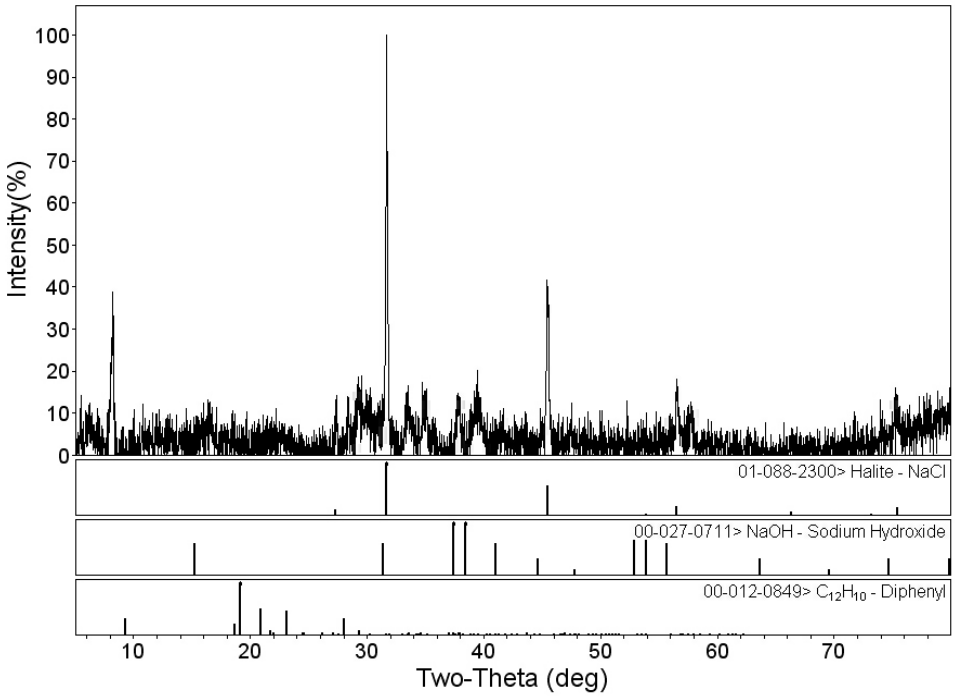

Figure 19. X-ray diffraction pattern of the wall deposit compared with known patterns of NaCl, sodium hydroxide, and biphenyl.

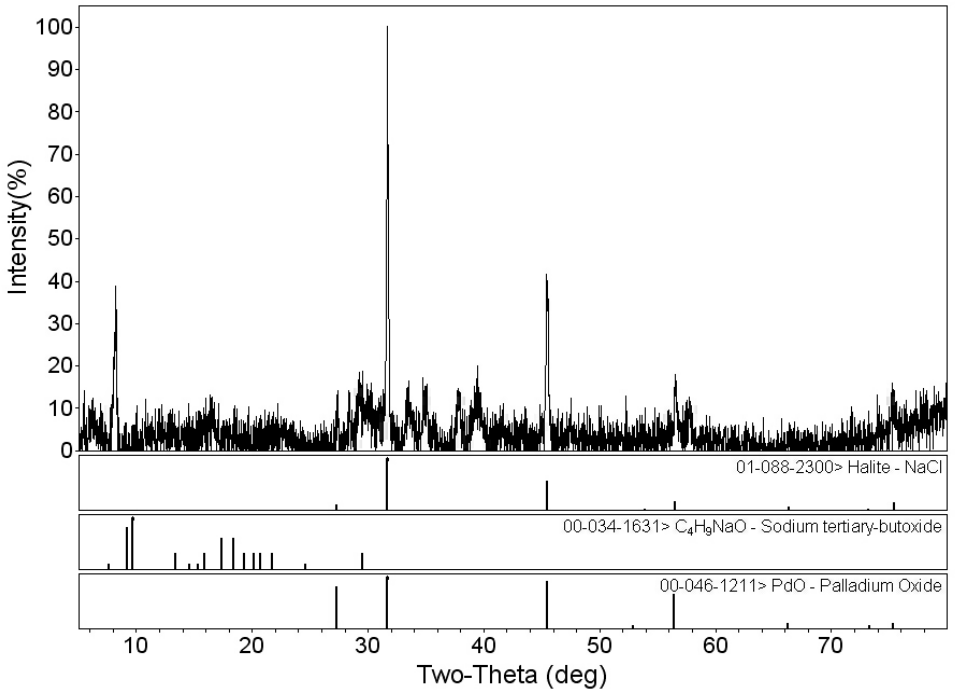

Figure 20. X-ray diffraction pattern of the wall deposit compared with known patterns of NaCl, sodium *tert*-butoxide, and palladium oxide.

General Procedure for Pd-Catalyzed Amination Reactions

An oven-dried volumetric flask (10.0 mL), which was fitted with a Teflon screw-cap septum, was charged with biphenyl (216 mg, 1.4 mmol) and the XPhos precatalyst (57.6 mg, 0.072 mmol). The vessel was evacuated and backfilled with argon (this process was repeated a total of 3 times) and then was charged with 4-chloroanisole (880 μL, 7.2 mmol), aniline (780 μL, 8.6 mmol) and 1.4-dioxane (~9 mL, to make the solution up to 10.0 mL) to give Solution 1. An oven-dried screw-top volumetric flask (10.0 mL), which was fitted with a Teflon screw-cap septum, was charged with NaOtBu (1.06 g, 11.0 mmol). The vessel was evacuated and backfilled with argon (this process was repeated a total of 3 times) and then was charged with 1.4-dioxane (~10 mL, to make the solution up to 10.0 mL) to give Solution 2. After vigorous mixing, Solution 2 was loaded into a Normject plastic syringe (10 mL) and filtered through a PTFE membrane filter (0.4 μm porosity) into an oven-dried screw-cap tube that had been purged with argon. These solutions were loaded into syringes (SGE glass or Normject plastic) and connected to the microfluidic system as diagrammed in Figure 21. The product stream was collected under argon and ethyl acetate and water were added. An aliquot of the organic layer was passed through a plug of silica, eluting with ethyl acetate and the reactions were analyzed by GC.

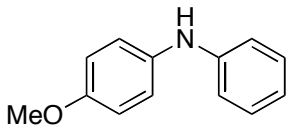

Procedure for obtaining an isolated yield of 4-methoxy-N-phenylaniline:[70] Solutions 1 and 2 were prepared following the general procedure described above, with the catalyst loading being changed to 0.5 mol% (28.8 mg, 0.036 mmol). The solutions were loaded into Normject plastic syringes and connected to the microfluidic system as diagrammed in Figure 21 and the solutions were injected (120 μL/min, τ = 1 min.) into FEP tubing (1/16" O.D., 1000 μm I.D., 240 μL heated, 360 μL total) submerged in an ultrasonic bath filled with water and heated to 80 °C. While sonicating, the flowrates and pressures were allowed to stabilized to a steady-state (5 reactor volumes) and a sample was collected under argon for 45

reactor volumes. The sample was diluted with ethyl acetate (EA) and water and mixed thoroughly. GC analysis of the organic layer determined the yield of **1** to be 84% relative to the biphenyl internal standard. The organic layer was separated and the aqueous layer was extracted 2 more times with EA. The combined organic layers were concentrated and purified by column chromatography (silica gel, Biotage Isolera, 50 g SNAP cartridge eluting with hexanes and 0-20% EA) to give the title compound as an off-white solid (620 mg, 80%), mp = 104-106 °C (lit. 104-106 °C). ^{1}H NMR (400 MHz, $CDCl_3$) δ: 7.24 (t, *J* = 8.0 Hz, 2H), 7.09 (d, *J* = 8.0 Hz, 2H), 6.86-6.94 (m, 5H), 5.51 (s, 1H), 3.81 (s, 3H) ppm. ^{13}C NMR (100 MHz, $CDCl_3$) δ: 155.4, 145.3, 135.8, 129.5, 122.3, 119.7, 115.8, 114.8, 55.7 ppm. IR (neat, cm^{-1}): 3395, 1598, 1515, 1493, 1322, 1298, 1247, 1178, 1029, 742, 693. Anal. Calc'd. for C13H13NO: C, 78.36; H, 6.58.

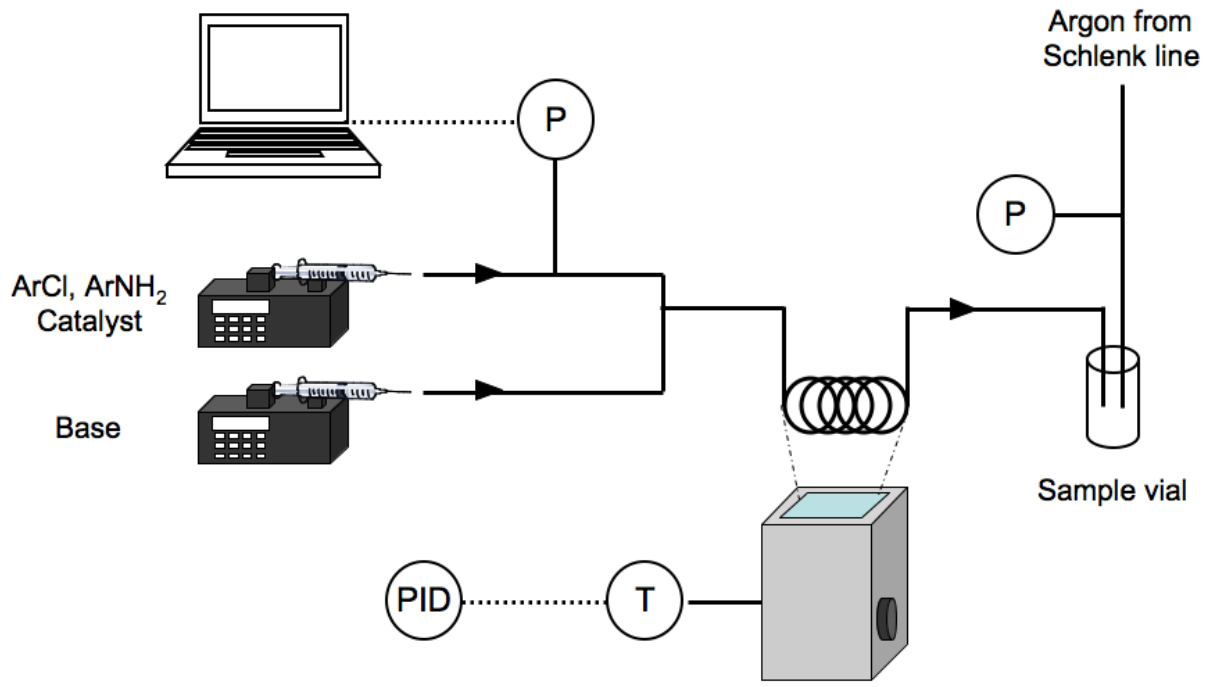

Figure 21. Experimental setup for experiments performed under acoustic irradiation

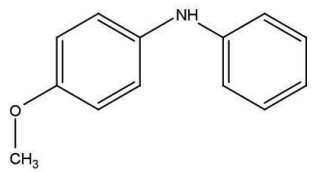
NH
O
CH3

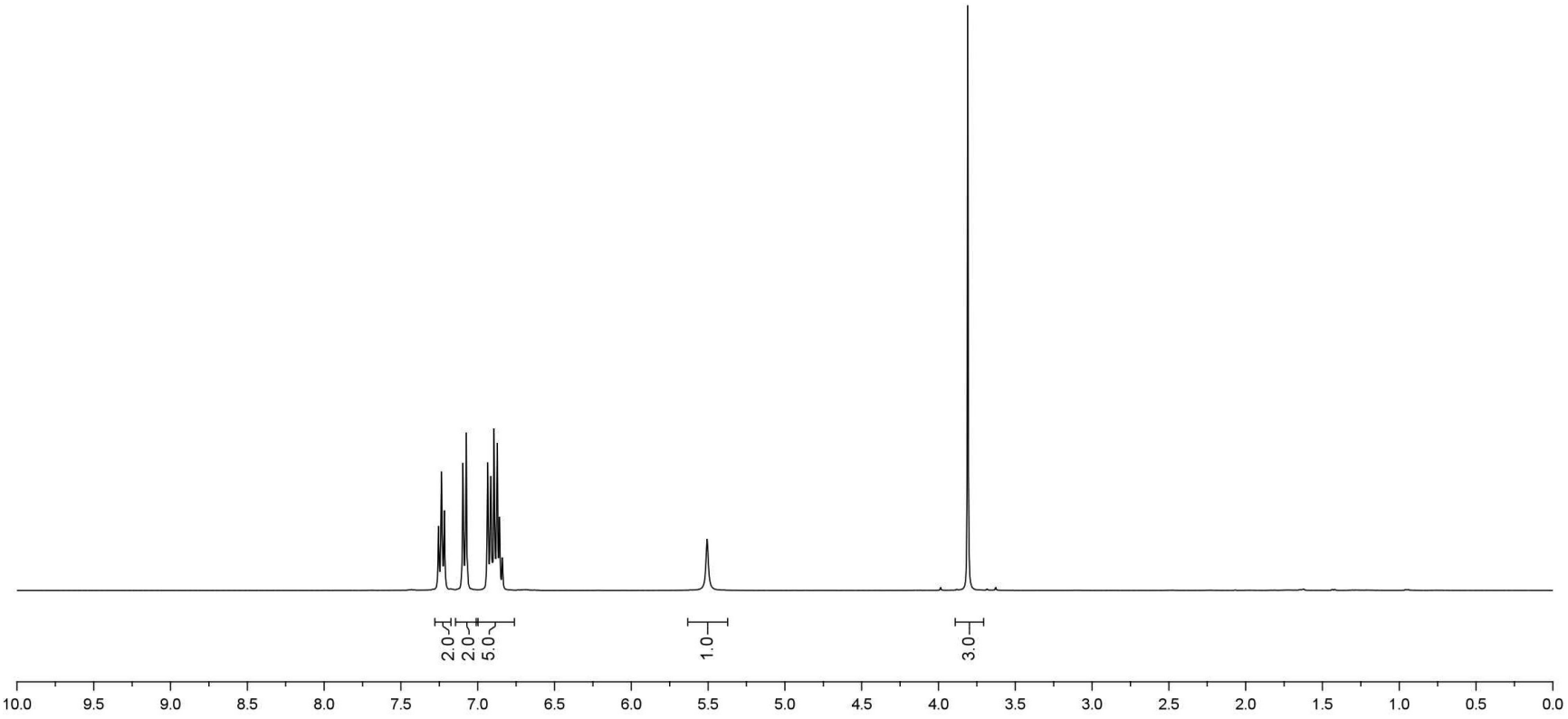
2.0
2.0
5.0
1.0
3.0
10.0
9.5
9.0
8.5
8.0
7.5
7.0
6.5
6.0
5.5
5.0
4.5
4.0
3.5
3.0
2.5
2.0
1.5
1.0
0.5
0.0

155.4
145.3
135.8
129.5
122.3
119.7
115.7
114.8
77.5
77.2
76.9
55.7
NH
O
CH3

4.5 References

1. Roberge, D. M.; Ducry, L.; Bieler, N.; Cretton, P.; Zimmermann, B. *Chem. Eng. Technol.* **2005**, *28*, 318-323.

2. Carey, J. S.; Laffan, D.; Thomson, C.; Williams, M. T. *Org. Biomol. Chem.* **2006**, *4*, 2337-2347.

3. Dugger, R. W.; Ragan, J. A.; Ripin, D. H. B. *Org. Proc. Res. Dev.* **2005**, *9*, 253-258.

4. Jensen, K. F. *Chem. Eng. Sci.* **2001**, *56*, 293-303.

5. Fletcher, P. D. I.; Haswell, S. J.; Pombo-Villar, E.; Warrington, B. H.; Watts, P.; Wong, S. Y. F.; Zhang, X. L. *Tetrahedron* **2002**, *58*, 4735-4757.

6. Jahnisch, K.; Hessel, V.; Lowe, H.; Baerns, M. *Angew. Chem.-Int. Edit.* **2004**, *43*, 406-446.

7. Pennemann, H.; Watts, P.; Haswell, S. J.; Hessel, V.; Lowe, H. *Org. Process Res. Dev.* **2004**, *8*, 422-439.

8. Hessel, V.; Lowe, H. *Chem. Eng. Technol.* **2005**, *28*, 267-284.

9. Jensen, K. F. *MRS Bull.* **2006**, *31*, 101-107.

10. deMello, A. J. *Nature* **2006**, *442*, 394-402.

11. Mason, B. P.; Price, K. E.; Steinbacher, J. L.; Bogdan, A. R.; McQuade, D. T. *Chem. Rev.* **2007**, *107*, 2300-2318.

12. Watts, P.; Wiles, C. *Chem. Commun.* **2007**, 443-467.

13. Watts, P.; Wiles, C. *Chem. Eng. Technol.* **2007**, *30*, 329-333.

14. Hartman, R. L.; Jensen, K. F. *Lab Chip* **2009**, *9*, 2495–2507.

15. Ehrfeld, W.; Hessel, V.; Lowe, H. *Microreactors: New Technology for Modern Chemistry*; Wiley-VCH: Weinheim, Germany, 2000.

16. Jensen, K. F. In *New Avenues to Effcient Chemical Synthesis: Emerging Technologies*; Seeberger,

P. H., Blume, T., Eds.; Springer-Verlag Berlin: Heidelberg, 2007, p 57-76.

17. Haswell, S. J.; O'Sullivan, B.; Styring, P. *Lab Chip* **2001**, *1*, 164-166.

18. Losey, M. W.; Schmidt, M. A.; Jensen, K. F. *Ind. Eng. Chem. Res.* **2001**, *40*, 2555-2562.

19. Baxendale, I. R.; Deeley, J.; Griffiths-Jones, C. M.; Ley, S. V.; Saaby, S.; Tranmer, G. K. *Chem. Commun.* **2006**, 2566-2568.

20. Wiles, C.; Watts, P.; Haswell, S. J. *Lab Chip* **2007**, *7*, 322-330.

21. Poe, S. L.; Cummings, M. A.; Haaf, M. R.; McQuade, D. T. *Angew. Chem. Int. Edit.* **2006**, *45*, 1544-1548.

22. Kockmann, N.; Kastner, J.; Woias, P. *Chem. Eng. J.* **2008**, *135*, S110-S116.

23. Song, H.; Chen, D. L.; Ismagilov, R. F. *Angew. Chem. Int. Edit.* **2006**, *45*, 7336-7356.

24. Horie, T.; Sumino, M.; Tanaka, T.; Matsushita, Y.; Ichimura, T.; Yoshida, J. *Org. Proc. Res. Dev.* **2010**, 10.1021/op900306z.

25. Conant, T.; Karim, A.; Rogers, S.; Samms, S.; Randolph, G.; Datye, A. *Chem. Eng. Sci.* **2006**, *61*, 5678-5685.

26. Li, W.; Pharn, H. H.; Nie, Z.; MacDonald, B.; Guenther, A.; Kumacheva, E. *J. Am. Chem. Soc.* **2008**, *130*, 9935-9941.

27. Kobayashi, J.; Mori, Y.; Okamoto, K.; Akiyama, R.; Ueno, M.; Kitamori, T.; Kobayashi, S. *Science* **2004**, *304*, 1305-1308.

28. Shestopalov, I.; Tice, J. D.; Ismagilov, R. F. *Lab Chip* **2004**, *4*, 316-321.

29. Trachsel, F.; Tidona, B.; Desportes, S.; Rudolf von Rohr, P. *J. Supercrit. Fluids* **2009**, *48*, 146-153.

30. Nagasawa, H.; Mae, K. *Ind. Eng. Chem. Res.* **2006**, *45*, 2179-2186.

31. Takagi, M.; Maki, T.; Miyahara, M.; Mae, K. *Chem. Eng. J.* **2004**, *101*, 269-276.

32. Khan, S. A.; Jensen, K. F. *Adv. Mat.* **2007**, *19*, 2556.

33. Khan, S. A.; Gunther, A.; Schmidt, M. A.; Jensen, K. F. *Langmuir* **2004**, *20*, 8604-8611.

34. Yen, B. K. H.; Gunther, A.; Schmidt, M. A.; Jensen, K. F.; Bawendi, M. G. *Angew. Chem. Int. Ed.* **2005**, *44*, 5447-5451.

35. Di Carlo, D.; Irimia, D.; Tompkins, R. G.; Toner, M. *P. Natl. Acad. Sci. USA* **2007**, *104*, 18892-18897.

36. Yamada, M.; Seki, M. *Lab Chip* **2005**, *5*, 1233-1239.

37. Kuntaegowdanahalli, S. S.; Bhagat, A. A. S.; Kumar, G.; Papautsky, I. *Lab Chip* **2009**, *9*, 2973-2980.

38. Huang, L. R.; Cox, E. C.; Austin, R. H.; Sturm, J. C. *Science* **2004**, *304*, 987-990.

39. Kralj, J. G.; Lis, M. T. W.; Schmidt, M. A.; Jensen, K. F. *Anal. Chem.* **2006**, *78*, 5019-5025.

40. Pamme, N. *Lab Chip* **2007**, *7*, 1644-1659.

41. Laurell, T.; Petersson, F.; Nilsson, A. *Chem. Soc. Rev.* **2007**, *36*, 492-506.

42. Nilsson, A.; Petersson, F.; Jonsson, H.; Laurell, T. *Lab on a Chip* **2004**, *4*, 131-135.

43. Petersson, F.; Aberg, L.; Sward-Nilsson, A. M.; Laurell, T. *Anal. Chem.* **2007**, *79*, 5117-5123.

44. Petersson, F.; Nilsson, A.; Holm, C.; Jonsson, H.; Laurell, T. *Lab on a Chip* **2005**, *5*, 20-22.

45. Hartman, R. L.; Naber, J. R.; Zaborenko, N.; Buchwald, S. L.; Jensen, K. F. In *AIChE Annual Conference* Nashville, TN, 2009.

46. Hartman, R. L.; Naber, J. R.; Zaborenko, N.; McMullen, J. P.; Jensen, K. F. 2009.

47. Surry, D. S.; Buchwald, S. L. *Angew. Chem. Int. Ed.* **2008**, *47*, 6338-6361.

48. Buchwald, S. L.; Jiang, L. In *Metal-Catalyzed Cross-Coupling Reactions*; deMeijere, A.,

Diederich, F., Eds.; Wiley-VCH: Weinheim, 2004, p 699.

49. Hartwig, J. F. *Acc. Chem. Res.* **2008**, *41*, 1534-1544.

50. Marion, N.; Nolan, S. P. *Acc. Chem. Res.* **2008**, *41*, 1440-1449.

51. For references pertaining to palladium-catalyzed amination reactions in microflow see: Mauger, C.; Buisine, O.; Caravieilhes, S.; Mignani, G. J. Organomet. Chem. 2005, 690, 3627-3629. Murphy, E. R.; Martinelli, J. R.; Zaborenko, N.; Buchwald, S. L.; Jensen, K. F. Angew. Chem. Int. Ed. 2007, 46, 1734-1737. Popa, D.; Marcos, R.; Sayalero, S.; Vidal-Ferran, A.; Pericàs, M. A. Adv. Synth. Catal. 2009, 351, 1539-1556. Shore, G.; Morin, S.; Mallik, D.; Organ, M. G. Chem.-Eur. J. 2008, 14, 1351-1356. Bazinet, P.; McMullen, J. P.; Naber, J. R.; Musacchio, A.; Jensen, K. F.; Buchwald, S. L. Angew. Chem. Int. Ed. 2010 (submitted). Naber, J. R.; Buchwald, S. L. Angew. Chem. Int. Ed. 2010 (submitted).

52. Huang, X.; Anderson, K. W.; Zim, D.; Jiang, L.; Klapars, A.; Buchwald, S. L. *J. Am. Chem. Soc.* **2003**, *125*, 6653-6655.

53. Ramachandran, V.; Fogler, H. S. *J. Fluid Mech.* **1999**, *385*, 129-156.

54. Vitthal, S.; Sharma, M. M. *J. Colloid Interf. Sci.* **1992**, *153*, 314-336.

55. Muecke, T. W. *J. Petrol. Tech.* **1979**, *31*, 144-150.

56. Wyss, H. M.; Blair, D. L.; Morris, J. F.; Stone, H. A.; Weitz, D. A. *Phys. Rev. E Stat. Nonlin. Soft. Matter Phys.* **2006**, *74*, 061402.

57. Ramachandran, V.; Fogler, H. S. *Langmuir* **1998**, *14*, 4435-4444.

58. Song, L. F.; Elimelech, M. *J. Colloid Interf. Sci.* **1994**, *167*, 301-313.

59. Marshall, J. K.; Kitchener, J. A. *J. Colloid Interf. Sci.* **1966**, *22*, 342-351.

60. Hartman, R. L.; Sultana, M.; Nagy, K. D.; Marre, S.; Jensen, K. F. *Langmuir* **2010**, (submitted).

61. Mason, W. P. *Physical Acoustics*; Academic Press, 1982.

62. Coakley, W. T. *Trends in Biotechnology* **1997**, *15*, 506-511.

63. Hawkes, J. J.; Barber, R. W.; Emerson, D. R.; Coakley, W. T. *Lab Chip* **2004**, *4*, 446-452.

64. Thompson, L. H.; Doraiswamy, L. K. *Ind. Eng. Chem. Res*. **1999**, *38*, 1215-1249.

65. Mason, T. J. *Chem. Soc. Rev.* **1997**, *26*, 443-451.

66. Barge, A.; Tagliapietra, S.; Tei, L.; Cintas, P.; Cravotto, G. *Curr. Org. Chem.* **2008**, *12*, 1588-1612.

67. Johansson, L.; Johansson, S.; Nikolajeff, F.; Thorslund, S. *Lab Chip* **2009**, *9*, 297-304.

68. Yang, Z.; Goto, H.; Matsumoto, M.; Maeda, R. *Electrophoresis* **2000**, *21*, 116-119.

69. Biscoe, M.R.; Fors, B.P.; Buchwald, S.L. *J. Am. Chem. Soc*. **2008**, *130*, 6686-6687.

70. Fors, B.P.; Davis, N.R.; Buchwald, S.L. *J. Am. Chem. Soc*. **2009**, *131*, 5766-5768.

Chapter 5 – Packed Bed Reactors for Continuous Flow C–N Cross-Coupling

5.1 Introduction

Continuous flow technology is becoming a point of emphasis for many companies in the pharmaceutical industry as the push for lean manufacturing intensifies.[1,2] The reduction in the number of isolated intermediates, the reduction of the capital equipment footprint and better control over the production line are some of the key benefits of these methods. While many chemical transformations are easily modified to facilitate the move from more traditional batchwise operation to continuous flow operation, a large number of reactions, which are vital to the preparation of pharmaceuticals, require significant modification in order to be run in flow.[3] Multi-phase reactions are one category where the change from batch to flow is problematic. For reactions where there are liquid/liquid or liquid/gas phases, mixing and mass transfer become major issues, and with liquid/solid phases, clogging of the system is a problem; practical methods are required to overcome these obstacles.

Microfluidics have found considerable application in this area of research, as the ability to perform a large number of reactions without the need for a large amount of reagents and solvents is desirable for lab scale research. With the ability to perform a large number of reactions allowing for efficient reaction optimization and can also allow for studies that can reveal the kinetic parameters of the reaction aiding in the transition from lab scale to production scale.[4]

The palladium-catalyzed amination reaction of aryl halides/pseudohalides is one of the most utilized transformations in the pharmaceutical industry[5], and as such a general method for performing this reaction in flow[6] would greatly aid in the development of flow syntheses of active pharmaceutical ingredients (API's). However, while a great deal of research has been devoted to the development of highly active catalyst systems that can facilitate the coupling of a wide range of aryl electrophiles with a host of amine nucleophiles, the vast majority of these methods involve insoluble inorganic bases and/or form insoluble salt byproducts.[7] Moreover, attempts to use soluble organic bases in these reactions have seen limited success.[8]

We postulated that a biphasic system of an organic solvent and water, which could solubilize both the organic and inorganic components of these reactions, could be a general solution to solids formation in flow.[9,10] Precedent for biphasic amination reactions using both sodium and potassium hydroxide as the base have shown that the use of these bases, which could provide significant economic savings,[11] can provide effective catalytic systems.[12] The first report of Pd-catalyzed C–N bond formation using NaOH as a base was by Boche in 1998.[12a] In 2001, Grasa and Nolan reported the coupling of aryl bromides with indoles using an N-heterocyclic carbene (NHC) ligand and NaOH as the base with the reaction being performed in 1,4-dioxane.[12b] Similar conditions were later reported by Gooβen and Rivas-Nass.[12f] A 2002 paper by Kuwano and Hartwig more thoroughly examined the use of hydroxide bases, and reported a method employing KOH or NaOH, an equimolar amount of water and a phase transfer catalyst (PTC).[12c] Similar conditions were later reported by Urgaonkar and Verkade.[12e] Reactions using KOH in tert-butanol, as well as the first examples of amination performed in water, without a cosolvent were reported by Huang, et al in 2003.[12d] Additional reports include the use of KOH in water with small amounts of t-BuOH by Gong and Xu,[12g] the use of toluene and highly concentrated KOH under microwave conditions by Van Baelen and Maes,[12h] and reactions run in water with a KOH and a PTC by Lipshutz.[12i] However, a general method that allows for the complete solubility of all of the components of the reaction, which would be imperative for flow synthesis, remains an elusive goal.

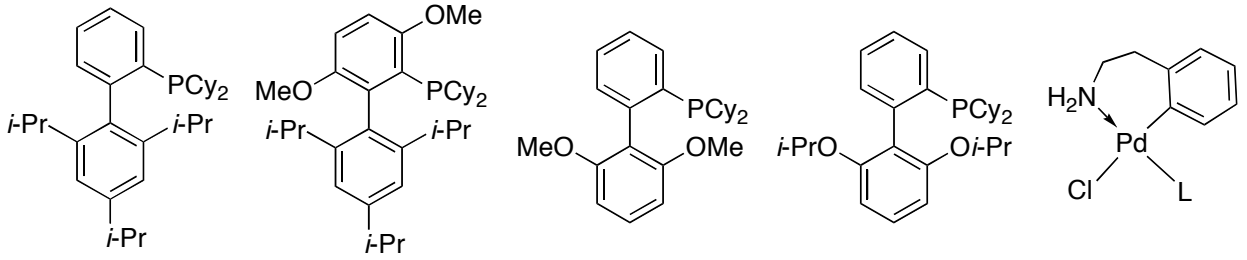

XPhos **1** BrettPhos **2** SPhos **3** RuPhos **4** **5;** L = **1** **6;** L = **2**

Figure 1. Biaryl Monophosphine Ligands.

5.2 Results and Discussion

The methods that had previously been described for Pd-catalyzed amination reactions using hydroxide base fell into two categories; those that used very small amounts of water in an organic solvent, and those that used water as the solvent. For our work, it was decided to work with equal volumes of water and organic solvent to ensure complete solubility of both the organic and inorganic reagents and products. Initial studies were performed using the XPhos precatalyst (**5**)[13] with toluene as a solvent and aqueous KOH as the base, and were performed under batch conditions. The reaction of 4-chloroanisole and aniline using 1 mol% of **5** at 80 °C for 1 hour resulted in only a 32% yield (Table 1, entry 1).

Table 1. Examination of phase transfer catalysts (PTC) for the biphasic amination reaction.

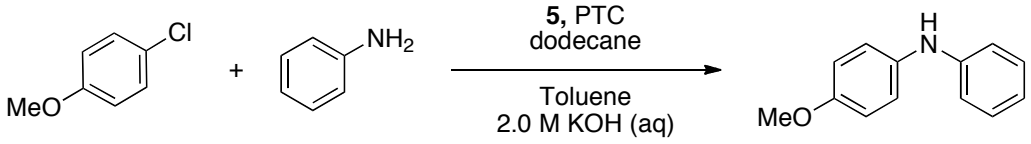

Entry	PTC	PTC (%)	Temp (°C)	Time (min)	Yield (%)[b]
1	none	-	80	60	32
2	$Bu_4N^+Br^-$	10	80	60	73
3	$Bu_4N^+OAc^-$	10	80	60	42
4[c]	$Bu_4N^+OH^-$	-	80	60	51
5	$Me_3NBn^+Br^-$	10	80	60	10
6	$Et_3NOct^+Br^-$	10	80	60	18
7	$Ph_4P^+Br^-$	10	80	60	22
8	$Bu_4N^+Br^-$	1	80	120	99
9	"	5	80	120	99
10	"	10	80	120	99
11	"	50	80	120	27
12	"	1	100	60	99

[a] Reaction Conditions; 0.5 mL of Solution 1, 2 M ArCl, 2.4 M $ArNH_2$, 0.4 M dodecane in toluene; 0.5 mL of Solution 2, 0.004 M of **5** in toluene; 1.0 mL of Solution 3, 2 M Base in water; PTC added as a solid. [b] GC Yield. [c] 1.0 mL of a 2.0 M solution of $Bu_4N^+OH^-$ in water was used in place of KOH.

Because phase transfer catalysts had been shown to accelerate similar coupling reactions that used KOH as the base, a selection of these catalysts were examined. Tetrabutylammonium salts (Table 1, entries 2-4) all provided an increase in yield, with the bromide giving the best result at 73% (Table 1, entry 2). Other quaternary ammonium bromides and a phosphonium bromide were also examined and gave decreased yields in all cases (Table 1, entries 5-7). Next, the effect of the amount of tetrabutylammonium bromide (TBAB) was investigated. No difference in yield was observed using between (Table 1, entries 8-10). However, when the quantity was increased to 50 mol% a drastic decrease in yield was observed (Table 1, entry 11).

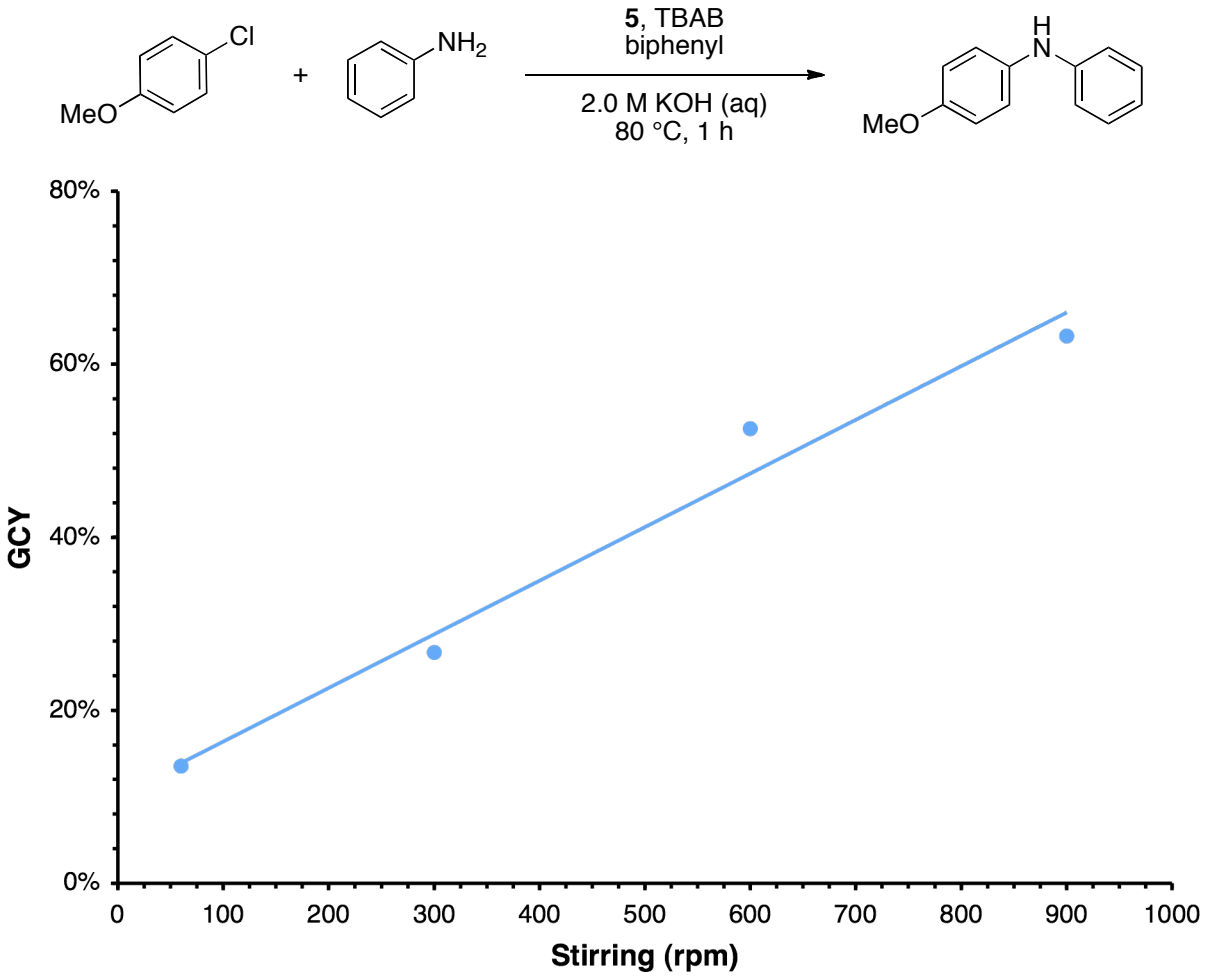

Figure 2. Stirring rate dependence for the coupling of 4-chloroanisole (1.0 mmol) and aniline (1.2 mmol) catalyzed by **5** (1 mol%) with TBAB (5 mol%) as a phase transfer catalyst and biphenyl as an internal standard (20 mol%) performed in toluene with 2.0 M KOH (aq) as the base.

During the course of these optimization reactions it was observed that the efficiency of the reaction was strongly influenced by the effectiveness of the mixing. As seen in Figure 2, the stirring rate was found to be directly proportional to the reaction yield; an increase of the stirring rate from 60 rpm to 900 rpm resulted in an increase of the yield of desired product from 13% to 60%.

Table 2. Examination of bases for the biphasic amination reaction using **2**.

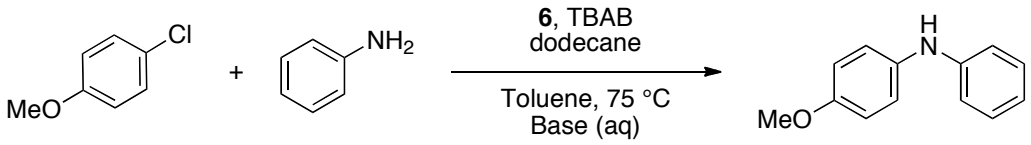

Entry	PTC (mol%)	Base	Base (M)	Time (min)	Yield (%)[b]
1	-	KOH	2.0	17	12
2	1	KOH	2.0	17	24
3	5	KOH	2.0	17	63
4	10	KOH	2.0	17	74
5	5	KOH	2.0	10	50
6	5	K_3PO_4	2.0	10	14
7	5	Cs_2CO_3	2.0	10	20
8	5	K_2CO_3	2.0	10	30
9[c]	5	KOH	2.0	10	14
10[d]	5	KOH	1.0	20	51
11	5	KOH	2.0	20	78
12[e]	5	KOH	4.0	20	90

[a] Reaction Conditions; 0.5 mL of Solution 1, 2 M ArCl, 2.4 M $ArNH_2$, TBAB, 0.4 M dodecane in toluene; 0.5 mL of Solution 2, 0.004 M of **6** in toluene; 1.0 mL of Solution 3, 2 M Base in water. [b] GC Yield. [c] 1,4-dioxane used in place of toluene. [d] 2.0 mL of 1.0 M KOH. [e] 0.5 mL of 4.0 M KOH.

In addition to these initial studies that were performed with **1** as the supporting ligand, experiments were performed using **2**, which gives rise to a more active catalyst than **1**; however, is also more expensive.[14,15] When reactions were performed using a reduced loading of **6,** it was found that the effect of the PTC loading was more evident, with higher amounts resulting in increased yields of the cross-coupled product

(Table 2, entries 1-4). While 10 mol% of TBAB gave the highest yield, it was found to be above the solubility limit of TBAB in toluene. Thus, 5 mol% TBAB was used for the remainder of the study. Several other inorganic bases besides KOH were also investigated, however, only moderate levels of conversion were observed when K_3PO_4, Cs_2CO_3 or K_2CO_3 were employed (Table 2, entries 5-8).

With the base and PTC chosen, an experiment was performed using 1,4-dioxane in place of toluene to determine whether increasing the miscibility of the two phases would increase the efficiency of the reaction (Table 2, entry 9). This solvent change resulted in decreased yield of product, therefore, toluene was used as the organic solvent for the remainder of our studies. Next, the effect of the base concentration on these reactions was explored (Table 2, entries 10-12). The use of a more concentrated base gave a higher yield, however, as the method was being developed for use in flow, the increase was not sufficient to compensate for the increased viscosity of the base, which would lead to an unacceptable pressure drop when the reaction was performed under flow conditions.

Table 3. Examination of catalyst stability for the biphasic amination reaction using BrettPhos.

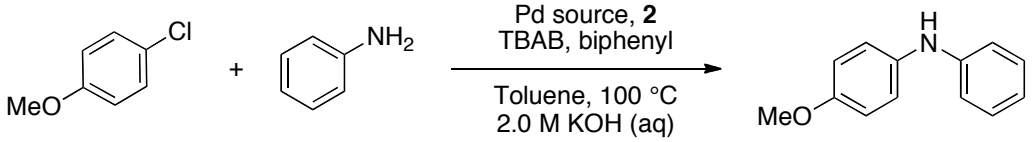

Entry	Pd Source	Pd (mol%)	Ligand (mol%)	Aging (h)[b]	Time (min)	Yield (%)[c]
1	**6**	0.5	0.1	0	3	88
2	**6**	0.5	0.1	24	3	70
3	**6**	0.5	0.1	24	6	96
4	$(AllylPdCl)_2$	0.5	0.6	0	3	45
5	$(AllylPdCl)_2$	0.5	0.6	24	3	45
6	$(AllylPdCl)_2$	0.5	0.6	24	6	94

[a] Reaction Conditions; 0.5 mL of Solution 1, 2 M ArCl, 2.4 M $ArNH_2$, 0.1 M TBAB, 0.4 M biphenyl in toluene; 0.5 mL of Solution 2, 0.01 M Pd, 0.012 M Ligand in toluene; 1.0 mL of Solution 3, 2 M KOH in water. [b] Time between prepartion and use of Solution 2. [c] GC Yield.

Lastly, we focused on the long-term stability of the catalyst precursors used for these experiments. In the same way that the method was developed to give complete solubility of the reagents to facilitate its use in flow, it was important to have reagents and catalysts that could be stored as solutions for the duration of an experiment. While large scale flow equipment can incorporate a solution making step to compensate for reagents with less solution stability, lab scale experiments require stock solutions, which are loaded onto pumps at the beginning of a reaction, that are stable throughout the experiment. Because of this a test was performed where the three solutions used in these experiments were prepared and then stored for 24 hours. In the case of **6** (Table 3, entries 1 and 2), it was found that the activity of the catalyst decreased over the course of the 24 hours of storage. The reaction performed with the fresh solutions for 3 min at 100 °C using 0.5 mol% Pd gave an 88% yield while the same experiment performed the next day gave only a 70% yield. This issue could be circumvented by switching from the precatalyst to allyl palladium chloride dimer (APC) as the Pd source for these reactions. Performing the same experiment with APC and **2** gave a 45% yield for both the freshly made and aged catalyst solutions. The yield was lower with the APC, attributable to a slower activation, but once the active catalyst was formed both reactions provided excellent yields (Table 3, entries 3 and 6).

We next applied our optimized reaction conditions to experiments in flow. The strong influence on the efficiency of the mixing that was observed for the batch reactions was also observed when the reaction was performed in continuous flow. While microscale reaction conditions are generally believed to allow for excellent mixing due to the small length scales that allow for short diffusion times, the use of immiscible liquid phases leads to segmented flow, which does not provide the same kind of mixing that is possible in a mechanically stirred reaction. Because of this we found that when the reaction conditions that had been optimized in batch were transferred to a flow system, the reaction proceeded with greatly reduced efficiency. A variety of approaches were examined, including modification of the flow reactor dimensions and changes in the microfluidic connections, in an attempt to overcome this mixing issue. However, all initial efforts resulted in only minor increases in reaction efficiency.

Due to the observed influence of mixing on reaction proficiency, we tested the effect of a commercially available microfluidic mixing tee on this reaction. The immiscibility of the two phases used in this reaction meant that while the mixing tee provided efficient mixing, the two phases quickly separated to segmented flow upon exiting the mixer and no improvement in the reaction was observed. This result suggested that a more continuous source of mixing was required. It was discovered that the use of reactors packed with stainless steel spheres could provide both the appropriate reactor volumes and the required biphasic mixing necessary for these reactions.

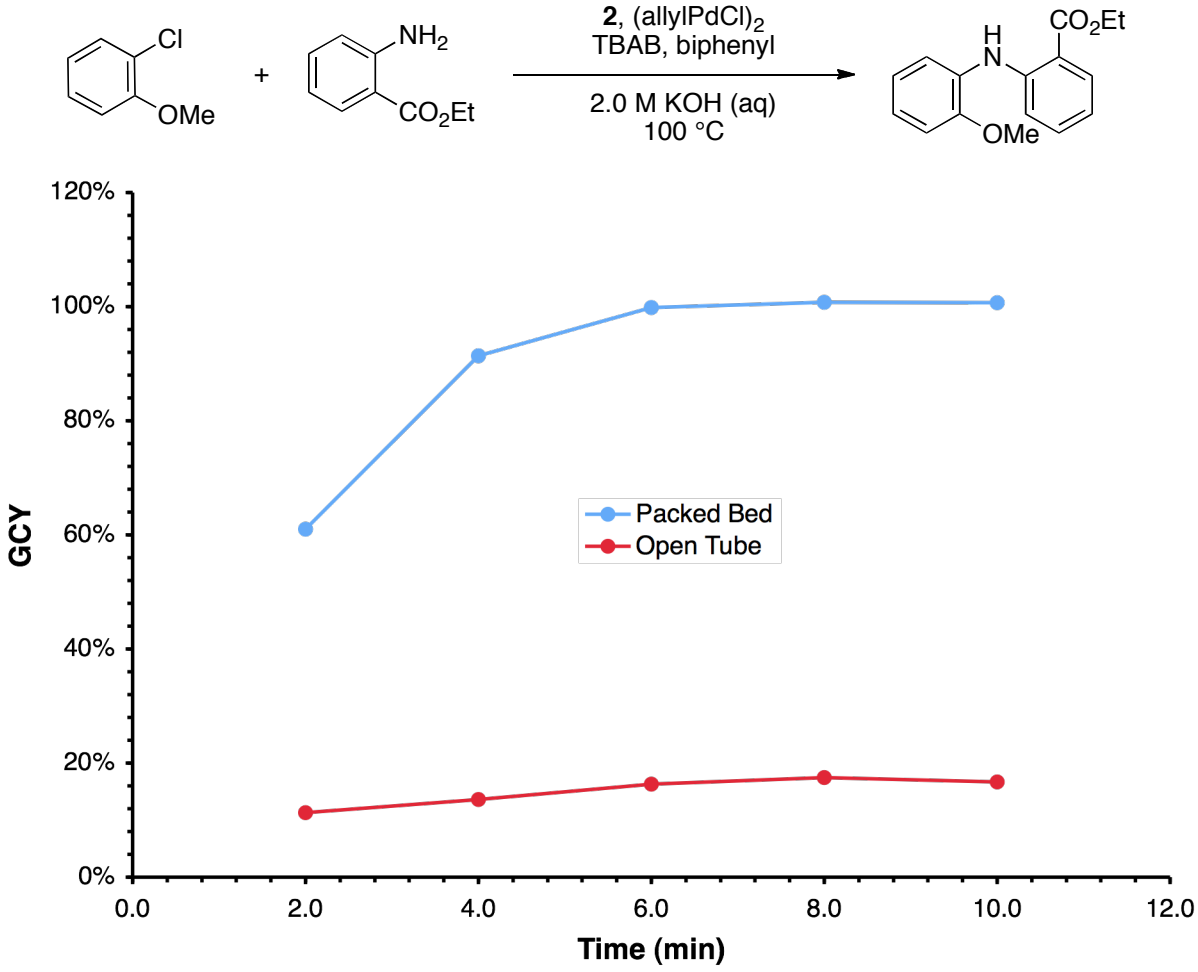

Figure 3. A packed bed reactor versus an open tube for the coupling of 2-chloroanisole (1.0 equiv) and ethyl 2-aminobenzoate (1.2 equiv) performed with **2** (0.6 mol%) and APC (0.25 mol%) using TBAB (5 mol%) as a phase transfer catalyst and biphenyl as an internal standard (20 mol%) performed in toluene with 2.0 M KOH (aq) as the base.

As seen in Figure 3, when the reaction of ethyl 2-aminobenzoate and 2-chloroanisole was run in 0.04" PFA tubing (56 cm, 448 μL), less than 20% of the product was observed for residence times of 2-10 minutes. When the tubing reactor was replaced with a packed bed reactor with a void volume equal to that of the tubing, which should give better mixing, the same reaction gave full conversion after a residence time of 6 minutes. These results clearly demonstrate the importance of effective mixing for these reactions. Further, this shows that the combination of a toluene/water biphasic system and the packed bed reactor result in an effective protocol for Pd-catalyzed amination reactions of aryl halides in flow.

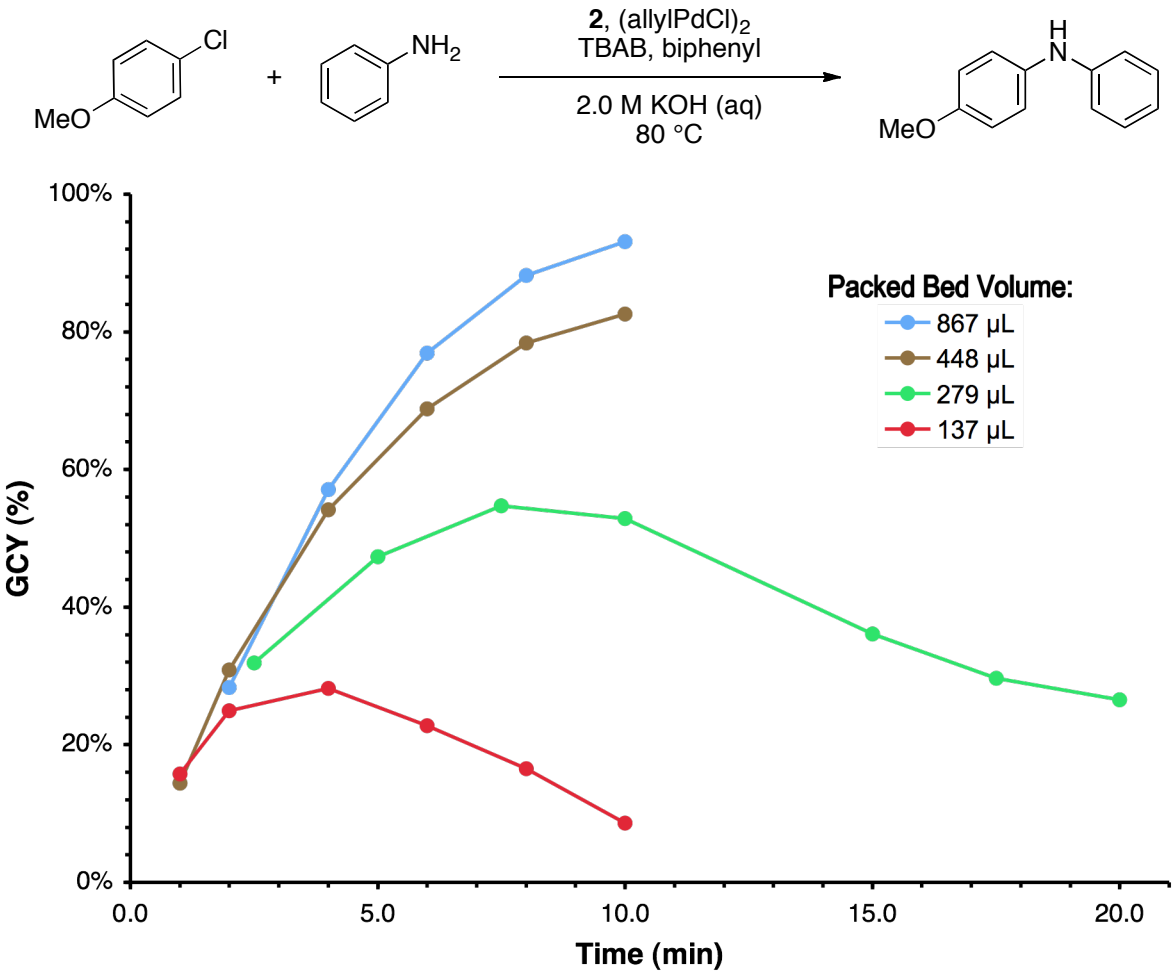

Figure 4. Flowrate dependence for the coupling of 4-chloroanisole (1.0 equiv) and aniline (1.2 equiv) with **2** (1.2 mol%) and APC (0.5 mol%) using TBAB (5 mol%) as a phase transfer catalyst and biphenyl as an internal standard (20 mol%) performed in toluene with 2.0 M KOH (aq) as the base.

Encouraged by our initial results using a biphasic system in a packed bed reactor, we next wanted to examine the range of reaction conditions that could be used. The results in Figure 4 demonstrate the effect of reactor size on the yield of the reaction. The reactions in Figure 4 were performed using a series of four packed beds with increasing volumes. In the largest packed bed, the results tracked very closely with the results obtained for this reaction in the batch process, with high stirring rates. As the size of the packed bed was decreased the yield of the reaction was also decreased. Interestingly, in the two smallest packed beds, it was found that after a certain point the reaction yield began to decrease with increased residence time (decreased flowrate). In these cases the reaction conversion was in agreement with the reaction yield implying that the product was not degrading over time. Because of this, it was postulated that the biphasic mixing in packed beds was related to the flowrate of the two reaction streams. This suggested that the biphasic amination method presented herein will be most effective for reaction with short reaction times where moderate flowrates can be maintained. Further studies to quantify the hydrodynamic parameters of the packed beds are underway.

A benefit of working with microfluidic systems is the ability to access reaction conditions that are more difficult to achieve or are unsafe in standard batch systems. The most common example of this is the use of high temperatures and pressures. In the biphasic amination system we thought that the use of high temperatures could allow for the reduction of the residence time needed for the complete conversion of the amination reactions that we were studying, and could, therefore, increase the number of possible reactions that could be performed efficiently in a biphasic manner using packed beds.

Figure 5 shows the effect of increasing the temperature and pressure for a Pd-catalyzed amination reaction. In this experiment the reaction time was held constant and the temperature was systematically increased from 80 °C to 200 °C. It was found that the reaction rate was greatly enhanced by the increased temperature up to a point where catalyst decomposition began to take place. However, a reaction that only proceeded to ~30% yield under the standard conditions could be taken to completion through increased temperature. This suggests that a wide range of reactions could be performed using this method by optimizing catalyst loading, reaction time and reaction temperature. In addition to the ability to push

difficult reactions to completion with increased temperature, this approach can also be used to decrease the amount of catalyst needed for these reactions, as shown in Figure 4 where only 0.15 mol% Pd was used. Another benefit of the ability to perform flow reactions under forcing conditions is the potential to use less expensive supporting ligands to form the catalysts for these reactions. As can be seen in Figure 5, while **2** provided the most active catalyst, it was possible to achieve the same levels of reactivity using **1**, which at present is considerably cheaper.[15]

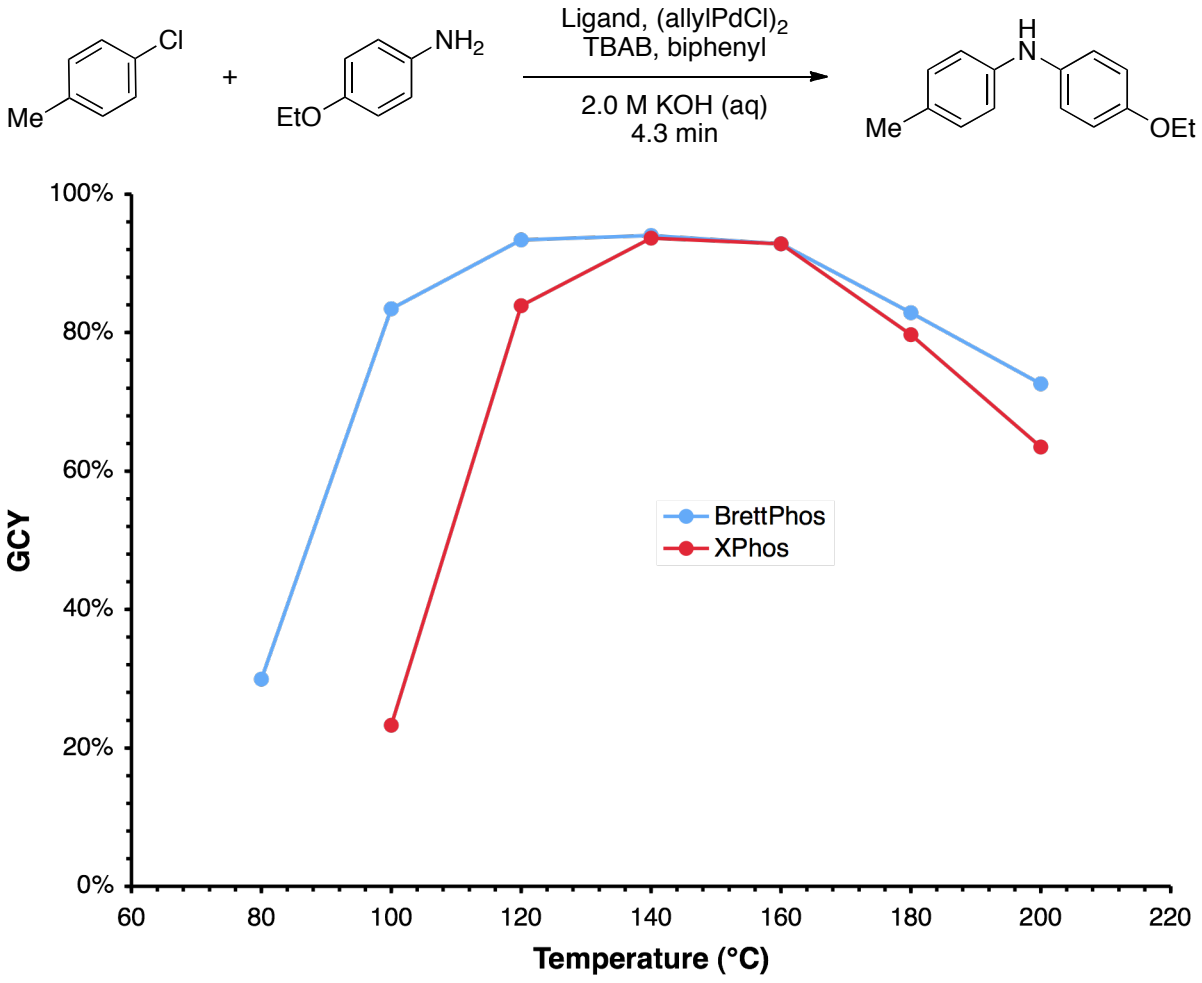

Figure 5. Temperature dependence for the coupling of 4-chlorotoluene (1.0 equiv) and *p*-phenetidine (1.2 equiv) with **1** or **2** (0.3 mol%) and APC (0.075 mol%) using TBAB (5 mol%) as a phase transfer catalyst and biphenyl as an internal standard (20 mol%) performed in toluene with 2.0 M KOH (aq) as the base.

5.3 Conclusion

In conclusion, conditions were developed for Pd–catalyzed C–N bond forming reactions, in a continuous flow manner. The optimized conditions employ aqueous KOH, toluene as a reaction solvent, TBAB as a phase transfer catalyst and a packed bed microreactor. Moderate flowrates (>40 uL/min) are necessary for efficient mixing. High temperature and pressure reaction conditions are easily accessed allowing for greatly enhanced reaction rates in some cases.

5.4 Experimental

Materials: Endcaps from standard 1/4" HPLC columns were recycled for the preparation of the packed beds used in this study. Sintered stainless steel (SS) frits were purchased from IDEX Health and Science, formerly Upchurch Scientific. Several sizes and porosities are available with 0.189" diameter frits having a 10 μm pore size were used for these packed beds. Nuts and ferrule sets, 1/4" and made of SS, were purchased from Swagelok. The tubing, 0.25" OD x 0.21" ID in 316 SS, was purchased in 12" lengths from McMaster Carr and was cut to length with a standard tubing cutter. Stainless steel beads were purchased from Duke Scientific, a subsidiary of Thermo Fisher and were spherical in shape with a size distribution from 60 – 125 μm. Microfluidic connections were made with standard Upchurch fittings (IDEX Health and Science), either 10-32 coned fittings, or 1/4-28 flat-bottomed fittings for 1/16" OD tubing.

Procedure for preparing a packed bed reactor: During the initial stages of the method development for the biphasic amination, a variety of materials were examined for use as the packing material for a packed bed reactor. Sand and borosilicate glass were two of the first candidate materials that were examined. Mesh sieves were used to obtain a uniform size distribution, and the particles were packed in a piece of 1/8" OD PFA tubing to make a simple packed bed. Control experiments showed that both the sand and borosilicate glass suffered from chemical compatibility issues when they were exposed to the strong aqueous base used in these reactions. Silica gel was similarly dismissed as a possible packing material. Polymeric beads were also examined, but the tendency for these materials to swell in the

presence of organic solvents prevented their use for this application. Finally, stainless steel beads were examined. The excellent chemical compatibility, specifically tolerance for strongly basic solutions, the absence of any swelling issues, and their commercial availability in a uniform size distribution (60 – 125 μm from Thermo Fisher) made these beads the ideal choice for a packed bed filler material. For a packed bed to have maximum efficiency it is generally accepted that the diameter of the bed should be more than 10x the diameter of the particles used as packing. For this reason, as well as for ease of construction we decided to use 1/4" tubing for the housing of the packed bed. In order to connect the 1/16" OD fluoropolymer tubing that we use for most of our microfluidic work and the 1/4" tubing of the packed bed, a 1/16" to 1/4" adapter was needed. This type of connection is commonplace in HPLC applications and the endcaps of HPLC columns could be used for this application. As such, an analytical HPLC column served as a model for our experimental setup.

a) 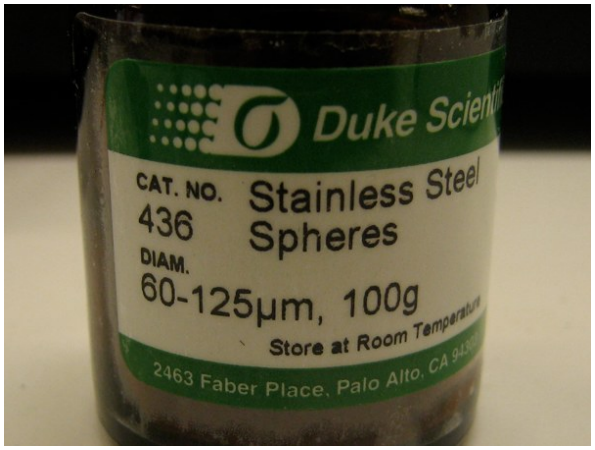

b) 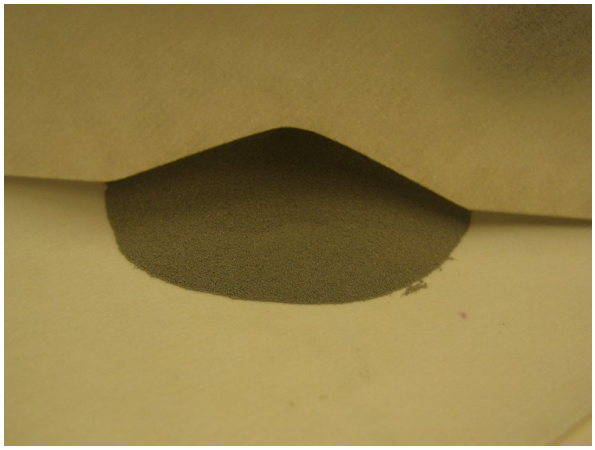

Figure 6. a) Stainless steel spheres from Duke Scientific (through Thermo Fisher). b) Close up.

When separated into its constituent components an HPLC column consists of two endcaps, two frits to hold in the packing material, a piece of SS tubing, two Swagelok nut/ferrule sets and the packing material. Standard HPLC columns come fitted with frits will very small pore sizes, often 0.2 μm, that result in the need for significant pressures to drive solvents through the frit at moderate flowrates (>100 μL/min). As the beads used to fill the packed bed were much larger than the particles used in liquid chromatography, a coarser frit could be used to reduce the pressure drop across the reactor. Frits in a wide range of sizes,

porosities and materials are available from IDEX Health and Science. For the packed beds in this study it was necessary to choose a frit with an OD of 0.25", and a pore size of <60 μm (size of the packing material). Figure 7 shows the frits used for the construction of a packed bed. The pore size was 10 μm and the diameter was 0.189". The frit is packaged in a polymeric ring with an OD of 0.254" to facilitate its use in applications involving 1/4" tubing. The frit fits snuggly in the bottom of the endcap and is held in place firmly by the tubing inside the endcap. Figure 8 shows the endcaps, a nut and a two-piece ferrule set. The ferrules are placed between the endcap and nut and when the nut is tightened the ferrule is compressed which forms the fluidic seal on the tubing.

Figure 7. a) Sintered stainless steel frits from Upchurch Scientific. b) Close up. c) Endcaps from HPLC columns. d) Endcap with frit installed.

To assemble the packed bed one endcap was fitted with a frit and attached to the 1/4" tubing. The nut, ferrules and endcap (with the frit) are placed on the tubing as shown in Figure 8 and the nut tightened to finger tightness. Once finger tight, the end assembly should be tightened one full turn to compress the ferrules to the tubing and ensure a leak proof connection. At this point the tube was filled with the SS beads. The high density of the SS along with their spherical shape makes them very easy to work with as they pour from a piece of weighing paper in a very regular way allowing them to be poured into the tube with little difficulty. The outside of the tubing tapped with a spatula to facilitate tight packing.

a) 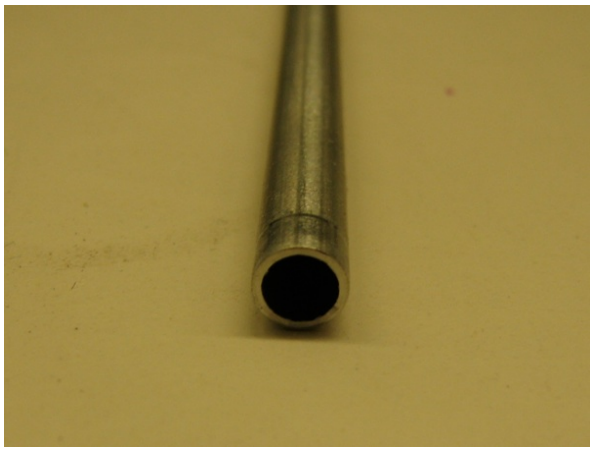 b) 

c) 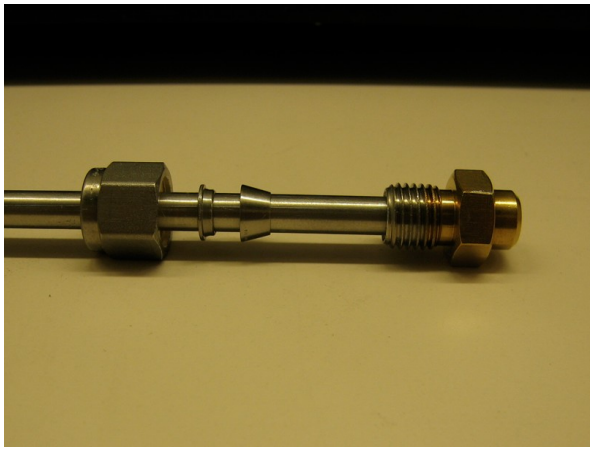 d) 

Figure 8. a) Stainless steel tubing (type 316, 0.25" OD x 0.21" ID). b) Swagelok nut and ferrule set. c) Complete end assembly before tightening. d) Packed bed assembly.

Additional packing was added to fill any space created by the tamping process. The nut and ferrules were then carefully passed over the open end of the tube. It is important that the nut and ferrules not be put in

place before the tube is filled as any packing material that spills over the edge of the tube can get caught in the nut and ferrule making it very difficult to tighten the nut and endcap, leading to leaks in the connection. Once the nut and ferrules are in place, the second endcap (with frit) can be placed on the tubing. At this point the packed bed can be laid flat or inverted as long as the endcap is held in place. The reactor is finished by tightening the nut to the endcap, one turn past finger tight as with the other end. Figure 10 shows a completed packed bed reactor.

a) 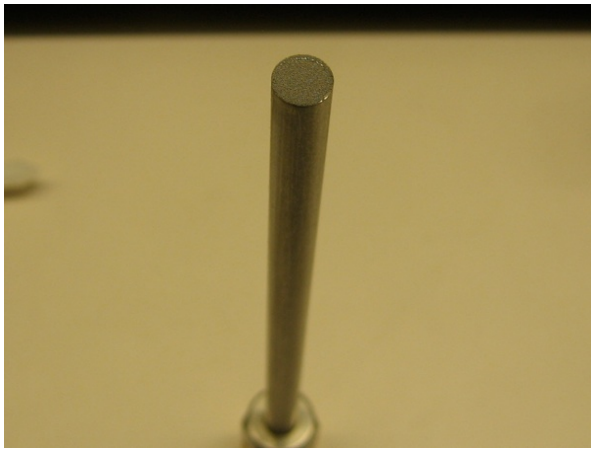 b) 

Figure 9. a) Stainless steel tubing filled with packing material. b) Filled tube with second end assembly.

The mass of the empty tube was subtracted from the mass of the packed bed and the volume of the packing was calculated based on the density of stainless steel (8.0 g/mL). The percentage of volume occupied by the packing material was consistently found to be between 63% and 65%.

Figure 10. Completed packed bed reactor.

Experimental setup. The equipment configurations that were used for the biphasic amination experiments are described in Figures 11 and 12. Figure 11 depicts the setup used for the majority of the experiments where three Harvard Apparatus PHD2000 syringe pumps were used to deliver reagents from Normject plastic syringes to the packed bed reactor. The reactor (preparation described above) was submerged in an bath of silicon oil. The temperature of the bath was monitored with a thermocouple and maintained by a Waage immersion heater controlled by a J-KEM Scientific Gemini PID controller. A fourth syringe pump was used to deliver a dilution quench stream to the reaction stream after it exited the heated zone. The diluted reaction stream was then fed into a collection vial. The system was plumbed with PFA capillary tubing (1/16" OD x 500 μm ID) and all fluidic connections were made using either 1/4-28 flat-bottomed flangeless fittings or 10-32 coned fittings (IDEX Health and Science).

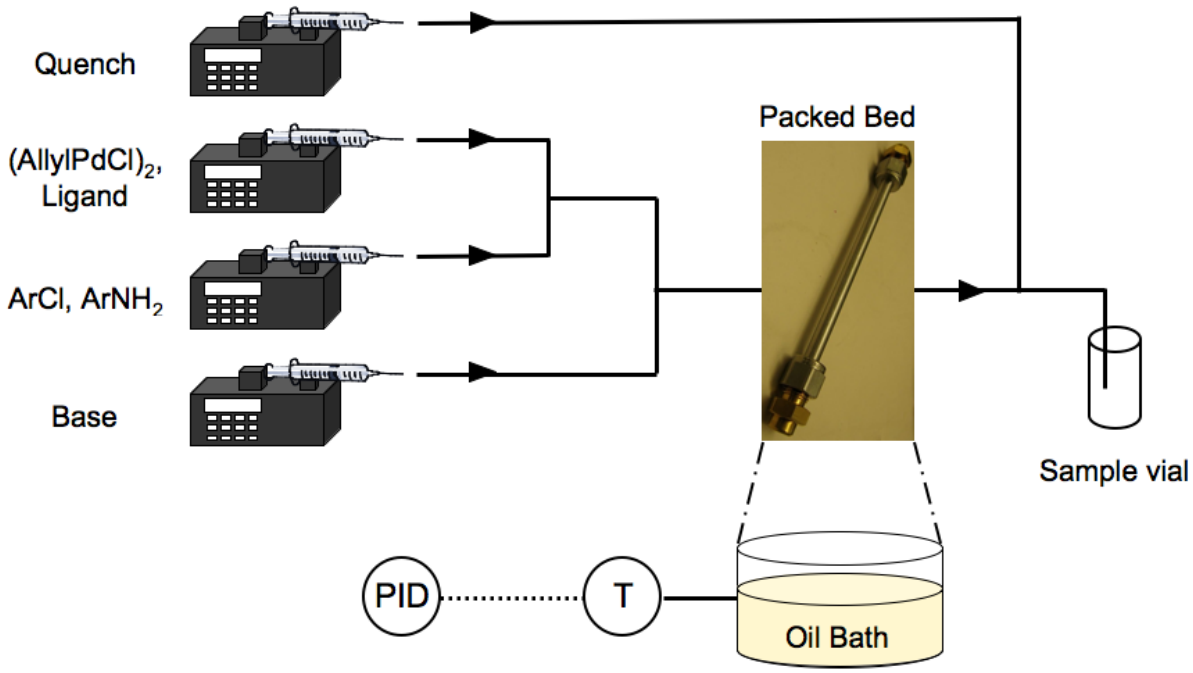

Figure 11. Completed packed bed reactor.

Experiments performed at elevated temperatures necessitated the modified equipment setup described in Figure 12. Three of the syringe pumps used in system shown in Figure 11 were replaced with Chromtech P-1500 dual stainless steel piston HPLC pumps. These pumps delivered the reagents to the packed bed

that was submerged in the bath of silicon oil that was heated in the same manner as described above. Upon exiting the heated zone, the reaction tubing was passed through an aluminum cooling block that was maintained at 4 °C using recirculating chilled water. The cooled reaction stream was then connected to a 1000-psi backpressure regulator (BPR, IDEX Health and Science). Two syringe pumps were used to deliver a dilution quench stream to the reaction stream after it exited the BPR. The diluted reaction stream was the n fed into a collection vial. The system was plumbed with a combination of PEEK and SS capillary tubing (1/16" OD x 250 μm ID) and all fluidic connections were made using either 1/4-28 flat-bottomed super flangeless fittings or 10-32 coned fittings in stainless steel (IDEX Health and Science).

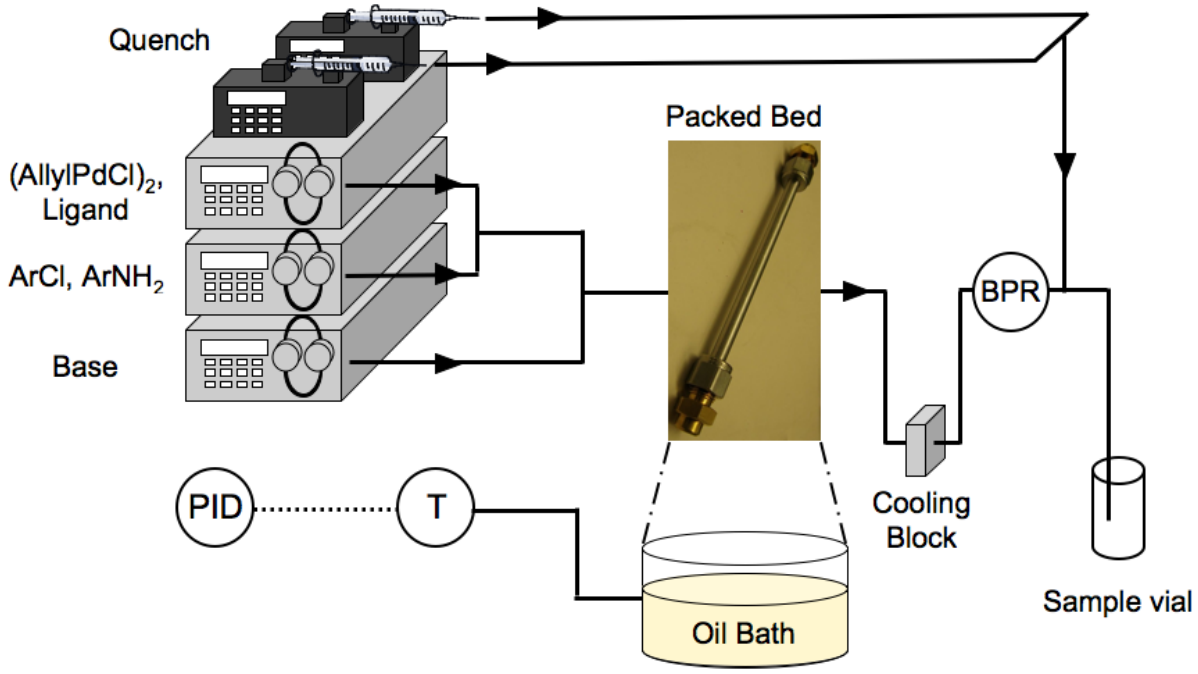

Figure 12. Completed packed bed reactor.

Reagents and analytical. All experiments were carried out using reagent grade solvents, and all solutions were prepared under argon atmospheres. Aryl halides, amines, biphenyl, tetrabutylammonium bromide (TBAB) and toluene were purchased from Sigma-Aldrich chemical company and used as received. Allyl palladium chloride dimer was purchased from Strem Chemicals and was stored in the refrigerator when not in use. The aqueous solution of potassium hydroxide solution was purchased from Alfa Aesar and

was used as received. XPhos, BrettPhos, the XPhos precatalyst and the BrettPhos precatalyst were prepared according to literature procedures.[12d,13,14] Reaction solutions were prepared in screw-cap, oven-dried volumetric flasks. For the continuous flow experiments, three solutions were prepared. The first solution contained the base (KOH), was prepared in de-ionized water and was degassed by sonication under reduced pressure followed by backfilling with argon prior to use. The second solution contained the aryl halide, amine, internal standard (biphenyl) and phase transfer catalyst (TBAB) catalyst and was prepared in toluene. The third solution contained the palladium source (APC) and ligand, and was also prepared in toluene. Reagents that were solids were added to the volumetric flasks that were then evacuated and refilled with argon. This process was repeated a total of 3 times. Liquid reagents were added by syringe, and the solutions were made up to the desired volume with toluene or water. These solutions were then either loaded into syringes and attached to syringe pumps as described in Figure 10, or connected to the HPLC pumps shown in Figure 11.

All compounds were characterized by ^{1}H NMR, ^{13}C NMR and IR spectroscopy. Copies of the ^{1}H and ^{13}C spectra can be found at the end of the experimental section. Nuclear Magnetic Resonance spectra were recorded on a Bruker 400 MHz instrument. All ^{1}H NMR experiments are reported in δ units, parts per million (ppm), and were measured relative to the signals for residual chloroform (7.26 ppm) in the deuterated solvent, unless otherwise stated. All ^{13}C NMR spectra are reported in ppm relative to deuterochloroform (77.23 ppm), unless otherwise stated, and all were obtained with 1H decoupling. All IR spectra were taken on a Perkin – Elmer 2000 FTIR. All GC analyses were performed on a Agilent 6890 gas chromatograph with an FID detector using a J & W DB-1 column (10 m, 0.1 mm I.D.). Elemental analyses were performed by Atlantic Microlabs Inc., Norcross, GA.

Workup and yields. Samples were collected in test tubes and were diluted with equal volumes of ethyl acetate and water and mixed vigorously. An aliquot of the organic phase was filtered through a short plug of silica gel and analyzed by GC. Yield and conversion were determined based on the peak area, relative to the internal standard. In certain cases, the phases were separated, the water phase was extracted with

ethyl acetate a total of three times and the organic phases were combined and concentrated. The crude material was then purified by column chromatography. Isolated yields were found to be in excellent agreement with the GC yields.

Procedure for Figure 1

An oven-dried screw-top vial that was equipped with a magnetic stir bar and fitted with a Teflon screw-cap septum, was charged with the **5** (8.0 mg, 0.01 mmol), TBAB (16.1 mg, 0.05 mmol) and biphenyl (30.8 mg, 0.2 mmol). The vessel was evacuated and backfilled with argon (this process was repeated a total of 3 times) and then 4-chloroanisole (120 μL, 1.0 mmol), aniline (110 μL, 1.2 mmol) and toluene (1 mL) were added. The reaction was stirred to allow the dissolution of the solid reagents and the base, 2 M KOH (1 mL) was added. The reaction solution was mixed vigorously for 5 s, and then stirred at 60–900 rpm for 1 h at 80 °C. The tube was removed from the oil bath, cooled to room temperature and ethyl acetate and water were added in equal portions (2 mL). The reaction solution was mixed vigorously, an aliquot of the organic layer was passed through a plug of silica gel, eluting with ethyl acetate, and the sample was analyzed by GC.

Procedure for Figure 2

An oven-dried screw-top volumetric flask (5.00 mL) that was equipped with a magnetic stir bar and fitted with a Teflon screw-cap septum, was charged with **2** (32.2 mg, 0.06 mmol) and $(allylPdCl)_2$ (9.2 mg, 0.025 mmol). The vessel was evacuated and backfilled with argon (this process was repeated a total of 3 times) and toluene was added to make the solution up to volume (~5 mL). Solution 1 was stirred for 5 min to allow complete dissolution of the solid reagents. A second oven-dried screw-top volumetric flask (5.00 mL) that was equipped with a magnetic stir bar and fitted with a Teflon screw-cap septum, was charged with biphenyl (308 mg, 2.0 mmol) and TBAB (161 mg, 0.5 mmol). The vessel was evacuated and backfilled with argon (this process was repeated a total of 3 times) and then 2-chloroanisole (1.21 mL, 10.0 mmol) and ethyl 2-aminobenzoate (1.77 mL, 12.0 mmol) were added and toluene was used to make the solution up to volume. Solution 2 was stirred to allow the dissolution of the solid reagents.

Solutions 1 and 2 were loaded into plastic syringes and fitted to syringe pumps as described in Figure 10 (448 μL packed bed). Three other syringes were filled with KOH (2 M), ethyl acetate and water, respectively, and were fitted to the remaining syringe pumps. The reagents were flowed through the packed bed reactor with the appropriate flowrates to give residence times of 2–10 min. Samples were collected, diluted with ethyl acetate and water, mixed vigorously, and an aliquot of the organic layer was filtered through a plug of silica eluting with ethyl acetate and the sample was analyzed by GC. In the second experiment, the packed bed reactor was replaced with a length of 0.04" ID PFA (56 cm, 448 μL). The reagents were prepared, flowed and analyzed in the same manner as described above.

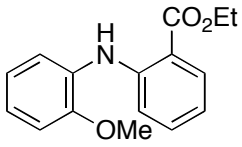

Ethyl 2-((2-methoxyphenyl)amino)benzoate. In addition to the samples collected for GC analysis, one sample was collected for 71 min (2.0 mmol, 8 min residence time, 56 μL/min total flowrate, 14 μL/min for solution 2). The sample was diluted with ethyl acetate and water and was mixed vigorously. The organic layer was separated and the aqueous layer was extracted 2 more times with EA. The combined organic layers were concentrated and purified by column chromatography (silica gel, Biotage Isolera, 25 g SNAP cartridge eluting with hexanes and 0-20% EA) to give the title compound as yellow oil (530 mg, 98%). ^{1}H NMR (400 MHz, $CDCl_3$) δ: 9.57 (s, 1H), 8.03 (d, *J* = 8.0 Hz, 1H), 7.31-7.39 (m, *2*H), 7.02-7.05 (m, 1H), 6.93-6.97 (m, *2*H), 6.76 (t, *J* = 8.0 Hz, 5H), 4.40 (q, *J* = 7 Hz, 2H), 3.88 (s, 3H), 1.42 (t, *J* = 7 Hz, 3H) ppm. ^{13}C NMR (100 MHz, $CDCl_3$) δ: 171.7, 168.4, 151.4, 147.2, 133.9, 131.8, 130.2, 123.2, 120.5, 120.3, 117.2, 114.4, 113.2, 111.3, 60.7, 55.7, 14.4 ppm. IR (neat, cm^{-1}): 3324, 2979, 1684, 1595, 1578, 1525, 1258, 1081, 1029, 744.

Procedure for Figure 3

Solutions were prepared as described in the procedure for Figure 2. Solution 1 contained **2** (129 mg, 0.24 mmol) and $(allylPdCl)_2$ (36.6 mg, 0.1 mmol) and was made up to 10.00 mL with toluene. Solution 2

contained biphenyl (616 mg, 4.0 mmol), TBAB (322 mg, 1.0 mmol), 4-chloroanisole (2.46 mL, 20.0 mmol) and aniline (2.18 mL, 24.0 mmol) and was made up to 10.00 mL with toluene. The solutions were loaded into syringes and connected to the pumps as described in the procedure for Figure 2, and the reagents were flowed through the packed bed reactor with the appropriate flowrates to give residence times of 1–20 minutes. Samples were collected, diluted with ethyl acetate and water, mixed vigorously, and an aliquot of the organic layer was filtered through a plug of silica eluting with ethyl acetate and the sample was analyzed by GC. In the subsequent experiments, the packed bed reactor was replaced with packed beds of different volumes. The reagents were prepared, flowed and analyzed in the same manner as described above.

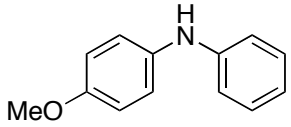

4-Methoxy-*N*-phenylaniline.[16] In addition to the samples collected for GC analysis, one sample was collected for 46 min (2.0 mmol, 10 min residence time, 87 μL/min total flowrate, 22 μL/min for solution 2). The sample was diluted with ethyl acetate and water and was mixed vigorously. The organic layer was separated and the aqueous layer was extracted 2 more times with EA. The combined organic layers were concentrated and purified by column chromatography (silica gel, Biotage Isolera, 25 g SNAP cartridge eluting with hexanes and 0-20% EA) to give the title compound as pale yellow solid (374 mg, 94%) mp = 104-106 °C (lit. 104-106 °C). ^{1}H NMR (400 MHz, $CDCl_3$) δ: 7.28 (t, *J* = 8.0 Hz, 2H), 7.12 (d, *J* = 9 Hz, *2*H), 6.92-6.98 (m, 5H), 5.55 (s, 1H), 3.84 (s, 3H) ppm. ^{13}C NMR (100 MHz, $CDCl_3$) δ: 155.3, 145.3, 135.9, 129.5, 122.3, 119.7, 115.8, 114.8, 55.7 ppm. IR (neat, cm^{-1}): 3387, 1595, 1513, 1501, 1298, 1250, 1182, 1033, 752, 696.

Procedure for Figure 4

A large oven-dried volumetric flask (100.0 mL) that was equipped with a magnetic stir bar and fitted with a rubber septum, was charged with biphenyl (6.16 g, 40.0 mmol), TBAB (3.22 g, 10.0 mmol). The vessel

was evacuated and backfilled with argon (this process was repeated a total of 3 times) and then 4-chlorotoluene (23.7 mL, 200 mmol) and *p*-phenetidine (31.1 mL, 240 mmol) were added and toluene was used to make the solution up to 100.0 mL. This solution was transferred to a Strauss flask for storage and was connected to an HPLC pump as described in Figure 11 for the experiments. Solution 2 was prepared in an oven-dried screw-top volumetric flask (10.00 mL) that was equipped with a magnetic stir bar and fitted with a Teflon screw-cap septum. The flask was charged with **2** (32.2 mg, 0.06 mmol) and $(allylPdCl)_2$ (5.5 mg, 0.015 mmol). The vessel was evacuated and backfilled with argon (this process was repeated a total of 3 times) and toluene was added to make the solution up to 10.0 mL. Solution 2 was stirred for 5 min to allow complete dissolution of the solid reagents. The solution was connected to an HPLC pump as described in Figure 11. A flask of the KOH solution (2 M) and the quench solutions were also connected to the system. The reagents were flowed through the packed bed reactor with a constant flowrate to give a residence time of 4.3 min. Samples were collected after an equilibration time and the temperature of the oil bath was stepped up from 80 °C – 200 °C. The samples were diluted with ethyl acetate and water, mixed vigorously, and an aliquot of the organic layer was filtered through a plug of silica eluting with ethyl acetate and the sample was analyzed by GC.

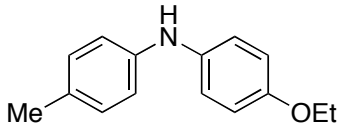

4-Ethoxy-*N*-(*p*-tolyl)aniline.[17] In addition to the samples collected for GC analysis, one sample was collected for 20 min (2.0 mmol, 4.3 min residence time, 200 μL/min total flowrate, 50 μL/min for solution 2). The sample was diluted with ethyl acetate and water and was mixed vigorously. The organic layer was separated and the aqueous layer was extracted 2 more times with EA. The combined organic layers were concentrated and purified by column chromatography (silica gel, Biotage Isolera, 25 g SNAP cartridge eluting with hexanes and 0-20% EA) to give the title compound as pale yellow solid (409 mg, 90%) mp = 66-68 °C (lit. 67-68 °C). ^{1}H NMR (400 MHz, $CDCl_3$) δ: 7.10-7.17 (m, 4H), 6.94-6.97 (m, 4H), 5.50 (s, 1H), 4.09 (q, *J* = 7.0 Hz, 2H), 2.41 (s, 3H), 1.52 (t, *J* = 7.0 Hz, 3H) ppm. ^{13}C NMR (100

MHz, $CDCl_3$) δ: 154.2, 142.6, 136.7, 130.0, 129.3, 121.5, 121.2, 116.7, 115.5, 63.9, 20.8, 15.2 ppm. IR (neat, cm^{-1}): 3415, 2975, 1613, 1514, 1294, 1253, 1116, 1051, 812, 518.

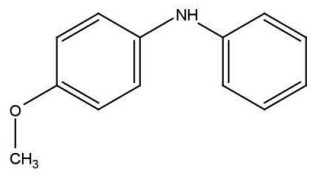
NH
O
CH3

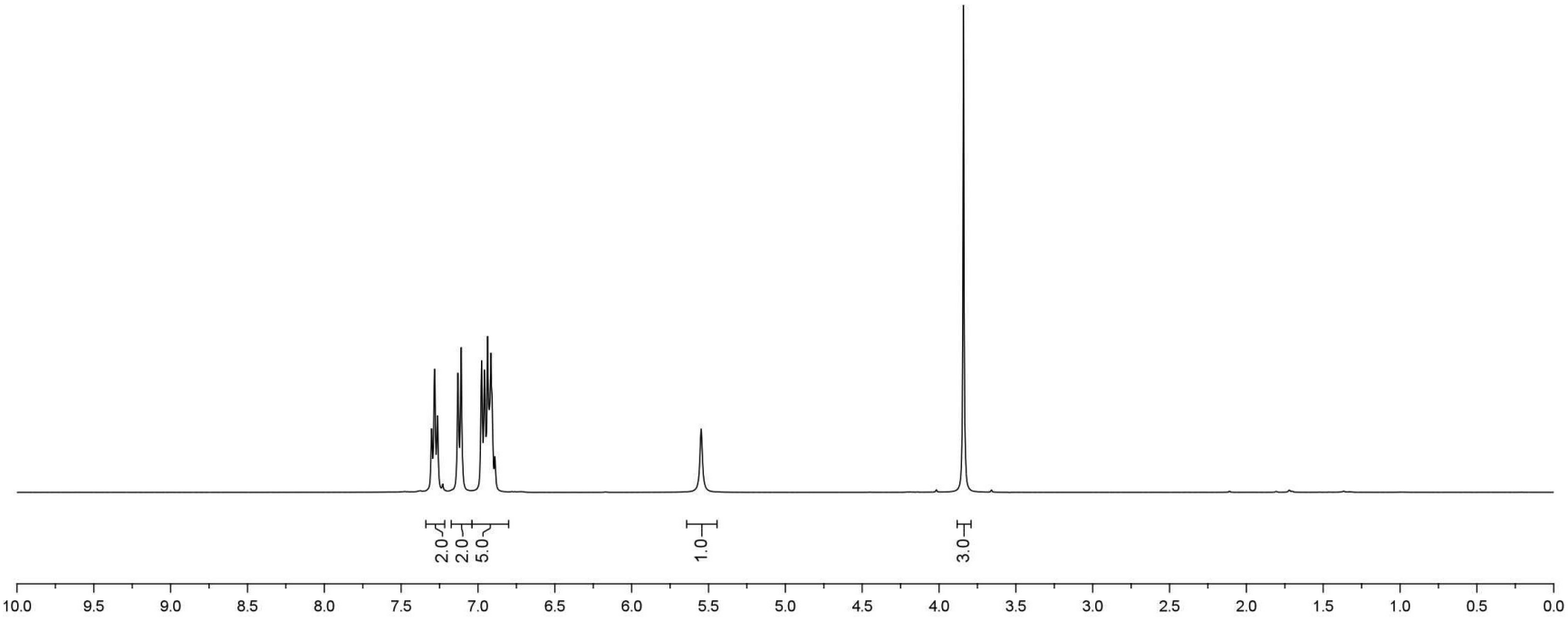
2.0
2.0
5.0
1.0
3.0
10.0
9.5
9.0
8.5
8.0
7.5
7.0
6.5
6.0
5.5
5.0
4.5
4.0
3.5
3.0
2.5
2.0
1.5
1.0
0.5
0.0

155.3
145.3
135.9
129.5
122.3
119.7
115.8
114.8
77.6
77.3
77.0
55.7
NH
O
CH3

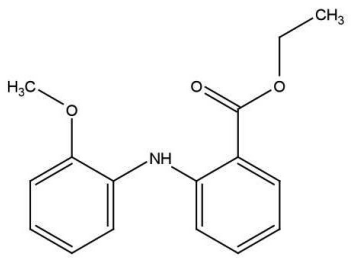
CH3
H3C
O
O
O
NH

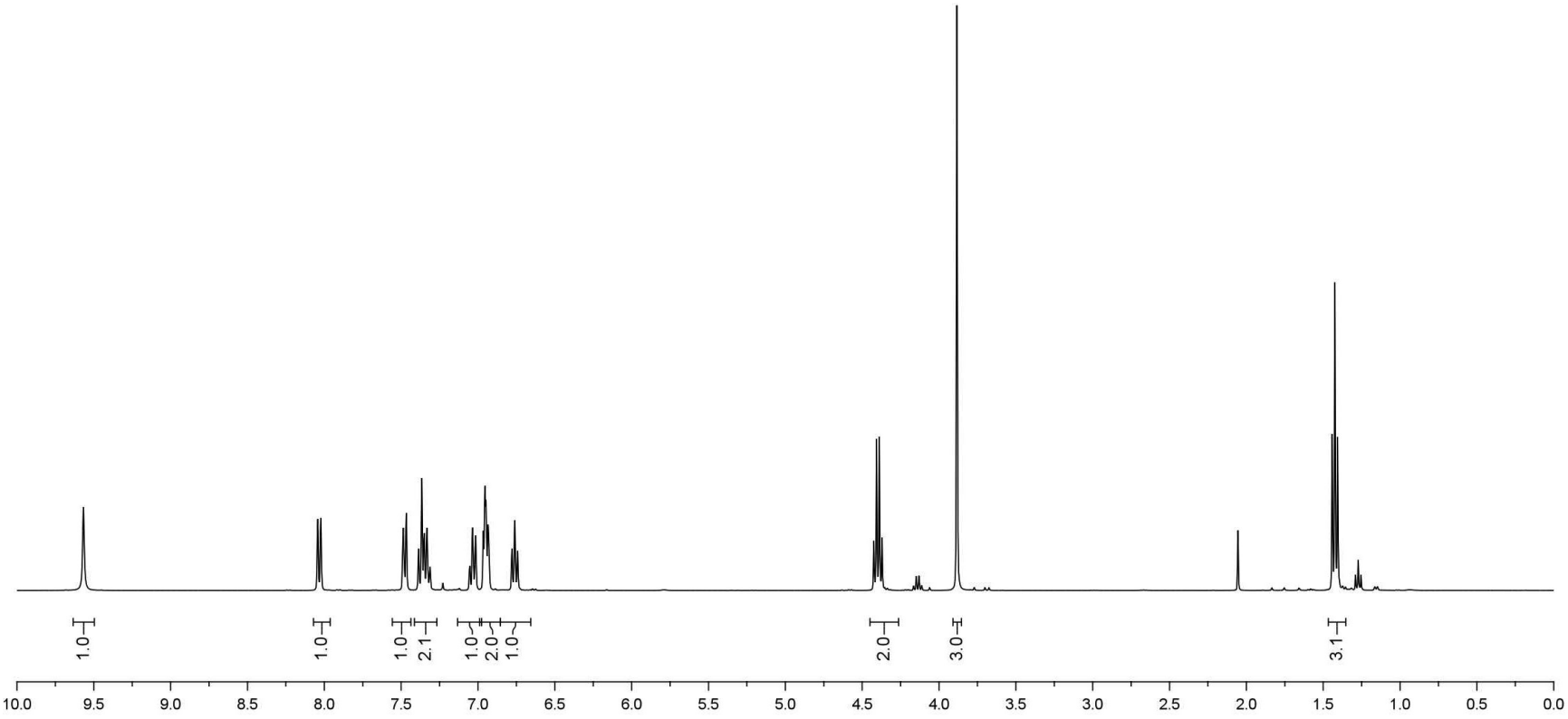
1.0
1.0
1.0
2.1
1.0
2.0
1.0
2.0
3.0
3.1
10.0
9.5
9.0
8.5
8.0
7.5
7.0
6.5
6.0
5.5
5.0
4.5
4.0
3.5
3.0
2.5
2.0
1.5
1.0
0.5
0.0

171.1
168.4
151.4
147.2
133.9
131.8
130.2
123.2
120.5
120.3
117.2
114.4
113.2
111.3
77.6
77.3
77.0
60.7
60.4
55.7
21.1
14.4
14.3
CH3
O
O
NH
O
H3C
-10
0
10
20
30
40
50
60
70
80
90
100
110
120
130
140
150
160
170
180
190
200
210

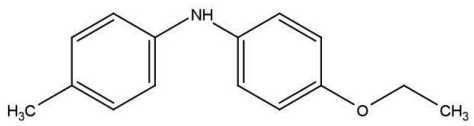
NH
H3C
O
CH3

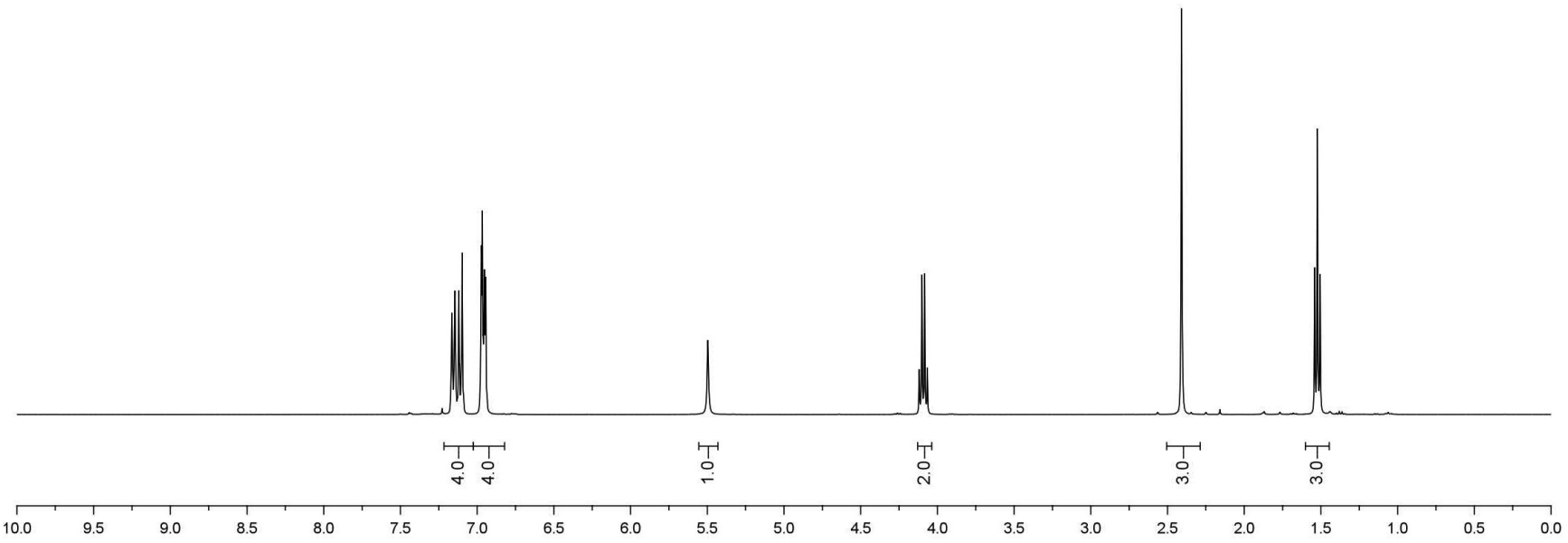
4.0
4.0
1.0
2.0
3.0
3.0
10.0
9.5
9.0
8.5
8.0
7.5
7.0
6.5
6.0
5.5
5.0
4.5
4.0
3.5
3.0
2.5
2.0
1.5
1.0
0.5
0.0

154.2
142.6
136.7
130.0
129.3
121.5
121.2
116.7
115.5
77.7
77.4
77.1
63.9
20.8
15.2
NH
O
CH3
H3C

5.5 References

1. For references on lean manufacturing, see: a) T. Ohno, *Toyota Production System: Beyond Large-Scale Production*; Productivity Press: University Park, IL, 1988. b) J.P. Womack, D.T. Jones, D. Roos, *The Machine That Changed the World: The Story of Lean Production*; HarperCollins: New York, NY, 1991. c) J.M. Gross, K.R. McInnis, *Kanban Made Simple*; American Management Association: New York, NY, 2003.

2. For an application of Lean Manufacturing to the drug industry, see: H.N. Weller, D.S. Nirschl, E.W. Petrillo, M.A. Poss, C.J. Andres, C.L. Cavallaro, M.M. Echols, K.A. Grant-Young, J.G. Houston, A.V. Miller, R.T. Swann, *J. Comb. Chem*. **2006**, *8*, 664-669.

3. a) D.M. Roberge, L. Ducry, N. Bieler, P. Cretton, B. Zimmermann, *Chem. Eng. Technol.* **2005**, *28*, 318-323. b) J.S. Carey, D. Laffan, C. Thomson, M.T. Williams, *Org. Biomol. Chem.* **2006**, *4*, 2337-2347. c) R.W. Dugger, J.A. Ragan, D.H.B. Ripin, *Org. Proc. Res. Dev.* **2005**, *9*, 253-258.

4. a) K.F. Jensen, *Chem. Eng. Sci.* **2001**, *56*, 293-303. b) P.D.I. Fletcher, S.J. Haswell, E. Pombo-Villar, B.H. Warrington, P. Watts, S.Y.F. Wong, X.L. Zhang, *Tetrahedron* **2002**, *58*, 4735-4757. c) K. Jahnisch, V. Hessel, H. Lowe, M. Baerns, *Angew. Chem. Int. Ed.* **2004**, *43*, 406-446. d) H. Pennemann, P. Watts, S.J. Haswell, V. Hessel, H. Lowe, *Org. Process Res. Dev.* **2004**, *8*, 422-439. e) V. Hessel, H. Lowe, *Chem. Eng. Technol.* **2005**, *28*, 267-284. f) K.F. Jensen, *MRS Bull.* **2006**, *31*, 101-107. g) A.J. deMello, *Nature* **2006**, *442*, 394-402. h) B.P. Mason, K.E. Price, J.L. Steinbacher, A.R. Bogdan, D.T. McQuade, *Chem. Rev.* **2007**, *107*, 2300-2318. i) P. Watts, C. Wiles, *Chem. Commun*. **2007**, 443-467. j) P. Watts, C. Wiles, *Chem. Eng. Technol.* **2007**, *30*, 329-333. k) R.L. Hartman, K.F. Jensen, *Lab Chip* **2009**, *9*, 2495–2507. l) W. Ehrfeld, V. Hessel, H. Lowe, *Microreactors: New Technology for Modern Chemistry*; Wiley-VCH: Weinheim, Germany, 2000. m) K.F. Jensen, In *New Avenues to Effcient Chemical Synthesis: Emerging Technologies*; P.H. Seeberger, T. Blume, Eds.; Springer-Verlag Berlin: Heidelberg, 2007, p 57-76.

5. For a selection of recent papers that use Pd-catalyzed aminations to make biologically active compounds, see: a) F.W. Goldberg, R.A. Ward, S.J. Powell, J.E. Debreczeni, R.A. Norman, N.J. Roberts, A.P. Dishington, H.J. Gingell, K.F. Wickson, A.L. Roberts, *J. Med. Chem*. **2009**, *52*, 7901-7905. b) S. Guo, Y. Song, Q. Huang, H. Yuan, B. Wan, Y. Wang, R. He, M.G. Beconi, S.G. Franzblau, A.P. Kozikowski, *J. Med. Chem*. **2010**, *53*, 649-659. c) V. Sandanayaka, B. Mamat, R.K. Mishra, J. Winger, M. Krohn, L.-M. Zhou, M. Keyvan, L. Enache, D. Sullins, E. Onau, J. Zhang, G. Halldorsdottir, H. Sigthorsdottir, A. Thorlaksdottir, G. Sigthorsson, M. Thorsteinnsdottir, D.R. Davies, L.J. Stewart, D.E. Zembower, T. Andresson, A.S. Kiselyov, J. Singh, M.E. Gurney, *J. Med. Chem*. **2010**, *53*, 573-585. d) M. Decker, Y.-G. Si, B.I. Knapp, J.M. Bidlack, J.L. Neumeyer. *J. Med. Chem*. **2010**, *53*, 402-418.

6. For references pertaining to palladium-catalyzed amination reactions in microflow see: a) C. Mauger, O. Buisine, S. Caravieilhes, G. Mignani, *J. Organomet. Chem*. **2005**, *690*, 3627-3629. b) D. Popa, R. Marcos, S. Sayalero, A. Vidal-Ferran, M.A. Pericàs, *Adv. Synth. Catal*. **2009**, *351*, 1539-1556. c) G. Shore, S. Morin, D. Mallik, M.G. Organ, *Chem.-Eur. J*. **2008**, *14*, 1351-1356. d) P. Bazinet, J.P. McMullen, J.R. Naber, A. Musacchio, K.F. Jensen, S.L. Buchwald, *Angew. Chem. Int. Ed*. **2010** (submitted).

7. For recent reviews of Pd-catalyzed aminations, see: a) D.S. Surry, S.L. Buchwald, *Angew. Chem. Int. Ed.* **2008**, *47*, 6338-6361. b) S.L. Buchwald, L. Jiang, In *Metal-Catalyzed Cross-Coupling Reactions*; A. deMeijere, F. Diederich, Eds.; Wiley-VCH: Weinheim, 2004, p 699. c) J.F. Hartwig, *Acc. Chem. Res*. **2008**, *41*, 1534-1544. d) N. Marion, S.P. Nolan, *Acc. Chem. Res*. **2008**, *41*, 1440-1449.

8. a) R.E. Tundel, K.W. Anderson, S.L. Buchwald, *J. Org. Chem*. **2006**, *71*, 430-433. b) E.R. Murphy, J.R. Martinelli, N. Zaborenko, S.L. Buchwald, K.F. Jensen, *Angew. Chem. Int. Ed*. **2007**, *46*, 1734-1737.

9. For a reviews of metal catalyzed reactions in water, see: a) M. Carril, R. SanMartin, E.

Dominguez, *Chem. Soc. Rev*. **2008**, *37*, 639-647. b) K.H. Shaughnessy, *Chem. Rev*. **2009**, *109*, 643-710.

10. a) A.S. Dallas, K.V. Gothelf, *J. Org. Chem*. **2005**, *70*, 3321-3323. b) S.R. Stauffer, M.A. Steinbeiser, *Tetrahedron Letters* **2005**, *46*, 2571-2575.

11. B. Schlummer, U. Scholz, *Adv. Synth. Catal*. **2004**, *346*, 1599-1626.

12. a) G. Wullner, H, Jansch, S. Kannenberg, F. Schubert, G. Boche, *Chem. Commun*, **1998**, 1509-1510. b) G.A. Grasa, M.S. Viciu, J. Huang, S.P. Nolan, *J. Org. Chem*. **2001**, *66*, 7729-7737 c) R. Kuwano, M. Utsunomiya, J.F. Hartwig, *J. Org. Chem*. **2002**, *67*, 6479-6486. d) X. Huang, K.W. Anderson, D. Zim, L. Jiang, A. Klapars, S.L. Buchwald, *J. Am. Chem. Soc*. **2003**, *125*, 6653-6655. e) S. Urgaonkar, J.G. Verkade, *J. Org. Chem*. **2004**, *69*, 9135-9142. f) L.J. Goosen, J. Paetzold, O. Briel, A. Rivas-Nass, R. Karch, B. Kayser, *Synlett* **2005**, *No. 2*, 275-278. g) C. Xu, J.-F. Gong, Y.-J. Wu, *Tetrahedron Letters* **2007**, *48*, 1619-1623. h) G. Van Baelan, B.U.W. Maes, *Tetrahedron* **2008**, *64*, 5604-5619. i) B.H. Lipshutz, D.W. Chung, B. Rich, *Adv. Synth. Catal*. **2009**, *351*, 1717-1721.

13. M.R. Biscoe, B.P. Fors, S.L. Buchwald, *J. Am. Chem. Soc*. **2008**, *130*, 6686-6687.

14. B.P. Fors, D.A. Watson, M.R. Biscoe, S.L. Buchwald, *J. Am. Chem. Soc*. **2008**, *130*, 13552-13554.

15. Prices from the Strem Chemicals online catalog: XPhos [564483-18-7] $36/g based on price for 10 grams, BrettPhos [N/A] $264/g.

16. B.P. Fors, N.R. Davis, S.L. Buchwald, *J. Am. Chem. Soc*. **2009**, *131*, 5766-5768.

17. K. Abe, M. Takahashi, A. Kunugi, *Chem. Express* **1990**, *5*, 385-388.

Appendix – Miscellaneous Microfluidic Work

6.1 Fluoropolymer tubing

Fluoropolymer tubing provides a highly chemical resistant, transparent medium for transporting reagents to and from reactors, and can also serve as a simple flow reactor. The availability of a range of tubing sizes, both outside diameter (OD) and inside diameter (ID), allows for the complete customization of the flow systems used in this research. While a range of different fluorinated polymers are used for tubing, perfluoroalkoxy (PFA) or high-purity PFA was found to provide an excellent mix of durability, transparency and chemical compatibility. In the 1/16" OD size, there are four different internal diameters ranging from 0.01" (250 μm) to 0.04" (1000 μm). The smallest of these, 0.01", is useful for small reactor systems where it is desirable to have a minimum amount of dead volume both before and after the reactor as this tubing has a volume of only 0.5 μL/cm. Conversely, the largest tubing, 0.04", can be used to make large volume reactors without the need for long lengths of tubing as it has a volume of 8 μL/cm. However, one of the intermediate sizes, 0.02", has proven to be the most useful for this work. The 0.02" tubing has the best tradeoff between wasted volume with only 1 μL/cm and backpressure; 1 mL/min flow of water through 100 cm of this tubing only generates 1.5 psi of backpressure, compared to 27 psi for the same flow through and equal length of 0.01" tubing.

The fittings used to form the connections between different pieces of tubing, or between tubing and the other microreactors described in this work were purchased from IDEX Health and Science. Three kinds of fittings were used: 1) Flangeless 10-32 coned fittings were used for connections to both the packed beds used in Chapter 5 and the compression chucks used with the silicon microreactors, 2) Flangeless 1/4-28 and 3) Super flangeless 1/4-28 fittings were used for connections to flat-bottomed ports that made up the bulk of the connections in the equipment setups. The major differences between the two types of 1/4-28 fittings involve the ferrules used to create the seal between the tubing and the bottom of the port. In the flangeless fittings a single piece ferrule that has a sloped backside is used; when the nut is tightened it compresses the ferrule on the tubing, which provides a good seal and allows both the ferrules and the nuts to be reused multiple times. The disadvantage of this type of connection is that the ferrule is compressed

by the nut and, as such, the two are locked leading to twisting of the tubing when the fitting is tightened. The super flangeless fittings have a two piece ferrule that consists of one piece that is very similar to the one used by the flangeless fittings and a locking ring that has a flat backside. When the nut is tightened, the locking ring is pressed onto the ferrule forming a compression seal. This design allows the flat backside of the locking to slide freely on the nut, which alleviates the tubing twist associated with the flangeless fittings. The disadvantage is that once the locking ring is compressed onto the ferrule it cannot be removed and must be discarded after use. The nuts can be reused as with the flangeless nuts.

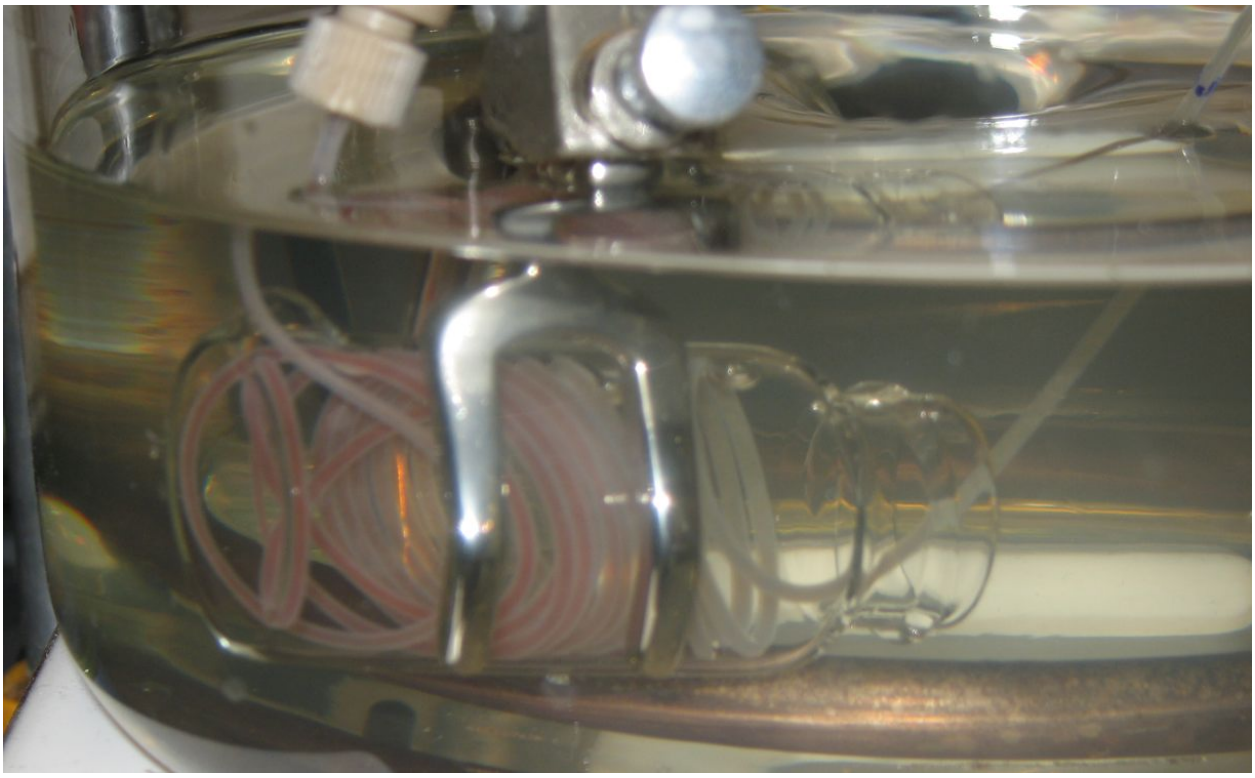

Figure 1. Tubing coiled inside a glass vial to facilitate submersion in an oil bath.

The first experiments were performed in simple reactors comprised of lengths of PFA tubing that were submerged in an oil bath to provide heating. As can be seen in Figure 1, longer lengths of tubing can be difficult to handle and submerge in an oil bath. This is further complicated in systems where it is desirable to have the reagent stream mix prior to heating and the mixing connection cannot be submerged with the tubing. While standard batch chemistry is usually performed in test tubes or flasks that can be

easily held in a bath by a clamp, PFA tubing is easily deformed or pinched and, as such, cannot be directly clamped in an oil bath. One solution to this problem was to place coils of the tubing inside of a rigid housing that could then be held with a clamp. Figures 1 and 2 show two examples of this where a glass vial, and the barrel of a glass syringe were used to hold the coiled tubing and still allow visualization of the tubing during the reaction. While this did enable the tubing to be held in the bath, the difficulty in assembly of such systems prompted us to devise simpler solutions.

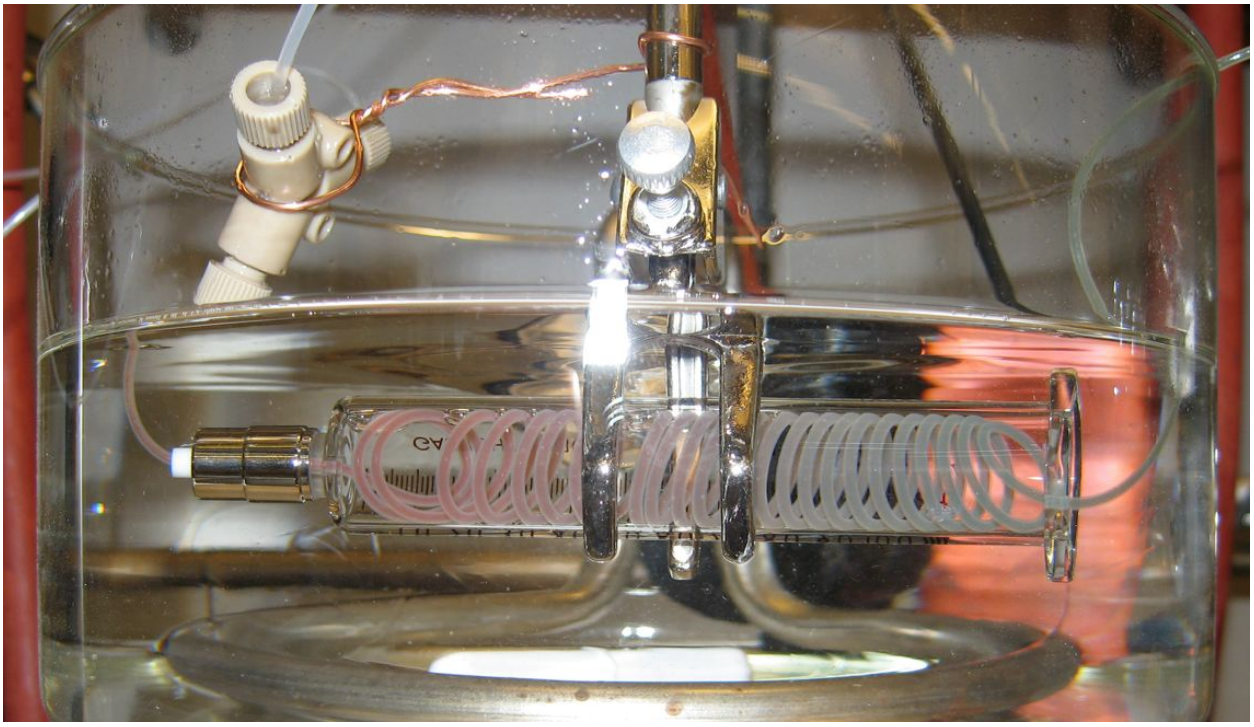

Figure 2. Tubing coiled inside a glass syringe barrel to facilitate submersion in an oil bath.

The use of short lengths of stainless steel (SS) tubing, which allowed for a predetermined shape to be maintained, was one successful strategy in overcoming this problem. Figure 3 shows one such system where pieces of 0.02" SS tubing (10 cm) were connected to the PFA tubing with a PEEK union. The steel tubing permitted the inlet and outlet to hold their shape and held the mixing zone out of the bath. The use of the unions to make the connections between the types of tubing provided an attachment point for the clamp and enabled the reactor to be submerged securely in an oil bath. It was also found that loose coils of PFA tubing were easier to work with than the tight coils that were first attempted, and that copper

wire could be used to hold the coils together; however, care is needed when copper wire is used as the PFA tubing can be easily pinched or constricted by the wire.

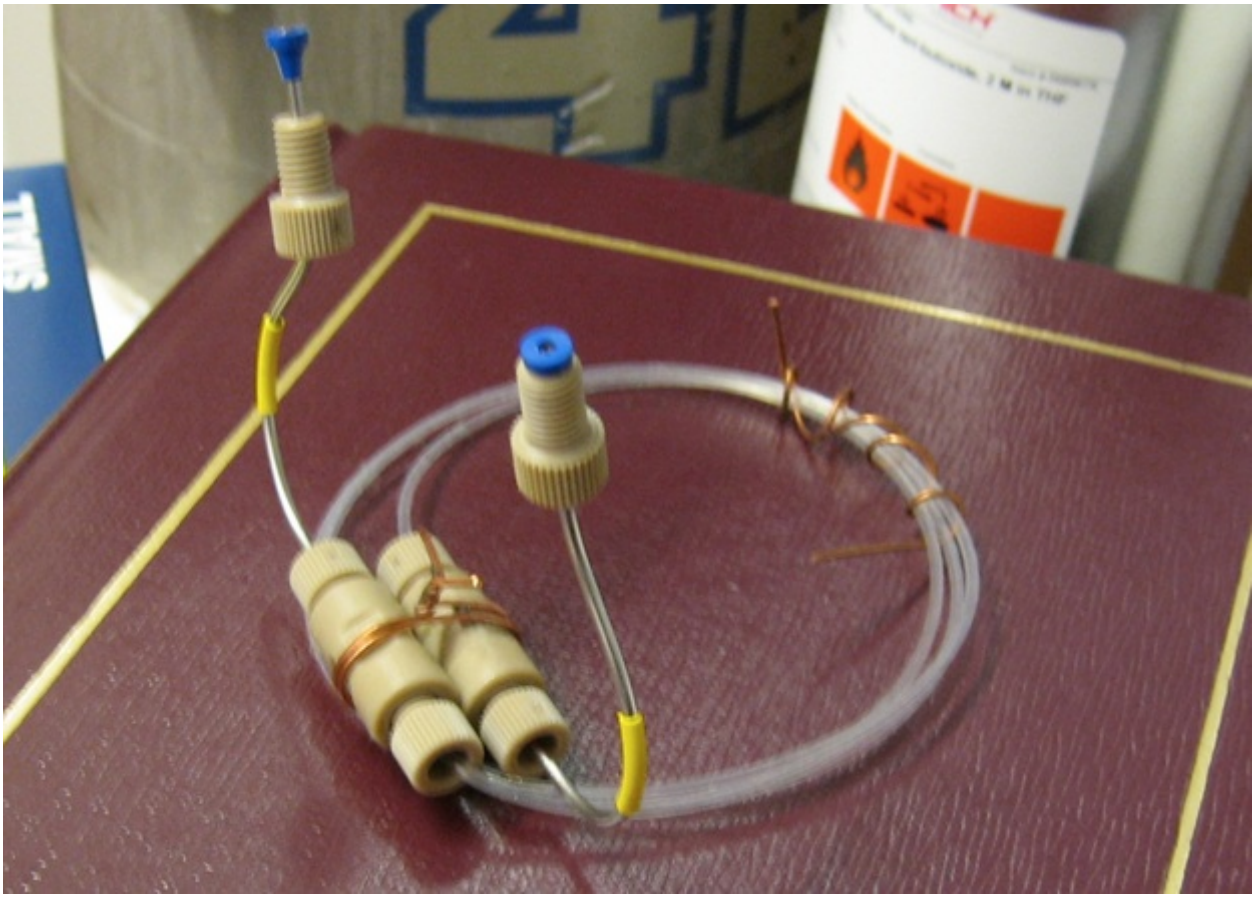

Figure 3. Reactor made from 0.02" PFA tubing and secured using PEEK unions.

In addition to its use as a simple reactor, PFA tubing was used in the bulk of the equipment setups for connecting either the syringes on the syringe pumps or the HPLC pumps to the reactors, and for transporting the reaction stream from the reactor to the outlet for collection. A variety of fittings and connectors are available from IDEX Health and Science with unions, tees, crosses, Luer adapters and Y connectors being among the most commonly used in this work. In addition to the PFA tubing commonly used, polyetheretherketone (PEEK) tubing is a more durable, albeit opaque, type of polymer tubing that is available in long pieces and can be cut to length. Further, stainless steel tubing is available in precut lengths. While scissors can be used to cut the polymer tubing and commercial tubing cutters are

available, razor blades provide the cleanest cuts.

6.2 Silicon microreactors

This research toward the development of palladium-catalyzed reactions in continuous flow is a collaborative effort with Prof. Klavs Jensen's research group in the chemical engineering department here at MIT. One of the focuses of their research is the fabrication and use of silicon based microfluidic devices. Two of these devices are pictured in Figure 4. The reactor on the left is referred to as the spiral reactor and is based on a four port template with three inlet ports that enter a serpentine mixing region that leads to the reaction zone comprised of a single gradually curved channel that exits through the fourth port. The opening between the mixing zone and the main channel is referred to as a halo etch and allows for the two sections of the chip to be maintained at different temperatures without imparting undue stress to the silicon chip. The reactor on the right is called the serpentine reactor and was laid out on the same template as the spiral reactor. The uniformity in the placement of the inlet and outlet ports as well as the size of the chip allows for a single system of fluidic connections and heaters to be used for the two chips.

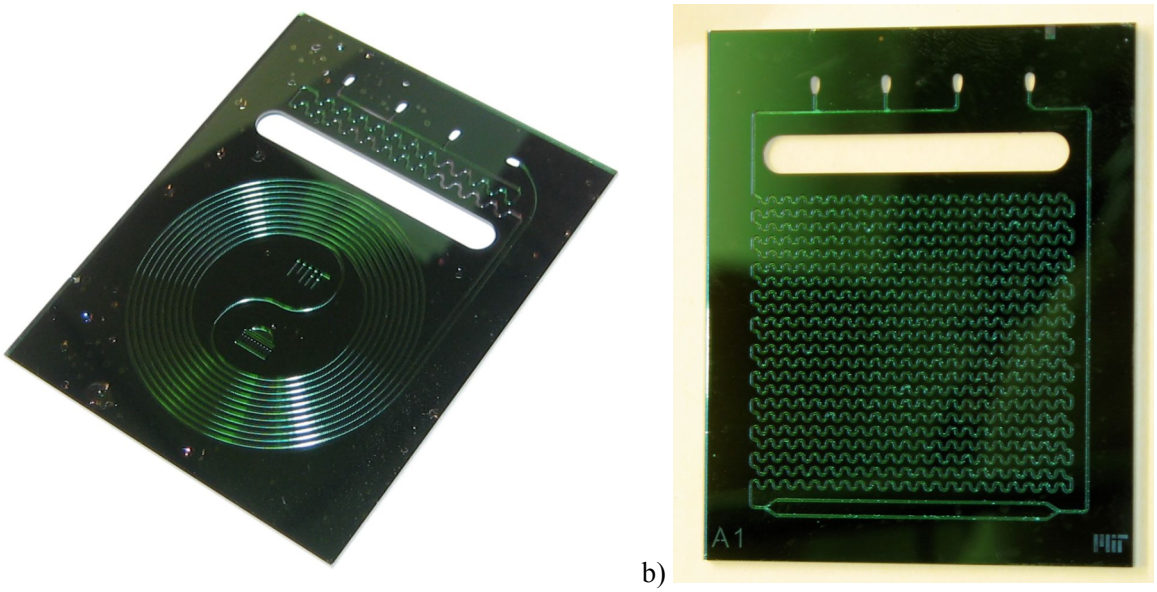

Figure 4. (Left) Spiral microreactor fabricated from silicon and coated with a layer of silicon nitride. (Right) Serpentine microreactor.

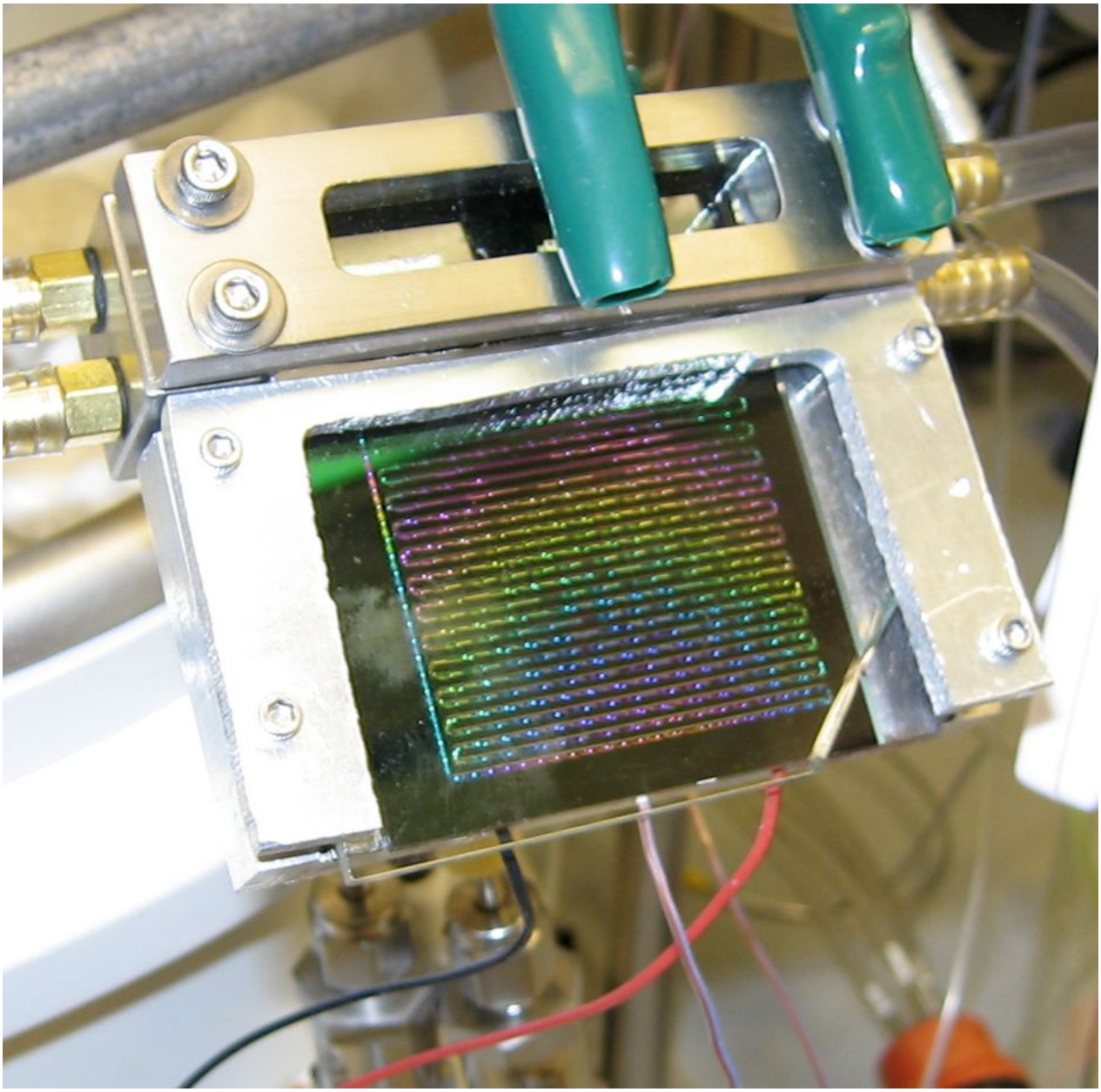

Figure 5. Silicon microreactor with a stainless steel chuck for fluidic connections and an aluminum heating chuck attached.

Figure 5 shows a third type of four-port silicon microreactor. This chip is called the straight channel, or 180 ° turn reactor, and is shown packaged with a fluidic chuck and a heating chuck. The fluidic chuck is machined from stainless steel and has four 10-32 coned ports on the back that are positioned to align with the outlet and three inlets. The bolts on each corner of the chuck are tightened to compress the two parts

of the chuck onto the top of the chip. Kalrez o-rings are used to make the seals between the steel chuck and the silicon reactor. The window in the top of the chuck allows for visualization of the inlets and outlet during the course of the reaction.

The aluminum heating chuck uses a similar compression design for its attachment to the chip. A piece of Pyrex glass is used on the top of the chip to provide an even distribution of the pressure over the chip. The chuck also contains a void space behind the chip that allows for the insertion of a Pelletier thermoelectric heater (the leads can be seen exiting the bottom of the chuck). The assembly is completed by sandwiching a thin layer of graphite between the back of the chip and the heater for uniform heat distribution.

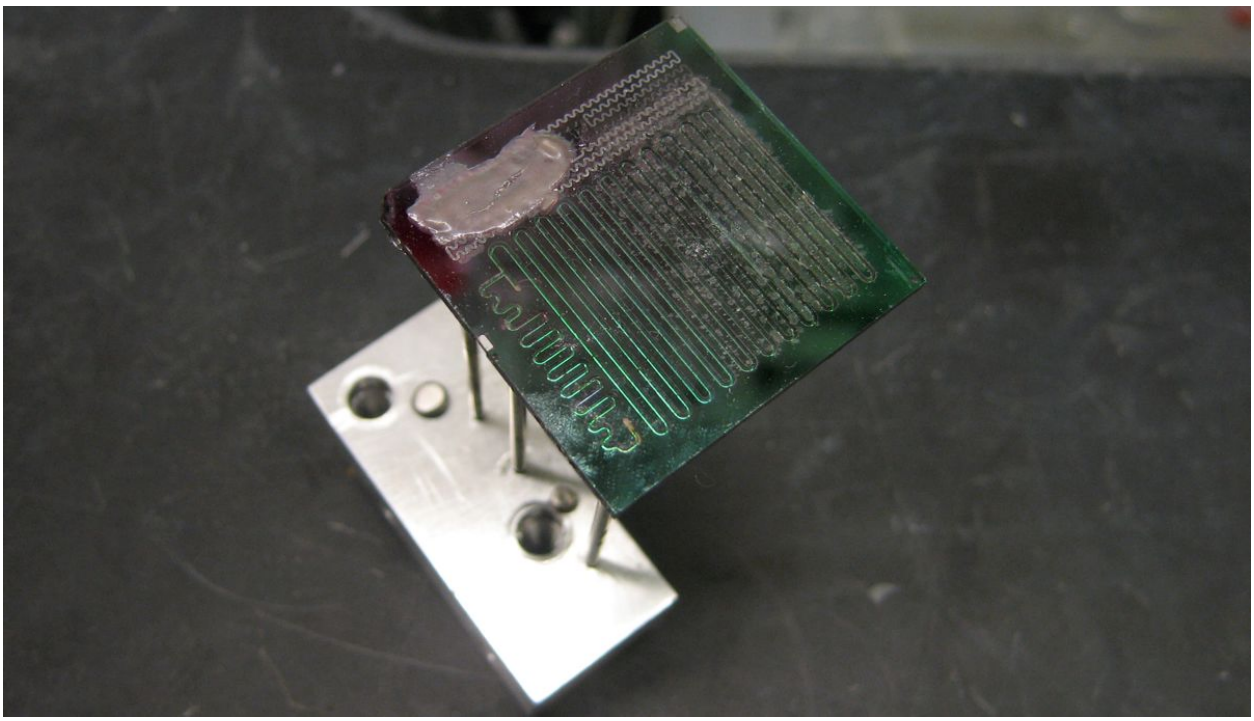

Figure 6. Five-port silicon microreactor.

Another type of microreactor design was the five-port design pictured in Figure 6. This reactor construction incorporates three inlets that feed into a narrow channeled mixing zone (top in picture) that leads into the main reactor channel. A fourth inlet combines with the reaction stream at the end of the channel to provide a quench, which then proceeds to the outlet through the fifth port. This reactor is

defined by its small reactor volume of only 70 μL and provides excellent mixing for homogeneous reactions. As can be seen in Figure 6, the five-port chip was packaged in a different manner than the four port chips. In this case, the inlets were soldered to the chip that had been prepared through a gold sputtering process around the ports. The stainless steel tubing that was soldered to the chip could then be connected to tubing leads via standard unions, or could be compressed in a stainless steel chuck, as pictured. This chuck forms a compression seal around the tubing, and provides standard 1/4-28 flat-bottomed connections for the tubing leads.

6.2.1 Biphasic reactions in silicon microreactors. Before it was discovered that packed bed reactors could provide excellent mixing and activity for the biphasic reactions the use of silicon reactors was explored. The silicon chips provided excellent heat and mass transfer properties along with the option for facile pressurization to allow for reactions at elevated temperatures. The steel barrels below the chip in the background of Figure 5 are backpressure regulators (Swagelok) that allow for the reaction to be run at temperatures above the boiling point of the reaction solvents. Unfortunately, continued operation of the silicon based system under the biphasic reaction conditions at elevated temperatures resulted in a rainbow color pattern on the reactor (Figure 5); initially the chip was a uniform green color, as the reactors in Figure 4. Over the course of the reaction, the strongly basic aqueous phase (2 M KOH) of the reaction began to etch away the silicon nitride layer of the microreactor. This etching reduced the thickness of the layer and resulted in a change in the diffraction of visible light and provided the rainbow of colors. After extended periods of time (7 hours), the color of the bottom channels faded to white implying complete removal of the nitride layer, and the reaction solution quickly etched through the underlying silicon oxide layer leading to failure of the device. Because of this, it was determined that silicon based microreactors would not be suitable for reactions involving aqueous hydroxide solutions that are run at elevated temperatures.

6.3 Packed beds

Prior to the development of the packed beds described in Chapter 5, several prototypes were explored. The early versions of the packed beds used PFA tubing as the reactor housing and glass wool as the end capping material. A piece of glass wool was inserted into the end of the PFA tubing (1/8" OD x 1/16" ID) and the tubing was connected to a length of our standard 0.02" ID (1/16" OD) tubing with a Teflon union to complete the end assembly. In order to pack the column, a Luer connector was installed on the open end of the tubing and a plastic syringe was used as a funnel for the packing material. The outside of the column was tapped with a spatula to facilitate the packing and the open end of the column was capped in the same manner as the first. One of these early packed beds is shown in Figure 7, and a close up of the glass wool plug used in the end capping is shown in Figure 8.

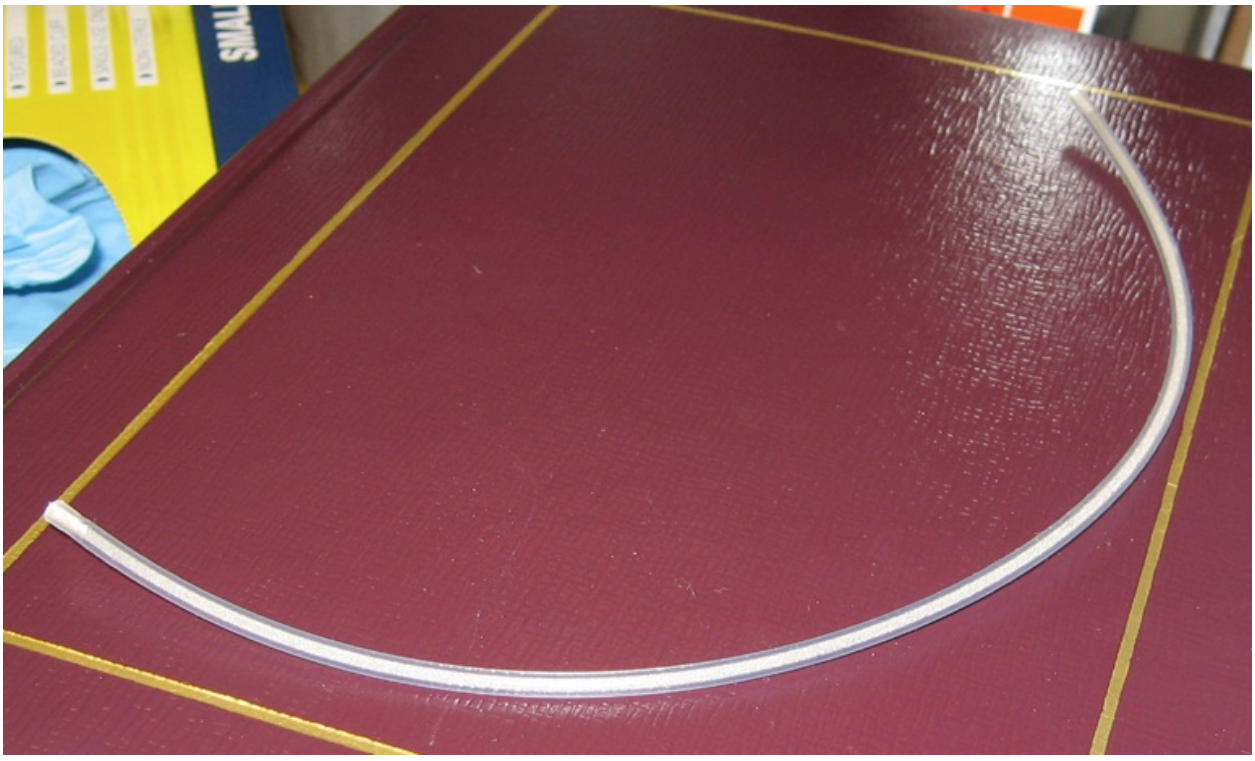

Figure 7. Packed bed column made from 1/8" PFA tubing.

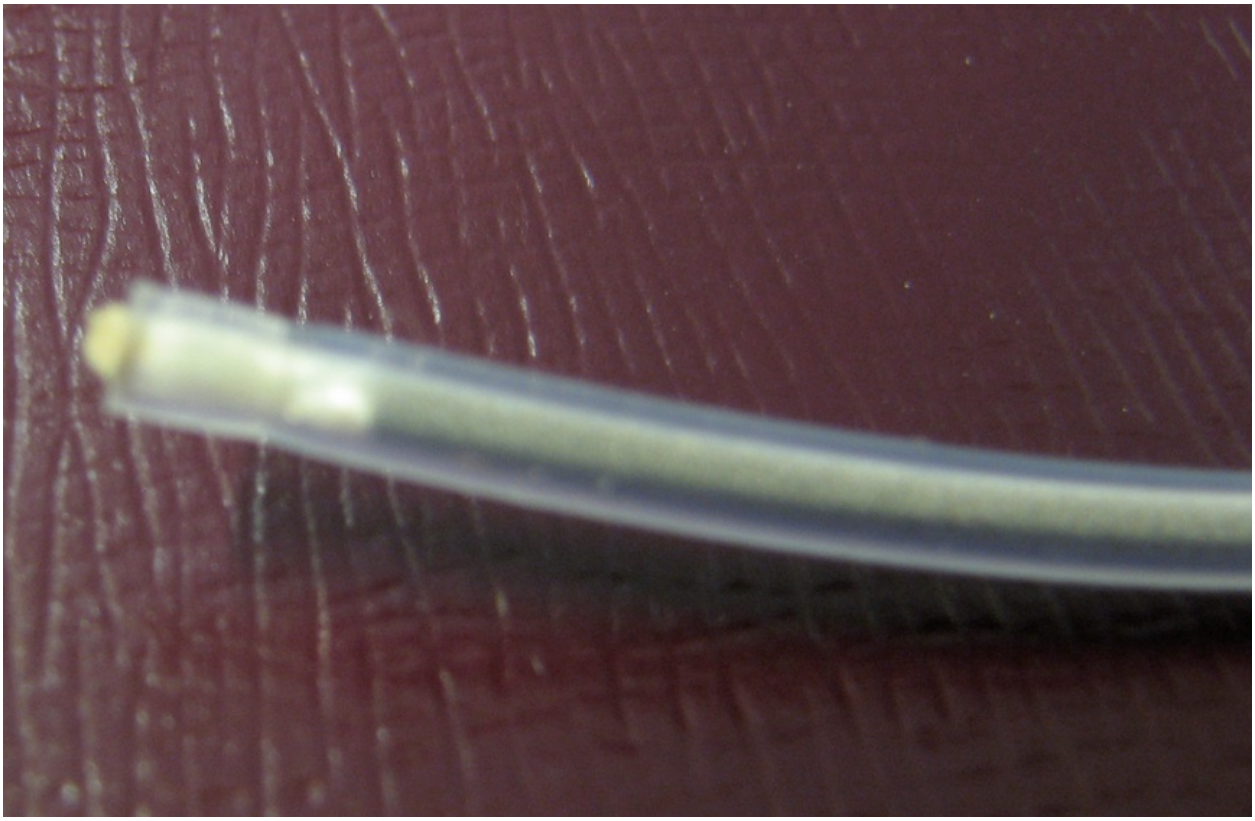

Figure 8. Close up of a packed bed made from 1/8" PFA tubing. End capped with glass wool.

Early experiments in packed bed construction often focused on the type of packing material that could be used to provide durable packed beds. The first beds were packed with borosilicate glass from standard culture tubes. The tubes were crushed and ground in a mortar and pestle to a fine powder. Commercially available mesh sieves were used to separate the glass powder into particle sizes, and packing material ranging in distribution from 40-60 μm to 125-160 μm were used to make packed beds. The mass of the empty tube was subtracted from the mass of the packed bed and the volume of the packing was calculated based on the density of borosilicate glass (2.23 g/mL). The percentage of volume occupied by the packing material was consistently found to be between 63% and 65%. As noted in Chapter 5, extended operation of these packed beds in the biphasic amination reaction lead to a degradation of the packing material that led to an increase in the back pressure of the system and resulted in syringe failure. Experiments were also performed using sand as the packing material. Standard lab grade sand was separated by particle size using the same sieves used for the glass powder. Similar degradation issues were observed with the sand packing material.

While the use of glass packing material was eventually discarded as a viable option, the initial results were very promising as the packed beds provided excellent mixing and efficient reactions. As such, a variety of different packed beds were constructed and used in these experiments. In addition to the borosilicate glass that was ground and separated in our lab, one commercially available source of glass beads was tested (Mo-Sci Specialty Products Corporation). The spheres were 38-45 μm in diameter and were ideal for making smaller volume packed beds. The beads were packed in 0.04" ID PFA tubing (1/16" OD) using the Luer connector and plastic syringe barrel technique described above. The ends of the column were capped with inline filters that were available from IDEX Health and Science. The completed column is shown in Figure 9. While the calculated volume of the bed was only 45 μL, minimizing the amount of starting materials required, the small size of the glass beads led to a pressure drop across the column that was prohibitively high for use with syringe pumps and plastic syringes.

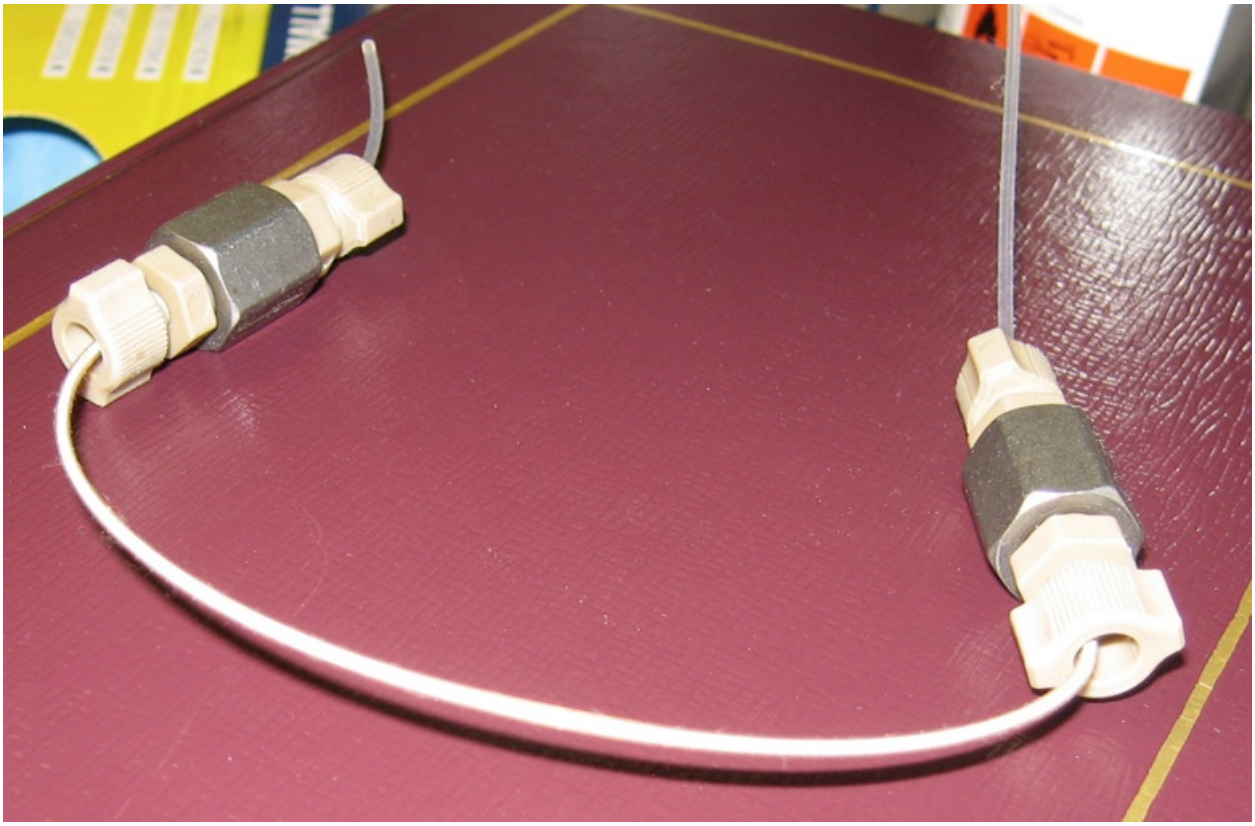

Figure 9. Packed bed reactor made from 1/16" OD x 0.04" ID PFA tubing and capped with inline filters.

The second generation packed beds that were used for the work described in Chapter 5 were constructed based on the model of an analytical HPLC column. One of these columns is pictured in Figure 10. As can be seen, short lengths of stainless steel tubing were used on each end of the packed bed and enabled connections to the 0.02" PFA tubing used for reagent delivery and product flow. The rigid stainless steel housing of the packed beds provided a convenient point of attachment for positioning the reactors in heating baths. Figure 11 shows a standard packed bed setup where the column is secured by a clamp and submerged in an oil bath. It is worth mentioning that unlike fluoropolymer tubing the stainless steel connectors do not suffer from curing and degradation after prolonged heating. Additionally, care must be used when using PEEK fittings to make the connection between the tubing and the packed bed. In the high temperature experiments described in Chapter 5, it was found that the fittings began to melt at 180 °C, and, therefore, stainless steel connections were required.

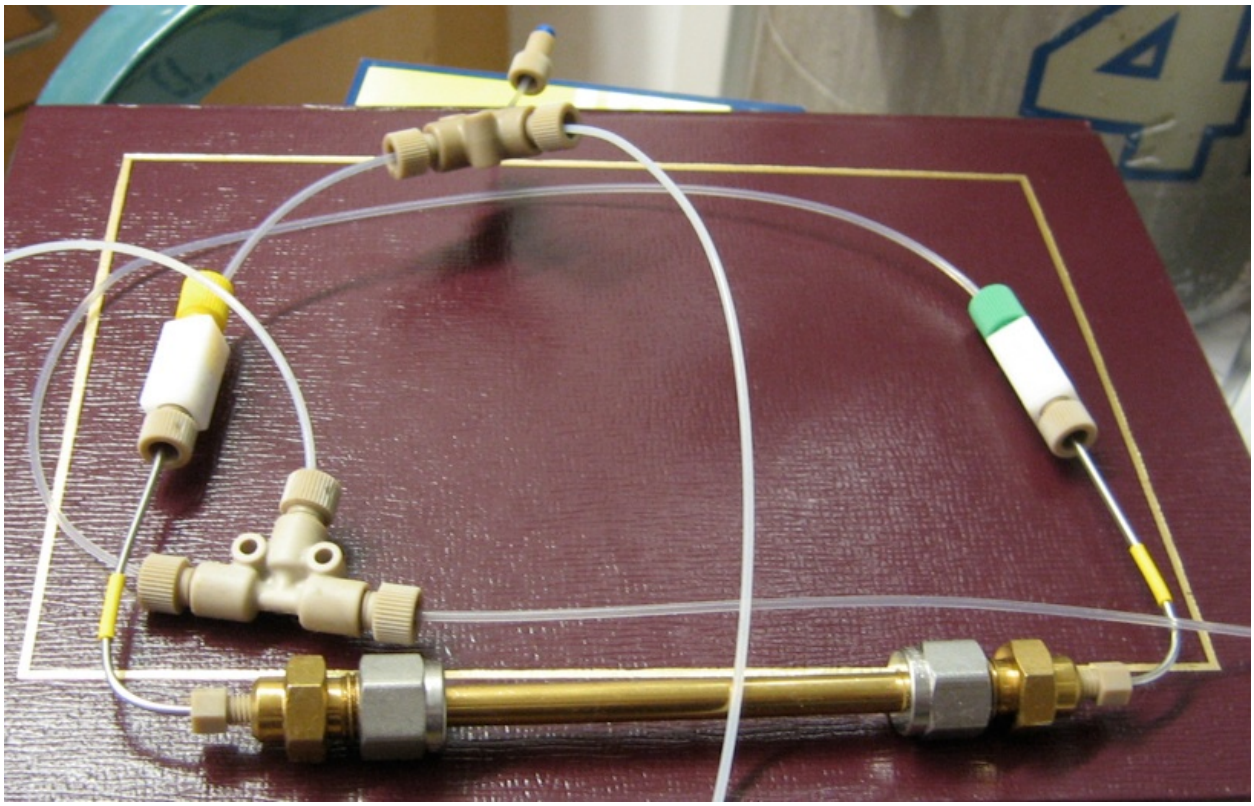

Figure 10. Packed bed reactor with 1/16" tubing connections.

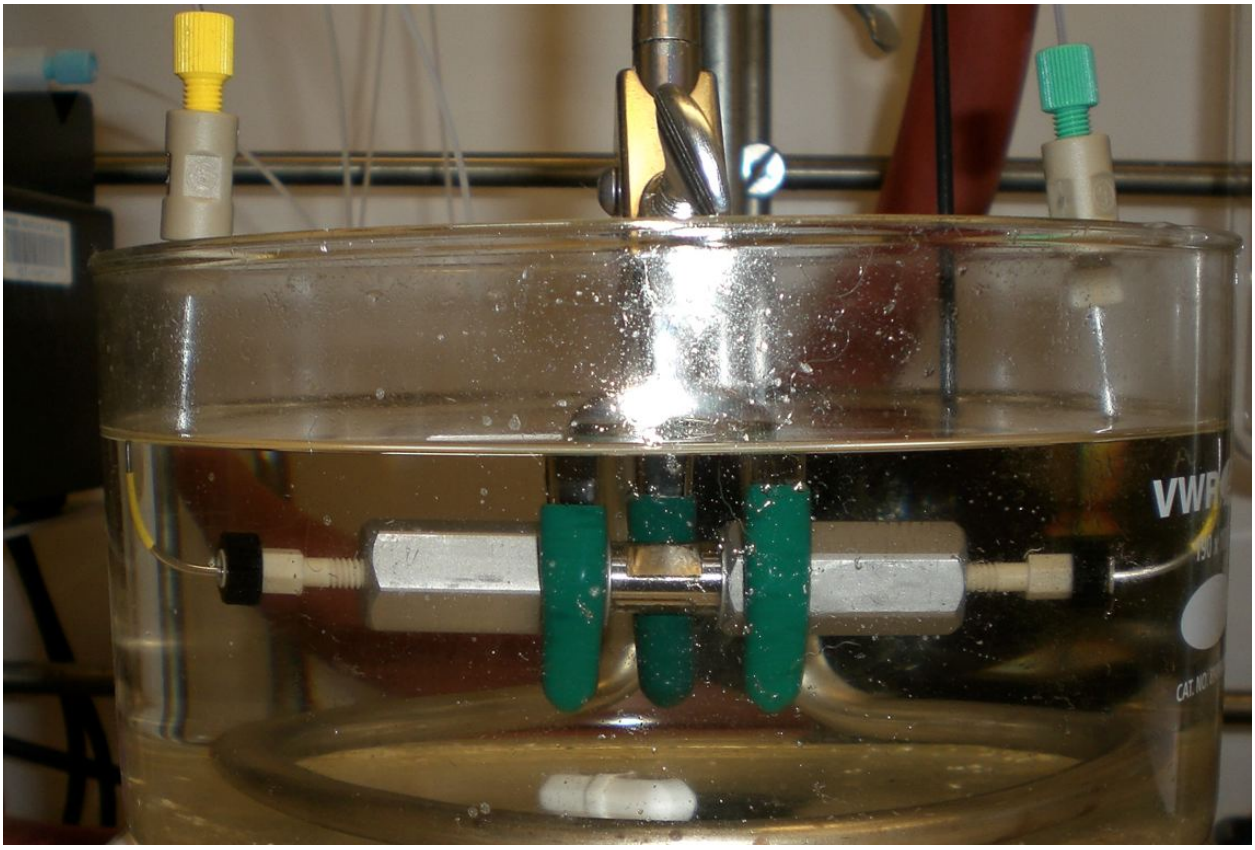

Figure 11. Packed reactor submerged in an oil bath.

While no loss of activity was observed with prolonged use of the packed bed reactors, it was important to periodically clean the reactors to prevent buildup of salts, reagents, or palladium decomposition materials. In general flushing the column with toluene and water after each experiment was sufficient to maintain proper flow in subsequent experiments. However, after long periods of operation a wash with a polar water-soluble solvent, such as acetone, would often result in the removal of some dark solids. Additionally, running the acetone wash in the opposite direction of the flow resulted in the most effective cleaning of the column. In general the pressure drop across the columns packed with the SS beads was low enough to allow for high rates of flow using plastic syringes by hand.

6.4 Auger Reactor

During the initial stages of the solids handling project many possible solutions were explored. One possibility was to use a mechanical force to either break up clogs, or to move the solids that were formed through a reactor. In analogy to an auger used for transporting grain, or an Archimedes screw used for water transport, it was postulated that a threaded rod inside of a smooth barrel could both provide a continuous channel for flow and if turned mechanically provide a physical push for the reaction stream, whether it was liquid, solid or a combination of the two. A reactor based on this premise was designed and the reactor was fabricated by the MIT central machine shop. The reactor was fabricated from 316 stainless steel with the barrel coming from a piece of 1" rod (8" long) and the threaded piece coming from a length of 0.25" rod (12" long). The rod was threaded (1/4-40) and a 0.25" channel was bored in the barrel (7.75" deep). Six 1/4-28 flat-bottomed ports were bored into the barrel to a depth of 0.25". Four of the ports were bored 0.5" from the open end of the barrel as inlets and were placed with 90° separation. The fifth port was 6" from the inlets and was installed as a quench. The final port was the outlet and was installed 7" from the inlets. A 0.75" diameter pocket was bored in the open end of the barrel to a depth of 0.25". The 1/4" rod was threaded for 7" starting 0.25" from one end. A 0.75" stopper, that was designed to incorporate three o-rings, two face mounted and one around the edge of the stopper, was fixed on the rod 7.75" from the end. Finally an endcap was designed to thread over the end of the barrel and compress the o-rings into the pocket and form the fluidic seal.

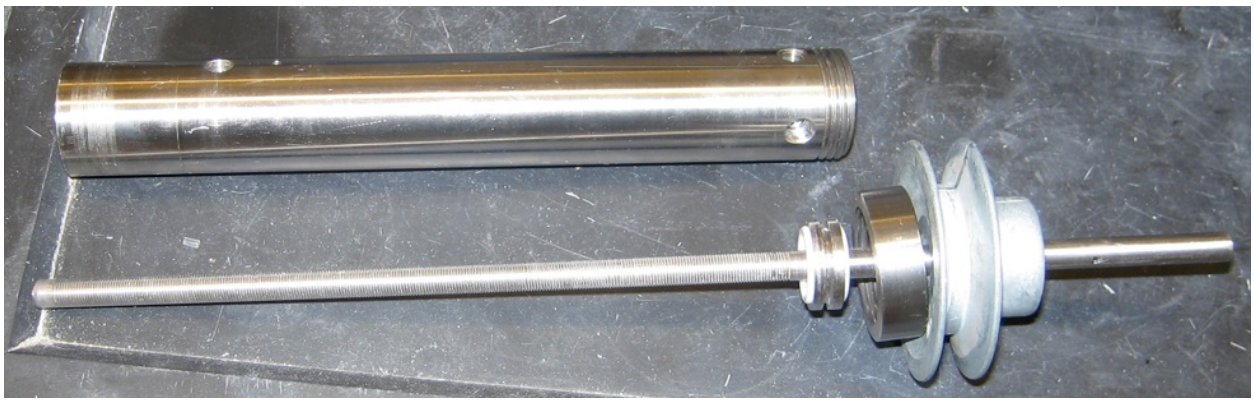

Figure 12. Auger reactor.

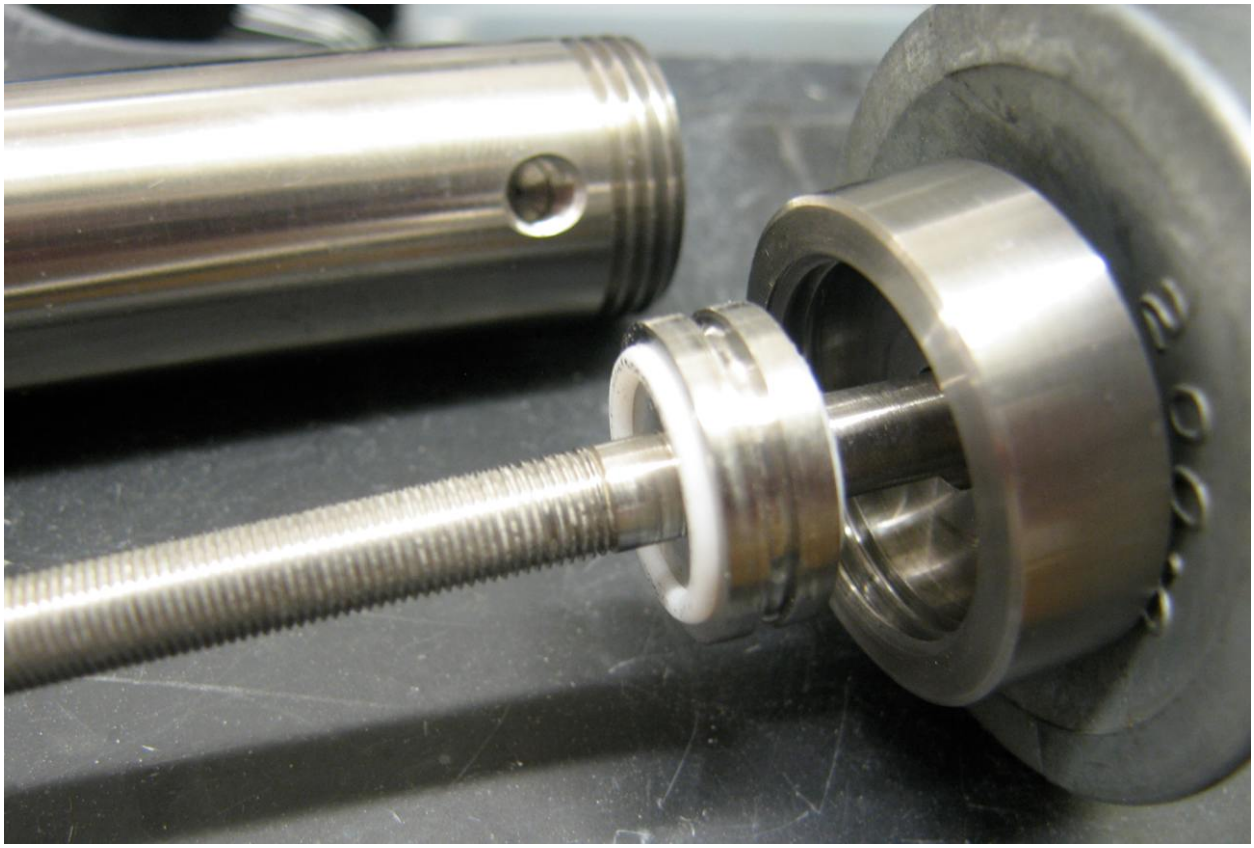

Figure 13. Close up of the threaded rod and stopper with o-rings.

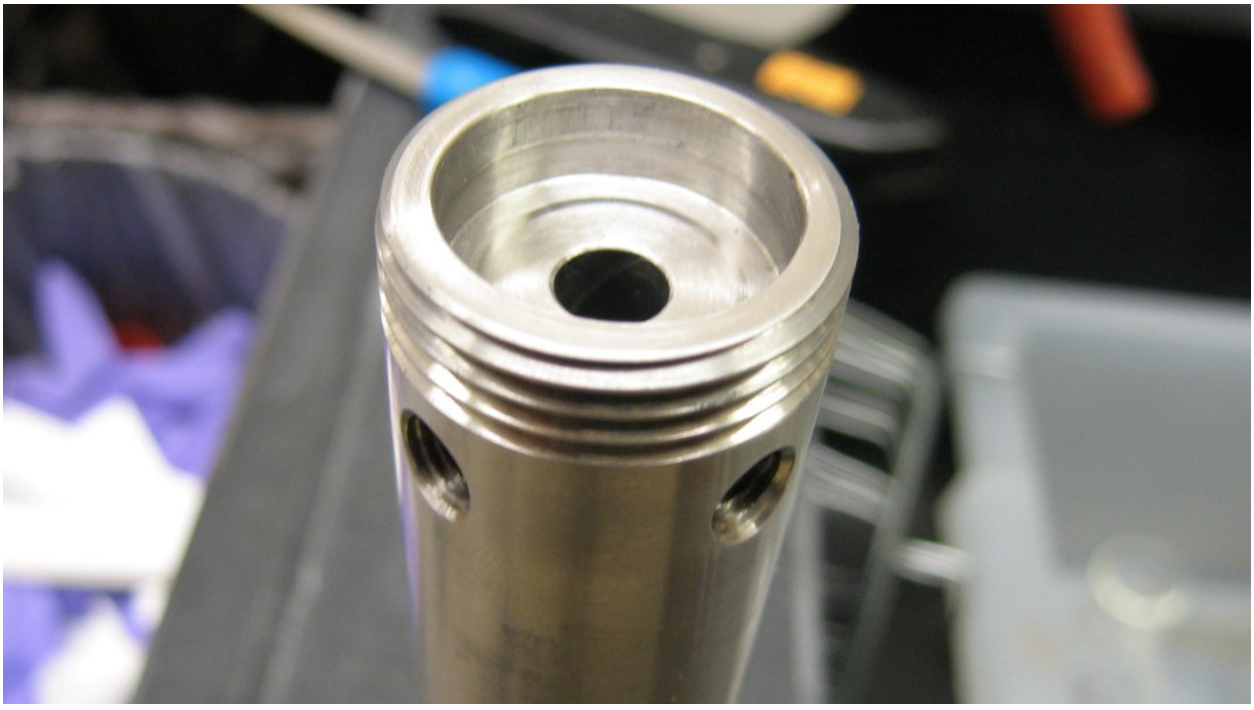

Figure 14. Close up of the barrel with recessed pocket.

Figure 15. Equipment setup for fast rotation of the auger reactor.

When the reactor was assembled it was found that the side mounted o-ring generated a significant amount of friction made turning the threaded rod very difficult. In addition to this, when Viton o-rings were used, the friction between the o-ring mounted on the back face of the stopper and the end cap resulted in a gradual tightening of the end cap when the rod was rotated clockwise and caused the reactor to seize up. Because of this, the PTFE o-rings pictured in Figure 13 were found to be better suited to the task.

Several options were explored to turn the threaded rod. The first option that was explored was to use an overhead stirrer to turn the threaded rod. However, when the stirrer was connected to the end of the rod, it was found that there was too much friction for the limited torque of the stirrer to overcome. The next option was an extension of this plan and involved using an electric drill in place of the overhead stirrer. The difficulties surrounding the perfect alignment of the drill and the reactor suggested that directly attaching the rod to the drill through the chuck of the drill was not a viable option. As such, a flexible alternative was devised similar to the setup for a mechanical stirrer. A length of rubber tubing was used to connect the threaded rod and the shaft that was mounted in the drill's chuck as shown in Figure 15. The trigger for the drill was locked in the on position with a zip-tie and the drill was connected to a variable AC voltage controller to allow for variable speeds of rotation. The reactor was wrapped in electrical heating tape and a thermocouple was inserted between the heating tape and barrel of the reactor. A control reaction was performed and over the course of the experiment the rod became more difficult to turn until it reached a point where the rubber tubing was not able to overcome the friction and began to twist on itself. When the reactor was opened it appeared that the high rate of rotation resulted in wear of the PTFE o-rings, and the fine shavings of PTFE may have lead to the increase in friction as they became lodged between the stopper and the walls of the recessed pocket.

A second system that was explored for turning the rod was the use of a low speed, high torque gear motor. While gears, chains and belts were all options for connecting the gear motor to the shaft, it was determined that a standard v-belt would be the simplest solution to the problem. In order to facilitate this, a pulley was mounted on the end of the threaded rod after a portion of the rod was flattened to receive a

setscrew. An aluminum base was used to attach both the gear motor and the auger reactor. Two mounts were designed and fabricated by the MIT central machine shop, from aluminum blanks, to hold the reactor in place. Adjustable length v-belting was used to connect the pulleys and the leads of the gear motor were wired to a standard three-pronged plug. The completed setup is pictured in Figure 16. This setup resulted in regular slow rotation of the threaded rod inside the auger reactor. This setup has the potential to find application in both solids handling applications and in reactions were mixing is important such as the biphasic chemistry described in Chapter 5.

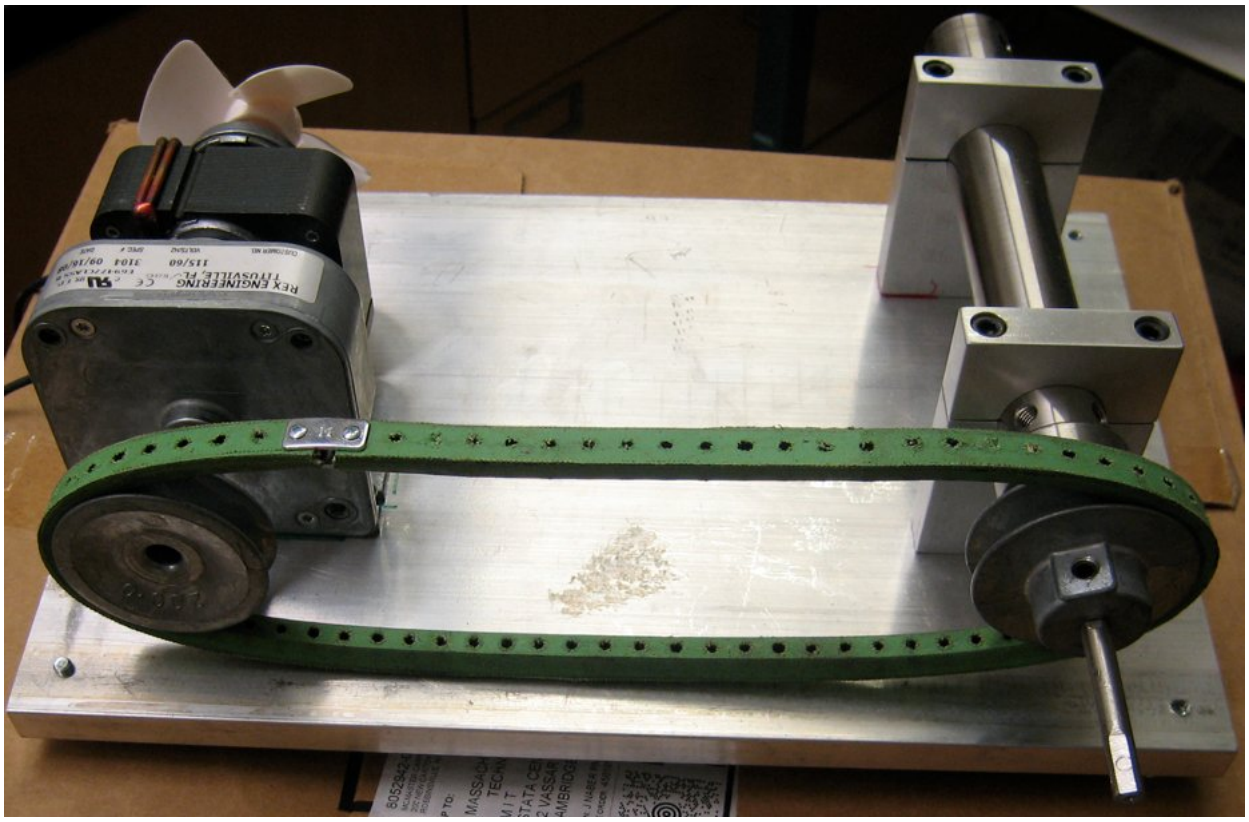

Figure 16. Equipment setup for slow rotation of the auger reactor.

NOTE: When working with rotating equipment and equipment that uses belting, caution is needed to avoid potential entanglement.

6.5 AM Technology Coflore

The Coflore system was purchased from AM Technology in the UK and is advertised as a system capable of handling suspensions and slurries in a continuous flow manner. The design is based on a reactor block that consists of 10 reaction cells that are connected by a single channel. Each cell contains an agitator that fits loosely and allows for flow around it, and through the cell. When the reaction block is connected to the Coflore (shaker), the system oscillates and the reaction block is shaken from side to side. The agitators shake in the cells and provide several benefits including grinding of any particles that are formed, mixing of the reaction solution, and also provide a "push" for any solids to pass to the next cell.

Figure 17. Equipment setup for the experiments with the Coflore system.

The equipment setup for the Coflore system can be seen in Figure 17 and includes a recirculating bath for temperature control, a compressed air source (hidden behind the water bath), the Coflore itself and pumps for delivering the reagent streams to the system. Experiments were performed with HPLC pumps (Chromtech), peristaltic pumps (Cole-Parmer) and syringe pumps (Harvard Apparatus). As long as chemical compatibility was not a problem the peristaltic pump provide an excellent combination of flowrate variability and multi-stream flow. The oscillation of the shaker was driven by the compressed air supply and a pressure of 80 psi was found to give the best results.

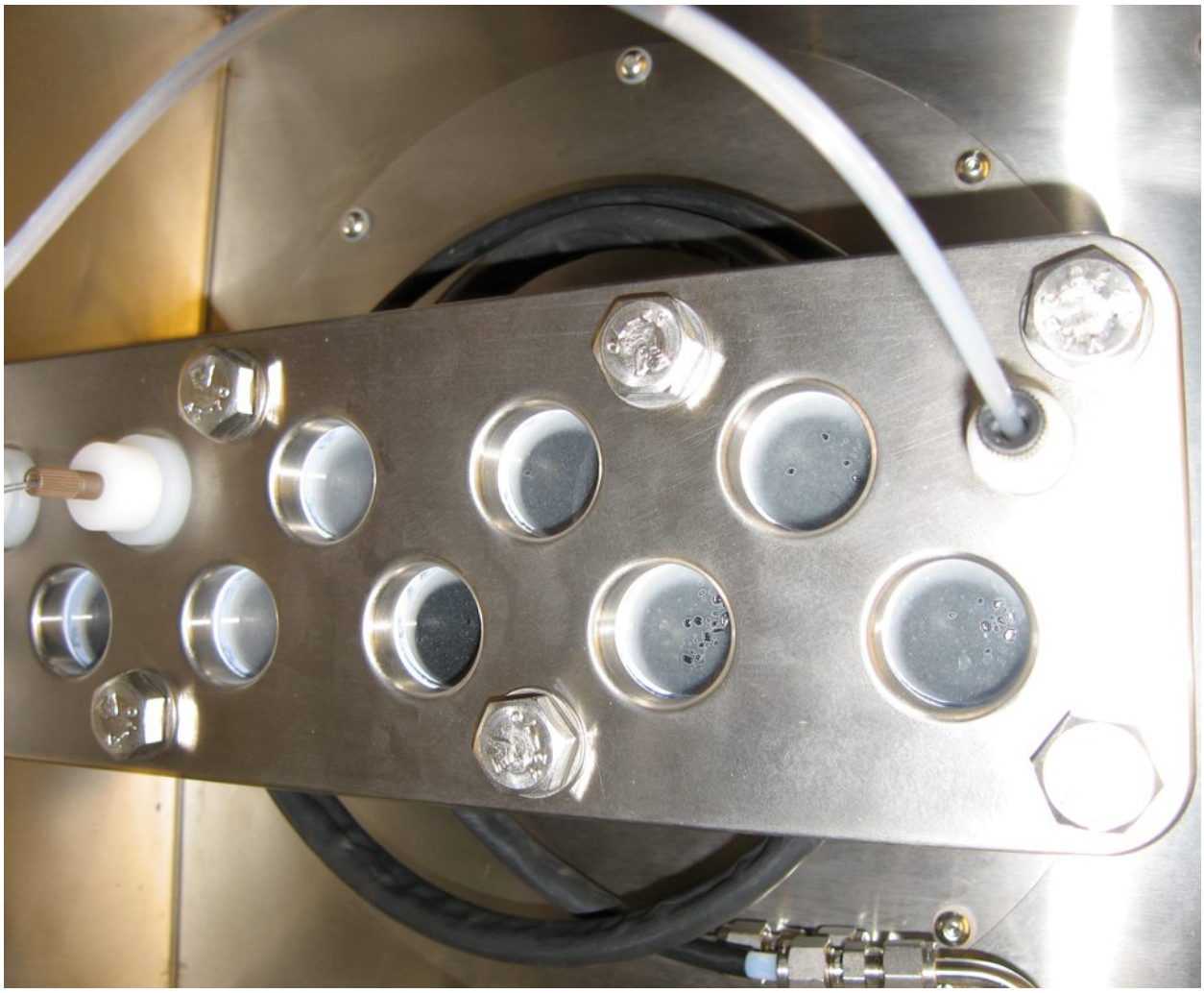

Figure 18. Reaction block for the AM Technology Coflore reactor.

The reaction block shown in figure 18 is very modular and can be customized in a variety of ways. The agitators can be removed and several different sizes are available. Additionally, other types of agitators are available and include mesh baskets for supported reagents or catalysts and heavy wire coils for increased mixing. The reactor block is very large compared to the types of volumes usually encountered in lab scale reactions with a liquid volume of ~40 mL when the largest agitators are installed. The windows of the individual cells can also be replaced with additional injection ports to allow for multiple reaction steps, or sequential addition of a reagent. The block that we purchased is made of PTFE and as such has excellent chemical compatibility although the maximum operating temperature is 100 °C. The

agitators are designed have a pair of o-rings that act as runners for the agitator when it moves around the cell. However, the standard Viton o-rings have very poor compatibility with organic solvents and were removed. The Teflon coated agitators that were purchased with the reactor were later recalled, and a second set of ceramic agitator were provided. This replacement set of agitators came with a set of Kalrez o-rings that have an excellent chemical compatibility profile.

Several test experiments were performed with the Coflore and it was found to handle a considerable amount of solids in the reaction stream without plugging. However, while the system did not clog, there was a buildup of white solid on the glass of the individual cells implying a slow deposition that could lead to clogging during extended runs. The major limitation with this equipment is the size of the reactor. The 40 mL reactor volume necessitates a large amount of starting materials and solvents to run a flow experiment as one commonly discards the first 5 reactor volumes before collecting the reaction stream.

6.6 Abbreviations

APC ---------- allyl palladium chloride dimer
API ---------- active pharmaceutical ingredient
BPR ---------- back pressure regulator
t-BuOH ---------- *tert*-butanol
CsF ---------- cesium fluoride
DCM ---------- dichloromethane
DIEA ---------- diisopropylethylamine
DME ---------- 1,2-dimethoxyethane
DMF ---------- dimethylformamide
DPPP ---------- diphenylphosphinopropane
EA ---------- elemental analysis
KF ---------- potassium fluoride
KOH ---------- potassium hydroxide
$CDCl_3$ ---------- deuterated chloroform
GC ---------- gas chromatography
HCl ---------- hydrochloric acid
HPLC ---------- high-pressure liquid chromatography
ID ---------- inside diameter
μTAS ---------- micro total analysis system
NaOH ---------- sodium hydroxide
NHC ---------- *N*-heterocyclic carbene
OD ---------- outside diameter
PEEK ---------- polyether ether ketone
PFA ---------- perfluoroalkoxy
PID ---------- proportional-integral-derivative
PTC ---------- phase transfer catalyst
PTFE ---------- polytetrafluoroethylene
SEM ---------- scanning electron microscopy
SS ---------- stainless steel
τ ---------- residence time
TBAB ---------- tetra-n-butylammonium bromide
TBAF ---------- tetra-n-butylammonium fluoride

John R. Naber

Education

Ph.D. Organic Chemistry — *Massachusetts Institute of Technology*, Cambridge, MA — 2010

- Thesis: Recent Advances in Palladium–Catalyzed Carbon–Carbon Bond–Forming Reactions and Continuous Flow Methods for Palladium–Catalyzed Carbon–Nitrogen Bond–Forming Reactions
- Advisor: Prof. Stephen L. Buchwald

B.Sc. in Chemistry — *University of Victoria*, Victoria, BC — 2004

Professional Experience

Academic Research

Graduate Research – Prof. Stephen L. Buchwald (MIT)	2005-2010
Undergraduate Research – Prof. Tom Fyles (UVic)	2003-2004

Teaching Experience

Massachusetts Institute of Technology	2004-2005

Industrial Research

Merck Frosst Canada Ltd., Kirkland, QC	5/2004 – 8/2005
Shire Biochem Inc., Laval, QC	5/2003 – 8/2003
Xerox Research Centre of Canada, Mississauga, ON	5/2002 – 8/2002
NOVA Chemical Corporation, Calgary, AB	5/2001 – 12/2001
ALS Chemex Vancouver, Vancouver, BC	5/2000 – 8/2000

Honors and Awards

- University of Victoria Coop Workterm Award — 2004
- John F. Reeves Memorial Scholarship — 2003
- NSERC Undergraduate Student Research Award — 2001, 2002, 2003
- University of Victoria Excellence Scholarship — 1999, 2000, 2001, 2002
- University of Victoria Dean's List — 2000, 2001, 2002
- Russel Hodges Memorial Scholarship — 1999
- Saskatchewan Academic Excellence Scholarship — 1999

Publications

John R. Naber and Stephen L. Buchwald, "*Continuous Flow Pd-Catalyzed CN Bond Formation.*" Prepared Manuscript.

Ryan L. Hartman, John R. Naber, Nikolay Zaborenko, Stephen L. Buchwald and Klavs F. Jensen, "*Overcoming the challenges of bridging and constriction during Pd-catalyzed C-N bond formation in micro-flow.*" Prepared manuscript.

Patrick Bazinet, Jonathan P. McMullen, John R. Naber, Andrew J. Musacchio, Klavs F. Jensen and Stephen L. Buchwald, "*Automated Optimization of Sequential Biphasic Pd-Catalyzed Amination and Suzuki-Miyaura Cross-Coupling Reactions.*" Prepared Manuscript.

Tarek M. Shazly, Aaron B. Baker, John R. Naber, Adriana Bon, Krystyn J. Van Vliet and Elazer R. Edelman, "*Augmentation of post-swelling surgical sealant potential of adhesive hydrogels*." Submitted paper.

Ryan L. Hartman, John R. Naber, Stephen L. Buchwald and Klavs F. Jensen, "*Multi-step Microchemical Synthesis Enabled by Microfluidic Distillation*." *Angew. Chem. Int. Ed.* **2010**, *49*, 899.

John R. Naber, Brett P. Fors, Xiaoxing Wu, Jonathan T. Gunn and Stephen L. Buchwald, "*Stille Cross-Coupling Reactions of Aryl Mesylates and Tosylates Using a Biarylphosphine Based Catalyst System*." In Press, *Heterocycles*, DOI: 10.3987/COM-09-S(S)105.

John R. Naber and Stephen L. Buchwald, "*Palladium-Catalyzed Stille Cross-Coupling Reaction of Aryl Chlorides using a Pre-Milled Palladium Acetate and XPhos Catalyst System." Adv. Synth. Catal.* **2008**, *350*, 957.

Greg Hughes, Paul N. Devine, John R. Naber, Paul D. O'Shea, Bruce S. Foster, Daniel J. McKay and R. P. Volante, "*Diastereoselective Reductive Amination of Aryl Trifluoromethyl Ketones and a-Amino Esters." Angew. Chem. Int. Ed.* **2007**, *46*, 1839.